Assessing the macro and microscale surface changes following citric acid mediated attack on polished and natural human enamel in vitro

Mylonas, Petros

Awarding institution:
King's College London

KING'S COLLEGE LONDON DENTAL INSTITUTE AT GUY'S, ST. THOMAS' AND KING'S COLLEGE HOSPITALS

Assessing the Macro and Microscale Surface Changes following Citric Acid Mediated Attack on Polished and Natural Human Enamel in vitro

Thesis submitted for the degree of
Doctor of Philosophy

Petros Mylonas

BDS MJDF RCS (Eng) MFDS RCPS (Glasg)
MMedEd FHEA(UK)

Faculty of Dentistry, Oral and Craniofacial Sciences
King's College London,
Centre for Oral, Clinical and Translational Sciences
Guy's Hospital
London SE1 9RT
United Kingdom
July 2019

Abstract

This thesis investigated the effect of short- and long-term citric acid mediated erosion on polished and natural human enamel and determined which characterisation methods were suitable to create and measure artificial dental erosion lesions on polished and natural human enamel.

Firstly, an in vitro study characterising early erosion in polished and natural human enamel was conducted. Changes to the enamel surface after citric acid erosion were measured with 3D-step height change (μm), surface roughness (Sa, μm), surface microhardness (KHN), surface reflectivity with optical coherence tomography (OCT) and surface morphology using tandem scanning confocal microscopy (TSM). In polished enamel, mean (SD) 3D-step height change (μm) was measurable after 60s (0.24±0.1), after 10s mean (SD) surface roughness (μm) was 0.270(0.013) and mean(SD) Knoop microhardness decreased to 316(1.82). Only surface roughness change was detectable in natural enamel after 120s (0.830(0.125)).

Secondly, further work determined how to create/detect/characterise early and late dental erosion in natural human enamel only. This was conducted in 4 separate but interconnected investigations. The first determined the minimum detection threshold of non-contacting laser profilometry (NCLP) in measuring changes in surface form (0.279μm) and roughness (0.072μm) in natural enamel, the second, calculated the effect of thermal variation on NCLP sensor displacement according to different scanning periods and NCLP conditions (open vs closed). The third determined the optimum scanning parameters for assessing/scanning surface form change in natural human enamel (3.5x3.5mm grid, 351x351 points, with step over

distance 10 μm). The fourth then validated a new in vitro dental erosion lesion model using natural human enamel; in this model, the erosion lesion could be defined using changes in step height (ISO and non-ISO methods), surface roughness, surface reflectivity (OCT), and surface morphology (TSM).

Thirdly, this new natural enamel dental erosion model was further tested according to different factors that are seen clinically which would affect the erosion process; this consisted of 3 further studies. The effect of three factors were all separately tested for their effect (if any) on dental erosion lesion formation using this new model: sodium fluoride toothpaste pre-treatment (factor 1) reduced mean (SD) step height formation (0.38(0.20)), acquired enamel pellicle (factor 2) did not produce any significant protective benefit against mean (SD) step height formation (1.22(0.75)), and an experimental calcium silicate/sodium phosphate/sodium monofluorophosphate toothpaste (factor 3) also reduced mean (SD) step height formation (0.51(0.22)).

Overall, the effects of early and late citric acid erosion could be measured on both polished and natural human enamel. Most importantly, however, enamel loss could be measured and quantified on the natural enamel surface as step height formation using both ISO and non-ISO methods. This new in vitro model using natural human enamel is a closer representation of the clinical scenario (versus using polished enamel). The methods developed have potential applications beyond those demonstrated in this Thesis.

Acknowledgements

To the other members of the Toothwear Gang: Rasha, Polis, and Sami; it's been an honour to have known you guys, you've made this difficult journey easier and worthwhile!

And last but not least, to my family whom I love so much, thank you for being there when I needed you and for being so supportive; I couldn't have finished this PhD without all of you.

Declaration of collaborative work

Professor David Bartlett, Dr Rebecca Moazzez, and Dr Andrew Joiner all contributed to the design, analysis, and discussion of all Chapters within this Thesis.

Mr Tom Bull contributed to the design and analysis of Chapter 3, Section 3.3.2 (detection threshold determination) and 3.3.5.1 (analysing barrier creation). The experimental data for Section 3.3.3 (influence of thermal variation) was gathered by Tom at the Nanometrology Laboratory in the Faculty of Engineering and the Environment at the University of Southampton; Figure 31 and Table 3 were provided accordingly.

The Applications and Support Team from Digital Surf, creators of MountainsMap software, provided technical support for the design and analysis of Chapter 3, Section 3.3.5.3.2 (MountainsMap method).

I am grateful for the collaborative help and support received in this Thesis, all remaining work is my own and references cited accordingly.

Petros Mylonas

July 2019

Publications and Presentations

Listed below are the publications, presentations, and prizes obtained as a result of the work conducted during the PhD and presented in this Thesis.

<u>Publications</u>: [peer-reviewed research papers]

1. **Mylonas, P**., Bull, T., Moazzez, R., Joiner, A. & Bartlett, D.W. Detection Threshold of Non-Contacting Laser Profilometry and Influence of Thermal Variation on Characterisation of Early Surface Form and Textural Changes in Natural Human Enamel. Dental Materials 2019 35(7) e140-e151

2. O'Toole, S., **Mylonas, P**. & Bartlett, D. W. Practice-Based Risk Assessment– a Practical Guide for Oral Healthcare Teams: Tooth Wear. Dental Update 2018, 46(2) 176-178

3. **Mylonas, P**., Austin, R. S., Moazzez, R., Joiner, A. & Bartlett, D. W. In vitro evaluation of the early erosive lesion in polished and natural human enamel. Dental Materials 2018 34(9) 1391-1400

4. Mullan, F., **Mylonas, P**., Parkinson, C., Bartlett, D. & Austin, R. S. Precision of 655nm Confocal Laser Profilometry for 3D surface texture characterisation of natural human enamel undergoing dietary acid mediated erosive wear. Dental Materials 2018 34(3) 531-537.

<u>Publications</u>: [peer-reviewed abstracts]

1. **Mylonas, P**., Moazzez, R., Joiner, A. & Bartlett, D.W. Erosion-Protective Benefit of Calcium Silicate Toothpaste On Natural Enamel Erosion. Jul 2019, In: Journal of Dental Research, 98, (Spec Iss A) - 3794

2. **Mylonas, P**., Bull, T., Moazzez, R., Joiner, A. & Bartlett, D.W. Thresholds of Non-contacting Laser Profilometry in Detecting Enamel Erosive Wear. Jul 2018, In: Journal of Dental Research, 97, (Spec Iss B) - 2275

3. **Mylonas, P**., Moazzez, R., Joiner, A. & Bartlett, D.W. Characterising early erosive lesions in polished and natural human enamel. Jul 2017, In: Journal of Dental Research, 96, (Spec Iss B) – 090

Media publications:

1. **Mylonas, P**. Detecting tooth enamel erosion with Mountains®. Surface Newsletter, Spring 2019, 6-7

Publications: [submitted or under review]

1. **Mylonas, P**., Bull, T., Moazzez, R., Joiner, A. & Bartlett, D.W. The effect of single application fluoride pre-treatment on step height formation in natural unpolished human enamel – a dental erosion in vitro model. ***manuscript submitted to Journal of Dentistry, pending review***

2. **Mylonas, P**., Moazzez, R., Joiner, A. & Bartlett, D.W. Erosion-protective benefit of calcium silicate toothpaste on natural enamel erosion in vitro– a natural enamel dental erosion in vitro model. ***manuscript being reviewed by Unilever and to be submitted to Dental Materials***

Presentations, posters, prizes

2019
1. International Association of Dental Research (IADR): Vancouver, Canada.

   Abstract Control ID: 3179709, Session Type: poster

   Title: Erosion-Protective Benefit of Calcium Silicate Toothpaste On Natural

   Enamel Erosion

2018
1. International Association of Dental Research (IADR): London, England.

   Final Presentation ID: 2275, Session Type: <u>oral</u>

   Title: Thresholds of Non-contacting Laser Profilometry in Detecting Enamel

   Erosive Wear

2. BSSM 13th International Conference on Advances in Experimental

   Mechanics: Southampton, England. Session Type: <u>oral</u>

   Title: The detection threshold of non-contacting laser profilometry and

   characterisation of microscale surface changes in natural human enamel

   following citric acid-mediated attack

3. 20th Dentistry Postgraduate Research Day; KCL, London, England.

   Session type: <u>oral</u>

   Title: The detection threshold of non-contacting laser profilometry in

   detecting enamel erosive wear

   <u>Prize winner: best oral presentation</u>

2017
1. British Society of Oral and Dental Research (BSODR): Plymouth, England.

   Final Presentation ID: 090, Session Type: <u>oral</u>

   Title: Characterising early erosive lesions in polished and natural human

   enamel

Contents

List of Figures

List of Tables

Overall Thesis structure

This thesis is split into 7 Chapters as outlined in Figure 1.

Chapter 1	Literature review, overall aims and objectives, overall null hypotheses
Chapter 2	Evaluating the early erosive lesion in polished and natural human enamel
Chapter 3	Developing a novel in vitro model to evaluate the early and late erosive lesion in natural human enamel
Investigation 1	Detection Threshold Determination of NCLP
Investigation 2	Characterising the influence of thermal variation on NCLP system stability
Investigation 3	Determining optimum scanning parameters for surface form measurement on natural human enamel
Investigation 4	Characterising effects of early citric acid-induced enamel erosion on natural human enamel
Chapter 4	Effect of single application fluoride treatment, and the acquired enamel pellicle on step height formation in natural human enamel
Chapter 5	Effect of calcium silicate/sodium phosphate treatment on early and late erosion in natural human enamel
Chapter 6	Overall Discussion, Limitations, and Conclusions
Chapter 7	Suggestions for future work

Figure 1 – Overall structure of Thesis

Chapter 1 – Literature Review

1.1 Human Enamel Ultrastructure

Human enamel is a non-vital densely packed mineralised structure, consisting primarily of calcium (Ca^{2+}) and phosphate (PO_4^{3-}) in the form of calcium hydroxyapatite (CaHAp); chemical formula, $Ca_{10}(PO_4)_6(OH)_2$. The exact composition of enamel differs between people, tooth, and area of tooth. Generally, enamel consists of (by weight) 95% CaHAp, 1% organic enamel matrix, and 4% water (Finke et al., 2001; Ganss et al., 2012; Cui and Ge, 2007; Zavala-alonso et al., 2012; Esfahani et al., 2016).

Enamel ultrastructure is arranged in hexagonal prisms separated by an inter-prismatic area whose mean width is 100nm. Enamel prisms form the basic building block of enamel and consist of millions of hydroxyapatite crystallites arranged tightly in a thin rod or prism formation (Berkovitz et al., 2009; Cui and Ge, 2007) (Figure 2). Prism dimensions vary according to the literature but have been reported between 50-70 nm (width) by 20-25 nm (height) respectively, with length varying between 300-600 nm (Ganss et al., 2012; Finke et al., 2001; Zavala-alonso et al., 2012).

The chemical composition and concentration of the mineral constituents of human enamel varies according to the distance/depth of enamel towards the boundary between the enamel and dentine, known as the dentino-enamel junction (DEJ). The outer or surface layer of enamel contains the highest concentrations of calcium (Ca^{2+}) and phosphate (PO_4^{3+}) ions and lowest concentrations of impurities such as carbonate (HCO_3^-) and magnesium (Mg^{2+}). As the DEJ is reached, the calcium and

fluoride content of enamel decreases whilst carbonate and magnesium content increases (Berkovitz et al., 2009; Cuisinier and Robinson, 2007; Cui and Ge, 2007).

The hierarchical organisation of enamel prisms varies according to their position from the enamel surface towards the DEJ (Kunin et al., 2015). The outer surface of enamel is primarily aprismatic – i.e. lacking a defined prism structure – with least organic constituents between prisms and presents a highly topographically variable surface with features such as perikymata (wave patterns), peaks and troughs, and prism-end markings (Figure 3).

The physicochemical and mechanical properties of enamel are determined by the chemical composition and hierarchical arrangement of the enamel prisms (He and Swain, 2007; Berkovitz et al., 2009; West and Joiner, 2014). The outer surface of enamel is considered the most clinically significant and relevant part of the enamel because this is in direct contact with the oral environment. It is significantly harder, less porous and less soluble compared to subsurface enamel towards the DEJ. Previous studies have demonstrated how the surface enamel layer is much more acid resistant to acid-erosion attack in-vitro (Zheng and Zhou, 2007; Zheng et al., 2010) and in-vivo (Mullan et al., 2017a) when compared with enamel surfaces which have been artificially polished to remove this layer.
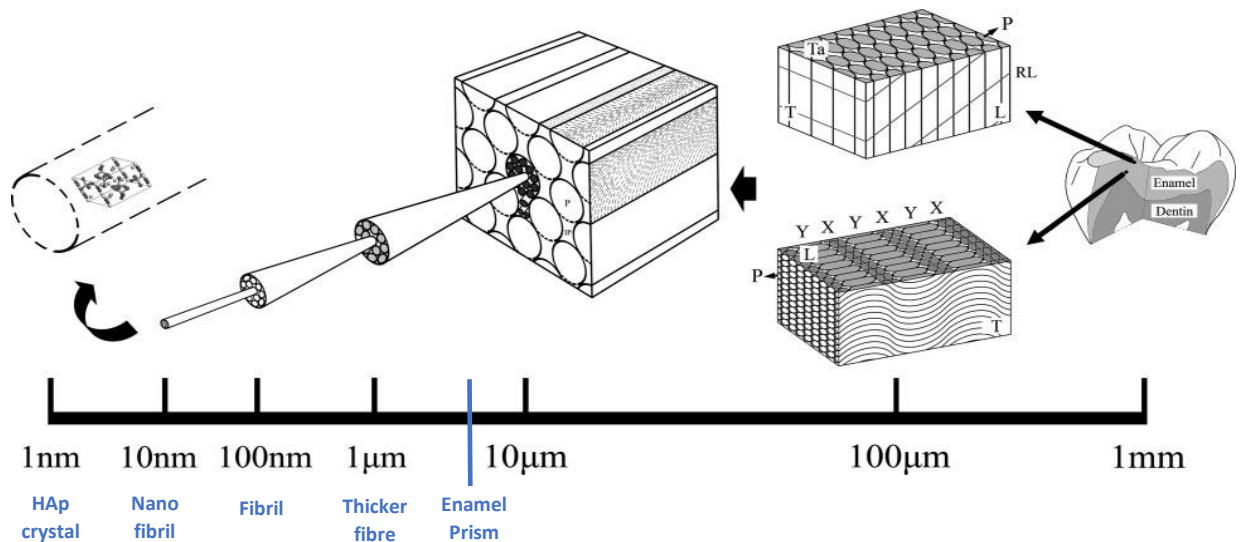
Figure 3 – The hierarchical assembly and typical cross sectional diameters of human enamel demonstrated schematically from crystal to prism: HAp crystals (1nm), mineral nanofibrils (30-40 nm), thicker fibres (80-130 nm), prisms (6-8 µm). Adapted from (Cui and Ge, 2007)
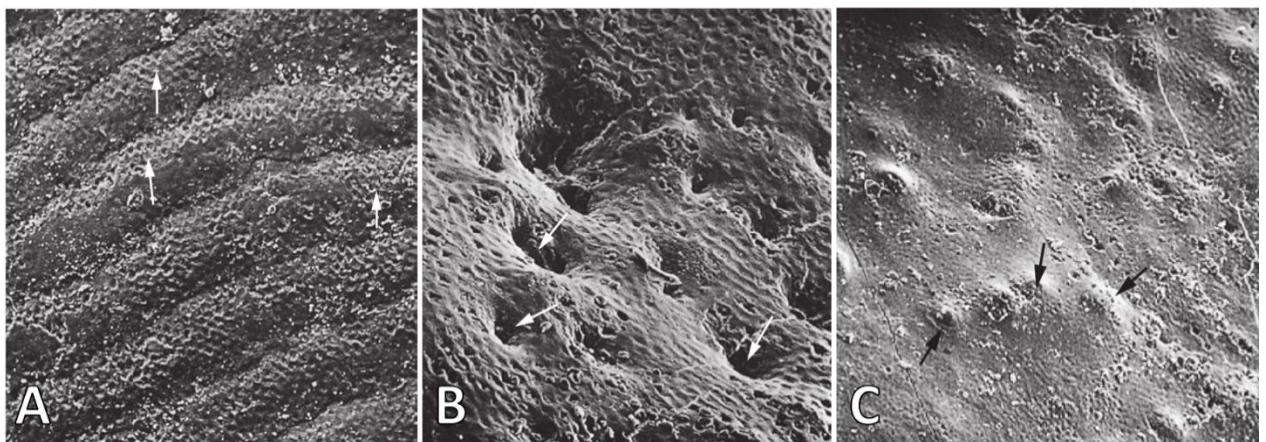
Figure 2 – The outer surface of human enamel using SEM indicating (A) prism-end markings visible on the surface (white arrows), (B) focal holes/depressions (white arrows), and (C) enamel caps (black arrows). Images (A), (B), (C) were taken at x300, x400 and x150 respectively and indicate the topographical complexity of the enamel surface layer. Adapted from (Berkovitz et al., 2009)

1.2 Erosive Tooth Wear in Human Enamel

1.2.1 <u>Definitions</u>

1.2.1.1 Dental Erosion vs Erosive Tooth Wear

Dental erosion is the chemical process of mineral loss from enamel and dentine due to acids of non-bacterial origin whether from extrinsic or intrinsic sources. This process occurs when mineral ion content of the surrounding aqueous environment is undersaturated with respect that of tooth structure it is contact with This mineral loss is called demineralisation and can result in bulk enamel loss if the acid attack is sustained (Eisenburger and Addy, 2002a; Huysmans et al., 2011b; Shellis et al., 2014).

However, the term erosive toothwear describes the irreversible loss of tooth structure due to a multifactorial process which starts from an initial episode of enamel or dentine demineralisation. In this process the tooth structure is eroded, minerals are lost to the erosion solution, and bulk tissue loss occurs due to additional factors such as toothbrushing (foreign body abrasion) or tooth-to-tooth contact (attrition) (Finke et al., 2000; Eisenburger and Addy, 2002b; Huysmans et al., 2011a; Lussi et al., 2011; Bartlett, 2016).

1.2.2 <u>Mechanisms of Erosive Toothwear</u>

1.2.2.1 Chemistry

Erosive demineralisation of enamel is the earliest form of acid attack which occurs within the erosive tooth wear process and is characterised by alteration of the physical and chemical characteristics of the enamel surface. This process can be modified according to the type of acid, contact/immersion period, and saliva quality (Hughes et al., 2000; Eisenburger and Addy, 2002b). The acid softened enamel that

is formed differs in thickness according to the literature, and has been reported between 0.2 μm and 5 μm (Amaechi et al., 1999; Eisenburger et al., 2001, 2004; Wiegand et al., 2007; Cheng et al., 2009; Voronets and Lussi, 2010; Lussi et al., 2011; Arsecularatne and Hoffman, 2014).

This disease process progresses with irreversible loss of enamel depending on whether the erosive, attritive or abrasive factors are maintained or introduced (Lussi et al., 2011; Shellis et al., 2011a). Clinically, teeth are continuously bathed in saliva and there is a continuous exchange of Ca^{2+}, PO_4^{3-} and OH^- ions between the enamel surface and saliva. If the saliva contains a higher concentration of Ca^{2+} and PO_4^{3-} compared to the enamel (i.e it's saturated) there will be mineralisation of the enamel surface. However, the opposite occurs if saliva is undersaturated with respect to enamel, leading to higher rate of mineral loss from the enamel surface (Shellis et al., 2014).

The concept of the 'critical pH of enamel' has been described as the pH of the surrounding solution which will cause enamel demineralisation; for enamel this occurs at pH 5.5 (Shellis et al., 2011a; Lussi et al., 2011). When the surrounding solution pH is below this critical pH, the solution is said to be undersaturated with respect to enamel and can dissolve the enamel due to the net loss of Ca^{2+} and PO_4^{3-} ions from the outer enamel surface into solution (Shellis et al., 2014).

This concept has been reported as critical in the formation of dental caries (tooth decay)(Featherstone, 2008; Berkovitz et al., 2009). Previous authors have also attempted to attribute this to erosion lesion formation; however, others have demonstrated that there is no 'critical pH' below which erosion will occur. Instead,

advocating that enamel erosion is more likely to be affected by: erosive solution temperature, flow rate of erosive solution, degree of calcium and phosphate saturation of erosive solution compared to the enamel surface, and flow characteristics of the erosive solution over the enamel surface (Shellis et al., 2011a; Lussi et al., 2011; West and Joiner, 2014).

1.2.2.2 Histopathology

The clinical process of erosion is influenced by saliva, the composition of the enamel surface and the strength and type of acid attack (Shellis et al., 2014). Laboratory investigations suggest, initial demineralisation of the enamel surface layer occurs after repeated short duration acid attack (Young and Tenuta, 2011). This causes the loss of minerals such as: calcium, phosphate, and fluoride, and may increase enamel surface roughness (Lussi et al., 2011). This results in the formation of a softened enamel layer approximately 0.2-5 µm thick which is susceptible to further loss from physical wear and/or continued exposure to an erosive solution (Figure 4) (Eisenburger and Addy, 2002a, 2002b; Lussi et al., 2011). The softened layer can be remineralised to regain its former mechanical properties (West and Joiner, 2014; Austin et al., 2016). The brittleness of this softened layer was previously demonstrated in a laboratory study which demonstrated that 5s of ultrasonication removed this layer leading to further enamel loss (step height increase/gain) of 2.3 µm (Eisenburger et al., 2001). There still significant difficulty in accurately assessing (both clinically and in vitro) the early effects of acid erosion on the natural human enamel surface.
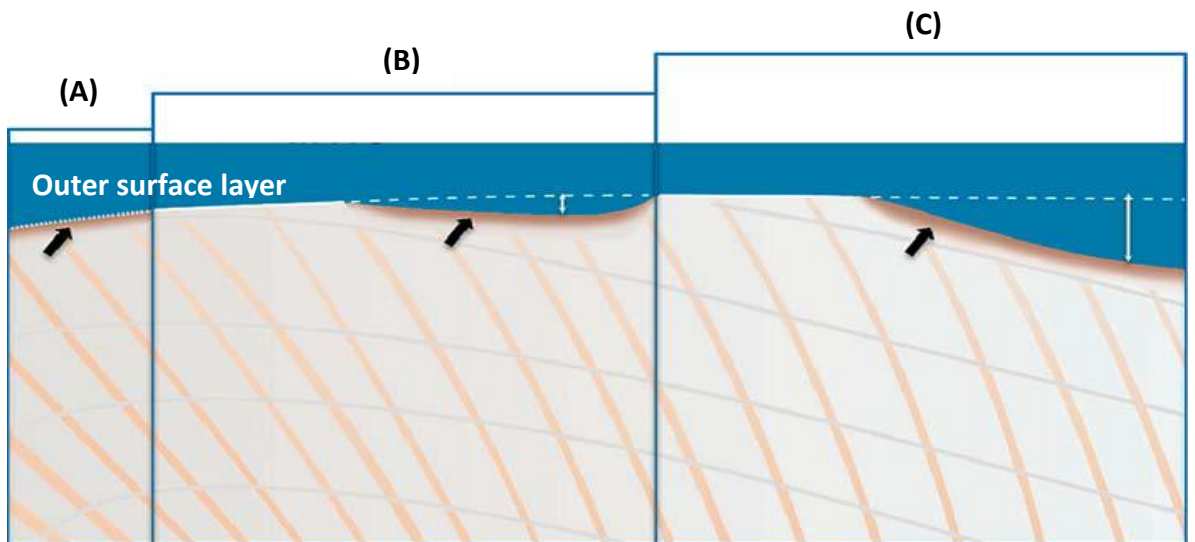
Figure 4 – Progression of the erosion lesion (A) initial surface softening with no bulk enamel loss, (B) partial loss of enamel and softening of the enamel subsurface, (C) significant loss of enamel. Typical thickness of enamel from outer surface layer to DEJ will vary from >1mm from occlusal surface down to <0.5mm at cervical margin. Adapted from (Lussi et al., 2011)

1.3 Factors Affecting Erosive Tooth Wear

1.3.1 Fluoride

1.3.1.1 Fluoride and Erosion

Studies have demonstrated fluoride alters the solubility of enamel to acid attack (Li et al., 2014). Fluoride in solution interacts with the surface layer of enamel and replaces the hydroxide (OH^-) ions in the calcium hydroxyapatite crystals producing fluorapatite (FAp) and stabilising the HAp crystals; FAp is less soluble and more resistant to acid dissolution (Shellis et al., 2014).

In addition, fluoride can be deposited onto the enamel surface via the formation of calcium fluoride (CaF_2) globules; free fluoride ions react and bind to calcium found either naturally in the saliva or artificially introduced through dental products such as toothpaste (Li et al., 2014; Shellis et al., 2014). In laboratory studies, this calcium fluoride-like deposition has been shown to provide two functions: acting as a sacrificial layer on the enamel surface and, as a reservoir for fluoride and calcium ions for remineralisation (Austin et al., 2011; Petzold, 2001).

Many fluoride containing compounds have been used in dental oral care products such as varnishes, toothpastes, or mouthwashes; this literature review will concentrate on the three most commonly used compounds, sodium fluoride, sodium monofluorophosphate, and stannous fluoride (Lussi and Carvalho, 2015; Carvalho et al., 2014).

1.3.1.2   Types of Fluoride

1.3.1.2.1   Sodium Fluoride

Sodium fluoride (NaF) is the most widely used form of fluoride in dental care products and is found at varying concentrations. It can be found in toothpastes, mouthwashes and professionally applied dental varnishes. It is used for the management of both dental caries and dental erosion. It has been advocated as an excellent component in the prevention of dental decay in individuals with limited or poor access to normal fluoride containing oral care products. It has also been advocated in the management of patients with severe tooth wear and has been described as providing erosive-protective and remineralising benefits on acid-affected enamel (Teixeira et al., 2016; Public Health England, 2014).

Toothpastes typically consist of a mixture of silica particles, flavourings, artificial sweeteners, and fluoride of concentrations up to 1000ppm (paediatric toothpaste formulations), 1450ppm (adult toothpaste formulations), 2800 ppm and 5000ppm (professionally prescribed toothpaste formulations); these concentrations have been advocated for preventing and managing dental caries and erosive tooth wear by the Delivering Better Oral Health Toolkit (Public Health England, 2014). The erosive-protective benefits of toothpaste have been shown as early as 1977 with both high (1450ppm and above) and low concentrations (below 1450ppm) formulations providing protective benefits (Teixeira et al., 2016; Davis and Winter, 1977). It is disputed whether there is a dose-response effect for the erosive protective efficacy of NaF containing toothpastes (Magalhaes et al., 2009). Lower concentration formulations have been shown to provide limited erosion-protective benefits versus non-fluoride formulations. Hara et al 2009 demonstrated the erosive-protective

effect of 1,100 ppm NaF toothpaste formulation on erosion (25 mins, grapefruit juice, pH 3.47) in polished bovine enamel, with toothpaste treated samples demonstrating less surface microhardness loss versus non-fluoride toothpaste treated samples. Additionally, 1098 ppm NaF toothpaste has also been demonstrated to provide erosion-protective benefits compared to non-fluoridated toothpastes in polished human enamel subjected to erosion (5 mins, cola); with average enamel wear depths and surface microhardness loss lower in NaF treated vs non-fluoride toothpaste groups (Magalhães et al., 2006). The use of dietary sources of acid provides a clinically relevant model to assess the effect of low-concentration NaF toothpaste in vitro, and thus provides an indicator of the likely clinical impact. High concentration NaF toothpastes have also been demonstrated to provide erosive-protective benefits. Ganss et al 2011 demonstrated better erosion protection from 14500 ppm toothpaste slurries compared with 1100 ppm slurries with less enamel loss following six 2-min erosion cycles (Ganss et al., 2011). However, Lussi et al 2008 demonstrated that fluoride content of different toothpastes containing between 1100 – 1450ppm NaF showed no significant differences in their erosive protective abilities against erosion (3 mins 1% citric acid pH4) in polished human enamel. However, they also concluded that toothpastes applied before erosive challenge provided better erosion protection compared with application after erosion (Lussi et al., 2008). This suggests that the topical application of NaF toothpaste is best before an erosive challenge.

Oral mouthwashes are advocated for use between meals to minimise the effects of erosion, these products primarily consist of water, ethanol, flavourings and surfactants, and contain much lower levels of sodium fluoride compared to toothpastes; concentrations can vary from 225-250 ppm (over-the-counter

formulations) up to 900ppm (prescribed formulations). A dose response in the erosive-protective benefit of oral mouthwashes has been described previously (Magalhaes et al., 2009). Gracia et al 2010 demonstrated better erosive-protective effects of a new 450ppm fluoride (NaF) mouthwash compared to known commercial formulations containing 100 – 225 ppm NaF (Gracia et al., 2010). Similarly, previous studies have demonstrated that using higher fluoride containing mouthrinses (450ppm) resulted in less surface microhardness loss compared with those containing lower concentrations of NaF (Maggio et al., 2010; Venasakulchai et al., 2010). However, Hjortso et al 2009 demonstrated no protective benefit of a 0.42% w/v NaF laboratory grade-solution (4200 ppm, pH 7.3) against short duration acid erosion (2 mins) (Hjortsjö et al., 2009). The protective benefit of NaF containing mouthwashes has been previously attributed to its pH as well as its fluoride concentration with acidified solutions providing more protective benefits compared to neutral solutions (Hjortsjö et al., 2009).

Dental varnishes contain the highest concentrations of NaF available and are a applied by a dental healthcare professional (dentist/hygienist/nurse) onto regions of interest on patients' teeth. These consist of a mixture containing a solvent (e.g ethyl acetate, ethanol), a base (e.g. colophonium, polyurethane), flavourings, and fluoride (NaF) in concentrations of, 1000 ppm (Ivoclar, 2010), 1450 ppm (Ivoclar, 2011), 22,600 ppm (Colgate-Palmolive, 2010) and 45,200 ppm (VOCO-GmbH, 2010). The NaF concentration of the varnish has a direct impact on its erosion protection properties with 22,600 and 45,200 ppm NaF varnish previously demonstrated as providing best protective outcomes against dietary acid erosion compared with 1000 ppm varnish (Sar Sancakli et al., 2015). However, Alexandria et al 2017 demonstrated

the protective benefit of NaF varnish (22,600 ppm) was not as significant compared to a calcium containing fluoride varnish, when treated enamel samples were eroded for six 1-minute erosion cycles (cola soft drink, pH 2.58); with enamel loss comparable to the deionised water negative control (Alexandria et al., 2017). The effect of NaF varnishes has been demonstrated to either provide or not provide protective benefit against enamel erosion, which could be explained by the lack of the acquired salivary pellicle (AEP) which will act as both a reservoir of fluoride and a diffusion-barrier (Magalhaes et al., 2009). Clinical guidelines recommend the use of NaF varnishes in the management and treatment of dental erosion clinically (Public Health England, 2014).

1.3.1.2.2   Sodium Monofluorophosphate

Sodium monofluorophosphate (SMFP) formulations are extensively used for the treatment of dental caries and for their erosive-protective benefits (Shellis et al., 2014; Volpe et al., 1993; Carvalho et al., 2014; Fan et al., 2008). The fluoride ion in SMFP is covalently bonded to the phosphorous ion of the phosphate group and its liberation occurs via hydrolysis of this bond via phosphatase enzymes found naturally in human saliva (Wood et al., 2018; Hornby et al., 2009; Tenuta and Cury, 2013). As a result, the protective benefits of SMFP compared with other fluoride formulations vary according to the study type and method of erosion assessment. In contrast with NaF which dissociates in water to release its fluoride ion readily.

Qasthari et al 2018 demonstrated the erosive-protective benefit of SMFP containing toothpaste (1450ppm F) on polished human enamel samples eroded in vitro using Coca-Cola. Enamel samples were treated with a toothpaste test slurry for 5 minutes,

and then followed by a long-duration acid-exposure (75 minutes). Results indicated a statistically significant increase in surface roughness after SMFP toothpaste application, indicative of a deposition on the enamel surface, and statistically significantly lower surface roughness after erosion when compared to the negative control (no toothpaste) (Qasthari et al., 2018). This suggests surface roughness could be used an indicator of surface change occurring after acid attack and maybe a useful metric when comparing oral healthcare products.

Wood et al 2018 demonstrated the erosion-protective benefit of SMFP toothpaste compared to non-fluoridated toothpaste in an interproximal enamel erosion model. Results indicated the lowest surface microhardness change demonstrated by the SMFP and alkaline phosphatase group; this was significantly less than the SMFP toothpaste group which did not have this enzyme (Hornby et al., 2009). As a result, studies which utilise SMFP as their source of fluoride should ideally utilise a method, where practical, to liberate the fluoride which is covalently bonded to the phosphate group, either by the addition of pure alkaline phosphatase or using a suitable incubation solution containing this enzyme such as whole human saliva. However, this study utilised inter-proximal enamel as their test surface which is not the tooth surface typically in direct contact with acids of dietary or intrinsic origin; therefore, the comparison of their results to other studies which have used the buccal or palatal/lingual enamel surface may be difficult.

Studies which have not utilised phosphatase enzymes or an incubation solution such as whole human saliva which would contain this enzyme, in order to correctly activate/liberate the fluoride present in SMFP, have demonstrated inferior

properties of SMFP compared to NaF and SnF$_2$ (Eversole et al., 2014; Faller et al., 2011).

1.3.1.2.3 Stannous Fluoride

Stannous fluoride (SnF) formulations form a layer/glaze-like coating on the enamel surface; providing erosion-protective benefits in vitro (O'Toole et al., 2016, 2015; Schlueter et al., 2009; Hove et al., 2006) and in situ (West et al., 2017; Li et al., 2014; Shellis et al., 2014; Ganss et al., 2004). This glaze-like layer consists of SnF$_2$ deposits that adsorb onto the enamel surface, and which has been reported as more acid resistant when compared to CaF$_2$ deposits produced with other fluoride types such as NaF and SMFP (Khambe et al., 2014; Ellingsen, 1986; Lussi and Carvalho, 2015).

Stannous fluoride is currently available in commercial toothpaste and mouthwash formulations, and has been investigated for its effects during in vitro and in situ erosion studies (Magalhaes et al., 2009). Its erosion protection ability has been previously linked to the stability of the stannous formulation which exhibits superior erosive protective properties at acidic (pH 3.9) compared with neutral pH (pH7), due to the increased incorporation of stannous and fluoride ions into the calcium hydroxyapatite of the enamel surface layer (Wiegand et al., 2009; Hove et al., 2006).

Interestingly, the studies indicating the superior erosion protective properties of SnF formulations versus other formulations such as NaF or SMFP, have utilised SnF solutions in their optimum working pH which is acidic (pH 3.9) and are not the same for NaF and SMFP formulations. Wiegand et al 2009 for example treated polished bovine enamel with SnF, NaF or an amine fluoride solution at equal pH 3.9 and equimolar with respect to fluoride (5000 or 10,000 ppm). Samples treated with SnF

solution demonstrated the lowest step height formation compared to NaF and AF solutions. Moreover, a previous study compared the erosion-protective efficacy of commercial grade mouthwashes containing SnF and NaF used at their respective pH of 3.8 and 6.0, with equal fluoride concentration 225 ppm. Results indicated step height formation was lowest for all groups pre-treated with stannous fluoride (pure solution and commercial mouthwash) compared to sodium fluoride groups (O'Toole et al., 2015).

Additionally the efficacy of SnF containing toothpastes was also demonstrated as superior to other fluoride types including NaF and SMFP (Magalhaes et al., 2009). Eversole et al 2014 demonstrated SnF containing toothpastes performed better then NaF and SMFP containing toothpastes placed on polished human enamel, all at the same fluoride concentration (1100 ppm), without indicating the pH of the respective toothpaste slurries. The toothpaste slurries were all produced using pooled human saliva and may therefore suggest that another factor other than pH may have contributed to the superior erosion-protective benefits of SnF. However, further analysis of the saliva utilised was not conducted to determine the levels of phosphatase enzyme present (or absent) which aids in the liberation of F from SMFP.

The erosive-protective benefit from stannous fluoride containing formulations is derived not only from the total concentrations of tin and fluoride present, but also from the ratio between stannous and fluoride ions in the formulation tested (Schlueter et al., 2009). Schleuter et al (2009) indicated that stannous:fluoride ratios of 1.8 or higher demonstrated the best erosive-protective benefits, with lowest step

height formation, compared to formulations with ratios 1.4 and less (Schlueter et al., 2009).

1.3.2   Calcium and Phosphate

Oral concentrations of calcium and phosphate ensure there is an equilibrium between calcium/phosphate loss (demineralisation) and gain (mineralisation) from the outer enamel surface. Previous studies demonstrated an inverse relationship between calcium and phosphate concentration in human saliva and incidence of dental caries (Sewon and Makela, 1990; Tanaka and Kadoma, 2000) and erosive tooth wear (Shellis et al., 2014; Carpenter et al., 2014). Many in vitro studies investigated the erosive protective mechanisms of calcium and phosphate; increasing calcium delivery to the tooth surface was found to be twenty times more effective in inhibiting enamel demineralisation than increasing phosphate delivery alone (Tanaka and Kadoma, 2000; Li et al., 2014). The optimum rate of enamel remineralisation, in vitro, can be achieved when the calcium/phosphate ratio of a given oral care product is 1.6 (Li et al., 2014; Exterkate et al., 1993). The main calcium-based products investigated for their erosive protective benefits are: calcium silicate, calcium phosphate and or calcium phosphopeptides (Kaidonis et al., 2018; Li et al., 2014). These will be explored further in this literature review.

1.3.2.1   Calcium silicate

These materials have been widely reported for use in medical and dental procedures including: bone graft substitutes in bone fracture repair (Sanmartin de Almeida et al., 2018), regenerative endodontics (Dutta and Saunders, 2014), regenerative restorative dentistry (Watson et al., 2014) and oral healthcare products such as

toothpaste for their erosion-protection properties (Hornby et al., 2014; Parker et al., 2014; Sun et al., 2014; Joiner et al., 2014).

The mode of action of a calcium silicate/phosphate-based (CaSi/PO$_4$) toothpaste formulation has been previously investigated (Sun et al., 2014). Polished human enamel samples were manually brushed with calcium silicate slurries: CaSi dispersed in phosphate solution CaSi/PO$_4$ mixture, pH7), calcium silicate/water, or a CaSi/PO$_4$ salts (monosodium phosphate and trisodium phosphate) and fluoride toothpaste formulation (SMFP, 1450ppm F). Scanning electron microscope (SEM) analysis indicated enamel surfaces treated with calcium silicate/phosphate and calcium silicate/sodium phosphate and fluoride toothpaste showed significant amounts of particle and mineral deposition which under energy dispersive X-ray spectroscopy (EDX) and transmission electron microscopy (TEM) analysis was revealed as calcium silicate particles and hydroxyapatite crystals; whilst very few particles and minerals were observed for calcium silicate/water only. This demonstrated that a CaSi/PO$_4$ salt and fluoride toothpaste slurry can induced deposition of hydroxyapatite on the enamel surface in vitro (Sun et al., 2014). This later was not investigated further with regards to its thickness or mode of formation on the enamel surface or its physical properties.

Hornby et al 2014 demonstrated the remineralising benefits of a calcium silicate containing toothpaste formulation on citric acid erosion. Polished bovine enamel underwent an erosion – remineralisation cycling protocol, 10-minute erosion (1%, pH3.6 citric acid), 1-minute toothpaste slurry treatment and 2 hours in neutral buffer, 2 minute or 30 second demineralisation and final 1-minute toothpaste slurry

treatment and 18 hours neutral buffer. Samples were treated with toothpaste containing $CaSi/PO_4$ and SMFP (1450ppm F) and evaluated for surface microhardness (mean Vickers SMH) after acid challenge, 3-day remineralisation, and 7-day remineralisation. Results demonstrated improved and higher surface microhardness values for all samples treated with $CaSi/PO_4$ and SMFP formulation, compared with SMFP alone, and non-fluoridated control toothpaste slurries after 3 and 7 days remineralisation (Hornby et al., 2014).

Similarly, the protective and reparative efficacy of calcium silicate against dental enamel erosion was investigated (Parker et al., 2014). The deposition of calcium silicate particles onto sound and pre-eroded polished bovine enamel was demonstrated. There was an initial rapid release of calcium from the $CaSi/PO_4$ mixture within the first minute of application reaching a maximum release after 10 minutes. Atomic force microscopy (AFM) and SEM analysis revealed deposition of calcium silicate particles and formation of hydroxyapatite crystals on the enamel surfaces treated with calcium silicate/phosphate. These depositions provided sufficient erosive protective benefits when subsequently exposed to citric acid demineralisation with a 39% reduction in calcium loss from the enamel surface versus non-treated enamel samples (Parker et al., 2014).

Wood et al 2018 demonstrated the superior erosion-protective benefits of calcium silicate/sodium phosphate containing toothpaste formulation on an interproximal enamel erosion model when compared to fluoride only and non-fluoride control toothpaste formulations (Wood et al., 2018). The highest values for surface microhardness were obtained in the $CaSi/PO_4$ and SMFP toothpaste treatment group

indicating these samples exhibited the least surface softening following acidic demineralisation with citric acid (Wood et al., 2018).

1.3.2.2 Calcium phosphate

Calcium phosphates are a group of biologically active synthetic materials most frequently used in the form of hydroxyapatite, $Ca_{10}(PO_4)_5(OH)_2$, or as tri-calcium phosphate ($Ca_3(PO_4)_2$) due to their osteoconductive (helping to serve as a scaffold for new bone growth), and biocompatible properties (LeGeros, 1991; Albrektsson and Johansson, 2001; Al-Sanabani et al., 2014). These materials have been in use since the 1920s in medicine as bone substitutes or for bone grafting procedures (Al-Sanabani et al., 2014). The first dental application of a calcium phosphate material was reported in 1975 whereby tri-calcium phosphate was demonstrated to regenerate and repair surgically induced periodontal bone defects in dogs (Nery et al., 1975). The use of calcium phosphate materials in dental erosion prevention was described according to mechanism of action and use (Reynolds, 2009; LeGeros, 1991; Al-Sanabani et al., 2014). The effectiveness of calcium phosphates in dental erosion prevention has been demonstrated in vitro and in vivo, and the effectiveness of these materials is attributed to the methodology utilised in order to allow precipitation of carbonate-hydroxyapatite on to the enamel surface (Kensche et al., 2016; Al-Sanabani et al., 2014). The addition of calcium phosphate as hydroxyapatite nanoclusters into toothpaste and mouthwash formulations has been previously investigated for their erosive protective in vitro (Kensche et al., 2016). These have been demonstrated to produce an erosion protective benefit in the presence of an AEP already present on the surfaces of polished human enamel, suggesting a biological interaction between the material and the AEP. Interestingly, the pH of the

respective test solutions/toothpaste slurries affected the release of calcium and phosphate; the more acidic the slurry the more calcium and phosphate release that occurred (Kensche et al., 2016).

Hornby et al 2009 investigated the erosive protective benefit of a toothpaste formulation containing hydroxyapatite particles and fluoride (1450ppm SMFP) against citric acid (pH 3.5 50mM) cyclic demineralisation in vitro study. Polished bovine enamel samples underwent 6 cycles of treatment with the HAp/SMFP toothpaste slurry for 3 minutes, and acid erosion for 5 minutes, before being placed in human saliva for 1 hour. Surface microhardness was measured at before and after the cycling regime with change in surface microhardness measured, and results indicated that the HAP/SMFP toothpaste significantly reduced effects of enamel demineralisation due to in vitro pH cycling, with the lowest values of surface microhardness change (Hornby et al., 2009).

Poggio et al 2010 demonstrated the erosive remineralising efficacy of toothpaste utilising hydroxyapatite nano-crystals against soft drink (Coca-Cola) induced demineralisation of polished human enamel (4x 2-minute cycles). Samples were treated (4x 3-minute treatment cycles) and subsequently eroded, and surface effects characterised using AFM; surface roughness (R_{rms}) and lesion depth were determined. Surface roughness and lesion depth were both lower after treatment with hydroxyapatite toothpaste compared with the negative control and similar to a fluoride (NaF) toothpaste positive control. This indicated that the hydroxyapatite nano-crystals provided remineralising effects on enamel following acid erosion (Poggio et al., 2010).

The clinical use of calcium and phosphate ions for remineralisation of dental erosion and dental caries lesions has been limited due to the low solubility of calcium phosphate especially in the presence of fluoride ions (Reynolds, 2009). Calcium phosphates are generally insoluble and difficult to apply onto the tooth surfaces as an acidic pH is required to solubilise calcium phosphate to produce ions which can interact with the enamel surface (Reynolds, 2009). Due to their insoluble properties, soluble calcium and phosphate ions can only be used at very low concentrations, and may not provide sufficient concentration gradients to promote surface remineralisation (Reynolds, 2009).

To overcome this deficit, casein phosphopeptide-amorphous calcium phosphate (CPP-ACP) was developed to produce a stabilised high concentration formulation of calcium and phosphate ions that can bind to the enamel pellicle and the enamel surface. Casein phosphopeptide (CPP) contains the active sequence -Ser(P)-Ser(P)-Ser(P)-Glu-Glu- which binds to calcium and phosphate ions forming amorphous calcium phosphate (ACP) nanocomplexes, thereby stabilising calcium and phosphate (Reynolds, 2009).

The use of CPP-ACP in preventing enamel erosion was previously investigated by Poggio et al (2014) who utilised polished human incisor enamel and surface roughness as the measurement outcome before and after erosion. Samples either underwent pre-treatment then erosion, or erosion first then treatment. Samples were eroded in Coca-cola for 2 minutes, which was repeated at 4 time periods (0,8,24,36hrs) for total cumulative erosion time of 8 minutes; treatment agents were applied for 3 minutes at 4 time periods (0,8,24,36 hours) for total treatment time of

12 minutes. They demonstrated using atomic force microscopy, that surface roughness of those samples treated with CPP-ACP were statistically significantly lower compared to the control (untreated group). Additionally, CPP-ACP particle formation occurred on the surface of the enamel blocks, indicating the formation of a protective layer on the surface; this was evidenced by higher surface roughness values versus the control group (Poggio et al., 2014). Interestingly, Wang et al 2011 conducted an in vitro study to determine the erosive protective effects of different calcium phosphate containing products; calcium sodium phosphosilicate (NovaMin) and CPP-ACP with and without fluoride (900ppm F as NaF). This study utilised polished human enamel samples, which underwent 4 days of pH cycling consisting of: salivary pellicle formation (2hrs), toothpaste slurry application (3 mins), erosion (orange juice, 3 mins), human saliva incubation (4 hours), toothpaste slurry application (3 mins), erosion (orange juice, 3 mins). Their results indicated that none of the toothpastes tested demonstrated erosive protective benefits versus control (no treatment), and concluded that neither calcium phosphate containing products had erosive-protective properties (Wang et al., 2011a). This study design did not provide any periods of immersion in a remineralising solution such as artificial saliva (Sun et al., 2014) or whole human saliva (Hornby et al., 2009), to allow for the effects of both calcium phosphate containing products to take effect.

1.3.2.3   Other protein-based products

Chitosan is a natural polymer derived from the deacetylation of chitin which is found in the shells of crustaceans (Lussi and Carvalho, 2015). It has been previously demonstrated to adsorb and form a layer on the surface of enamel which provides erosive-protective benefits against subsequent erosive attack (Ganss et al., 2011).

The reason for this is because chitosan has a strong positive zeta potential (measure of the electrostatic difference between solids and liquids) and is therefore able to adsorb and form a layer on the surface of enamel which has a strong negative zeta potential. Chitosan containing toothpaste has been previously evaluated against conventional NaF containing toothpaste, and has been demonstrated to reduce enamel loss by 30% in polished human samples subjected to a total erosion period of 12 minutes (citric acid, pH 2.4) (Ganss et al., 2011). Interestingly, the chitosan formulation did not contain any fluoride and still produced an erosive effect. Chitosan can readily bind to the AEP present on enamel (van der Mei et al., 2007) and is able to form an organic multilayer in the presence of mucins (Svensson et al., 2006).

1.3.3   Saliva and The Acquired Enamel Pellicle

In vitro dental erosion studies investigating the effects of saliva on early and late acid exposure have utilised either natural human saliva or laboratory-made artificial saliva. There is no agreement in the literature regarding the correct or perfect in vitro saliva model to simulate the clinical environment (Hornby et al., 2009; Wang et al., 2011a).

1.3.3.1   Natural Human Saliva

Natural human saliva is a complex mixture of biological fluids produced from the major and minor salivary glands, and gingival crevicular fluid, comprising 99.5% water, a variety of electrolytes, organic and inorganic components and nitrogenous compounds (Carpenter, 2013; Humphrey and Williamson, 2001; Buzalaf et al., 2012). The constituent components provide saliva with a number of key important roles and functions which include (Humphrey and Williamson, 2001; Marsh and Martin, 2009; Carpenter, 2013):

(1) saliva pH modulation and buffering capacity is provided by the bicarbonates, phosphates, and urea;

(2) saliva lubricating, cleaning and aggregation capacity is provided by mucins and statherin;

(3) antibacterial/microbial action of saliva is provided by immunoglobulins and enzymes; and

(4) modulation of demineralisation and remineralisation is provided by calcium, phosphate, and statherin

The type of saliva used in dental erosion studies varies from whole mouth saliva, obtained from volunteers expressing saliva into a container and used without further modification, centrifuged saliva, which is whole mouth saliva centrifuged to remove any debris with the remaining supernatant used, or saliva collected from specific salivary glands (Humphrey and Williamson, 2001; Carpenter, 2013). Saliva collection can either be stimulated (chewing a neutral paraffin wax) or unstimulated; these saliva types have different characteristics. Stimulated saliva has a higher pH, a greater capacity for buffering pH and is more lubricating compared with unstimulated saliva. Stimulated whole mouth saliva is most commonly utilised as this is clinically representative of the salivary conditions present during normal chewing function and is in direct contact with teeth before/during/after an erosive challenge (Shellis et al., 2011a; Carpenter, 2013; Schlueter et al., 2011).

To overcome the complexity and diversity of human saliva, previous guidance from Shellis et al 2011, suggested the collection of whole human saliva from multiple healthy participants pooled into one saliva sample (Shellis et al., 2011a). The use of pooled whole human saliva is very common in dental erosion literature to overcome the issues of saliva quality and content variability.

1.3.3.2 Artificial Saliva

Artificial saliva has been extensively used in dental erosion research to account for the variability in whole human saliva as discussed previously. The ingredients, content, and quality of artificial saliva can be controlled in a laboratory environment and its effects on dental erosion can be individually accounted for if so required (Eisenburger et al., 2001; Shellis et al., 2011a). There is no consensus in the literature

on the formulation for artificial saliva and there are broadly four main formulations utilised according to the following studies: (1) Klimek et al 1982, (2) Amaechi et al 1998b, (3) Eisenburger et al 2001, and (4) De Mello Vieira et al 2005, whose constituents can be seen in Table 1 (Klimek et al., 1982; Amaechi et al., 1998b; Eisenburger et al., 2001; De Mello Vieira et al., 2005). The first use of artificial saliva containing organic components (pork mucin) was reported by Klimek et al (1982) who conducted a study using artificial saliva to grow an artificial acquired enamel pellicle (AEP) on polished bovine enamel to determine fluoride uptake into both the pellicle and enamel surface (Klimek et al., 1982). Very few studies have been conducted which have evaluated the protective effect of artificial saliva on subsequent enamel erosion, whilst more research has focused on the remineralising effects of artificial saliva on previously eroded enamel.

The erosive protective effect of artificial saliva has been investigated through the addition of mucins derived from gastric porcine or bovine origin, or through the use of carboxymethyl cellulose (Batista et al., 2016). Mucins in artificial saliva have been previously demonstrated to form an artificial AEP on polished human and bovine enamel samples, and have been reported to change the rheological properties of artificial saliva to almost match those of natural saliva (Jordão et al., 2017; Vissink et al., 1985). However, the impact of the added mucins on the erosive-protective properties of artificial saliva is unclear, some studies report a protective benefit whilst others do not.

Wang et al 2011 produced an artificial AEP on polished human enamel in vitro utilising artificial saliva containing porcine mucins after 7-days of incubation and

demonstrated no protective benefit against 1-mins citric acid erosion (pH 2.23). However, interestingly after 4-days storage in artificial saliva after erosion, samples demonstrated remineralisation with the effect of remineralisation more pronounced after 24 hours storage (Wang et al., 2011b). Similarly, Ionta et al 2014 utilising the same artificial saliva formulation to produce an artificial AEP demonstrated a remineralising effect on polished bovine enamel samples eroded for 15s erosion with citric acid (pH 2.5, 0.05M), rather than a protective benefit against subsequent erosion. This therefore suggests that artificial saliva mucins may not provide a protective benefit as the artificial AEP is incomparable to the natural saliva AEP but may instead provide the minerals required for remineralisation of eroded enamel.

However, Jordao et al 2016 demonstrated that an in vitro formed 2-hrs artificial AEP, produced by immersing polished bovine enamel in artificial saliva containing porcine mucins, produced comparable erosive-protective benefits compared to an in-situ formed natural saliva AEP. No statistically significant differences in surface microhardness after 4-min citric acid (1.0%, pH 3.6) were determined between samples with artificial and natural AEP. Interestingly, the same artificial saliva formulation without the mucins conferred no protective benefit with the same post-erosion surface microhardness change as samples pre-treated with deionised water (Jordão et al., 2017).

The use of carboxymethyl cellulose (CMC) to modify artificial saliva has been demonstrated to reduce its remineralising effect on previously eroded enamel samples (Ionta et al., 2014). The mechanism by which this occurs was previously studied and was attributed to the formation of complexes between CMC and the

calcium and phosphate ions present within artificial saliva solution, thereby reducing

their availability to initiate remineralisation of previously demineralised enamel

(Amaechi and Higham, 2001; Vissink et al., 1985; Gelhard et al., 1983). There have

been no reported studies indicating polished enamel pre-treatment with CMC-

containing artificial saliva in vitro results in a protective effect against subsequent

erosion.

Compound	Artificial Saliva Formulations			
	According to Klimek et al 1982	According to Vieira et al 2005	According to Amaechi et al 1998	According to Eisenburger et al 2001
$C_6H_8O_6$	2 mg/l	-	-	-
$C_6H_{12}O_6$	30 mg/l	-	-	-
NaCl	580 mg/l	-	-	-
$CaCl_2$	170 mg/l	-	-	-
KCl	1,270 mg/l	11,182.50 mg/l	624.73 mg/l	2,236.50 mg/l
NaSCN	160 mg/l	-		
KH_2PO_4	330 mg/l	-	326.620 mg/l	544.360 mg/l
CH_4N_2O	200 mg/l	-	-	-
Na_2HPO_4	340 mg/l	-	-	-
Mucin	2,700 mg/l	-	-	-
$Ca(NO_3)_2 \cdot 4H_2O$	–	60.12 mg/l	-	-
NaF	–	0.066 mg/l	-	-
$NaH_2PO_4 \cdot 2H_2O$	–	160.19 mg/l	-	-
$C_4H_{11}NO_3$ Tris buffer	–	12,114.00 mg/l	-	-
K_2HPO_4	–	-	804.712 mg/l	-
$CaCl_2 \cdot 2H_2O$	–	-	166.130 mg/l	77.960 mg/l
$C_8H_8O_3$	–	-	2,000 mg/l	-
CMC-Na	–	-	10,000 mg/l	-
$MgCl_2 \cdot 6H_2O$	–	-	58.96 mg/l	-
$MgCl_2$	–	-	-	19.04 mg/l
$C_8H_{18}N_2O_4S$ HEPES	–	-	-	4,766.20 mg/l
Deionized water	1,000 ml	1,000 ml	1,000 ml	1,000 ml
pH	6.4	7.0	6.75	7.0
Hydroxyapatite	6.51	6.69	11.26	9.50
Octacalcium phosphate	1.57	1.20	2.46	1.89
Dicalcium phosphate dehydrate	1.15	0.54	1.66	1.06

Table 1 – Artificial saliva formulations commonly utilised in dental erosion research.

Adapted from   (Klimek et al., 1982; Amaechi et al., 1998b; Eisenburger et al., 2001; De

Mello Vieira et al., 2005; Batista et al., 2016).

1.3.3.3   Effect of the Acquired Enamel Pellicle

The formation of the AEP is one of the most important functions of human saliva in its ability to protect and remineralise teeth against acid erosion; this is formed in two phases. The first phase occurs within seconds of the surface layer of enamel being exposed to saliva with an initial 10-20nm thick protein-rich pellicle formation occurring and consisting of selectively adsorbed precursor proteins such as statherin and acidic proline-rich proteins. In the second phase the pellicle thickness increases to between 100-1000nm consisting of globular protein aggregates (Vukosavljevic et al., 2014; Hannig and Joiner, 2006; Lindh et al., 2014). The AEP is a semi-permeable membrane regulating and modifying the demineralisation/remineralisation process at the tooth surface (Hannig and Hannig, 2012). The protective ability of the AEP is determined by: its composition, thickness, and time-to-formation, but will also be influenced by the nature of the erosive challenge such as acid exposure, type of acid, and acid concentration (Hove et al., 2006).

Nieu Amerongen et al 1987 demonstrated that mucins present in natural saliva contribute to the development of the AEP on polished human enamel surfaces which in turn confers erosive-protective ability against citric acid (1-mins, 1.0% citric acid) erosion (Nieuw Amerongen et al., 1987). This study utilised dialysed samples of human saliva to produce concentrated amounts of mucins to produce their AEP, which explains the total protective benefit of the AEP created using concentrated mucins. The AEP formed using natural human saliva (un-dialysed) can reduce the effects of acidic demineralisation but cannot completely inhibit the acid-related changes that may occur to the enamel surface (Hannig and Hannig, 2012).

In an in vitro early erosion model, Nekrashevych and Stosser 2003 demonstrated the variable protective effect of a 24-hrs formed AEP. This pellicle, formed on polished bovine enamel, protected samples against 0.1% and 1.0% citric acid after 1- and 5-minutes erosion; with higher microhardness levels after erosion for AEP treated samples versus non-AEP samples. However, after 10- and 30-mins erosion, there were significant differences between AEP and non-AEP treated samples, with higher microhardness values seen in AEP treated enamel after erosion (Nekrashevych and Stosser, 2003). This indicated that the 24-hrs AEP has a protective effect against short duration citric acid erosion which is lost after longer duration acid-attack of stronger citric acid concentration. Similar results were also obtained from Wetton et al 2006, demonstrating a time-dependant relationship between in vitro AEP formation time and subsequent erosion protection properties (Wetton et al., 2006).

However, the in situ formed AEP has been demonstrated to provide superior erosion-protective benefit compared with the in vitro AEP. Hannig et al 2004 demonstrated that samples with a 3-min AEP, formed in situ, demonstrated less calcium loss and higher surface microhardness values compared with non-AEP treated enamel; the protective effect did not increase with time of AEP formation (Hannig et al., 2004a). This would suggest the initial surface adsorption of salivary protein could provide some level of protection equivalent to an AEP formed over several hours. Additionally the AEP formed in situ over 30 mins, 1 and 2 hrs, and for 2, 6, and 12 hrs respectively did not differ in their ability to protect against enamel demineralisation (Hannig et al., 2004a, 2005). However, when compared to the in vitro AEP, it has been shown that a short duration (2 mins) AEP produced no significant erosion-protective benefit versus 60, 120, and 240 mins AEP, when eroded using citric acid (0.3%, pH

3.2) (Wetton et al., 2006). Similarly, Hall et al 1999 demonstrated that the protective effect of human saliva is significantly reduced when used to incubate polished enamel samples in vitro, compared with when volunteers are asked to wear an intraoral appliance housing similar samples to form an in vivo AEP. However, the differences between the AEP formed on the polished and natural human enamel surface have yet to be studied; it is unknown whether is a difference in the formation, thickness, or protective nature of the AEP depending on which surface its formed on.

Interestingly, Mutahar et al 2017 demonstrated that an in vitro formed 24-hrs AEP altered the acid erosion process from one of dissolution into a softening process. After five 10-mins erosion cycles using citric acid (0.3%, pH 3.2), AEP (natural human saliva) coated samples demonstrated the lowest step height formation but highest surface microhardness change, compared to those immersed in water only.

Whilst a number of studies have been previously conducted studying the impact of the AEP, formed over different human saliva immersion periods, on dental erosion in vitro, most have been conducted on polished enamel (human or bovine), and very few on natural unpolished human enamel.

1.4 Laboratory Methodologies Investigating Erosive Tooth Wear

1.4.1 Enamel Type and Preparation

The specimen/substrate/surface used erosion in the laboratory depends on the type of study and erosive mechanism being evaluated. Polished enamel samples have been used for the majority of in vitro and in situ studies to evaluate the effect of different erosive solutions on enamel, whilst natural enamel surfaces have been primarily studied for their behaviour compared to polished enamel (Young and Tenuta, 2011; Zheng et al., 2009, 2010).

1.4.1.1 Human

1.4.1.1.1 Polished Human Enamel

Polished enamel samples have been most commonly used to study short- and long-term acid exposure on enamel, and other factors that influence the dental erosion process. This is due to the ease and standardisation of sample production, simplicity in barrier utilisation/isolation with an acid-resistant barrier, and ease in characterising surface changes after erosion (Young and Tenuta, 2011; Shellis et al., 2011)

The polishing process, however, removes the outer surface layer of enamel which has been demonstrated to be more resistant to acid dissolution compared to enamel towards the DEJ (Zheng et al., 2010). Polished enamel samples are therefore more susceptible to erosion compared with natural enamel samples; natural samples are favoured for their relevance to the clinical scenario but are much more technique sensitive to utilise in vitro (Young and Tenuta, 2011; Ganss et al., 2000).

The increased susceptibility of polished human enamel has been previously demonstrated using both long and short acid-erosion durations, and both in vitro and in situ study models. Whilst long duration acid erosion methods are not clinically representative, their use helps demonstrate the erosion behaviour differences between natural and polished enamel. Ganss et al 2000 eroded polished and natural enamel for 3 hours and demonstrated statistically significantly higher mean(SD) enamel loss for polished 115(44.6) μm compared to natural 70.3(16.2) μm enamel samples (Ganss et al., 2000). Their method utilised human enamel samples created from the same extracted teeth to ensure parity in comparison during experimentation. Likewise, this method has been previously utilised by Lin et al 2016 demonstrating similar results using a short duration citric acid erosion model, comparing polished and natural enamel samples prepared from the same human teeth. After three and six 1-min erosion cycles (1% citric acid, pH 3.6), greater calcium loss, surface loss, and microhardness loss was shown from polished enamel versus natural enamel (Lin et al., 2016). This indicated that, regardless of the erosion time, polished enamel exhibited more demineralisation and tissue loss compared with natural enamel. Similarly, the use of surface roughness changes between polished and natural human enamel has been demonstrated as evidence of different erosion behaviour between the two sample types. Mullan et al 2018 demonstrated in an in situ study, mean(SD) surface roughness values of natural enamel did not significantly differ after 45 minutes erosion (orange juice) compared to before erosion (0.20(0.08) vs 0.24(0.09) μm), whilst mean (SD) surface roughness increased significantly for polished enamel (0.04(0.01) vs 0.13(0.04) μm) (Mullan et al., 2018a). Natural enamel samples were therefore more resistant to citric acid erosion evidenced by the longer

duration acid-exposure required to produce a statistically significant detectable change in surface roughness, and alterations in surface morphology; confirming results obtained by Meurman and Frank 1991 (Meurman and Frank, 1991; Mullan et al., 2018a).

Further research using natural human enamel would provide further insights into the dental erosion process occurring on enamel surfaces as they are present clinically.

1.4.1.1.2 Natural (unpolished) Human Enamel

Natural human enamel samples have seldom been utilised in dental erosion studies due to the inherent complexities of enamel surface topography and composition which vary between individuals; hence the popularity of polished enamel samples. However, artificially flattened/polished enamel are not considered clinically representative. Utilising natural enamel in dental erosion studies in vitro provides a more clinically representative model (Young and Tenuta, 2011; Shellis et al., 2011a). The difference in erosive behaviour between natural and polished human enamel has been discussed previously and is due to the presence of the outer enamel surface layer which is known to be more resistance to acid erosion (Berkovitz et al., 2009; Zheng et al., 2010).

The difference in acid resistance of human enamel varies according to enamel depth was previously studied using enamel samples produced at difference depths relative to the DEJ (Zheng et al., 2010). After 3-mins citric acid erosion, the erosive behaviour of enamel at the outer, intermediate, and inner region (defined according to their proximity to the DEJ) could be demonstrated; acid resistance decreased in enamel according to the distance from the DEJ (Zheng et al., 2010). This method utilised

changes in nano-scratch behaviour and erosion depth to determine differences between the different enamel sample types.

However, other investigators have utilised changes in surface roughness to demonstrate the differences in erosive behaviour between natural and polished enamel. Mullan et al 2018 showed that after 45 minutes total citric acid erosion, the surface roughness (amplitude parameter, Sa) of natural human enamel exhibited no significant differences versus before erosion (0.3% citric acid, pH 3.2), compared with polished human enamel which increased significantly after erosion (Mullan et al., 2018a). However, in an in vitro study, differences in surface roughness and hence erosive behaviour were noted between natural and polished human enamel. Polished human enamel became rougher (higher Sa values) after 45 minutes erosion (orange juice pH 3.2), whilst natural human enamel became smoother (lower Sa values) when each were compared to their respective baseline Sa values; however, their post erosion Sa values were not significantly different (Mullan et al., 2018b). Therefore, indicating that natural enamel, tends to become smoother due to the destruction of the highly complex topographical features contributing to its high baseline Sa value, whilst polished enamel which is almost featureless (at baseline) due to the polishing process becomes exceedingly rough with sufficient erosion. This difference in erosive behaviour between the two sample types in vitro versus in situ can be explained by the presence of human saliva affecting the erosion process, as well as the differences in their respective surface topographies and chemical composition.

Optical changes before and after erosion using optical coherence tomography have been utilised to determine the differences in erosive behaviour of polished and natural enamel. Natural enamel has been demonstrated to require longer erosion times (10 mins or greater) before changes in specular reflection could be detectable (Chew et al., 2014), whilst in polished enamel this could be detected after short erosion times (1 min or greater) using changes in pixel intensity slope values (Aden et al., 2017). Two different analytical methods for OCT data were utilised, however, no study has been conducted so far to analyse both polished and natural enamel using the same analytical method.

The utilisation of natural human enamel samples will therefore provide for a more clinically representative substrate on which to test the effects of both short- and long-term acid exposure, as well as any factors which can impact on the dental erosion process. However, overcoming the issues of lesion creation and characterisation are necessary to allow for natural enamel to be used as a viable test substrate in vitro.

1.4.1.2 Non-Human

Enamel of non-human origin (bovine or ovine) have been extensively utilised in dental erosion studies due to their ease of collection and availability comapred with human enamel; the collection of suitable human teeth can be expensive, time-consuming and more difficult. These human enamel substitutes have been evaluated for their ability to mimic the erosion-behaviour characteristics of human enamel; however, there are conflicting reports as to their suitability as replacements of human enamel. Care must therefore be taken when extrapolating the findings

collected from these tissue types to the human clinical situation (Shellis et al., 2011a; Field et al., 2017; Laurence-Young et al., 2011).

Bovine enamel is the most commonly utilised human enamel substitute; however, its erosive characteristics have previously been described as either similar (Shellis et al., 2011a; Barbour and Rees, 2004) or different (Meurman and Frank, 1991; Field et al., 2017; White et al., 2010; Amaechi et al., 1999) to human enamel.

Amaechi et al 1999 demonstrated a significantly lower mineral loss and erosion lesion depth for human enamel compared with bovine enamel, concluding bovine enamel to be more susceptible to longer erosion periods due to the differences in its structure compared to human enamel (Amaechi et al., 1999). However, Field et al 2013 showed how human enamel exhibited greater maximum height change within the eroded lesion (0.70(0.20) μm) versus bovine enamel 0.41(0.20) μm. This effect may be due to the increased number of isolated profile peaks at baseline for human enamel versus bovine enamel, therefore suggesting human enamel is more susceptible to erosion.

White et al 2010 demonstrated the earliest erosion time required to produce a statistically significant decrease in surface nanohardness was 2s (human enamel) and 5s (bovine enamel), and for enamel tissue loss this was 20 mins (human enamel) and 10 mins (bovine enamel) (White et al., 2010). It was concluded for early erosion times polished bovine and human enamel displayed similar erosion characteristics, whilst at late erosion times the differences in the structure between both tissue types are apparent with bovine enamel demonstrating more rapid erosion progression

compared with human enamel; this was due to the larger crystallites and greater porosity of bovine enamel (White et al., 2010).

Field et al 2017 concluded that neither bovine nor ovine enamel could be used interchangeably with human enamel for the study of early erosion in vitro; recommending that human enamel be utilised where possible (Field et al., 2017). Similarly, baseline properties differ between polished enamel samples produced from human, bovine, and ovine teeth. Previously it has been demonstrated that bovine enamel possesses the smoothest (Ra=0.13 µm) and hardest (VHN=532) material characteristics compared to ovine and human enamel; ovine enamel is the roughest (Ra=0.19) and softest (VHN=293). This has been demonstrated to affect their respective erosive behaviours.

Overall, there are differences in the physicochemical and structural properties between human, bovine, and ovine enamel that affect their erosive behaviour. Erosion studies seeking to study the early and late erosive process and associated factors which impact on dental erosion are best to be conducted on human enamel samples, where feasible, to allow for better comparison to the clinical situation.

1.4.2 Acid Models (type of acid)

The erosive challenge utilised in studying dental erosion in vitro should be reflective of the clinical scenario being modelled, and these can either be extrinsic (dietary) acids or intrinsic (gastric) acids.

1.4.2.1 Extrinsic (Dietary)

Many clinical, laboratory, and epidemiological studies have previously linked excessive consumption of acidic drinks to erosive toothwear, these include: sports drinks, fruit juices, carbonated soft drinks, and alcoholic beverages (Young and Tenuta, 2011; Shellis et al., 2011a). In the UK, there has been an increase in consumption of fruit juices which has been linked to increasing erosive tooth wear in the adult population (Bartlett et al., 2013; Young and Tenuta, 2011; Huysmans et al., 2011a). The sources of common extrinsic acids found in dietary foodstuffs include: citric acid from citrus fruits, malic acid from apples and plums, tartaric acid from grapes and wine, phosphoric acid in carbonated soft drinks, and lactic acid in fermented foods (Shellis et al., 2012; Young and Tenuta, 2011).

Citric acid is the most commonly used erosive solution to model the effects of dietary acids on early and late erosion in vitro. This is the most frequent acid found in fruit juices and is most often present in concentration of 0.3% and pH 3.2 (West et al., 2000; Featherstone and Lussi, 2006; Young and Tenuta, 2011; Shellis et al., 2013).

Studies which have investigated the effect of early and late dietary erosion on enamel samples have primarily utilised pure citric acid solution, either neat or titrated to a certain pH with sodium hydroxide.

The erosive potential of citric acid was previously compared to hydrochloric acid and phosphoric acid on polished human enamel, over a range of different pH (West et al., 2001). Enamel loss was the highest for citric acid (0.3%) compared to phosphoric acid (0.1%) and HCL over pH range 2.15 – 6.0, suggesting that the chelating effect of citric acid (occurring at pH range 3.9-6.0) has an impact on potentiating enamel erosion at pH levels commonly present in orange juice. The erosive potential of citric acid was potentiated with further addition of trisodium citrate, a commonly added buffering agent to citric acid drinks to improve taste, resulting in higher enamel loss (West et al., 2001).

However, contrary findings regarding the chelating effect of citric acid and its erosive potential on polished bovine enamel were demonstrated by Asadi-Schossig et al 2016. This study utilised citric acid (0.3%) titrated to pH 7.00 which was pumped over the samples in a superfusion chamber consisting of a peristaltic pump which flowed the erosive solution over the samples at a flow rate of 2.47mm/s for 15 minutes. Results indicated the erosion rate of citric acid at pH 7.00 was negligible when compared with the amount of enamel loss using citric acid in its natural pH 2.17 (Azadi-Schossig et al., 2016). Similarly, Hughes et al 2000 also compared the erosive potential of citric, malic and lactic acids at a range of pH levels and concentrations and concluded that for the pH and concentrations found in common acidic beverages, lactic acid was the most erosive, and citric and malic acid were comparable in their erosive ability. Additionally 0.3% citric acid was deemed clinically representative, in vitro, of what is commonly found in dietary products (Hughes et al., 2000).

Citric acid at 0.3% concentration has been further utilised and investigated for its effects on the microscale and macroscale change occurring to the surface of polished enamel samples in early in vitro studies. The earliest known effect of 0.3% citric acid on polished human enamel was demonstrated to occur after 30s erosion, this was characterised with changes in surface roughness (Sa), using confocal laser scanning microscopy, and surface microhardness (KHN) (Austin et al., 2016). However, the earliest time period after which surface form change could be detected using citric acid was described by Lin et al 2016, after three 1-minute erosion cycles. This study utilised a higher concentration citric acid (1%, pH 3.6) and determined enamel loss in polished human enamel at 0.571 μm and 0.431 μm for natural enamel (Lin et al., 2016)

Overall, the use of 0.3% citric acid at a suitable pH such as 3.2 has been shown as a valid erosive solution for use in modelling dietary extrinsic acid erosion for early and late erosion.

1.4.2.2 Intrinsic (Gastric)

Gastro-oesophageal reflux disorder (GORD) affects approximately 60% of the UK population and involves the movement of gastric juice into the oesophagus (Bartlett et al., 1996; Moazzez et al., 2004). GORD has been associated with erosive toothwear and its effects are clinically manifested on palatal surfaces of the maxillary dentition (Bartlett et al., 1996; Gregory-Head et al., 2000). For modelling the effects of intrinsic acid exposure on enamel and thus the effects of GORD in vitro, the use of hydrochloric acid solution of an appropriate concentration and pH is necessary (Shellis et al., 2011a; Young and Tenuta, 2011).

The erosive nature of HCL against enamel is dependent on its pH; at its natural pH (1.0-2.0), as would be found in GORD patients, HCL is more erosive than other acidic carbonated beverages, whilst at higher pH (>3) it is less erosive in comparison to other acids at the same pH (Bartlett et al., 1996; West et al., 2001; Hannig et al., 2005). Therefore, to compare the early and late erosive effects of acids in vitro, it is important to ensure the acids are utilised at the pH that they would be encountered in the clinical scenario being modelled/investigated (Shellis et al., 2011a; Young and Tenuta, 2011).

The effects of the severity of GORD on polished enamel was previously studied in vitro. Mann et al 2014 utilised HCL at pH 1.5 (simulating severe GORD) and pH 3.0 (simulating moderate GORD) and a cyclic demineralisation model to determine the longitudinal effects of three stages of erosion, stage 1 (30s), stage 2 (30s) and stage 3 (60s). Samples eroded with pH 1.5 and 3.0 HCL exhibited statistically significantly higher surface roughness (Sa) after 30s erosion indicating the characterisation of early erosion in a GORD in vitro model is possible (Mann et al., 2014). Similar findings in the characterisation of early erosion in a GORD model using HCL were also demonstrated by Derceli et al 2016. In this model, polished bovine enamel samples were subjected to one of five single duration erosion times: baseline (0s), 10s, 20, 30s, or 40s, and then analysed using atomic force microscopy (AFM) before and after erosion. They demonstrated that surface roughness increase was characterisable after 10s using AFM and the Ra and Rms (root mean square) 2D parameters (Derceli et al., 2016).

1.4.3 Sample preparation and cleaning before use

For the creation of polished enamel samples, a standardised polishing procedure should be utilised to ensure a suitable flatness tolerance is achieved (Young and Tenuta, 2011).

The process of polishing, also known as lapping, removes the surface enamel layer which is the most acid-resistant layer. Polishing enamel samples flat requires the use of polishing discs of different abrasiveness utilised with a polishing machine and consists of two steps: grinding using course grit discs followed by polishing with finer grit discs. The process of grinding will remove most of the enamel surface producing a relatively flat sample and polishing with successively finer grit discs will remove the polishing marks from the grinding process and refine the sample flatness. The utilisation of diamond suspended paste particles has also been reported to achieve a similar polishing process instead of using finer polishing discs (Field et al., 2017). The reporting of the final flatness tolerances achieved from the polishing process is important to ensure sample preparation has been consistent. Flatness tolerances have been reported from $\pm$0.6 µm (Mistry et al., 2015), $\pm$0.4 µm (Austin et al., 2016; Mullan et al., 2018a, 2018b), and $\pm$0.3 µm (West et al., 2000; Eisenburger and Addy, 2003; Shellis et al., 2005).

There is no reported standardised method for polishing enamel nor a specified flatness tolerance to produce flat polished enamel samples.

The polishing process produces a smear layer measured at 0.27 µm thick on samples finished to 2000 grit (12 µm grain size) polishing disc, and 0.5 µm thick if finished with alumina oxide suspension (0.05 µm grain size) (Watari, 2005). This smear layer has

been shown to be acid-soluble (Sanches et al., 2009). Miten et al 2015 demonstrated polished human enamel samples with smear layer intact demonstrated greater enamel loss (step height) and surface microhardness loss compared to samples that were ultrasonicated after polishing to remove the smear layer (Mistry et al., 2015). Sample cleaning to remove this smear layer after polishing has been advised to ensure cleanliness and consistency of the enamel surface prior to, and minimise its effects on, subsequent acid erosion (Young and Tenuta, 2011). Ultrasonication for 15 minutes in distilled water can successfully remove the smear layer created and is advocated when preparing polished enamel samples for subsequent erosion (Austin et al., 2016; O'Toole et al., 2016; Mistry et al., 2015; Mullan et al., 2017a, 2018b).

Regardless of the biological origin of the enamel to be utilised in the creation of enamel samples for use in vitro, or in vivo, these samples must undergo a cleaning and preparation regime to ensure they are sterile for use or conform to the local ethical guidelines/standards (Shellis et al., 2011a). The most commonly utilised cleaning/sterilising methods have utilised either: chemical only, mechanical only, or chemo-mechanical methods.

Chemical cleaning methods described previously include use of sodium hypochlorite (NaOCl) (Lippert et al., 2004a, 2004b), thymol solution/crystals (Shellis et al., 2011a), sodium p-toluenesulphonylchloramide (Chloramine-T) (Field et al., 2014, 2017), and none have been demonstrated to significantly affect the enamel surface nor its physicochemical properties. High strength NaOCl (14%) has been demonstrated to have no significant impact on the surface physical properties nor erosive behaviour of enamel samples (Lippert et al., 2004a). Mechanical methods described include the

use of dental pumice to clean the collected teeth prior to polishing (Amaechi et al., 1999), a dental scaler instrument to remove any organic/inorganic surface contaminants (Klimek et al., 1982), whilst West et al 2000 described a chemo-mechanical method utilising 50% NaOCl solution, manual scraping of any remaining debris, washing in distilled water, and sonication in 70% ethyl alcohol before a final rinse using distilled water (West et al., 2000).

Natural enamel presents a complex surface to clean, isolate, erode, and measure accurately. Moreover, natural enamel samples produced using teeth donated by patients undergoing routine dental treatment or collected from animals from an abattoir, will be contaminated with different organic and inorganic contaminants.

Mechanical cleaning regimes previously described, consist of soft toothbrush and non-fluoridated toothpaste together with ethanol wipe, however the durations and cleaning pressure were not mentioned (Mullan et al., 2018a, 2017a). Another cleaning technique described the use of ultrasonication in deionised water followed by alcohol cleaning, again for unspecified time periods, was utilised for cleaning the natural samples (Mullan et al., 2018b). It is difficult to determine whether any organic and inorganic surface contaminants were still present on these samples at baseline, which could potentially impact on the erosive process; though this has not been previously determined. Chemical and mechanical cleaning methods for natural enamel would ensure a thoroughly cleaned surface for subsequent erosion (Young and Tenuta, 2011). Ganss et al 2000 described a similar cleaning method using dental pumice and the removal of residual soft tissue but did not describe how this was removed; however, samples were inspected for any defects of surface damaging

using stereomicroscopy (Ganss et al., 2000). The utilisation of physical abrasive substances may potentially lead to scratching and physical alteration of the outer enamel surface layer, and the use of non-abrasive methods would be indicated (Young and Tenuta, 2011).

1.4.4 <u>Barriers and Reference Region Creation</u>

A reference region of uneroded enamel is the commonly utilised surface for comparison to the eroded region for the purposes of erosion characterisation (Young and Tenuta, 2011). Sample analysis is simplified and experimental analytical time reduced, as the same samples can be utilised for comparing the effects of acid erosion, depending on the erosion model utilised (Shellis et al., 2011a; Young and Tenuta, 2011).

Many different barrier techniques have been previously described for use on polished enamel samples to allow creation of a localised erosion lesion using either early or later erosion time periods. Strips of adhesive tape are the most commonly utilised/reported barrier due to its simplicity of use, ease of removal and minimal to no risk of damaging the eroded surface on removal (West et al., 2000, 2001; Eisenburger and Addy, 2003; Shellis et al., 2005; Barbour et al., 2006; White et al., 2010; Paepegaey et al., 2013a; Mistry et al., 2015; Austin et al., 2016; O'Toole et al., 2016). Whilst the majority of studies have not described the exact material-type of adhesive tape utilised is either coloured or clear polyvinyl chloride tape (Mistry et al., 2015; Austin et al., 2016; O'Toole et al., 2016; Mullan et al., 2017a).

The use of nail varnish has been previously reported in dental erosion studies (Amaechi et al., 1998a, 1999; Ganss et al., 2005; Zheng et al., 2010), but they are used

mainly in dental caries studies whereby acid-demineralisation models can last weeks or even months on the same samples (Zhang et al., 2018a, 2018b). Using nail varnish as the protective barrier requires removal either through the careful use of a sharp instrument such as a scalpel or using an acetone wash to dissolve the nail varnish and rinsing with distilled water to remove the acetone (Amaechi et al., 1998b, 1999; Ganss et al., 2005; Zheng et al., 2010). This method is more technique sensitive and there is a risk of damaging the erosive lesion when compared to using adhesive tape.

Holme et al 2005 describes the use of dental amalgam restorative material as the reference region against which the enamel surface would be compared after erosion. The authors calculated difference in height between the unaffected amalgam, and etched enamel (Holme et al., 2005). Given that the samples were polished flat for use, the use of a much simpler barrier method, such as adhesive PVC tape would have been ideal, and would have forgone the requirement to modify the enamel surface through drilling and filling using dental amalgam.

A number of studies describe use of the embedding material itself for reference compared to the enamel sample after erosion. The use of self-setting plastic (Zheng et al., 2009) and acrylic resin (Ganss et al., 2000; Field et al., 2017) has been previously described. These methods are particularly useful as there is no requirement modifying the enamel experimental surface with any adhesive tape or nail varnish which will require removal afterwards.

Few studies have described a suitable barrier technique for use in creating reference regions on natural human enamel in dental erosion studies in vitro. Ganss et al 2000 describes the use of acrylic resin to cover certain regions of polished and natural

enamel samples that have been fixed to glass microscope slides. After samples were eroded, the acrylic resin was then described being carefully removed with a scalpel to reveal a clearly visible erosion lesion compared to the surrounding eroded region (Ganss et al., 2000). The study did not clarify how the acrylic was removed without risking damaging the erosion lesion, nor did they explain how the acrylic resin was applied without contaminating the exposed enamel experimental surface.

Barrier use in polished enamel samples are relatively straightforward, and the use of adhesive PVC tape is the simplest, most effective and easily retrievable method of choice. However, there is a paucity of evidence regarding their use in natural human enamel sample creation. Therefore, further study would be required to determine their suitability of use.

1.4.5 Erosion Regimes

In vitro models designed to mimic the erosive conditions during normal and excessive acid consumption, provide valuable insights into the acid-erosion process and performance of oral care products under erosive conditions (Young and Tenuta, 2011; Shellis et al., 2011a; West et al., 2017). Variables and factors that may impact the erosion process can be controlled or tested to understand the erosive process, as well as test oral care products.

Erosion regimes simulating the clinical scenario are advantageous; extensive erosion times should therefore be avoided. Additionally a balance between the erosion time utilised and the ability to measure subsequent change accurately is required to allow characterisation of the effects of the short duration acid exposure (Young and Tenuta, 2011; Shellis et al., 2011a).

In general, in vitro erosion models consist of single-exposure only or pH cycling methods. Both study types are considered valid as long as they are relevant to the clinical scenario being modelled (Young and Tenuta, 2011).

1.4.5.1 Early Erosion Models

There is no consensus on the acid exposure time that would constitute early or late erosion; erosion time must reflect the clinical scenario modelled in vitro. Erosion studies can broadly be categorised according to the length of individual acid exposures and the number of acid exposure cycles. Five minutes is generally regarded as representative of slow beverage consumption and an early erosion time period (Young and Tenuta, 2011; Hornby et al., 2014). However, early erosion periods previously reported, range from 10 – 120 minutes (Mathews et al., 2012; O'Toole et

al., 2015; Mistry et al., 2015), whilst shorter erosion periods described as early or very early range from several seconds up to 4 minutes of erosion (Lippert et al., 2004b, 2004a; Hjortsjö et al., 2009, 2010; Zheng et al., 2009, 2010; Mann et al., 2014; Derceli et al., 2016; Baumann et al., 2016).

Field et al 2017 demonstrated enamel loss could be detected after one 30s erosion using 1% citric acid (weakest erosion group) in polished human, bovine, and ovine enamel (Field et al., 2017). Austin et al 2016 demonstrated the effect of 30s citric acid (0.3%, pH 3.2) on polished enamel, resulting in statistically significant decrease in surface microhardness (KHN), and increase in surface roughness (Sa) versus baseline (Austin et al., 2016). As a result, when studying the effects of acid erosion, erosion times as quick as 30s are necessary to be evaluated. However, Derceli et al 2016 demonstrated statistically significant increase in surface roughness (Ra) after just 10s erosion using HCL in a GORD model (Derceli et al., 2016). Early erosion studies must therefore take into consideration very quick erosion periods. It has been previously demonstrated that increasing the concentration of citric acid increases the mineral loss that occurs in human and bovine enamel; 0.3% is considered the standard dietary citric acid concentration (West et al., 2001; Hughes et al., 2000).

Previous studies have also utilised the early erosion in vitro model to study the effects of the AEP on short duration acid-erosion.

Nekrashevych and Stösser et al 2003 studied the level of protection provided by the AEP against citric acid erosion by comparing the erosion lesions formed in polished bovine samples with and without AEP. This study demonstrated short duration exposure to citric acid (1 and 5-mins) even at 0.1% concentration resulted in early

erosive change, indicating the aggressiveness of citric acid against polished enamel even in the presence of AEP (Nekrashevych and Stösser, 2003). Nekrashevyich et al 2004 demonstrated the protective effect of AEP against 1-min erosion for both 0.1% and 1.0% citric acid; however, no protective effect was observed after 10 and 30 mins erosion (Nekrashevych et al., 2004). This early erosion model therefore was able to determine the early erosive effects of citric acid and how it was modified by the AEP.

The early erosion model is characterised either by the utilisation of acid durations of 5 minutes or less either as single erosion or multiple-erosion cycle exposures and should be designed to characterise micro and macroscale changes occurring to the enamel surface after short duration acid attack. Conducting in vitro studies at early erosion times ensures they are clinically relevant and thus allows a better understanding of the erosion process occurring clinically.

1.4.5.2 Late Erosion Models

Late erosion models consist of erosion times greater than 5 minutes, whether used as single exposure or multiple exposure. They have been used to study factors that impact on long term dental erosion which include oral care products, the AEP, and how erosion occurs on the natural enamel surface.

Mullan et al 2017 investigated orange juice (pH 3.2) erosion on both polished and natural human enamel. Samples were eroded for three cycles of 15-mins erosion and scanned with NCLP before and after erosion. Results indicated after 45-mins cumulative erosion the surface roughness of the natural and polished enamel samples were similar after erosion, despite at baseline the surface roughness of the natural enamel being statistically higher than the very smooth polished samples

(Mullan et al., 2017a). Surface textural change following erosion for natural and polished enamel are different i.e. natural enamel becomes smoother, and polished enamel becomes rougher, but both surfaces after a long enough erosion time have similar Sa values. This in agreement with Mullan et al 2017, surface roughness of polished enamel increased significantly, whilst natural enamel surface roughness decreased after 45-mins cumulative erosion (Mullan et al., 2017a).

Mutahar et al 2017 also utilised a late erosion dietary acid model to determine the impact of the AEP on polished human enamel erosion. Results indicated surface microhardness change and surface roughness values were highest for samples with AEP whilst the step height formed was the lowest for this group. The authors concluded that an in vitro AEP using natural whole human pooled saliva altered the erosion process from dissolution to a surface softening phenomenon (Mutahar et al., 2017). The long erosion cycling periods allowed for the longitudinal impact of the AEP in vitro; however, it would be interesting to determine whether this phenomenon is also evident for short duration acid erosion periods.

Very few studies have been conducted to determine enamel loss in the natural human enamel surface after quick erosion time periods due to difficulties in lesion creation and measurement technique sensitivity. Ganss et al 2000 described an interesting method to determine surface loss in natural human enamel utilising a very long duration (3-hrs) citric acid demineralisation in vitro model. Natural and polished human enamel samples were prepared from the same human molar teeth, and fixed on glass microscope slides, and partly covered with acrylic resin as a protective barrier. Mean(SD) erosion depths of 115(44.6) μm and 70.3(16.2) μm for

natural and polished enamel were obtained respectively (Ganss et al., 2000). Whilst the method utilised a long erosion period, it provided a valuable insight into how to potentially measure enamel loss on the natural surface; further work however is required to determine the accuracy of methodology utilised to determine mineral loss on such a complex surface for short more clinically relevant erosion times.

1.4.6 <u>In-Vitro Surface Characterisation Techniques</u>

The process of dental erosion results in alteration of the mechanical and physical properties of enamel, which are dependent on several factors discussed extensively previously. Methods utilised to study dental erosion in enamel have been dependant on the stage of the erosive lesion under investigation, the type of change anticipated in the erosive lesion, and the measurement output of interest (Barbour and Rees, 2004; Field et al., 2010; Shellis et al., 2011a; Young and Tenuta, 2011; Schlueter et al., 2011; Joshi et al., 2016).

In this section we will discuss the potential applications, advantages and limitations of existing techniques, in relation to the in vitro characterisation of the dental erosion lesions created on both polished and natural enamel surfaces utilising single or multiple short duration acid-exposure times.

1.4.6.1 Surface Hardness

Surface hardness testing techniques have been extensively utilised to investigate the hardness of the enamel surface before and after erosion or by comparing the eroded enamel to a region of protected/reference uneroded enamel. This technique works on the principle of measuring the resistance of the test surface to the penetration of an indenter of specified dimensions, at a specified loading force and indenter dwell

time (Field et al., 2010; Schlueter et al., 2011). There are three techniques commonly utilised to study surface hardness of eroded enamel: Knoop microhardness, Vickers microhardness, and nanoindentation (Barbour and Rees, 2004; Schlueter et al., 2011). Enamel hardness measurements are considered a robust method for determining surface enamel hardness properties as they are not susceptible to time-dependent change in morphology due to the low elasticity and little retraction of enamel (Schlueter et al., 2011).

1.4.6.1.1 Surface Microhardness

Both Knoop and Vickers surface microhardness (SM) techniques utilise a diamond indenter of known geometry to produce an indent analysed for its dimensions to produce either a Knoop hardness number (KHN) or Vickers hardness number (VHN).

Knoop microhardness utilises a pyramidal with a rhomboidal base diamond indenter which can penetrate the enamel surface approximately 1.5 µm whilst the tetra-pyramidal Vickers indenter would penetrate 5 µm when the usual loading forces of 50 – 200g are utilised (Featherstone, 1992). There is no consensus on the loading force nor indent dwell time utilised for either microhardness techniques when studying the erosive lesion, but loading can be performed using 1g up to 1000g force with any loading time. There is no consensus regarding which indenter is suitable for studying effects of early erosion, however, Knoop microhardness has been previously recommended due to its shallow penetration depth (Schlueter et al., 2011; Shellis et al., 2011a).

The effect of early citric acid erosion could be discriminated using Knoop microhardness with a statistically significant decrease after 30s compared to baseline

(baseline KHN) 363 (11) versus 319.0 (20), p<0.05) (Austin et al., 2016). However, Knoop microhardness was not possible on the natural enamel surface owing to the complexity of surface topography making Knoop indentation evaluation impossible. Similarly, it has been previously recommended that surface microhardness evaluation be limited to polished enamel surfaces owing to the ease and accuracy of indentation assessment before/after erosion (Shellis et al., 2011a; Schlueter et al., 2011).

Due to the greater depth/length ratio, Vickers indenters will indent and penetrate softened enamel more deeply compared to Knoop indenters, and thus the underlying sound enamel may influence indentation depth (Schlueter et al., 2011). However, Vickers microhardness has also been previously utilised to determine the impact of early erosion on enamel. Changes in VHN has been demonstrated to show the differences in surface microhardness characteristics of human, bovine and ovine enamel before and after erosion (Field et al., 2017). Vickers microhardness distinguished the effects of early erosion on bovine enamel eroded with different citric acid concentrations and erosion times and allowed for the determination of the erosive-protective effect of the AEP (Nekrashevych and Stösser, 2003).

1.4.6.1.2 Surface Nanohardness

Nanoindentation hardness utilises a similar principle to microhardness indentation but on a reduced scale. This technique utilises a trigonal pyramidal Berkovich diamond indenter which is maximally 1 µm in length, and with loading forces between 0.25 – 50 mN (0.025 – 5.1gf) together with AFM. This technique applies a steadily increasing load on the sample and loading is relaxed until partial or complete

relaxation of the sample occurs; this allows for the calculation of the sample's Young's modulus, nanohardness, time-dependent creep, plastic and elastic energy, and fracture toughness (Schlueter et al., 2011).

The earliest time at which nanohardness has been demonstrated as significantly different from baseline was after 2s of acid exposure for human enamel and after 5s of acid exposure for bovine enamel (White et al., 2010).

Zheng et al 2010 studied the erosive behaviour of human enamel polished to different depths from the surface layer down to the dentino-enamel junction (DEJ). Polished human enamel samples were eroded with citric acid (0.001M, pH 3.20) for 3 mins and evaluated for their nanohardness. Their results indicated compared to the uneroded reference surface, enamel nanohardness close to the outer surface decreased by 38% whilst nanohardness close to the DEJ decreased by 44%. Nanohardness demonstrated sensitivity to the changes in physical properties of enamel according to the depth from which the enamel sample was created, with nanohardness decreasing closer to the DEJ. (Zheng et al., 2010).

1.4.6.2 Optical Coherence Tomography

OCT is a high resolution, low coherence interferometric technique utilising a near-infrared laser (1305 nm) generating surface and subsurface images of enamel by measuring the intensity and time delay of backscattered light from the different layers of enamel (Attin and Wegehaupt, 2014; Huysmans et al., 2011a). This technique is analogous to ultrasound imaging used in medical diagnostics; however, light is used instead of sound.

Morphological cross-sectional images (B-scans) can be obtained utilising the differences in backscattered light (OCT signal) from the demineralised enamel surface. The decrease in OCT backscatter signal return, due to the altered optical properties of eroded enamel, has been utilised to characterise erosive change (Chan et al., 2013; Attin and Wegehaupt, 2014). Its use in determining early erosive change has been limited due to difficulty in data analysis owing to the intense specular reflections from the enamel surface (air-enamel interface) which can mask the light scatter information within the initial few micrometers below the enamel surface (Attin and Wegehaupt, 2014; Chew et al., 2014).

Austin et al 2017 demonstrated OCT backscatter analysis utilising the previously discarded OCT signal from the enamel surface. Firstly, the difference was calculated between OCT signal entering the tooth and OCT signal scattered in the enamel surface, this difference was then normalised according to the OCT signal entering the tooth; a value of 1 indicated 100% back-scattered OCT signal intensity indicative of no erosion (Austin et al., 2017). This method demonstrated after 60-mins erosion with orange juice, erosive change could be calculated within the first 33 μm of enamel previously discarded in other studies (Chew et al., 2014).

The exact nature of the optical changes occurring after erosion in polished and natural human enamel and their effect on OCT analysis is not fully understood and would therefore require further analysis and study.

Two other analytical methods of OCT data have been utilised to determine whether the effects of early erosion can be detected and characterised; surface projection/reflection image analysis and pixel intensity analysis.

OCT data can be processed to plot the individual pixel intensities in (x,y) and their corresponding axial direction (z), to produce a projected image for any given timepoint during scan acquisition; this is known as a surface projection or surface reflection intensity image (Aden et al., 2017).

Surface projection images were utilised together with pixel intensity analysis to determine the effects of early acid erosion (1% citric acid pH 3.8) on polished bovine enamel for cumulative erosion time-points 1, 2, 5, 10, 30, and 120 minutes. Results indicated pixel-intensity correlation decreased after 1-min erosion and for each subsequent time-point and was statistically significantly positively correlated with surface microhardness (VHN value); indicating as pixel-intensity correlation decreased which would be indicative of an erosive change, VHN value decreased also (Aden et al., 2017).

The exact method by which OCT measurements are affected by the morphological changes in enamel are still uncertain, however, this analysis method is promising and requires further investigation especially on the natural enamel samples, as it can be directly utilised in the clinical environment. An example of OCT and its associated outputs can be seen in Figure 5.
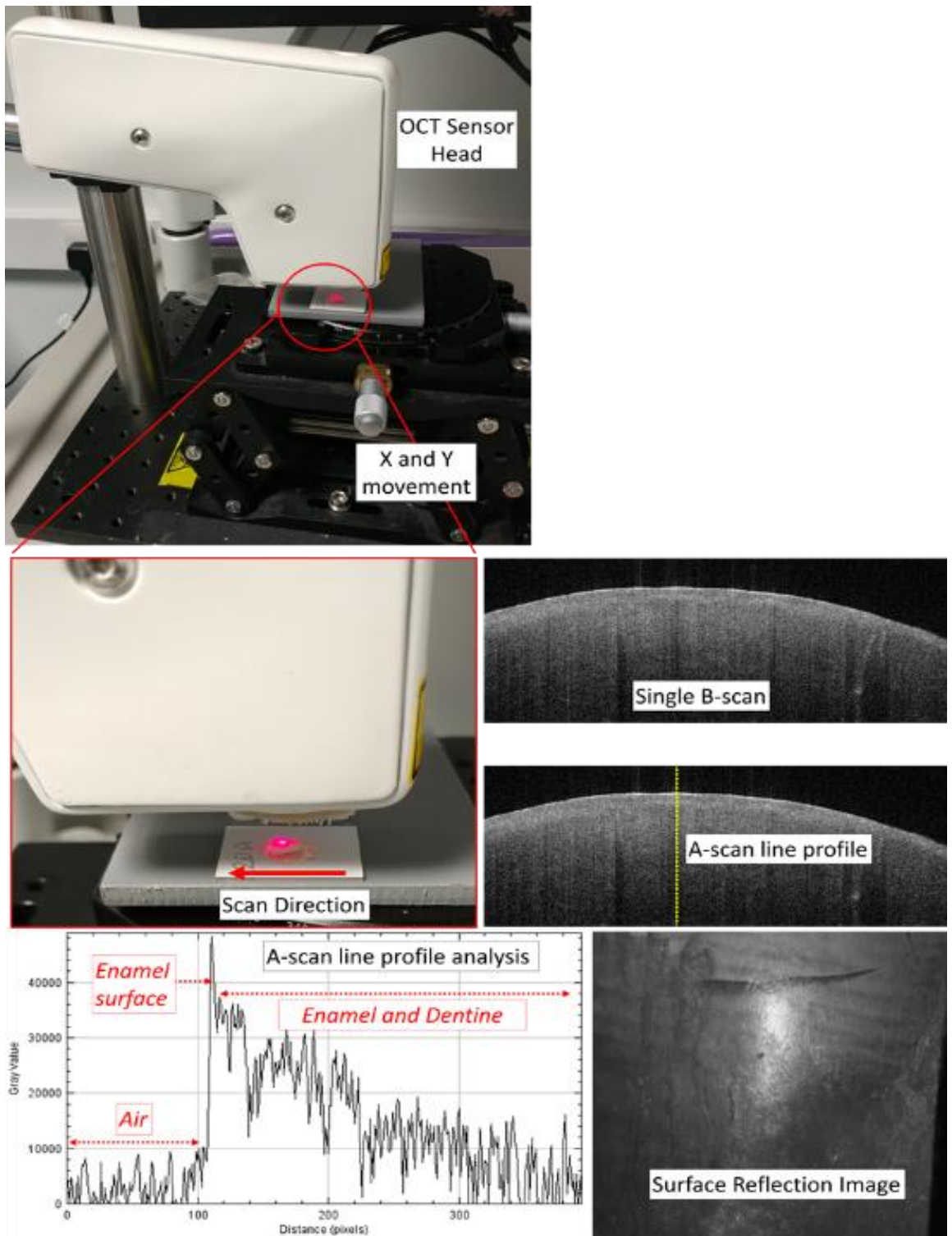
Figure 5 – Example of an OCT machine. The sensor moves in a raster pattern scanning the sample and producing multiple tomographic slices (B-scans). Single B-scans can be analysed for peak intensity profile analysis (A-scans). Multiple B-scans can be used to form a B-stack volume which can then be used to form a surface reflection image.

1.4.6.3 Tandem Scanning Confocal Microscopy

First described for use in Dentistry by Watson and Boyde, 1985, the term confocal refers to the use of an aperture in the focal plane of an objective lens both in the illumination and imaging pathways of the microscope. Only light which is within the focal plane of the lens can pass through the aperture, any stray light is blocked; producing high resolution confocal microscopic images. A scanning disk (Nipkow) allows for lateral scanning of a sample to produce highly detailed images. The enamel surface or subsurface can be imaged, and optical section thickness can be adjusted according to the Z-axis movement of the objective lens. Typically TSM can penetrate 100 μm into enamel and dentine or can be utilised to capture detailed surface reflection images using green or blue light (Watson, 1990, 1997; Watson and Boyde, 1985). Several studies have utilised TSM in surface characterisation of dental erosion lesions in vitro and in situ (Mullan et al., 2017a, 2018a, 2018b). TSM is particularly useful for the qualitative analysis of natural human enamel samples and has been previously demonstrated to aid in the characterisation of the surface morphology features which are affected by long duration citric-acid mediated erosion(Mullan et al., 2017a, 2018a, 2018b), but has yet to be demonstrated for short duration erosion in polished or natural human enamel.

This is a powerful and cost-effective imaging technique with rapid acquisition time, and does not require any surface alterations or other sample preparations to obtain images; this technique can be used for the longitudinal assessment of the same enamel samples in vitro.

1.4.6.4 Focus Variation Three-Dimensional Microscopy

Focus variation 3D microscopy (FVM) is a non-contact optical microscope image acquisition technique utilising the principle of focus variation whereby an object is kept stationary under an objective lens, and the lens is moved in the z-axis (utilising a piezo-control mechanism) towards or away from the sample. Multiple images are captured as the lens z-axis position is altered in relation to the sample and a 3D z-stack comprising multiple images is produced which can then be analysed for changes in surface form and texture using specialised software (Fujii et al., 2011; Joshi et al., 2016; Gyurkovics et al., 2017).

This technique has been utilised to quantify surface roughness change in early and late acid erosion models using common beverages (Fujii et al., 2011), fruit juices (Mita et al., 2013), and has also been used to quantify surface form change (enamel loss) in both polished and natural bovine enamel (Ren et al., 2009; Lin et al., 2016).

1.4.6.5 Quantitative Light Fluorescence Microscopy

Teeth have been previously demonstrated to exhibit auto-fluorescence when irradiated with blue-green light (often around 470nm) and fluoresce with a wavelength of 540nm; this is caused by the chromophores present in the organic component of dentine and particularly the DEJ (Pretty et al., 2004; Field et al., 2010; Joshi et al., 2016). The amount of fluorescence of a tooth is related to the mineral density of the enamel, with demineralised regions appearing darker as the amount of fluorescence radiance is lost due to mineral loss of the overlying enamel (Chew et al., 2014). QLF has been utilised to study natural human enamel carious lesions (Maia et al., 2016) and advanced dental erosion lesions (Pretty et al., 2004). Chew et al 2014

demonstrated that QLF can detect statistically significant loss of fluorescence (1.28%) after 10-mins erosion of natural human enamel samples and after every consecutive 20-min erosive challenge. This was strongly correlated with both OCT data and surface microhardness values which decreased with increasing erosion (Chew et al., 2014).

Whilst this technique is non-destructive, and provides longitudinal assessment of erosion, the setup is expensive, and its detectable limit has neither been defined nor been demonstrated for measuring early erosion lesion. The use of QLF has not been explored for early erosion characterisation in vitro or in vivo.

1.4.6.6 Scanning Electron Microscopy

Scanning electron microscopy (SEM) utilises an electron beam which is scanned across the surface of a sample to produce a highly detailed image which can be utilised to observe nano- and micro-scale surface morphology (Barbour and Rees, 2004). Its main use in dental erosion research is as a supporting characterisation technique in conjunction with other characterisation methods (Joshi et al., 2016).

SEM has been previously utilised to study the baseline differences between polished enamel samples derived from human, bovine, or ovine origin, together with contact profilometry and surface microhardness measurements (Field et al., 2014). Qualitative differences between all three polished enamel samples could be visualised under SEM and confirmed with profilometry. Ovine enamel surfaces appeared more particulate and irregular, whilst bovine enamel appeared the smoothest containing large ridges and valleys. These qualitative findings were confirmed with profilometric assessment of surface roughness with bovine enamel

samples the smoothest (Ra=0.13 μm) and ovine the roughest (Ra=0.19) (Field et al., 2014). Additionally, polished human enamel demonstrated a characteristic keyhole pattered with eroded enamel prism cores and raised interprismatic enamel regions, whereas ovine enamel demonstrated a sheet-like structure of overlapping prisms, whilst bovine displayed an even less regular surface morphology with more enamel pits with raised rolled edges (Field et al., 2017).

SEM has been additionally utilised to study the differences between the natural and polished human enamel surface in relation to their erosive behaviour. Mullan et al 2017 studied the measurement of surface roughness on polished and natural human enamel utilising changes in surface roughness (non-contact laser profilometry) and surface morphology (SEM). Results indicated samples eroded after 45-mins in orange juice (pH 3.2); polished enamel samples demonstrated surface destruction characterised by a honeycomb appearance with the enamel prism cores dissolved by acid attack and pronounced interprismatic enamel regions. However, natural enamel samples demonstrated a less homogenous appearance, with some enamel prism exposure and varying perikymata striations (Mullan et al., 2017a). The morphological appearance of enamel is therefore different dependant on the sample preparation, as visualised under SEM. Whilst SEM can provide ultrahigh resolution images for qualitative image analysis, this technique requires sample preparation (gold sputtering) to ensure accurate image acquisition. As a result, the longitudinal measurement of erosion on surfaces may not be possible utilising SEM due to the irreversible sample preparation required.

1.4.6.7 Atomic Force Microscopy

AFM is one of the most accurate measurement instruments available to study changes in surface form, texture, and morphology in both enamel and dentine following erosion at the nanometre resolution (Barbour and Rees, 2004). This is a scanning probe microscope technique which works by running a stylus (usual diameter 20-50nm) attached to a cantilever and optical sensor over the surface of a sample and measuring the forces between the stylus and sample. As the stylus moves across the surface the cantilever is deflected up and down due the surface features present. The cantilever deflection is quantified by the optical sensor laser beam being reflected according to the cantilever deflection, onto a photodetector (Poon and Bhushan, 1995).

AFM has been utilised to demonstrate that the erosive behaviour of human enamel after 3-min citric acid erosion is depth-dependant, with enamel samples produced at the enamel surface exhibiting fewer features of surface destruction compared to enamel samples produced close to the DEJ (Zheng et al., 2010). Similarly, AFM has been utilised to characterise very early erosion in polished bovine enamel in a GORD model; a statistically significant increase in surface roughness (Ra) was measured after 10s erosion (Derceli et al., 2016). Additionally, the effect of the 24-hrs AEP on enamel erosion was demonstrated with AFM; lower surface roughness (Sa) and fewer features of surface morphology destruction – fewer prism-like structures appearing and less prism core destruction – were evident (Mutahar et al., 2017).

AFM is a very accurate measurement technique providing nanometer precision measurement of surface topography; however, the scan area for AFM measurement

is usually limited to <0.5x0.5mm^2 and maximum sample height difference of 10-20 μm, which can take 60 mins to complete (Barbour and Rees, 2004; Häßler-Grohne et al., 2011).

Utilising this technique to determine quantification of surface form and texture change over a larger more representative region of the enamel surface will require multiple scans, which would be both time consuming and expensive for studies utilising large sample sizes and requiring multiple scans for longitudinal erosion assessment (Barbour and Rees, 2004; Field et al., 2010).

1.5 Dental Surface Metrology

1.5.1 <u>Human Enamel – Metrology Challenges</u>

The human tooth, as described earlier, consists of different layers of highly mineralised tissues organised hierarchically and designed for cyclic function under many different challenging conditions within the oral cavity. Enamel is the most highly mineralised substance in the human body and is the first layer of the tooth exposed to a continuous cycles of acid erosion, foreign-body abrasion, and tooth-to-tooth attrition forces (Berkovitz et al., 2009). The most significant clinical event relevant to surface metrology measurement and analysis, is the micro and macro scale surface changes occurring on the enamel surface due to chemical and mechanical wear sustained in the oral environment (Austin et al., 2015).

From an engineering perspective, the natural enamel surface is as freeform surface consisting of perikymata, overlapping projections, and varying peaks and valleys (Ganss et al., 2000; McBride et al., 2009; Austin et al., 2015). Measuring the micro and macro scale surface changes in vitro has been readily accomplished using polished enamel samples of human, bovine, and ovine biological origin; flatness tolerances previously reported include $\pm$0.6 µm (Mistry et al., 2015), $\pm$0.4 µm (Austin et al., 2016; Mullan et al., 2018a, 2018b), $\pm$0.3 µm (West et al., 2000; Eisenburger and Addy, 2003; Shellis et al., 2005). However, measuring these changes on natural enamel has posed significant problems.

The majority of in vitro studies on dental erosion have utilised polished enamel samples due to the ease of sample creation, standardisation, and measurement of

surface changes. However, utilising natural enamel will improve our understanding of the complex mechanisms involved in the dental erosion process.

Surface profilometry is considered the gold standard measurement technique for measuring bulk tissue loss in dental erosion studies in vitro (Schlueter et al., 2011; Rodriguez et al., 2012a).

1.5.2 <u>Surface Profilometry</u>

This is a measurement technique which utilises either a physical or a light-based stylus to produce a digitised 2D or 3D topographical measurement of the samples' surface (Leach, 2009). This method can be conducted using confocal laser scanning microscopy (CLSM), contact profilometry (CP) or non-contacting laser profilometry (NCLP) and will be explored further below.

1.5.2.1 Contact Profilometry

Contact stylus profilometry (CP) utilises a physical diamond stylus in direct contact with the sample surface, the stylus tip diameter can vary between 1.5-2.5 µm and loading can vary from 0.05 to 100 mg (Barbour and Rees, 2004; Field et al., 2010). As the tip is dragged across the sample surface the vertical movement of the stylus is converted into a signal and used for 2D profile or 3D measurements. This technique has been utilised to study the effects of early and late acid erosion on both polished and natural enamel (Barbour and Rees, 2004; Field et al., 2010; Young and Tenuta, 2011).

Ganss et al 2000 studied the effect of long duration (3 hrs) citric acid erosion on polished and natural human enamel using contact profilometry; however, no details regarding scan dimensions nor settings were provided by the authors. Enamel loss

was expressed as erosion depth, in the polished samples this was defined by the vertical distance between the highest and lowest point of a profile trace; whilst in natural enamel, this was expressed as the vertical distance between the highest points of the reference enamel and lowest point of eroded enamel within the first 0.3mm. Results indicated enamel loss was statistically less ($p<0.05$) in natural (70.3 $\pm$ 16.2 μm) versus polished (115.0 $\pm$ 44.6 μm) enamel. To the authors best knowledge, this was the first study to utilise contact profilometry to measure and attempt to characterise enamel loss on the natural enamel surface. However, a long acid duration was utilised which was not clinically representative. This technique cannot be used for measuring the same erosion lesion over time due to the eroded surface being affected by the scratch marks. The longitudinal assessment of erosion was not possible using this method.

Mita et al 2013 characterised the early and late erosive lesion on polished bovine enamel using contact profilometry to study the effect of calcium concentration on apple juice mediated erosion. Four 4mm length tracings across the reference and eroded enamel were measured per sample; the surface loss defined as the average vertical distance between the reference enamel and 3 random points on the eroded surface. Results indicated calcium concentration >1% resulted in surface loss (0.8 $\pm$ 0.66 μm) which was not statistically different from a deionised water control (0.28 $\pm$ 0.28 μm) (Mita et al., 2013). CP allowed for the measurement of enamel loss due to early erosion in a dietary in vitro model, however, the use of CP has been previously demonstrated to cause surface damage due to the direct contact of the stylus with soft eroded enamel layer (Heurich et al., 2010). It is unknown whether this would lead to an overestimation of the erosion lesion depth.

This phenomenon has been previously studied in the measurement of dental erosion lesions on polished human enamel (Heurich et al., 2010; Paepegaey et al., 2013a). Heurich et al 2010 eroded polished human enamel with citric acid (0.1M, pH 2.3, and 0.01M, pH 3.3) or water (pH 7.1) for 10, 20, and 40 minutes and dental erosion lesions were measured with CP, CLSM, and AFM. Samples were first analysed with CP, CLSM and AFM was used to analyse the depth of the 3 scratches produced by CP measurement. Results indicated CP produced detectable scratches in the eroded enamel lesion, between 57 – 608 nm deep, which increased with increasing erosion time and citric acid concentration; both erosion time and citric acid concentration statistically significantly influenced CP scratch depth (Heurich et al., 2010).

Similar results were obtained by Paepegaey et al 2013 who eroded polished bovine enamel with citric acid (0.05M, pH 2.26) or orange juice (pH 3.8) in a cyclic erosion/remineralisation model for a total acid exposure of 180 and 300 minutes. The resulting extensive erosion lesions were measured with CP, 2D line profile step height, CSLM, and NCLP for 3D step height formation; scratches from CP were measured with CLSM. Step height formation increased with increased erosion time for all three measurements, with excellent inter-method reliability (>0.95) and correlation (R^2>0.99) between all methods. However, scratch depths from CP could not be analysed by CLSM and were concluded to be <1 µm deep, beyond the measurement range of the CLSM. This study did utilise AFM to analyse the scratch depths which were found to be between 57 – 608 nm, however they concluded that once the CP values were adjusted to account for the scratch depths, the CP scratches did not affect their study conclusions (Paepegaey et al., 2013a). However, this study conducted their erosion lesion analysis by performing CP first then NCLP and lastly

CSLM. It would be interesting to determine whether there would be any differences in erosion lesion depths if CP was performed last. Additionally, their recordings were taken at the end of the erosion cycling protocol (24 erosion cycles in total), it is therefore unknown whether the scratch marks from CP would impact the longitudinal measurement and evaluation of erosion lesion formation.

Caution should be exercised when measuring erosion in enamel especially where the smallest changes in step height are expected to be detected at early erosion times, and where repeated measurements on the same samples are required; the use of non-contacting measurement methods such as CLSM and NCLP are advocated (Stenhagen et al., 2010; Mita et al., 2013; Austin et al., 2015).

The use of non-contacting measurement techniques are desirable to prevent potential surface contamination or damage which can occur as a result of using a mechanical stylus in contact profilometry (Boltryk et al., 2008). Future study on the impact of CP on measuring early erosion lesions in comparison to CLSM and NCLP would be interesting to determine whether scratch formation is detectable and if they have an impact on early erosion formation or characterisation.

1.5.2.2 Confocal laser scanning microscopy

Confocal laser scanning microscopy (CLSM) is a non-destructive 3D imaging technique utilising a laser source to scan the surface of an object using the principle of confocal imaging (similar in principle to TSM) to obtain high quality images at one depth level at a time with the removal of any out-of-focus light and 3D image reconstruction. This technique has gained popularity in dental erosion research due

to the speed of image acquisition, non-destructive scanning technique, and no requirement for sample preparation (Field et al., 2010).

Stenhagen et al 2010 utilised and compared enamel loss measuring with CLSM, CP and white light interferometry (WLI), in polished human enamel samples eroded for two cycles of 6-mins erosion using 0.01M HCL (pH 2.2) in a GORD in vitro model. Their results indicated excellent correlation between CLSM and WLI (R^2=0.98, p<0.001), and CP and WLI (R^2=0.85, p<0.001), with erosion depths measured between 5.1-6.0 μm and 10.4 – 11.7 μm after 6- and 12-mins erosion respectively. CLSM has also been previously utilised for studying surface textural changes occurring on polished human enamel in an in vitro dietary acid model (Austin et al., 2016).

1.5.2.3 Non-Contact Profilometry (NCLP)

Instead of a physical stylus which is in contact with the sample surface during measurement, non-contacting profilometers (NCLP) utilise a displacement sensor consisting of either a polychromatic or monochromatic light source to produce a stylus of focused light of known spot size. The sensor captures information from the light returned from the light spot, it is analysed by a spectrometer or a charge-coupled device (CCD) array, and is then plotted on a digital (x,y,z) grid. When the point measurement sensor is combined with a controllable stage platform, 3D topographical maps of a sample surface can be created consisting of hundreds, thousands, or millions of individually measured points on a digital (x,y,z) grid (Boltryk et al., 2008; Leach, 2009; McBride et al., 2009; Austin et al., 2015). Anything which can affect the reflection of light back to the sensor will impact on NCLP measurement capability (Leach, 2009).

The displacement sensors that have been utilised to measure the effects of early and late erosion on enamel include: confocal white light (WL) (Mistry et al., 2015; O'Toole et al., 2016), confocal laser (CL) (Mullan et al., 2018a, 2018b), and triangulation laser (TL) (Rodriguez and Bartlett, 2010; Rodriguez et al., 2012b, 2012a).

One of the biggest advantages of NCLP is, since it utilises light to produce a stylus, there is no direct contact between the profilometer and the sample surface and thus no surface scratching and damage of the soft eroded enamel is possible (Barbour and Rees, 2004; Austin et al., 2015). This allows for longitudinal assessment of the same erosion lesion over time. Additionally, an NCLP can be programmed to scan a batch of samples thereby increasing time efficiency of experimentation and analysis, as compared to CLSM and CP which can only scan individual samples at a time.

However, when measuring complex surfaces such as natural human enamel the optical stylus used to measure and capture the surface can be distorted resulting in sensor drop out due to the decrease in the sensor ability to capture the reflected light (Rodriguez et al., 2012a). Similarly, the spot size of the optical stylus must be sufficiently small to allow NCLP to accurately resolve troughs, and its gauge range sufficiently large to detect valleys and peaks (Boltryk et al., 2008).

Non-contacting measurement techniques such as NCLP and CLSM have now become increasingly popular for the study of micro- and macro scale changes occurring on both polished and natural enamel; these will be discussed according to surface form and surface roughness measurements using NCLP.

1.5.3 NCLP Surface Form Measurement and Analysis

Changes in surface form of enamel between the eroded lesion and reference uneroded enamel is one of the most common methods utilised to characterise and measure enamel loss due to erosion (Schlueter et al., 2011; Young and Tenuta, 2011; Austin et al., 2015). Different measurement techniques have been reported and different analysis methods have been used to define enamel loss. In this literature review, surface form change will defined by (a) the measurement technique and (b) the analysis method.

1.5.3.1 Measurement Technique

1.5.3.1.1 Single Scan

The use of a single post-erosion scan is the most commonly described measurement technique in dental erosion studies using NCLP (Young and Tenuta, 2011). Most have been conducted on polished enamel samples due to ease of creation, barrier isolation, and lesion characterisation, compared to natural enamel (Young and Tenuta, 2011; O'Toole et al., 2015, 2016; Mistry et al., 2015). Previous studies have reported that to calculate step height formation in natural human enamel a combination of before- and after- erosion scans are required to allow for analysis either via profile extraction and analysis of the residual data set, or via scan superimposition (Holme et al., 2005; Stenhagen et al., 2010; Rodriguez and Bartlett, 2010; Rodriguez et al., 2012b).

Interestingly, Ganss et al 2000 utilised a single after-erosion scan technique to calculate surface form change in natural human enamel, albeit requiring a very long citric acid erosion (3-hrs) and a regression line method to determine vertical height

change between the eroded trough and reference enamel; this study did not utilise any ISO standards in their enamel loss measurement, and therefore its accuracy and reproducibility for early erosion is uncertain (Ganss et al., 2000).

1.5.3.1.2   Profile Extraction

Profile extraction involves subtracting before- and after-erosion scan datasets using metrology software to produce a resultant or difference image/dataset; enamel loss is then calculated using this difference image/dataset (Holme et al., 2005; Stenhagen et al., 2010). This technique has been reported for use with (Holme et al., 2005) or without (Stenhagen et al., 2010) prior surface alignment of the before- and after-erosion datasets, and subsequent subtraction to produce the difference image/dataset.

The first dental study to utilise this technique was described by Holme et al 2005, who reported using alignment of before- and after-erosion datasets before subtracting them to produce a difference image from which enamel loss was calculated. Enamel loss was defined as change in surface height of enamel using an analysis program which calculated the depth distribution of the pixels in the region exposed to erosion relative to a reference region of uneroded amalgam material (Holme et al., 2005). The use of pre- and post-erosion scans and their subsequent alignment and subtraction allowed for the calculation of step height formation from the difference data using polished enamel samples. This technique has not been used with NCLP data and future study is required to determine its suitability in calculating step height formation in natural human enamel.

A similar method utilised by Stenhagen et al 2010 calculated step height formation in polished human enamel samples eroded for a total of 6 and 12 minutes using an HCL (0.01M) GORD model. Samples were scanned with WLI before and after each erosion period, the scan images were aligned, and subtracted from baseline, to produce two differences images for each erosion time point; step height was calculated as per Holme et al 2005. Results indicated this method allowed for calculation of step height of 5.1(1.1) μm and 10.4(1.9) μm after 6 and 12 mins respectively. This study did not mention the use of scan alignment prior to subtraction to produce their difference/resultant image, and therefore it is assumed this was not carried out. As a result, the use of subtraction may also be possible without the requirement of prior image alignment, as long as the scanning methodology is sufficiently robust. However, these techniques are subject to errors inherent to the scanning method itself which was not described in their study, but was briefly touched upon by Holme et al 2005.

Utilising before- and after- erosion scan data with or without scan alignment holds promise for calculating step height formation in natural human enamel using NCLP.

Previously, scan superimposition and subsequent analysis has been performed on data sets produced with NCLP (CL + TL); this has shown great promise as a method to determine enamel loss in natural enamel (Rodriguez and Bartlett, 2010; Rodriguez et al., 2012a; Kumar et al., 2018; O'Toole et al., 2019).

1.5.3.1.3   Superimposition alignment

Three-dimensional data sets produced by NCLP or other methods such as digital intra-oral scanners consist of a point-cloud of data analysable with specialist

metrology software, or 3D superimposition software (Rodriguez and Bartlett, 2010; Rodriguez et al., 2012a; Kumar et al., 2018; O'Toole et al., 2019). Superimposition and alignment of two data sets can be conducted utilising one of three different methods: landmark-based alignment, best-fit alignment, and a reference best-fit alignment; however, the exact mathematics utilised for dataset alignment is often hidden to the user for the ease of software use (O'Toole et al., 2019). Landmark-based alignment is performed manually by the user who selects common landmarks or points on each dataset they want to subsequently align with the software. This method is highly subjective and dependent on the comprehension and skill of alignment of the user (O'Toole et al., 2019). A best-fit alignment utilises an iterative closest point algorithm to align consecutive scan datasets, which can differ according to the specific software used, and does not involve user-based decision-making. This method aims to minimise the mesh distance error between each corresponding data point for the different datasets undergoing alignment. Due to the nature of the iterative algorithms' termination criteria, i.e. when the best-fit alignment finishes, the alignment process will minimise the mesh distance error and spread this error evenly over both positive and negative deviations between the datasets being aligned. As a result, using this method for analysing large deviations due to acid erosion, non-eroded regions appear to "gain" or grow over the measurement period, which is impossible (Tantbirojn et al., 2012; O'Toole et al., 2019). A reference best-fit alignment aligns datasets by restricting dataset alignment to sections defined by the user as areas whereby no change (due to erosion) would have occurred, this would therefore avoid the error of minimising the defect of interest to be measured,

although the requirement of user-input and thus user error is introduced (O'Toole et al., 2019).

Rodriguez and Bartlett 2010 conducted an in-vitro dietary erosion-abrasion study evaluating the effectiveness of TL NCLP and superimposition to determine enamel loss in polished human enamel samples. Results indicated a statistically significant (p<0.001) correlation ρ=0.76 between 2D and 3D step height values; however, 3D step height demonstrated statistically significant differences between the different fruit drinks tested, whilst 2D step height did not, and was only statistically significantly different versus the water control. This study is the first to utilise NCLP and superimposition techniques to determine enamel loss defined as either 2D or 3D step height; however, this study utilised a TL NCLP set up, polished enamel surfaces and very long erosion time periods (Rodriguez and Bartlett, 2010). This method has yet to be used for analysing early erosion in natural human enamel.

Kumar et al 2018 demonstrated the difficulty associated with utilising natural human enamel samples to calculate enamel loss due to dietary acid erosion in vitro. Superimposition software was used together with an iterative closest point (ICP) technique to align datasets according to pre-erosion dataset. Enamel loss was defined using the maximum profile decrease on the surface and average profile loss of the entire surface. Results indicated maximum and average profile loss increased after 120 mins from 33.4(10.3) to 72.8(42.3)µm and 9.2(5.1) to 18.6(16.2)µm respectively; both measurement outputs were significantly correlated with increasing erosion time maximum profile loss (r = 0.88, p<0.001) and average profile loss (r = 0.66, p<0.01) (Kumar et al., 2018). However, this study utilised long erosion

periods not clinically representative, and the large standard deviations obtained may potentially limit method applicability in detecting very small profile loss/changes. Additionally, the study did not utilise a reference area on the enamel surface to measure comparative enamel loss via step height formation using ISO 5436-1. The use of this intra-oral scanner was reported to produce a smoothening effect by interpolating data points to form triangles during digital surface creation, the size of the average triangle created by the intra-oral scanner software was 50 μm in all directions. Additionally, the ICP alignment method resulted in artefactual gain of enamel tissue with increasing erosion despite this being impossible; this was because of the issue with ICP alignment methods as described earlier.

1.5.3.2 Analysis Methods

Methods for analysing and quantifying enamel loss can be characterised into ISO and non-ISO methods.

1.5.3.2.1 *Step Height using ISO 5436-1*

Step height defined by ISO 5436-1 is one of the most commonly reported methods for defining enamel loss in early and late dietary erosion in vitro models. This method defines step height as the height from the central third region of the step (or eroded) zone subtracted from the average height from one or two reference (non-eroded) areas (ISO, 2000c); Figure 6.

This can be calculated either using one profile line across the sample and calculating the difference in height, known as single line mid-point step height (SPHC) (O'Toole et al., 2015). Alternatively it can be calculated by taking the average difference in height from multiple profile lines across the sample, known as mean single line mid-

point step height (MSPHC); this has been previously calculated from 10 (Mutahar et al., 2017) or 5 (Mistry et al., 2015) profile readings. This method works well on polished enamel surfaces where the erosion scar and associated reference enamel are relatively flat or exhibit slight deviation in form. Most studies utilising this method have reported using slope correction methods before analysis involving removal of plane of best fit using the least squares method (Mistry et al., 2015). The utilisation of single line profiles to determine step height may not necessarily be representative of erosion lesion as both the erosion lesion and reference enamel may not be uniform nor completely flat. However, the use of these techniques has not been evaluated for erosion in natural human enamel.
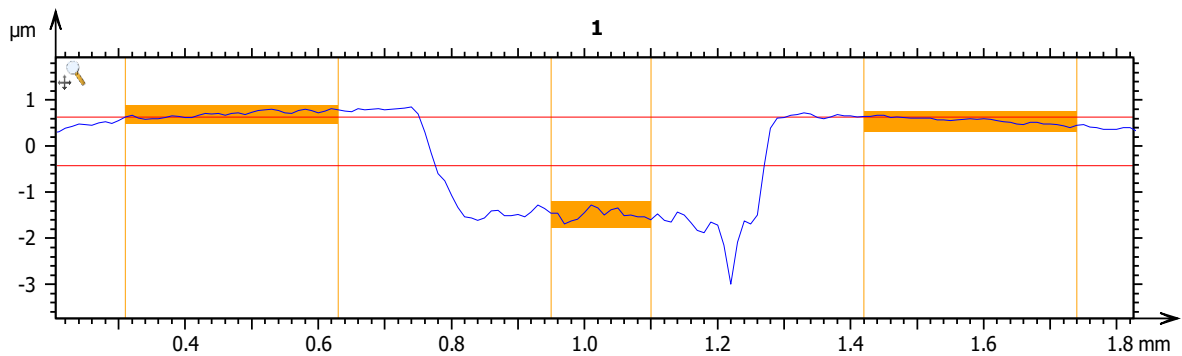
Figure 6 – Example of step height calculated using automated macro on MountainsMap software. The step height is calculated by analysing the difference in height between the two orange reference regions and reference region in the erosion trough.

Three-dimensional step height (3D SH) has been utilised to overcome this issue and is defined differently according to different studies. Previously it has been defined as the average step height (μm) across the entire erosion lesion by dividing the lesion volume (μm^3) by its surface area (μm^2) (Rodriguez and Bartlett, 2010; Paepegaey et al., 2013a); this technique does not utilise the defined ISO 5436-1 standard as its method of defining step height as the reference enamel is ignored, and it is technique sensitive and dependant on the user defining the edges of the erosion lesion. Another variation of 3D SH utilising ISO 5436-1 and automatic software calculation has been previously defined as the average height between the base of the eroded lesion and the reference enamel for the entire scan data set (Sar Sancakli et al., 2015). This has the added advantage of objectivity by utilising automatic software to analyse the step height and takes into consideration the whole data set during analysis.

These methods have been utilised on polished enamel surfaces and not on natural enamel surfaces due to the complexities of defining the reference and eroded regions for calculating height change for SPSH and MSPSH, and in the creation of isolated regions of erosion for the utilisation of 3DSH calculation defined previously (Schlueter et al., 2011; O'Toole et al., 2019).

1.5.3.2.2 Non-ISO Step Height

Ganss et al 2000 utilised a contact profilometer to measure the effects of 3-hour citric acid mediated erosion and characterised the bulk enamel loss post-erosion dataset; Figure 7. This study compared the effect of erosion on polished and natural human enamel. For polished enamel, this was defined as the vertical distance between the highest and lowest point of any given profile trace; six tracings were performed (200

µm apart, 1x1mm^2 area) with the mean erosion depth calculated accordingly. On natural enamel samples the profile tracing was adjusted to the x-axis using a regression line of 0.3mm length constructed as close as possible to the eroded lesion trace; erosion depth was then defined as the vertical distance between the highest point of the uneroded/reference enamel and lowest point of the eroded lesion within the first 0.3mm of the regression line. A very long erosion period was utilised to produce an extensive erosion lesion, and only a single profile trace was utilised. Additionally, this study did not provide information or details about the reproducibility and repeatability of this method. Its use for erosion scars produced using early erosion is unknown as this method depends on the ability of the measurement technique to accurately record the erosion scar and associated reference region; example illustrated in Figure 7.
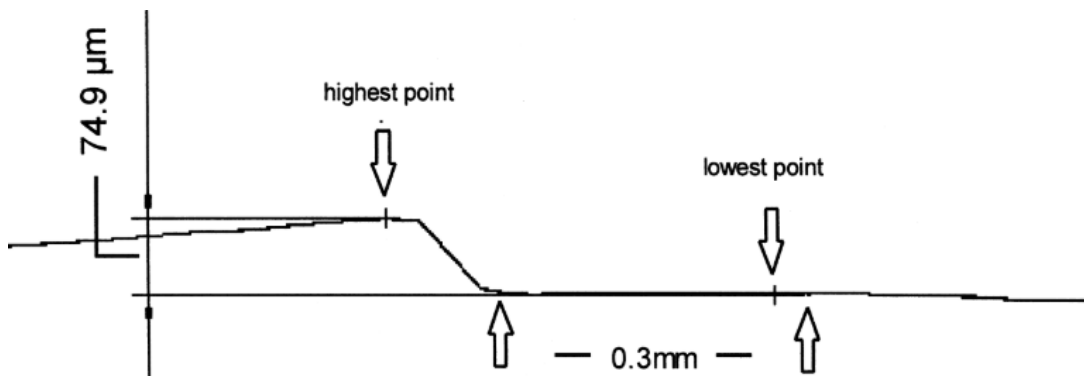
Figure 7 – Methodology utilised by Ganss et al 2000 demonstrating a step height in a natural enamel surface.

A similar technique was also utilised to determine enamel loss in polished human enamel, defined as the difference between maximum height of reference enamel and maximum depth of the lesion centre (Ren et al., 2011, 2009). This technique utilised a single after erosion scan from which step height was determined after 5, 10, and 15 days of erosion. The problem with this definition is in the variation that exists within natural enamel; the highest/lowest point within the defined erosive area need to be manually defined and will not be consistent across samples analysed; example illustrated in Figure 8.

Lin et al 2016 utilised a similar technique but instead compared before- and after-erosion scans obtained using focus variation microscopy for polished and natural human enamel. This technique defined step height as vertical distance between the highest and lowest point within the defined erosive area (Lin et al., 2016). This technique resulted in surface loss measurements for polished enamel 0.575(0.107) μm and 0.854(0.118) μm, natural enamel and 0.431(0.096) μm and 0.661(0.124) μm after 3 and 6 erosion cycles respectively. This study did not elaborate on their method of 3D scan alignment, nor how exactly they defined their region of interest for profile analysis. It is therefore difficult to determine if this technique is a form of point-cloud data best fit alignment superimposition or if it relies on matching unaltered fiducial markers as points of reference. Unfortunately, the authors did not provide an example figure.
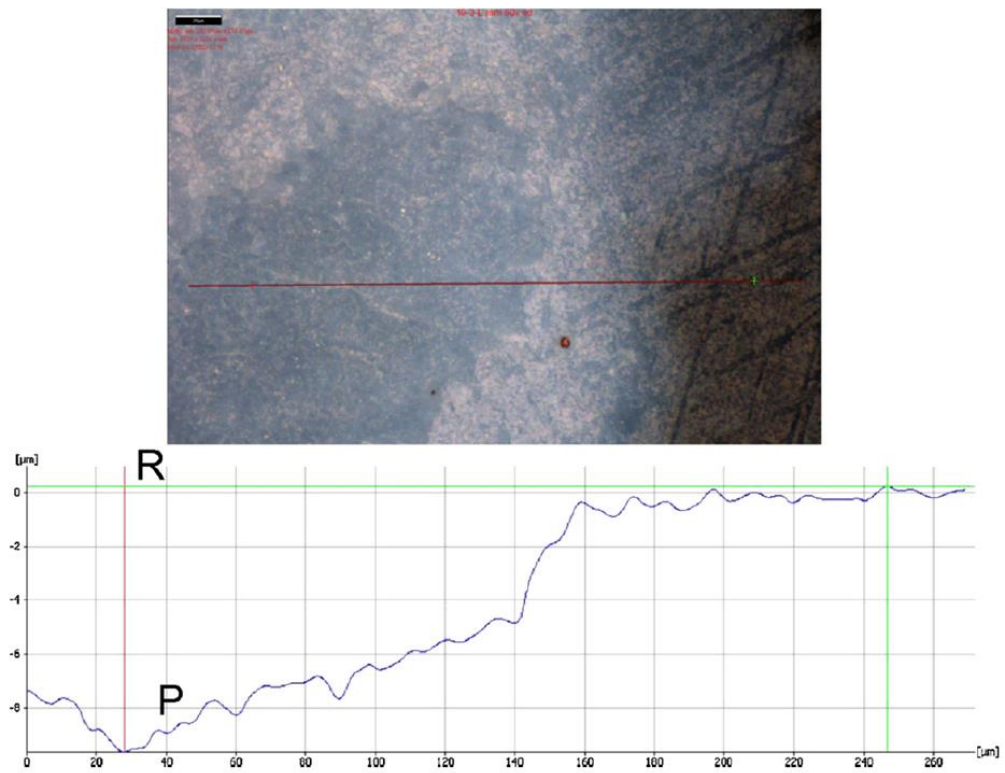
Figure 8 – Example of step height calculated as vertical distance between highest point on reference enamel and lowest point of eroded region (Ren et al., 2011)

1.5.4 NCLP Surface Texture Measurement and Analysis

Surface roughness is another component together with surface form that comprises the surface profile data obtained using profilometry (Mullan et al., 2018b). Changes in surface texture of enamel have been previously studied as a method to characterise the early and late surface changes occurring due to acid erosion; this has been characterised by changes in surface roughness before and after erosion (Field et al., 2010; Austin et al., 2015).

Surface roughness has been previously characterised utilising CP and 2D roughness parameters defined by ISO 4287 (ISO, 2000a; Nekrashevych and Stösser, 2003; Nekrashevych et al., 2004; Field et al., 2010; Mita et al., 2013; Field et al., 2014, 2017) with increasing popularity of NCLP, surface roughness has been defined using 3D roughness parameters defined by ISO 25178 (ISO, 2000b; Mann et al., 2014; Austin et al., 2016; Mullan et al., 2017a, 2017b, 2018a). Both methods are valid depending on the surface being measured, the measurement technique, and the analysis process; an example can be seen in Figure 9.
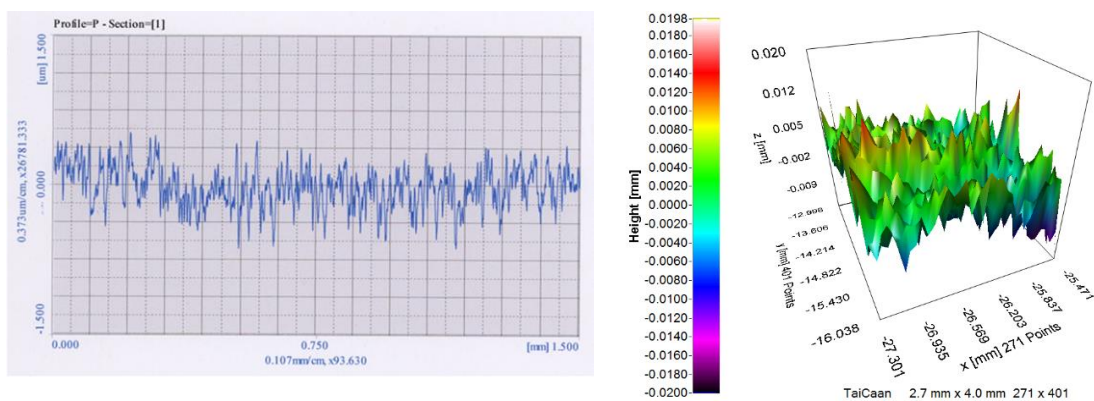
Figure 9 – Example of 2D roughness (left) measurement using CP and 3D roughness (right) measurement using NCLP

1.5.4.1   Measurement Technique

Surface roughness has been evaluated using both 2D (Mita et al., 2013; Field et al., 2017) and 3D roughness parameters (Mullan et al., 2017a, 2018b). The most common measurement techniques utilised for 2D roughness measurement involve the use of multiple single scan line profiles (Nekrashevych et al., 2004; Mita et al., 2013) whilst cluster scans are utilised for 3D roughness evaluation in both polished and natural enamel samples (Mullan et al., 2017a, 2018a). The use of a central cluster of five 0.2x0.2 mm (0.04mm^2) scans was demonstrated as representative of the surface roughness of both polished and natural human enamel (Mullan et al., 2017a).

1.5.4.2   Analysis Methods

1.5.4.2.1   2D Roughness Parameters (ISO 4287)

Studies utilising stylus profilometry have defined surface roughness using 2D roughness parameters as these techniques have been widely utilised for the purposes of characterising surface textural changes on enamel before and after early and late erosive challenge (Field et al., 2010; Schlueter et al., 2011). The most commonly used 2D parameter for surface texture analysis in dental erosion research is Ra which is defined as the average roughness of the resulting profile of the measured surface (Field et al., 2010).

Using Ra alone to quantify surface roughness has been argued as insufficient (Mita et al., 2013); others have suggested using bearing area parameters to provide a more complete understanding of the surface changes in an early erosion model, these include: Rpk (peak roughness), Rk (core roughness), Rvk (valley roughness), MR1 (material ratio of peaks) and MR2 (material ratio of troughs) (Field et al., 2013, 2017).

Two dimensional roughness parameters, can provide information regarding the surface textural features on enamel following early and late erosion models, however their ability to discriminate between tissue types is limited (Leach, 2013; Austin et al., 2015). 2D parameters are calculated from a single profile and may not be truly representative of complex surfaces of natural teeth, therefore the use of 3D areal roughness parameters has been advocated (Austin et al., 2015; Mullan et al., 2017a).

1.5.4.2.2   Areal Roughness Parameters (ISO 25178)

Use of areal roughness parameters has increased due to the increasing availability of non-contacting profilometric measurement methods using NCLP and CLSM (Austin et al., 2015; Joshi et al., 2016).

The most commonly utilised areal roughness parameter is Sa which is defined as the arithmetic mean height of the deviations of the surface measured; it reflects the deviation in height at each point from the arithmetic mean of the surface measured (Mullan et al., 2017a). This has been utilised as a possible predictor of early erosion.

In dental erosion studies the use of Sa alone has been sufficient to determine the impact of early erosion in GORD models (Mann et al., 2014), and dietary acid models (Austin et al., 2016). The use of a central cluster of five surface roughness scans has been demonstrated as sufficiently representative of both the polished and natural enamel surfaces, and has been recommended as the method of choice to study surface roughness change in these sample types (Mullan et al., 2018a, 2018b).

The use and interpretation of the Sa parameter is different depending on whether the enamel surface is polished or natural. In polished enamel it can be argued the Sa parameter can provide sufficient information on surface textural changes to indicate

erosive change after 30s (Austin et al., 2016), whilst for natural enamel erosion additional parameters may be necessary. In polished enamel, the Sa value has been demonstrated to increase with increasing erosion time (Mullan et al., 2017b) whilst in natural enamel the value decreases; this is a function of the higher baseline Sa value of natural enamel, which decreases as surface textural features are destroyed with increasing erosion indicating overall surface smoothening (Mullan et al., 2017a).

However, the use of Sa alone for the quantification and identification of surface textural wear due to other factors such as attrition and abrasion has been previously demonstrated as insufficient and other methods of defining surface roughness have been investigated (Hara et al., 2016; Austin et al., 2016; Ranjitkar et al., 2017). Area-scale fractal analysis has been conducted demonstrating how complex surface texture features are produced due to erosion. These lesions demonstrate complexity and anisotropy which may not be explained by using Sa only. Complexity measures the number of overlaying variations of microwear features at different scales of measurement, whilst anisotropy is a measure of directionality and orientation of the microwear features (Scott and Halcrow, 2017). Complexity parameters studied include area-scale fractal complexity (Asfc) and scale of maximum complexity (Smc), and the anisotropy parameter called exact proportion length-scale anisotropy of relief (eplsar) (Hara et al., 2016; Ranjitkar et al., 2017).

Higher values of complexity and lower values for anisotropy were observed for erosion only lesions, with the reverse trend observed for erosion-toothbrush abrasion surfaces (Hara et al., 2016), whilst tooth-tooth attrition was associated with

higher values of complexity and lower anisotropy which was indicative of enamel loss associated with attrition (Ranjitkar et al., 2017).

Overall these studies concluded the Asfc and Smc complexity parameters can provide further information on surface complexity and can be used for distinguishing eroded enamel from non-eroded enamel, whilst the eplsar anisotropy parameter can distinguish between toothbrush induced enamel loss, non-eroded enamel and enamel erosion only.

1.5.5 <u>Metrology Definitions</u>

Surface profile measurement consists of the measurement of a line across the surface of an object, which can be represented mathematically with each measured point having a value in the x and z axes. This is a form of two-dimensional data and can be produced with both optical and stylus profilometry (Leach, 2009).

Areal measurements, however, consist of multiple lines of 2D profile measurements to produce a 3D surface map; this form of measurement provides much more information about surface topography (Leach, 2009).

Resolution is the minimum distance between two lateral features on a surface which can be measured (Leach, 2009). The resolution of NCLP is determined by the axial (z) resolution of the NCLP sensor, the step over distance (x- and y-axis), and the lateral resolution of the sensor spot size (Boltryk et al., 2008; Mullan et al., 2018b).

Measurement precision is defined as the closeness of a set of measurements to a given true value, whilst accuracy is defined as the closeness in agreement of a measurement to the known true value; when combined, both are utilised to

determine the reproducibility and repeatability of a given measurement technique (Leach, 2009, 2013).

Most dental erosion studies have utilised long erosion time periods in order to mitigate potential measurement limitations and ensure erosion can be detected. However, by understanding the measurement limitations of a given measurement technique, a better understanding can be made of the results obtained using that measurement technique. This is necessary to ensure that changes in surface form and texture can be determined in both polished and natural human enamel following exposure to early acid-erosion; this has not been studied to date.

1.5.6 NCLP Accuracy and Detection Limitations

Determining the accuracy and precision of the surface profilometry will improve understanding of the micro and macro scale surface changes that occur on both polished and natural human enamel surfaces (Stenhagen et al., 2010); this will allow for the measurement of the earliest forms of change due to acid erosion. Studies should ideally analyse and characterise the repeatability and reproducibility accuracy and therefore detection limit/threshold of their chosen measurement technique; this will provide greater certainty for the values obtained during experimentation (Bell, 2001; Stenhagen et al., 2010; Austin et al., 2015).

An important concept by the guidelines of bioanalytical analysis state that the detection limit/threshold of a given measurement system is defined by the equation *mean + 3 x standard deviation*, (mean + 3D). This should ideally be defined (both for repeatability and reproducibility) for the quantification system and study methodology being utilised unless it has already been previously published (Shah et

al., 2000; Attin et al., 2009). This concept has been previously investigated by studies conducting in vitro erosion experimentation using CP (Attin et al., 2009), CLSM (Austin et al., 2016), and NCLP (Mullan et al., 2017b, 2018b; Rodriguez and Bartlett, 2010).

Attin et al 2009 reported the background noise for CP in their laboratory setup was recorded as the vertical displacement of the stationary stylus during 20s period which showed a mean of 0 ± 0.035 µm; the detection limit of CP was therefore calculated as 0.105 µm (Attin et al., 2009). This method describes the requirement for meticulous sample flattening during preparation to ensure the smallest surface form deviations are detectable; however, this is not translatable to the natural enamel surface. Additionally, this study captured single profiles to calculate form change which may not be representative of an erosion scar in biological samples.

For optical based measurement systems in dental metrology, it has been reported that ambient temperature variation is a main contributor to background noise (Holme et al., 2005). Holme et al 2005 identified ambient temperature change as an important factor which can impact on the accuracy of measurement of step height using optical based measurement. This study reported a 1K variation in ambient temperature lead to a positional variation between the sensor and the sample of 6.5 µm; the use of manual alignment of the sample stage was required to ensure scans were as closely aligned as possible before and after erosion (Holme et al., 2005). However, the authors did not report how the temperature was logged nor how the positional variation of the sensor was determined or calculated.

Rodriguez et al 2012 conducted a study to determine the accuracy of a TL NCLP system which utilised a 785nm wavelength triangulation laser with spot size diameter of 30 µm with sensor resolution 0.1 µm and angular tolerance 89.7°. This study determined the repeatability in measuring a steel gage block length was 1.6 µm with mean error of 1.3 µm, (Rodriguez et al., 2012a). A TL NCLP is useful when measuring whole teeth or casts of teeth due to its larger gauge range which can measure more of the whole tooth morphology. However, its use in measuring early erosion on polished or natural enamel sample in vitro is limited and the use of CL NCLP or CLSM with smaller stylus spot sizes would be recommended (Austin et al., 2015).

Austin et al 2016 analysed early erosion using CLSM in an in vitro dietary erosion model. This study demonstrated and recommended that lateral scan dimension <2.5 µm is required to allow scanning of the enamel surface with sufficient accuracy to ensure features of interest (enamel prisms), can be scanned and measured. Additionally, Gaussian filtering of five times the feature size of interest (approx. 5 µm for enamel prisms) was recommended (25 µm), to allow analysis of the enamel prisms before and after erosion (Austin et al., 2016).

Mullan et al 2018 studied the precision of CL NCLP utilising a 655nm displacement sensor for measuring surface roughness change on polished and natural human enamel. This study utilised 30 consecutive roughness scans, where each scan consisted of a 0.2x0.2mm square with 0.004 mm (4 µm) step-over distance. Five regions on the polished and natural enamel were scanned 30 times consecutively and precision of each scan was expressed as variability of measurement (SD in nm). Their results indicated the CL NCLP precision for surface roughness measurement was 5nm

(0.005 µm) in polished enamel and 23nm (0.023 µm) in natural enamel (Mullan et al., 2018b). However, the study did not outline the detection threshold for surface roughness measurement using their method, as defined by Attin et al 2009, or the limits in measuring surface form change (Attin et al., 2009).

1.5.7   Non-dental surface metrology

Within manufacturing, precision measurement and investigation of 3D surfaces is important as this allows for the quality assurance of many different manufactured products including: contact lenses, artificial hip replacements, and electrical contacts (McBride et al., 2004; McBride, 2009; Tuke et al., 2010). Three-dimensional measurement techniques and concepts which have been developed within the manufacturing and engineering sector, could also be applied to the study of biological surfaces within dental surface metrology.

Suk et al 1999 studied the progression of surface wear of a stainless-steel pin abraded across a plastic specimen using time-lapse photography and image difference analysis. Difference images between the initial (unworn) image from successive images of the surface as it undergoes wear were created through image subtraction, and the level of wear progression was calculated according to the surface area of the pixels in the difference images produced (Suk et al., 1999). However, whilst this method provided a visualisable analysis of wear on a metallic surface, it did not provide quantifiable topography measurements. Additionally, this method required a baseline image to be taken before wear occurred which may limit its applicability if samples have already undergone wear. This method is similar described earlier by Holme et al 2005 who utilised white light interferometry (Holme et al., 2005). Its application for dental surface metrology using CL NCLP has yet to be investigated.

The effect of temperature on optical profilometry in mechanical engineering applications has been previously studied by McBride et al 2001. The effect of ambient operating/scanning temperatures was characterised for a NCLP with a polychromatic (white light) sensor. The stability of the WL NCLP sensor was studied together with variations in ambient temperature under two conditions, NCLP in an enclosed space (Perspex enclosure) versus in an open space, with measurements occurring in a 24 hrs period. Housing the NCLP resulted in a vast improvement in sensor stability and measurement repeatability, by a factor of 3, when compared to NCLP in an open space; measurement standard deviation reduced from 72 µm to 15 µm accordingly (McBride et al., 2001). Whilst this phenomenon was evaluated in dental metrology for white light interferometry (Holme et al., 2005), this has not been studied for NCLP (chromatic or mono-chromatic); it is therefore unknown whether ambient scanning temperature would affect the performance of NCLP in measuring enamel erosion.

Similarly, the effects of NCLP sensor spot size and their effect on edge detection capabilities were previously studied on different engineering precision surfaces. An NCLP utilising two different sensors, a polychromatic (white light) sensor, and a monochromatic (red light) sensor, were tested for their respective capabilities in measuring different precision surfaces (McBride and Maul, 2004; Boltryk et al., 2009). The sensors tested were a white light sensor which had a 7 µm spot size, 10 nm z-axis resolution, 350 µm gauge range and 27° angular tolerance, whilst the red light sensor had a 2 µm spot size, 100 nm z-axis resolution, 600 µm gauge range, and 17° angular tolerance (McBride and Maul, 2004; Boltryk et al., 2009). McBride and Maul 2004 demonstrated that the red light sensor provided better edge detection performance and in detecting near vertical walls due to its large gauge range,

however for spherical and aspheric surfaces the white light sensor produced superior results with less data loss as function of the slope of the surface measured (McBride and Maul, 2004; Boltryk et al., 2009).

1.6   Summary of findings from literature review

- Human enamel varies in: thickness, chemical composition, and hierarchical organisation from the outer surface layer to the DEJ

- The physicochemical and mechanical properties of human enamel decrease as the DEJ is reached, this is correlated with fluoride and calcium content which also decreases towards the DEJ

- Human enamel used in in vitro studies can either be natural (unpolished) or polished artificially flat. There are significant differences in erosive behaviour of both sample types, natural enamel is more acid-resistant

- Human enamel polished artificially flat is the most common laboratory model for use in dental erosion and erosive toothwear research

- Previous work using natural unpolished human enamel slabs, has seldom been conducted due to difficulties associated with: sample preparation, standardisation, isolation, and lesion characterisation

- Majority of in vitro research involving the study of specific toothpaste technologies and formulations have been conducted on polished human enamel

- Profilometry has been primarily utilised for studying erosion on the polished enamel surface. There has been increasing work using natural enamel,

however, there is no standardised method for the preparation, isolation, and creation of erosion lesions on these surfaces

- Previous work on understanding profilometer instrument limitations has provided new insights into how surface roughness (Sa) change can be measured before/after erosion on natural enamel

- In long erosion times, surface roughness (Sa) of natural enamel decreases, whilst in polished enamel it increases. This is not been evaluated for short erosion times

- Previous work to determine surface form change in natural enamel has been limited to contact profilometry with limited success; none using NCLP and none using a robust method

- No work has been conducted to:

  o Study limitations of NCLP in measuring surface form change in natural enamel

  o Determine whether step height formation can be measured on natural enamel, as can be done on polished enamel

  o Study acid-erosion of natural enamel to create a viable in vitro laboratory model

1.7   Thesis Aims and Objectives

The overall (thesis) aims and objectives are as follows. Each objective relates to a specific chapter, with each chapter having their own sub-objectives; these are signposted in each chapter.

1.7.1   Thesis Aims

The overall aims of this PhD were to:

1.   To determine the minimum resolution and the in vitro conditions for NCLP to detect/measure the first signs of erosive change on human enamel

1.7.2   Thesis Objectives

1.   To characterise the micro and macroscale changes occurring on polished and natural human enamel and determine the detection limit using NCLP (step height and surface roughness), SM (Knoop), OCT (surface reflectivity), and TSM (surface morphology)

2.   To create a new in vitro model to characterise the micro and macroscale changes on natural human enamel

3.   To determine the impact of the AEP, single application sodium fluoride, and use of calcium silicate/sodium phosphate fluoride toothpaste, on the dental erosion process on natural enamel

1.8   Thesis Null Hypotheses

1.   NCLP cannot detect the earliest signs of erosion on polished and natural human enamel

2.   Changes in thermal variation will not affect NCLP measurement of surface form and roughness

3.   Surface form change cannot be measured in natural human enamel using NCLP

4.   The AEP will not have a protective effect on erosion in natural human enamel

5.   Sodium fluoride will not have a protective effect on erosion in natural human enamel

6.   Calcium silicate/sodium phosphate fluoride toothpaste will not have a protective effect on erosion in natural human enamel

2 Chapter 2 – Evaluating the early erosive lesion in polished and natural human enamel

2.1 Introduction

In this first Chapter, the early erosive lesion was explored on polished and natural human enamel samples. As discussed in Chapter 1, many studies have described creating early erosive lesions using different erosion times ranging from 5s (Derceli et al., 2016) to 2 hrs (Mathews et al., 2012) and using either single or multiple erosion cycles (Young and Tenuta, 2011). Erosion periods of 5 mins or quicker are considered representative of the clinical situation where patients' sip/ingest erosive substances either once or multiple times over the course of a day (Young and Tenuta, 2011; Shellis et al., 2011b). The shortest erosion time required to produce a detectable erosive lesion in either polished or natural human enamel has yet to be explored for a dietary acid (citric acid) in vitro model. This chapter focuses on the assessment of dietary erosion at varying erosion times using surface profilometry, surface microhardness, surface reflection and surface morphology analysis.

2.2 Chapter Aims, Objectives and Null Hypotheses

2.2.1 Chapter Aims

The aims of this Chapter were to:

1. Characterise the early erosive lesion in both polished and unpolished enamel samples.

2. Ascertain which measurement techniques can be utilised to detect an early erosive lesion and determine which would be most appropriate in future studies within the PhD.

3. Determine the minimum acid-erosion time required before early erosion can be detected using different measurement techniques

2.2.2   Chapter Objectives

The objectives of this Chapter are linked to and expand on Thesis Objective 1 (page 114)

1. Erode polished and natural enamel samples using an early erosion dietary-acid model (citric acid)

2. Characterise the early erosion lesions in polished and natural enamel using changes in: surface form (step height) and surface roughness (Sa) with NCLP, surface microhardness (Knoop), surface reflectivity (OCT), and surface morphology (TSM)

3. Determine the minimum erosion times required to produce a characterisable erosion lesion

2.2.3   Chapter Null hypotheses

1) Immersion of polished and unpolished human enamel samples in citric acid will produce no detectable quantitative nor qualitative differences according to immersion time period

2) The early erosive lesion will not be definable using surface roughness, 3D step height, surface microhardness, TSM, and OCT

2.3   Materials and Methods

An experimental overview can be seen in Figure 10.

2.3.1   Sample creation

Enamel slabs (n=120, 60 polished, 60 unpolished) were sectioned from the mid-buccal surfaces of previously extracted caries-free human molar teeth (REC ref 12/LO/1836), using a water-cooled 300 μm diamond wafering blade (XL 12205, Benetec Ltd., London, UK); as shown in Figure 11. Each slab was mounted, unpolished enamel surface down, in self-cured bisacryl material (Protemp™4, 3M ESPE, Seefeld, Germany) using a custom-made silicone mould (). A further sixty slabs were polished using successively finer silicon-carbide discs (Versocit, Struers A/S, Copenhagen, Denmark) of grit 500, 1200, 2000, and 4000 for 25s, 30s, and 60s respectively, using a water-cooled rotating polishing machine at 150 RPM and 10N constant pressure (LaboPol-30, Struers ApS, Ballerup, Denmark) removing approximately 300 μm of enamel and achieving a flatness tolerance of ±0.2μm.The newly polished surfaces were then ultrasonicated (GP-70, Nusonics, Lakewood, USA) in 100ml deionised water (pH 5.8) for 15 minutes to remove the smear layer and air-dried for 24 hours at room temperature (Mistry et al., 2015). Polyvinyl chloride (PVC) adhesive tape was placed using previously published protocols, on the polished enamel slab/bis-acryl embedding material surface such that each polished enamel surface had a 1mm x 3mm window of exposed enamel, protected by two zones of reference tape either side; allowing for comparison of eroded and protected enamel regions after erosion and after tape removal (Mistry et al., 2015). Examples of polished and natural samples can be seen in Figure 12.

Natural surfaces (n=60) underwent a standardised cleaning regime consisting of a 10-minute immersion in 4.7% sodium hypochlorite solution (Coventry Chemicals Ltd, Coventry, UK), followed by 30-minute ultrasonic cleaning in deionised water and air dried for 1 hour followed by a 2-minute clean with ethanol and cotton wipes, and final air dry for 1 hour. They were examined under TSM before and after cleaning to ensure surface cleanliness which was determined as the visible lack of surface material after cleaning and clear visualisation of enamel surface topography. Example of a before/after cleaning TSM image can be seen in Figure 13.
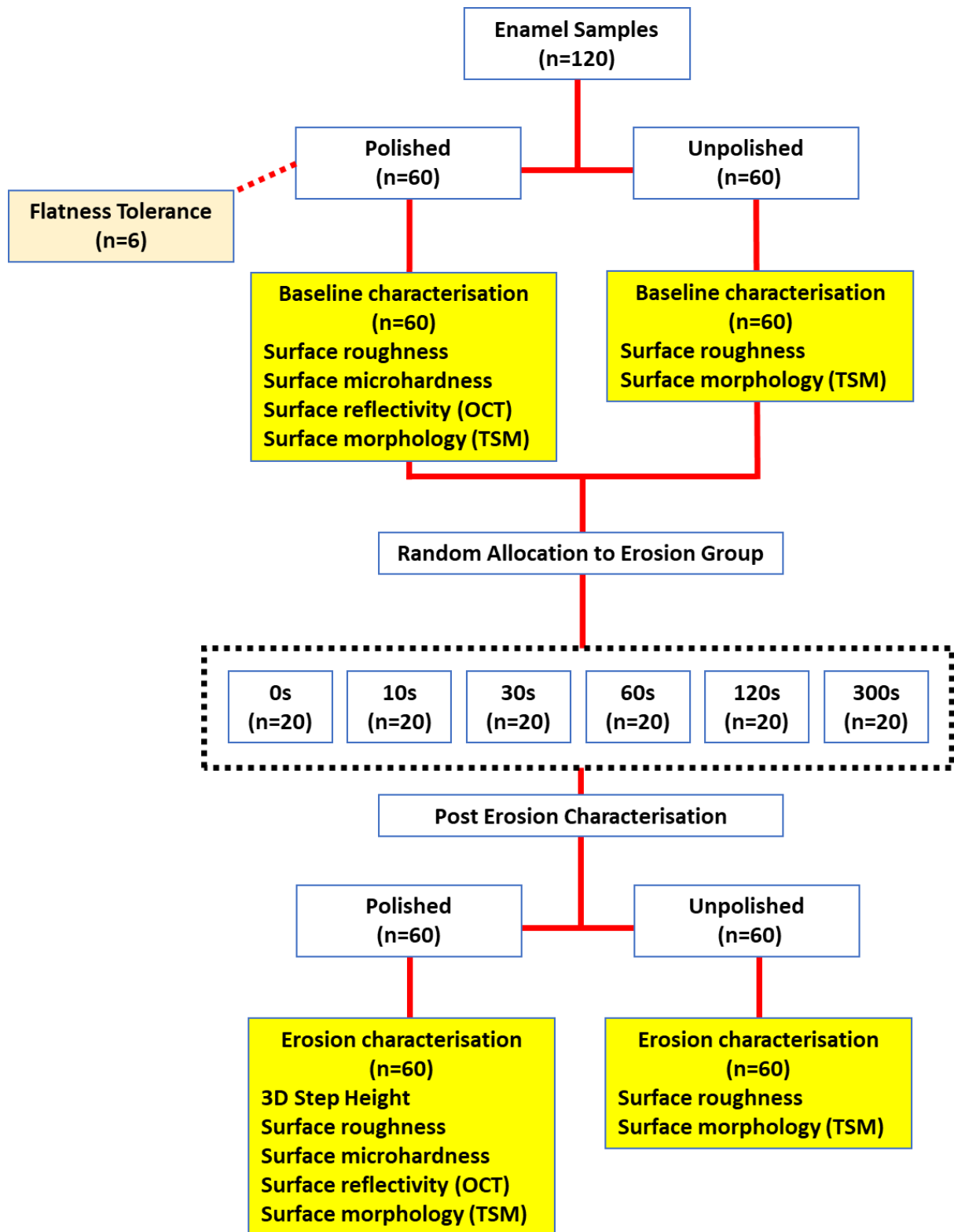
Figure 10 – Experimental Overview

| Step 1: separate crown from root | → | Step 2: split crown mesial - distal | → | Step 3: split each half into quarters to produce 4 enamel slabs |
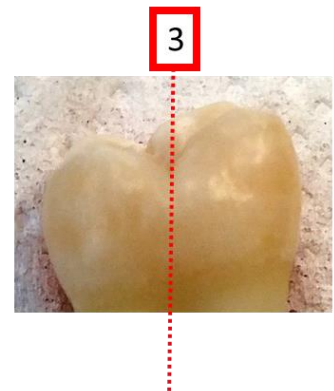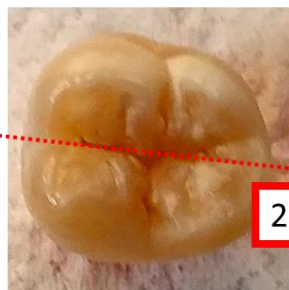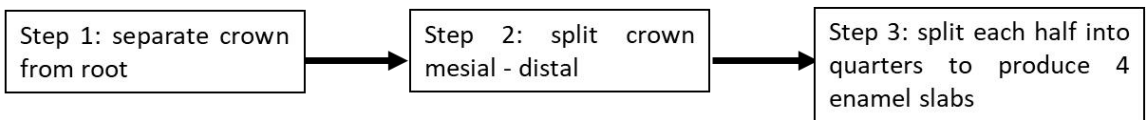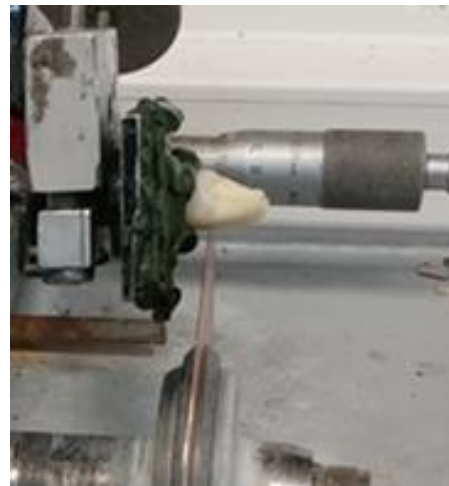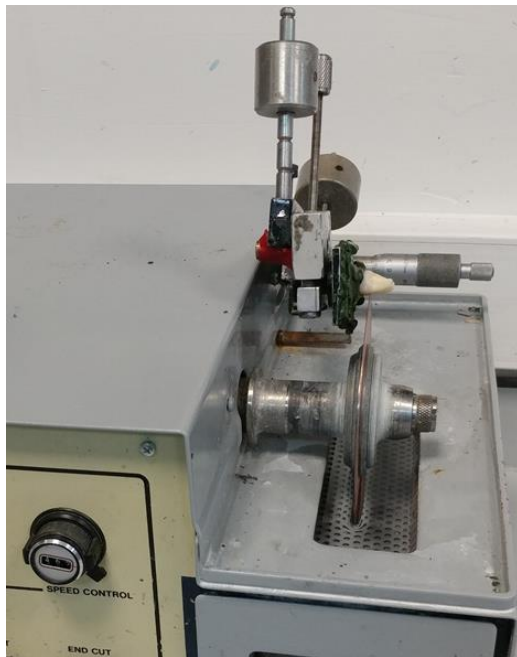
Figure 11 – Creation of enamel specimens was conducted using a cutting machine to section teeth in 3 places to produce the enamel slabs (Labcut 1010, Agar Scientific Limited, UK)
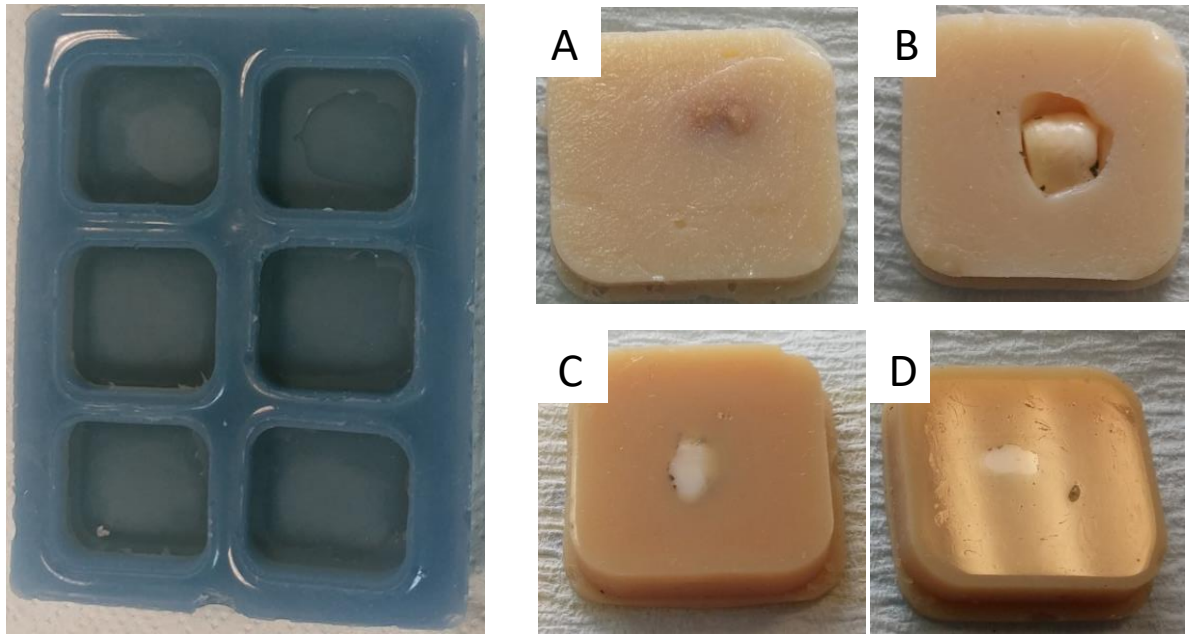
Figure 13 – Enamel slab placed into the silicone mould (left) are either then wholly embedded in bis-acryl composite (A) and polished to mirror finish (C) and (D) or left with an air gap as natural enamel samples (B)
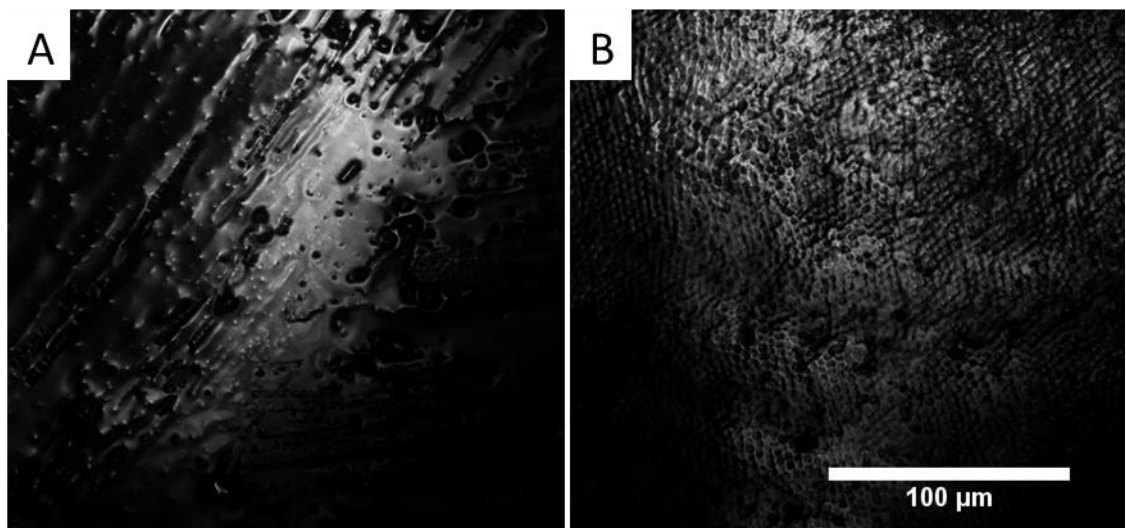
Figure 12 – TSM image in reflection mode showing unpolished enamel sample before (A) and after (B) cleaning regime for an unpolished enamel sample. This shows a very clean natural tooth surface free of any surface contaminants.

2.3.2 Erosion protocol

All samples were then randomly assigned to one of six treatment groups according to period of acid immersion: 0, 10, 30, 60, 120, or 300 seconds; 10 natural and 10 polished surfaces per group. Citric acid (0.3%w/w) was prepared, using previously published protocols, by adding anhydrous citric acid powder (Sigma Aldrich, Poole, Dorset UK) to deionised water, and the pH adjusted to 3.2 using 0.1 M sodium hydroxide (Sigma Aldrich, Poole, Dorset UK) (Austin et al., 2016; Mullan et al., 2017a). The titratable acidity was calculated according to the volume of sodium hydroxide required to increase the solution pH to 7, which was 18.0 ml (Austin et al., 2016; O'Toole et al., 2016). Each group of teeth were immersed in 100ml 0.3 % citric acid solution (10ml per sample) and agitated (62.5 rpm) using an orbital shaker (Stuart mini-Orbital Shaker SSM1, Bibby Scientific, England), at differing times for only 1 erosion cycle. All surfaces were washed with deionised water (pH 5.8) and left to dry overnight before data collection to ensure consistent profilometry scanning of all surfaces under the same scanning conditions (Austin et al., 2016; Mullan et al., 2017a).

2.3.3 Characterisation methods

Baseline surface microhardness was tested for all polished surfaces utilising a Knoop microhardness tester (Duramin-5, Struers Ltd, Rotherham, UK) and those surfaces outside the range 270 – 400 KHN were rejected (O'Toole et al., 2015). After acid immersion and drying, adhesive tape for polished enamel surfaces was carefully removed and surfaces assessed. Post erosion microhardness was conducted from 6 indentations produced 100 μm apart, selected conveniently in the eroded and

uneroded enamel regions, at 981.2 mN load and 10s press time and the mean change calculated from the difference between them according to previously published protocols and ASTM E384 17 (O'Toole et al., 2015; Austin et al., 2016; ASTM E384 - 17, 2017).

Profilometric measurement was conducted using a non-contacting laser profilometer (confocal laser) CL NCLP with a 655nm displacement sensor (Taicaan, XYRIS 2000, UK) with 2 μm spot size, 650 μm gauge range, 0.01 μm z height resolution. A (x,y) scanning interval of 10 μm, according to previously published protocols, was used for surface form measurements (Mistry et al., 2015; O'Toole et al., 2016). Two reference marks made using indelible pen on the bis-acryl material of each sample were used to allow scan co-localisation. Analysis for mean 3D step height was conducted using surface metrology software (MountainsMap®, Digitalsurf, France) using the ISO 5436-1 standard (ISO, 2000c).

Surface roughness was measured with CL NCLP according to previously published protocol (Mullan et al., 2017b) using a cluster of five representative areas in the intended erosion zone. Each scan area was 0.04 mm² (0.2x0.2mm, 51 x 51 points) and scanned using a scanning interval of 4 μm. To ensure enamel prism features were included in the scan analysis, a 25 μm Gaussian filter was applied to each scan in order to determine 3D roughness (Sa) data for each sample, according to previously published protocols and ISO 25178-2 (ISO, 2000b; Austin et al., 2016; Mullan et al., 2017a). Mean (SD) Sa (μm) was calculated for each erosion group.

OCT was conducted by a swept-source multi-beam clinical OCT machine (VivoSight™ Michelson Diagnostics, Kent, UK) utilising a near infra-red laser (1305 nm), with <7.5

μm optical resolution (Austin et al., 2017), on representative samples (n=2) of polished enamel surfaces for each erosion group. The refractive index of sound enamel has been previously approximated as 1.65 (Aden et al., 2017), the resolution of this system for measuring sound enamel was 4.06 μm (x direction) and 3.32 μm (z direction) in air respectively. Each sample was scanned in a raster pattern to produce B-stack volumes consisting of 500 B-stacks of (x,z) dimension (6 x 1 mm) with y-dimension of 4 μm between each scan. OCT data were semi-quantitatively analysed by using a stack analysis algorithm that was custom designed for this study to extract single full profile peak intensity average images from each B-stack volume; these images were known as surface projection/reflection images. These images were semi-quantitatively analysed using image processing software (ImageJ, Abramoff et al (Abramoff et al., 2004)) by assessing the peak intensity of the eroded enamel compared with non-eroded reference enamel in polished enamel surfaces. This method could not be used for the natural surfaces and thus they were only evaluated qualitatively with TSM.

TSM (Noran Instruments; Middleton, WI, USA) used a x20 objective lens (x20/0.35 NA objective) filtered light projection (green, 550 nm), to acquire representative (n=2, per group) 2D images of surfaces before and after acid erosion; the region of interest was the eroded region. A camera (iXon 885 EM-CCD Andor Technology; Northern Ireland, UK) and image acquisition software Micromanager v1.4.22 (Open Imaging; Inc. San Francisco, CA, USA), was used together with image processing software (ImageJ, (Abramoff et al., 2004)) to qualitatively analyse the 2D images (Mullan et al., 2018b). The images produced using TSM were evaluated qualitatively

to determine any visual changes between eroded and uneroded/protected enamel in polished surfaces, and between co-localised images of before/after eroded natural enamel surfaces. Co-localisation was conducted by means of utilising distinct surface features on each natural sample as fiducial markers for comparison of each sample against itself before/after erosion; in accordance with previous protocol (Mullan et al., 2018b).

2.3.4 <u>Statistical analysis</u>

All data was collected and tabulated using Excel (2018, Microsoft Corp, USA). From previous pilot data, a power calculation, using GPower 3.0.1, based on T-tests and ANOVA comparing between sample types (polished and unpolished) was conducted, and indicated a sample size of 60 per sample type (120 total sample size) would be required for an effect size 0.46 yielding 80% power. Statistical analysis was conducted using OriginPro 8.5 Statistical Software (OriginPro version 8.5, OriginLab Corp, MA, United States). Kolmogorov-Smirnov and Shapiro-Wilks tests confirmed data conformed to normal distribution, therefore means and standard deviations of each acid immersion group were calculated. Intra-group analysis compared with baseline values for uneroded enamel utilising dependent T-tests, whilst inter-group analysis was conducted with one-way ANOVA; $p<0.05$ was considered statistically significant. Non-linear regression analysis and Spearman rank correlation coefficient comparing 3D step height and surface microhardness (mean KHN) was conducted, whilst linear regression analysis and Pearson correlation coefficient was conducted to compare surface roughness (mean SA) with both 3D step height and surface microhardness; p

<0.05 was considered statistically significant and R^2 values expressed for all correlation measures and r values for the association between the variables.

2.4   Results

Surface microhardness results for the polished surfaces are shown in Table 2. Surface microhardness changes after 10 s, 30 s, 60 s, 120 s, and 300 s citric acid immersion were 40.9 (2.03) KHN, 60.7 (1.79) KHN, 91.7 (3.08) KHN, 100.1 (2.07) KHN, and 119.9 (4.34) KHN and were statistically significant for all groups compared to baseline (p<0.01). Polished enamel surfaces became statistically significantly softer with increasing citric acid immersion (p<0.01). Microhardness data could not be derived from natural surfaces.

Mean (SD) step height formation for 10, 30, 60, 120, and 300s using acid immersion groups for the polished surfaces were, 0.16(0.04) μm, 0.20(0.1) μm, 0.24(0.1) μm, 1.16(0.71) μm, and 2.01(0.47) μm respectively and these were statistically different compared to baseline (Table 2). Mean (SD) step height change was detected at all times but the number of surfaces that could be analysed was not consistent, the number of analysable surfaces for 10, 30, 60, 120, and 300 s were 5, 3, 7, 8, and 9 respectively. Results below 60 s were considered unreliable and discounted. Step height data was not obtainable from the natural surfaces.

The mean surface roughness for polished enamel for 10, 30, 60, 120, and 300 s acid immersion groups the mean (SD) surface roughness were, 0.27(0.024) μm, 0.30(0.028) μm, 0.51(0.068) μm, 0.95(0.201) μm, and 1.28(0.146) μm respectively and were statistically significant at all citric acid immersion time points compared to before erosion (p<0.05). The mean (SD) surface roughness for the natural enamel

decreased for all citric acid immersion time points compared to baseline (Table 2) but were only statistically significant at 120 s and 300 s; 0.83(0.125) μm and 0.80(0.140) μm respectively (p<0.01). Intergroup analysis revealed no statistically significant differences in mean surface roughness between immersion groups (p>0.05).

Correlation analysis between surface microhardness, surface profilometry, and surface roughness can be seen in Figure 14. There was a negative curvilinear relationship (r= -0.7676) and positive correlation (R^2=0.6593) between surface microhardness mean KHN and 3D step height (Figure 14A), positive linear relationship (r = 0.854) and positive correlation (R^2=0.7293) between surface roughness and 3D step height (Figure 14B), and negative linear relationship (r= -0.8811) and positive correlation (0.7764) between surface roughness and surface microhardness (Figure 14C); the correlation between each measurement output/method was highly significant (p<0.0001).

Percentage peak intensity analysis of representative polished enamel surfaces using OCT revealed significant differences in surface reflectivity between eroded and non-eroded regions for different citric acid immersion groups (see Figure 15). Percentage peak intensity change after 10s, 30s, 60s, 120s, and 300s were 88.8%, 86.8%, 77.9%, 69.2%, and 49.1% respectively and were statistically significant for all groups compared with baseline (p<0.01). Surface reflectivity analysis could not be determined for the natural surfaces.

TSM micrographic analyses of polished (Figure 16) and natural enamel (Figure 17) surfaces revealed differences between eroded and non-eroded surfaces for each acid erosion group. The honeycomb structure of polished enamel could be seen after 10s

erosion (Figure 16B) and progressed with increased erosion immersion time. The eroded regions became subsequently darker, and scratch marks present after the polishing process progressively were lost. This indicated that the erosive process resulted in further loss of enamel with increasing erosion time. Changes to the surface of natural enamel surfaces were subtler, with changes appearing to occur in the prism-inter prism interface after 10 s (Figure 17) and progressed to further generalised destruction of enamel prism structure and surface topography after 300s (Figure 17).

	Polished Enamel Group						Natural Enamel Group					
Erosion Time (s)	Mean(SD) 3D step height change (µm)	Analysable samples	Mean (SD) Surface Roughness (µm)	Analysable samples	Mean (SD) Microhardness Change (KHN)	Analysable samples	Mean(SD) 3D step height change (µm)	Analysable samples	Mean (SD) Surface Roughness (µm)	Analysable samples	Mean (SD) Microhardness Change (KHN)	Analysable samples
0	0	0	0.18(0.001)	10	4.4(1.44)	10	-	0	0.99(0.265)	10	-	0
10	0.16(0.04)	5	0.27(0.002)[*]	10	40.9(2.03)	10	-	0	0.95(0.098)	10	-	0
30	0.20(0.10)	3	0.30(0.028)[*]	10	60.7(1.79)	10	-	0	0.88(0.241)	10	-	0
60	0.24(0.10)	7	0.51(0.068)[*]	10	91.7(3.08)	10	-	0	0.86(0.4841)	10	-	0
120	1.16(0.71)[**]	8	0.95(0.201)[*]	10	100.1(2.07)	10	-	0	0.83(0.125)[**]	10	-	0
300	2.01(0.47)[**]	9	1.28(0.146)[*]	10	119.9(4.34)	10	-	0	0.80(0.140)[**]	10	-	0

Table 2 – Descriptive statistics for mean(SD) 3D step height change (µm), mean(SD) surface roughness (Sa, µm), and the number of analysable samples for each characterisation method for both polished and natural enamel groups. Data is represented as mean (SD) after citric acid erosion. Statistical significance is compared to baseline according to asterisk assignment * p<0.05, ** p<0.01
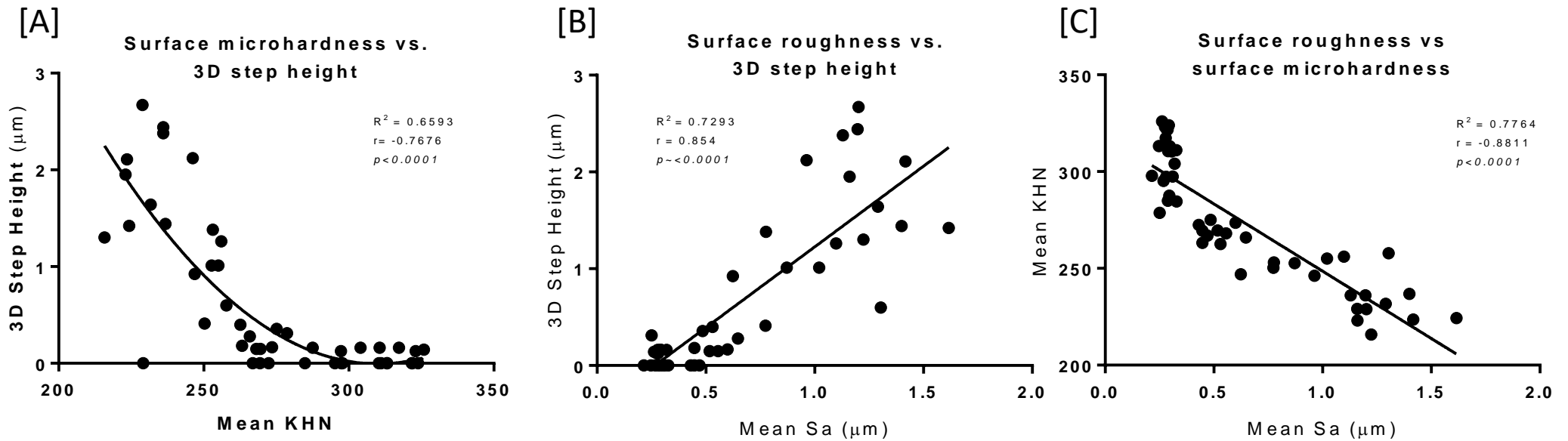
Figure 14 – [A] Negative curvilinear relationship and large correlation is demonstrated between surface microhardness (mean KHN) and 3D step height (μm) for all samples evaluated. [B] Positive linear relationship and large correlation is demonstrated between surface roughness (mean Sa, μm) and 3D step height (μm) for all samples evaluated. [C] Negative linear relationship and large correlation is demonstrated between surface roughness (mean Sa, μm) and surface microhardness (mean KHN) for all samples evaluated.
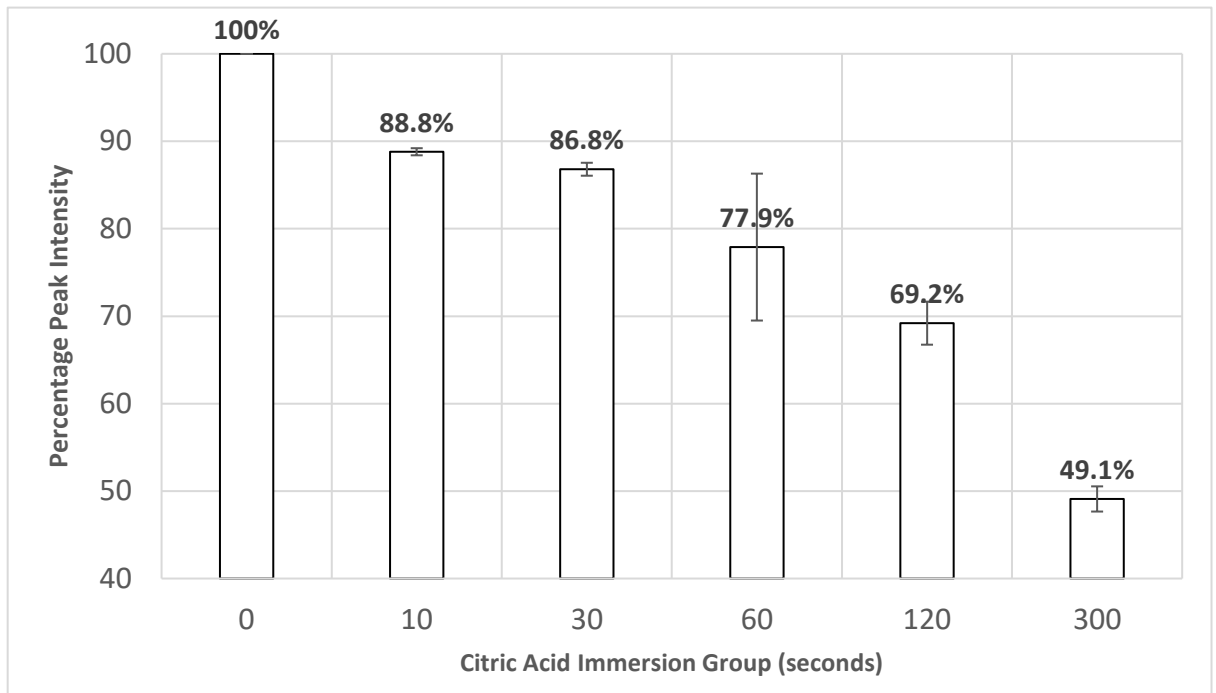
Figure 15 – Optical Coherence Tomography, surface reflectivity percentage peak intensity changes for representative samples from each acid erosion group compared with baseline/before acid erosion. A decrease in enamel surface reflectivity is evident after acid erosion and continues to decrease with increasing acid erosion.
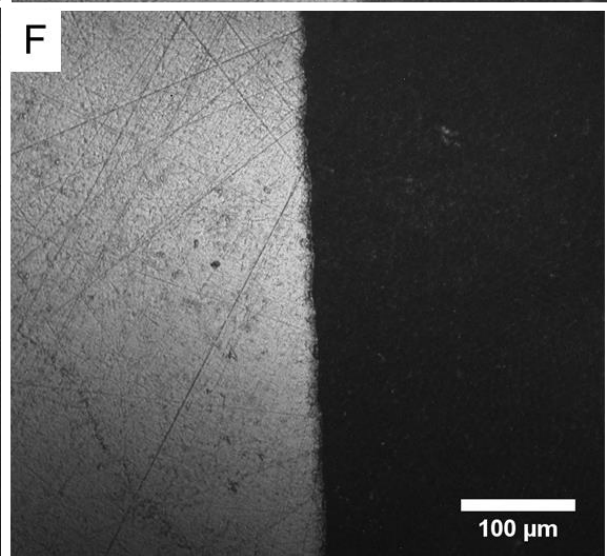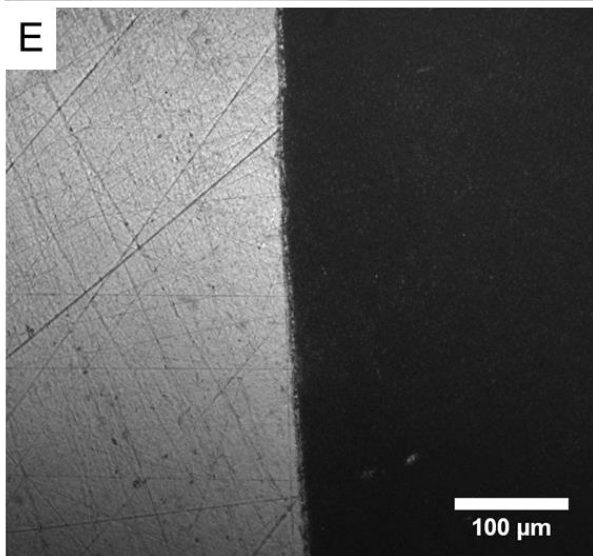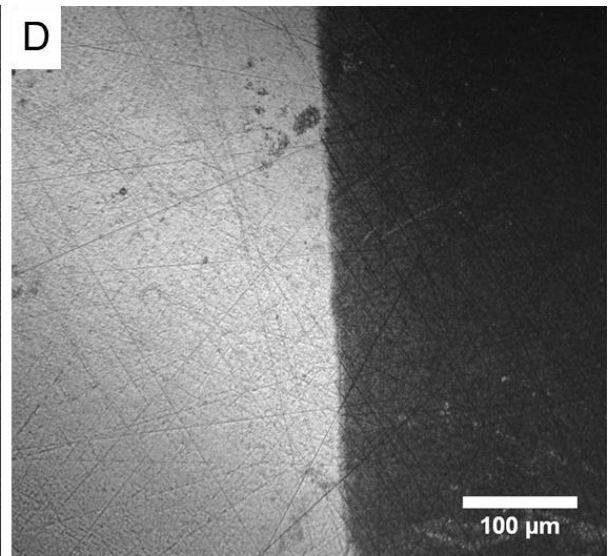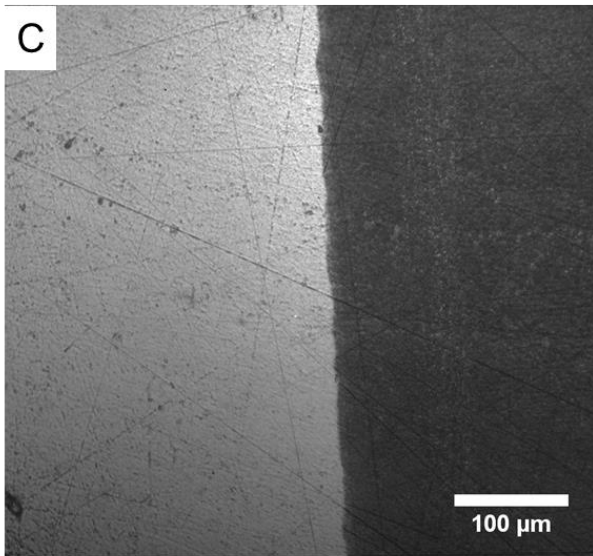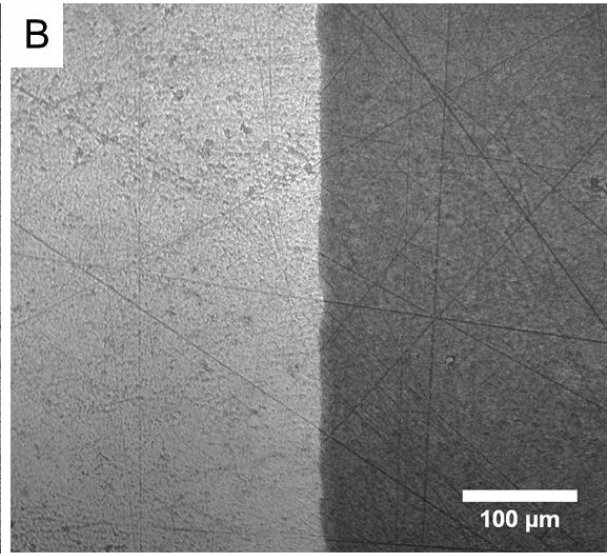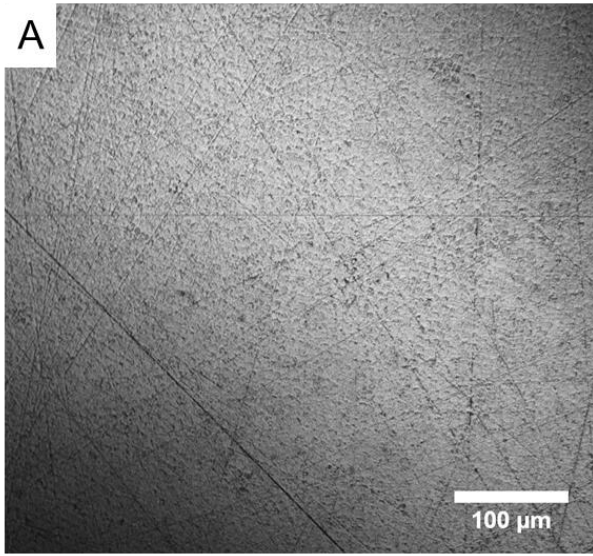
Figure 16 – Tandem scanning confocal microscopic assessment of polished enamel samples eroded after: 0s (A), 10s (B), 30s (C), 60s (D), 120s (E), 300s (F). Light areas on the left side represent the uneroded/protected enamel surface, darker areas to the right demonstrate change due to acid erosion. As acid erosion increased, the eroded regions became progressively dark.
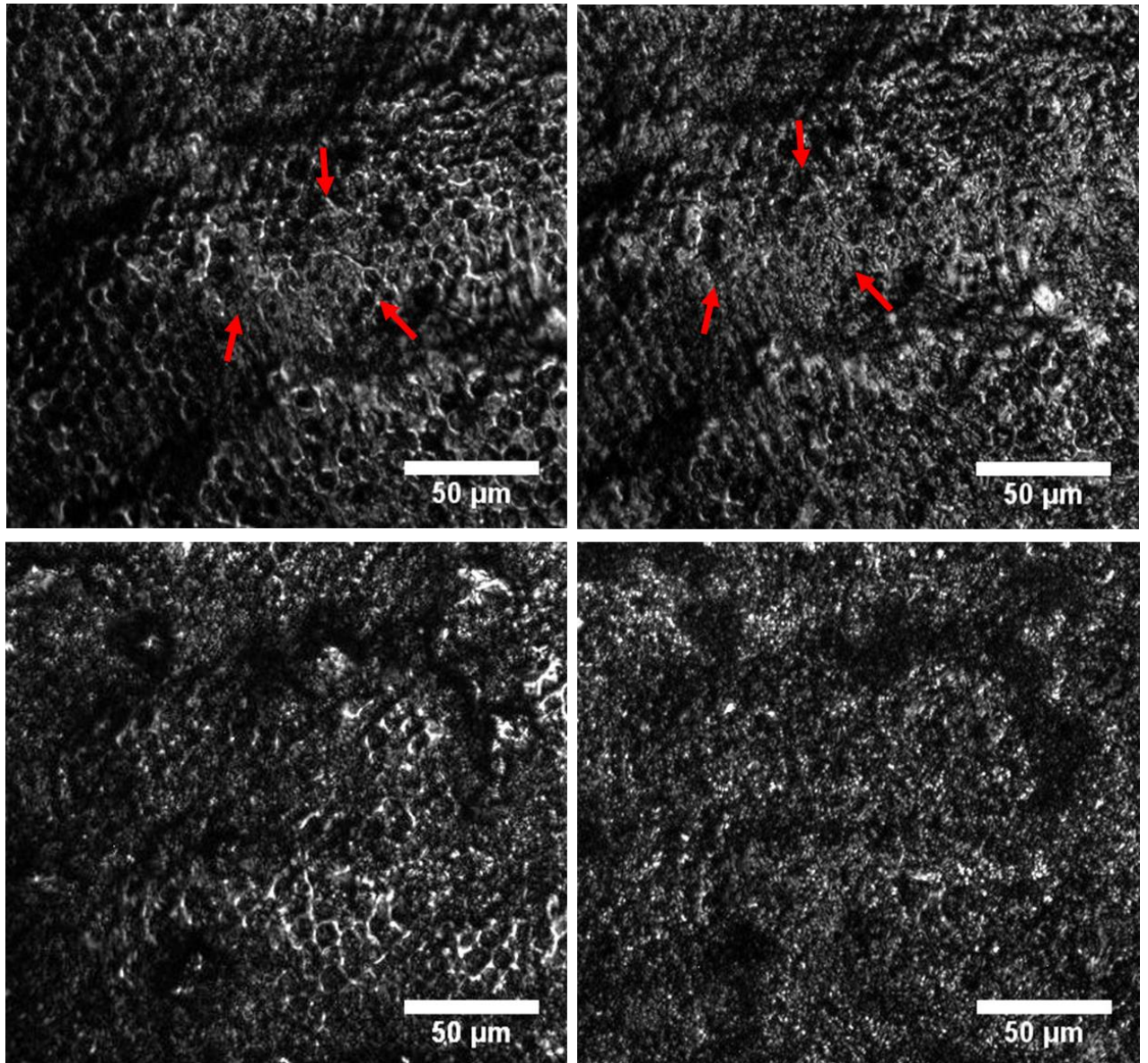
Figure 17 – Tandem scanning confocal microscopic assessment of changes in appearance of the enamel surface of natural enamel samples: before citric acid immersion (top left and bottom left); after citric acid immersion 10 s (top right) and 300 s (bottom right). Early changes include initial breakdown of prism-interprism interfaces(indicated with red arrows), further increasing size of the prisms relative to their 'Before' acid erosion image, loss of superficial and deeper topographical features.

2.5   Discussion

The surface microhardness results indicated surface softening of polished enamel surfaces occurred after 10 seconds, which is much earlier than previously reported in the literature (Austin et al., 2016). This suggests that the effects of citric acid on polished enamel, involving the processes of phosphate leaching and calcium chelation from the enamel surface, occur rapidly during acid exposure resulting in surface softening (Attin and Wegehaupt, 2014). It was not possible to obtain any accurate, reproducible, or measurable Knoop indentations on natural enamel surfaces to ascertain the minimum time that changes in surface microhardness occurred. This is partly due to the curvature of the enamel surface but also the variations in surface topography and profile that exist in all natural enamel surfaces, making the measurement of a standardised Knoop diamond indent impossible to conduct; which is why this technique is used only on polished uniformly flat enamel surfaces (Wiegand and Attin, 2011; Attin and Wegehaupt, 2014).

The findings from this study demonstrated that the current NCLP scanning settings and method was sufficient to measure the formation of the early erosive lesion in polished enamel (after 10s), and in natural enamel (after 120s) but only using surface roughness parameters. The surface roughness (Sa) data indicated that polished enamel statistically significant ($p<0.05$) increased compared to baseline and could be detected after just 10s citric acid erosion, whereas these changes could only be detected after 120 s in natural enamel (Table 2). The disparity in in the erosive characteristics between polished and natural enamel is likely to be due to the presence of the aprismatic enamel on the surface layer present on natural enamel

which is removed during polishing. This surface layer contains a higher concentration of fluoride and phosphate, and fewer impurities such as magnesium and carbonate, and has been previously shown to be more highly resistant to acid dissolution (Zheng et al., 2009, 2010). In a study by Zheng et al (Zheng et al., 2010) the mechanical properties of enamel differed according to its distance from the dentino-enamel junction (DEJ); erosion resistance decreased as the DEJ was reached and subsequent wear loss of eroded enamel was significantly lower for surface layer enamel versus enamel close to the DEJ. Further study of the natural enamel surface and the implications of changes in surface roughness following acid attack are required.

Within the scanning protocol and specifications of CL NCLP used in this study, we were able to detect significant changes in surface roughness after 10s of acid exposure, which is much earlier when compared with studies utilising longer erosion time periods (Lippert et al., 2004b; Zheng et al., 2009; Mann et al., 2014; O'Toole et al., 2015; Austin et al., 2016). Current findings are consistent with a previous report which demonstrated that changes in surface roughness, as a measurement output, could be detected after 10 s (Derceli et al., 2016); however, this was conducted on polished bovine enamel using pH 2 hydrochloric acid and atomic force microscopy as the measurement technique and Ra as the amplitude parameter for surface roughness. The earliest reported change in surface roughness for polished human enamel occurred after 30 s citric acid exposure (Austin et al., 2016). Enamel surfaces in the current study were polished to a higher flatness tolerance of $\pm$0.2 μm compared with some previous studies which utilised 0.4 μm (Austin et al., 2016) and 0.25 μm (Mann et al., 2014). This may have helped in the detection of the earliest

deviations in the polished enamel surface due to acid erosion in the current study. This is consistent with suggestions from previous reports indicating the importance of sample preparation and its potential influence on surface texture feature detection (Austin et al., 2016). The detection of surface roughness change after 10 s citric acid exposure using CL NCLP suggests that the physiological processes occurring during early erosive attack, such as calcium and phosphate release from the enamel surface, occur relatively quickly (Hannig et al., 2008; Mann et al., 2014; Austin et al., 2016). Although it was beyond the scope of this Chapter, further investigation would be required to correlate calcium and or phosphate release from the enamel surface with surface roughness; this would provide a better understand of what type of information the surface roughness parameter is providing.

The surface roughness of natural enamel surfaces decreased as acid immersion time increased, indicating smoothening of the aprismatic enamel surface, and contrasts to the results from polished surfaces which became rougher with increasing erosion. This difference in the wear behaviour and surface characteristics between polished and natural human enamel after erosion was also observed in a study by Mullan et al 2017 who found the median (IQR) surface roughness (Sa) of natural enamel reduced significantly (p<0.0001) (baseline Sa of 1.45(2.58) µm to 0.38(0.35) µm) after three 15-minute cycles of orange juice mediated erosion, whilst the median (IQR) surface roughness (Sa) for polished enamel increased (baseline 0.04 (0.17) µm to 0.27 (0.08) µm) after the same erosion period (Mullan et al., 2017a). This supports what is observed clinically in patients who suffer from erosive tooth wear, where natural

enamel surfaces become progressively smoother and shinier due to loss of surface structure and texture (Bartlett, 2016).

In the polished enamel group, there was a lack of consistent outputs for 3D step height formation in surfaces with citric acid exposure below 60 s. This could indicate that below this time the integrity of the enamel remains unchanged or was not detected using our non-contacting optical profilometry methods. The barrier method of choice, PVC taping in 1:3 ratio to leave an exposed region of enamel, has been widely published previously and has been shown to not influence the effect of acid-mediated erosion on enamel (O'Toole et al., 2015; Austin et al., 2016; Mullan et al., 2017a, 2018b). Additionally, the calculation of 3D step height using ISO 5435-1 utilises three relatively flat regions, two in the reference regions and one in the central portion of the eroded region; and thus any influence from the use of taping to protect the reference regions such as left over adhesive at the eroded-uneroded region or slight diffusion of acid under the tape is unlikely to affect 3D step height calculation (ISO, 2000c; Mistry et al., 2015). The progression from early erosive lesion to erosive tooth wear with measurable loss of enamel would appears to occur in the presence of prolonged citric acid attack greater than 60 s duration.

In natural enamel however, 3D step height change was undetectable. This was due to a number of technical challenges faced in trying to measure the natural enamel surface. The PVC tape barriers would not adhere to the natural enamel, which meant a referenced region of exposed enamel could not be produced. In addition, utilising a non-contacting optical profilometer to measure 3D step height on natural enamel was very difficult due to the curvature and non-uniform surface topography of the

natural enamel surface. These comparisons were conducted without either natural or artificial saliva and their impact is unknown. This study's aim was to assess the sensitivity of the measuring systems, the next will be to determine the influence of salvia.

This was the first study to correlate the use of changes in surface profilometry (3D step height), surface roughness (Sa) and surface microhardness (KHN) when measuring the same co-localised eroded regions to characterise the early erosive lesion within an in-vitro early-erosion model. Results indicated there was a strong positive correlation between all three measurement methods, whilst the association between each variable differed. The negative curvilinear relationship between surface microhardness and 3D step height indicates with bulk loss of enamel, the microhardness of the underlying enamel reduces. Additionally, there was a positive linear relationship between surface roughness – of the enamel surface at the base of the erosion trough – and 3D step height formation. Both these findings may be explained by the fact that surface microhardness and surface roughness was conducted on the acid- softened enamel left behind after bulk enamel loss occurred. This acid-softened enamel is formed as a result of the softening process that occurs during citric-acid mediated dental erosion where penetration of the acid into the enamel subsurface occurs before bulk superficial enamel is lost due to prolonged acidic attack (Attin et al., 2003; Shellis et al., 2014). The negative linear relationship between surface roughness and surface microhardness indicates that in polished enamel surfaces, surface roughness may be a surrogate marker for the enamel softening that occurs following citric acid erosion. Future studies will need to be

conducted to correlate surface roughness (Sa) changes with associated calcium release analysis to determine whether surface roughness can be used as a surrogate measurement for the chemical changes occurring on the eroded enamel surface.

OCT did not produce quantifiable data for enamel subsurface/depth changes for any of the acid exposure times. However, OCT allowed surface intensity changes of the profile of eroded surfaces to be quantified and analysed. The use of surface reflection/projection images derived from the B-stack volumes provided valuable information to determine differences in surface reflectivity between the eroded and non-eroded (reference) region of each sample. This was denoted by gradual decrease in percentage peak intensity, indicating that early acid erosion did result in changes in surface optical properties of enamel. This was likely due to the loss of calcium and phosphate from the enamel surface resulting in an increase in surface roughness and hence change in the optical properties of enamel producing a less reflective and more optically diffuse surface (Austin et al., 2017). Aden et al 2017 used OCT to conduct quantitative analysis of mean local pixel intensities on polished bovine enamel specimens in-vitro with increasing acid exposure time. Their results indicated pixel intensity decreased with increased acid erosion, suggesting that surface change due to acid exposure could be detected after 1, 2, and 5 minutes (Aden et al., 2017). However, longer acid exposure times were required to measure sub-surface changes using OCT in natural enamel in-vivo, for example, Austin et al 2017 demonstrated sub-surface changes in the superficial 33 µm of enamel after 60 minutes rinsing with orange juice *in-vivo*. Although saliva and salivary pellicle may affect the erosive process in-vivo, suggesting that short acid immersion periods produce alterations in

the enamel surface characteristics with minimal subsurface changes whilst more extended acid exposure times are required before subsurface changes in enamel occur (Austin et al., 2017). Significant additional changes to subsurface enamel may also be required before quantitative changes in 3D step height can be detected with the OCT as supported by the work of Chan et al (Chan et al., 2013) who reported that polarisation-sensitive OCT detected subsurface enamel changes after 6 hours immersion in a pH 4.5 demineralisation solution cycled over 2 days (Chan et al., 2013).

TSM images allowed qualitative assessment of the eroded zone for each erosion period, and as time increased the presence of the honeycomb-like structure of eroded enamel became more prominent and was best visualised after 300 s of citric acid exposure. This supports the work by Zheng et al (Zheng et al., 2009) who reported that after 5 minutes acid erosion, the formation of a honeycomb-like structure could be distinguished, which was due to the preferential dissolution of the prism inter-prism interface (Zheng et al., 2009). SEM could have also been used in our study to further corroborate surface structural changes; however, TSM allows for sample scanning without further surface modification.

The *in vitro* methods used in the current study demonstrate the formation of erosive lesions in polished enamel. Using polished enamel specimens, it was possible to detect relatively small changes in enamel surface characteristics following short acid exposures and sensitive enough to discriminate between different acid exposure times. Thus, polished enamel specimens are appropriate for studies that aim to investigate the formation of erosive lesions and studies that aim to investigate the

prevention or repair of erosive lesions. Indeed, such specimens are commonly used in the evaluation of enamel remineralisation agents and formulations (Hjortsjö et al., 2009; Attin and Wegehaupt, 2014; O'Toole et al., 2015, 2016). This study did not consider the impact of the acquired salivary pellicle on the formation of the early erosive lesion, as it was necessary to overcome the significant challenges in developing a working dry-field model first before additional influencing factors were introduced. The presence of saliva and/or the use of artificial saliva has been previously shown to influence the erosive patterns observed following acid mediated erosion of enamel for more extensive erosion periods, greater than 5 and 10 minutes, however there is a paucity of literature on the effect of the AEP on the formation and progression of the early erosive lesion; this will be the focus of future work in this area (Hannig et al., 2004b; Hara et al., 2008b; Austin et al., 2016; Mutahar et al., 2017).

One potential limitation of this study is that the resolution of the optical profilometer used to determine 3D step height change may not have been sufficient to detect changes consistently/reliably below 60 seconds in polished enamel surfaces. Any enamel loss which may be occurring during the initial 60 s citric acid exposure may not have been detected by the current non-contacting optical profilometer, and therefore whether or not enamel bulk material loss is occurring at such early erosion times may not be entirely excluded without further analysis, such as with atomic force microscopy. Additionally, this study sought to determine the level of dental erosion which could be detected using current and previously utilised scanning parameters/techniques and did not consider how different data acquisition variables

may affect the NCLP detection performance. Fleming et al 2016 explored the minimum data acquisition variables for contact profilometry on the measurement of artificial wear scars created on resin-based composite samples and determined the minimum x- and y- axis spacing required to ensure accurate quantification of mean total volumetric wear. Whilst their results may be extrapolated to non-contacting white profilometry, it is unknown whether this would be case for the NCLP used in this study which used a red-laser mono-chromatic based displacement sensor. Future study is therefore required to consider the effect of altering the scanning parameters on the accuracy of the measurements obtained using NCLP's that utilise this type of displacement sensor.

Using the current methods utilised, neither 3D step height nor surface microhardness data could be obtained in natural enamel surfaces. Future studies may consider using different measurement techniques to obtain quantifiable data for determining changes that occur in natural enamel surfaces after citric acid demineralisation.

2.6 Conclusion

Changes in surface roughness, surface microhardness and qualitative image analysis were evident for polished enamel surfaces and demonstrated that 0.3% citric acid (pH 3.2) alters the surface after only 10 s of citric acid exposure. Changes in surface roughness (Sa) and surface microhardness (KHN) were sensitive enough to allow the determination of the early erosive lesion; and their use in early enamel erosion studies is recommended. Natural enamel surfaces, however, required much longer erosion periods before any measurable change could be quantified; neither profilometric changes nor microhardness measurements were possible using the specific measurement equipment and data acquisition methods selected for this study.

3 Chapter 3 – Developing a novel in vitro model to evaluate the early and late erosive lesion in natural human enamel

3.1 Introduction

In Chapter 2 early acid erosion was characterised on polished enamel samples after 10s of citric acid immersion and assessed using changes in surface roughness, surface microhardness, surface reflectivity and surface morphology. Natural enamel samples required more than 120s acid exposure before detectable changes were characterised using surface roughness and surface morphology. Isolated erosion lesions were created in polished but not natural enamel. This Chapter focuses primarily on the assessment of unpolished, natural human enamel. It is split into 4 interconnected investigations. These investigations explore the limits of the CL NCLP setup, determine the optimum parameters for measuring surface form change on natural enamel, and develop a new in vitro model for creating and characterising dental erosion in natural human enamel.

3.2 Chapter Aims, Objectives and Hypotheses

3.2.1 Chapter Aims

The aims of these studies on natural enamel were to:

1. Determine the detection threshold of NCLP in measuring surface form and roughness

2. Characterise the influence of ambient thermal variation in NCLP system stability

3. Determine the optimum scanning measurement parameters for surface form measurement

4. Characterise the effect of early acid-induced erosion on natural enamel

3.2.2 Chapter Objectives

The objectives of this Chapter are linked to and expand on Thesis Objective 2 (page 114)

1. Calculate the repeatability and reproducibility error, and therefore detection threshold of NCLP measurement of surface form and roughness

2. Measure NCLP sensor displacement for temperature variation logged over short (30s), medium (20 mins), and long (2 hrs) evaluation periods with the NCLP enclosure closed and open

3. Measure surface form of natural enamel using different scanning dimensions and settings

4. Test a new taping method for suitability in creating erosion lesions in natural enamel

5. Utilise NCLP and OCT to characterise changes in surface form, surface roughness, and surface reflectivity

3.2.3 Chapter Null Hypotheses

1. NCLP sensor displacement will not be affected by ambient temperature variation

2. Changing NCLP step over distance will not impact on: total number of points measured, raw Sa value, and scan duration.

3. There will be no difference between using PVC strips and hole-punched PVC as an acid-resistant barrier on natural enamel

4. The early erosive lesion will not be definable in natural human enamel using changes in surface form, surface roughness, surface reflectivity, and surface morphology

3.3 Materials and Methods

3.3.1 Sample creation

Extracted human adult molar teeth, free from clinical disease or prior dental treatment, were collected under ethical approval (REC: 12/LO/1836) and with patient informed consent. The teeth were sectioned as described in Chapter 2 Section 2.3.1 to produce twelve enamel slabs approximately equal dimensions (5 mm x 5 mm x 3 mm). These slabs were bonded to glass microscope slides (Marienfield GmbH & Co. KG, Germany, dimension 76 mm x 26 mm x 1 mm) using epoxy resin (EverStick, Everbuild Products Ltd, UK) and each had four 4 enamel specimens bonded to the surface. A custom positioning jig was made for the glass microscope slides (as above) and positioned on an aluminium block, bonded with hot glue (Loctite Hot Melt Glue Gun Sticks, Henkel Adhesive Technologies, Germany) to create a one-way path of insertion to ensure repeatable placement onto the NCLP for scanning; Figure 18. Samples were cleaned following the method described in Chapter 2 Section 2.3.1. The NCLP utilised in all investigations was described in Chapter 2 Section 2.3.3.
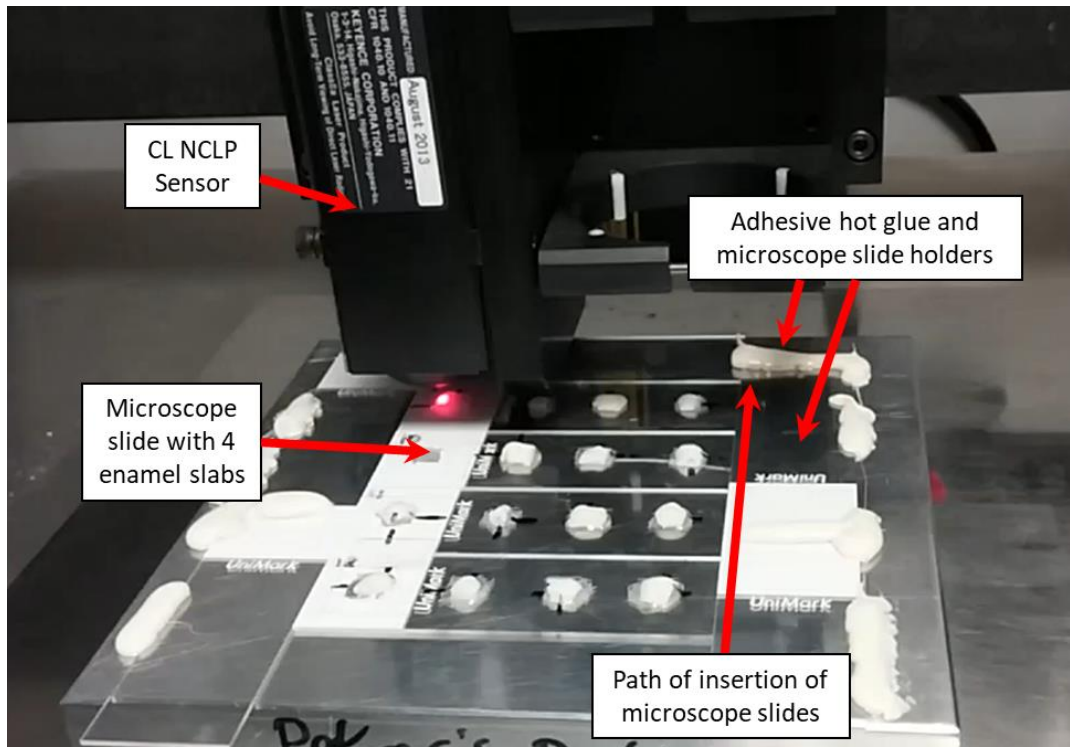
Figure 18 – Custom scanning jig created using microscope slides and adhesive hot glue. There is only 1 path of insertion of the microscope slides containing natural enamel slabs, there is no lateral movement of the slides.

3.3.2   Investigation 1 – Detection threshold determination

Repeatability error has been defined as "the error in repeated sample measurement under the same conditions"(Leach, 2009). In this investigation 20 measurements were used, 10 for repeatability and 10 for reproducibility; Figure 19. The data obtained by the NCLP consisted of all the data points and associated positions in x,y,z axis. When loaded into the metrology software (Boddies v1.92, Taicaan, Southampton UK), these data points were automatically plotted on a digital grid which represents the enamel surface scanned by the NCLP. This raw data (surface profile) was used to extract the surface form and surface roughness data; an example is shown in Figure 20.

To quantify NCLP repeatability and reproducibility error in measuring surface form and surface roughness, each digital grid was subtracted from the next to produce a difference data set. This contained the height differences (in µm) averaged for each measurement point; superimposed measurement grids after subtraction produced a difference data set (Figure 21). In total, 18 difference data sets were produced, and the mean (SD) height differences calculated and expressed as mean (SD) surface form difference and mean (SD) surface roughness difference; Figure 22.

The values for mean and SD obtained from the repeatability and reproducibility study for surface form and roughness were then used to calculate the detection threshold of NCLP was using the equation *mean $\pm$ 3SD* (Attin et al., 2009); this was expressed as NCLP repeatability and reproducibility for both surface form and roughness.
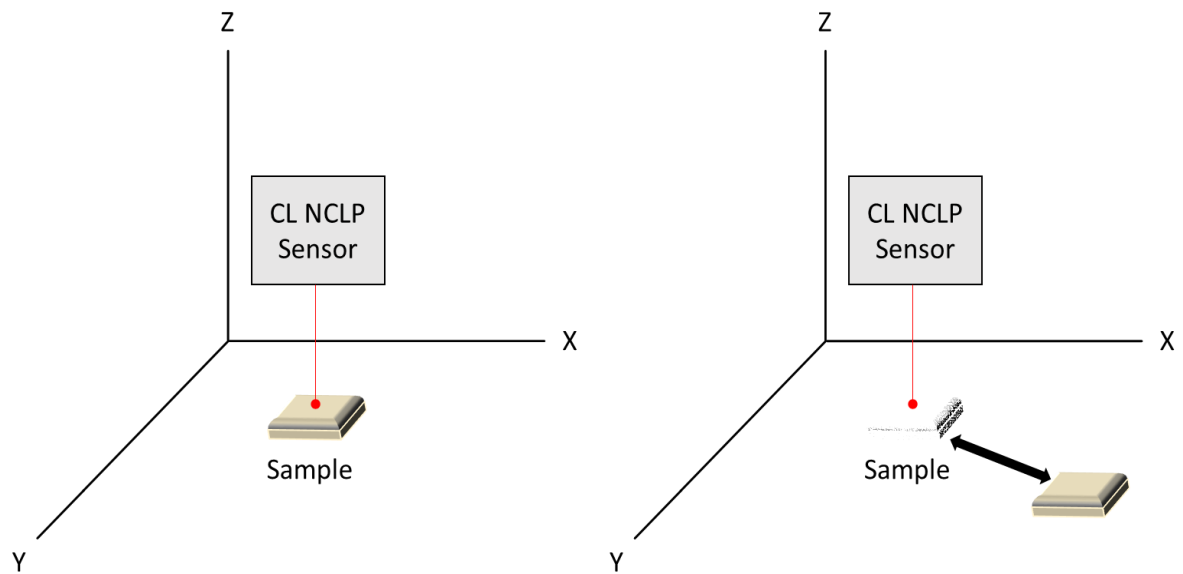
Figure 19 – Experimental setup for repeatability (left) and reproducibility (right) study. For the repeatability study, the sample was left untouched and NCLP programmed to scan the sample 10 times consecutively. For the reproducibility study, the sample was scanned, picked up and repositioned as close to the original position as possible, and scanned again; this was conducted 10 times consecutively
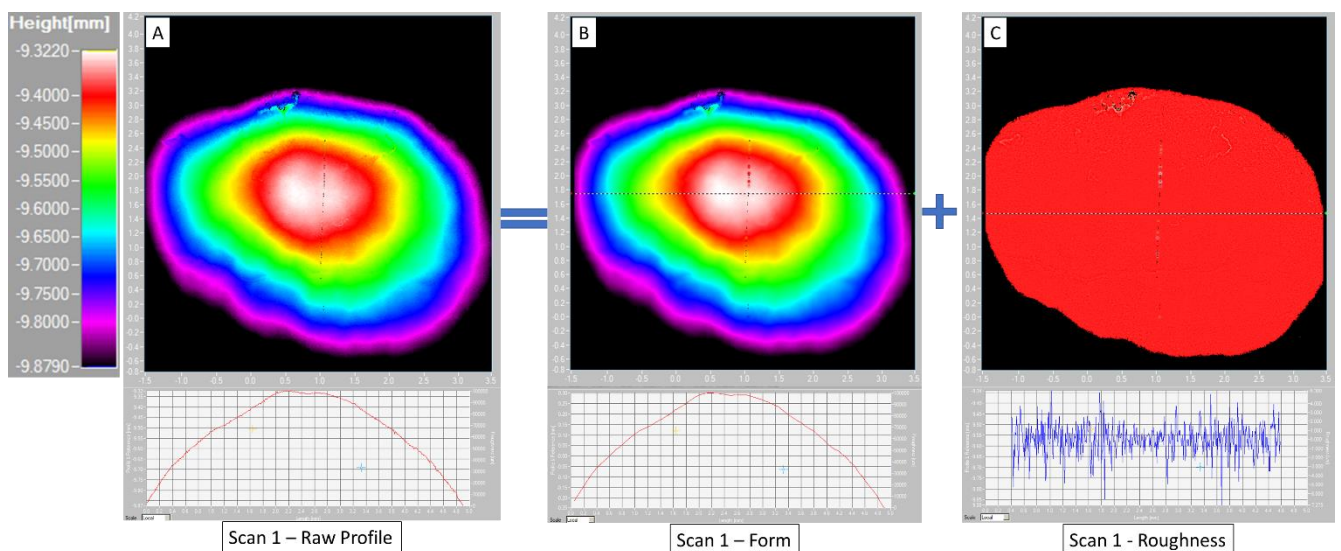
Figure 20 – The measurement grids produced after importing the data from the NCLP into surface metrology software Boddies. This indicates raw profile data (A), which after applying a Gaussian filter, can be separated into the form (B) and roughness (C) data sets; this can be used for further analysis.
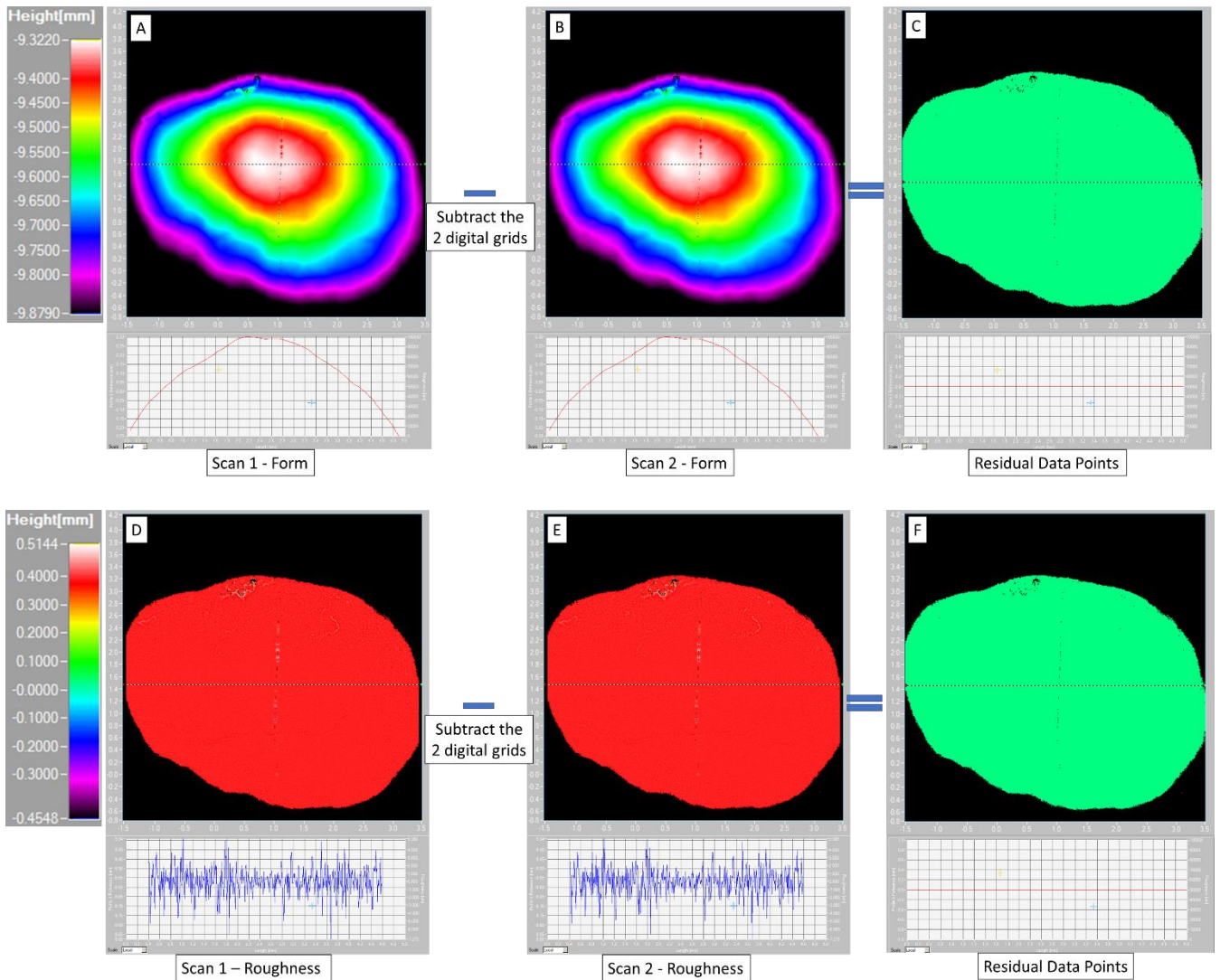
Figure 21 – If form (A, B) and roughness (D, E) data perfectly superimpose, after subtraction, there would be no residual data points remaining (C, F) and therefore no quantifiable average height differences. In this example, the same data sets were loaded twice and subtracted to demonstrate the lack of residual data points in the difference data set; shown in green (lack of residual points). In practice, this is impossible to achieve.
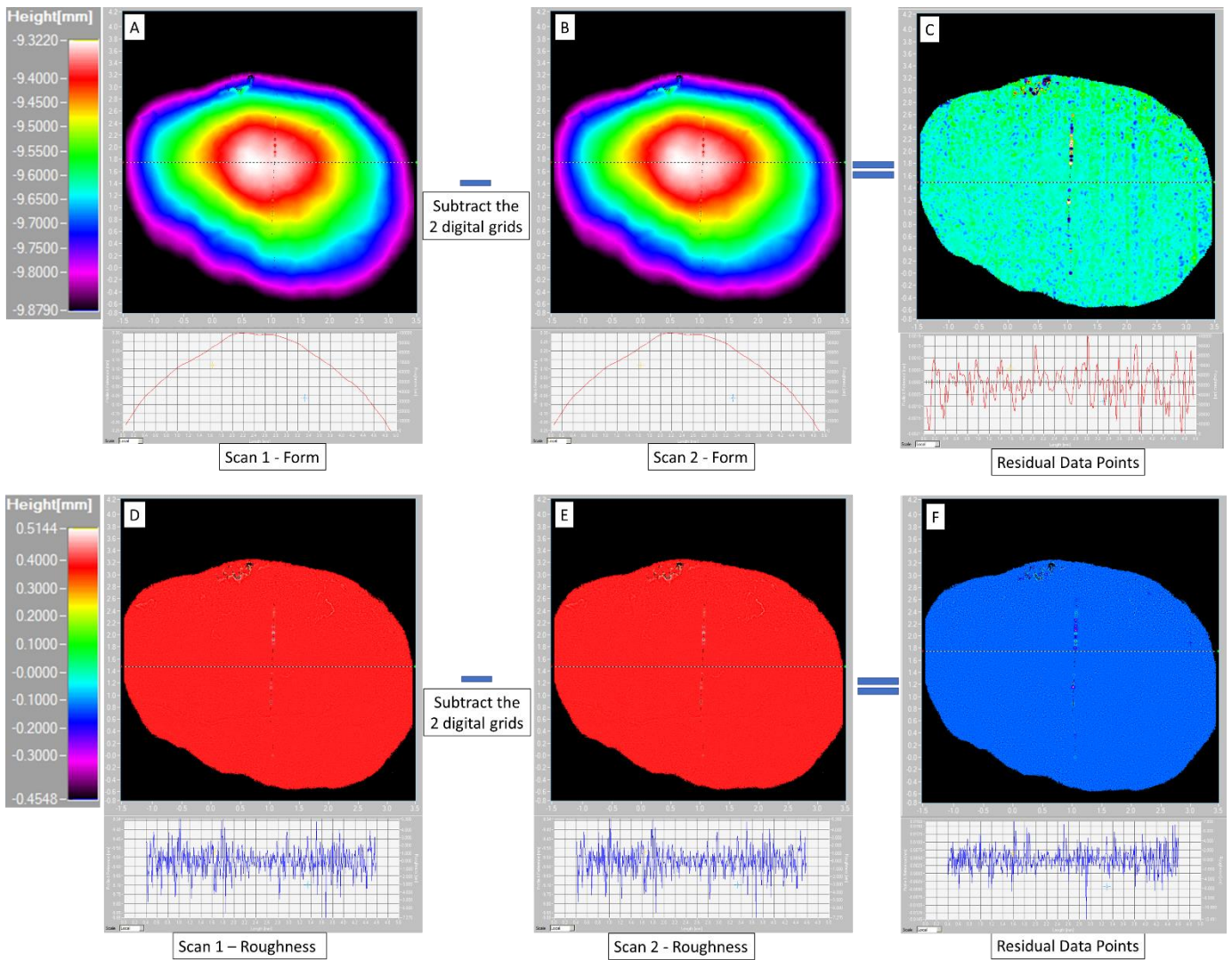
Figure 22 – In this example, two consecutive form (A, B) and roughness (D, E) data sets were subtracted to produce their respective difference data sets (C, F). Positional differences could be expressed using the average height difference for each measured point. The average height differences between the measurements could be quantified; 0.73 µm (C) and 2.63 µm (D). The difference in values obtained is due to the number of data points evaluated after filtering (more for roughness and fewer for form).

3.3.3 Investigation 2 – Characterising the influence of thermal variation on NCLP system stability

This investigation characterised the effect of thermal variation on NCLP sensor stability during scanning and was conducted by measuring NCLP sensor displacement (positional variation) against an optically flat surface placed under the measurement beam and displacement of the laser beam logged over several hours together with the changes in ambient temperature. The environmental control consisted of a laboratory air conditioning unit (RAV SM562KRT-E, Toshiba, Japan) with a temperature control set at 20 +/- 1°C. Temperature logging was conducted out-of-hours by one operator, to minimise variations in ambient temperature due to movement of people; the room was locked to ensure NCLP isolation. The experimental set up can be diagrammatically seen in Figure 23 and Figure 24.

A single calibrated optically flat surface (Edmunds Industrial Optics, USA) made of lithium-aluminosilicate glass with low coefficient of thermal expansion (α = 0.1 x10-6 ^{o}C-1), was used as the target surface. The surface was cleaned using an acetone rinse followed by distilled water and blown dry using dry nitrogen. The surface was arranged on the NCLP, perpendicular to the NCLP sensor laser beam at a distance of 6mm. A temperature and humidity logger (Lascar Electronics, UK) with 0.1 ^{o}C and 0.5 %RH resolution recorded environmental conditions at a rate of 0.2 Hz.

Temperature change and sensor positional variation were recorded at the NCLP as maximum peak to trough displacement (in μm). These were the highest and lowest values of distance between the NCLP laser beam and the optical flat and data captured continuously over the specified time. Thermal and positional variation were evaluated over three time periods which represent common scanning protocols in dental surface metrology: 1) short term (30s), 2) medium term (20 mins), and 3) long term (2 hrs) (Mullan et al., 2018b; Mistry et al., 2015). These scanning periods were investigated under two conditions: a) NCLP uncovered (open condition) and b) NCLP in protective Perspex enclosure (closed condition). The enclosure provided a basic level of protection from local air currents and thus stabilised the temperature at the NCLP.

The NCLP was programmed (Stages, Taicaan Technologies, Southampton, UK) to collect data on NCLP sensor positional variation at 25 Hz for the short-term measurement and 0.8 Hz for the medium- and long-term measurement. The number of data sets or samples collected over 30s, 20 mins, and 2 hrs were 690, 920, and 5500 samples respectively.

The data recorded in this investigation consisted of: temperature (^oC), positional variation (μm), and time of recording (hrs:mins:sec). This was tabulated in a spreadsheet (Microsoft Excel, Microsoft USA), and the standard deviation calculated for thermal variation (^oC) and positional variation (μm) for each time period. This allowed for determination of the influence of thermal effects according to the scanning time.
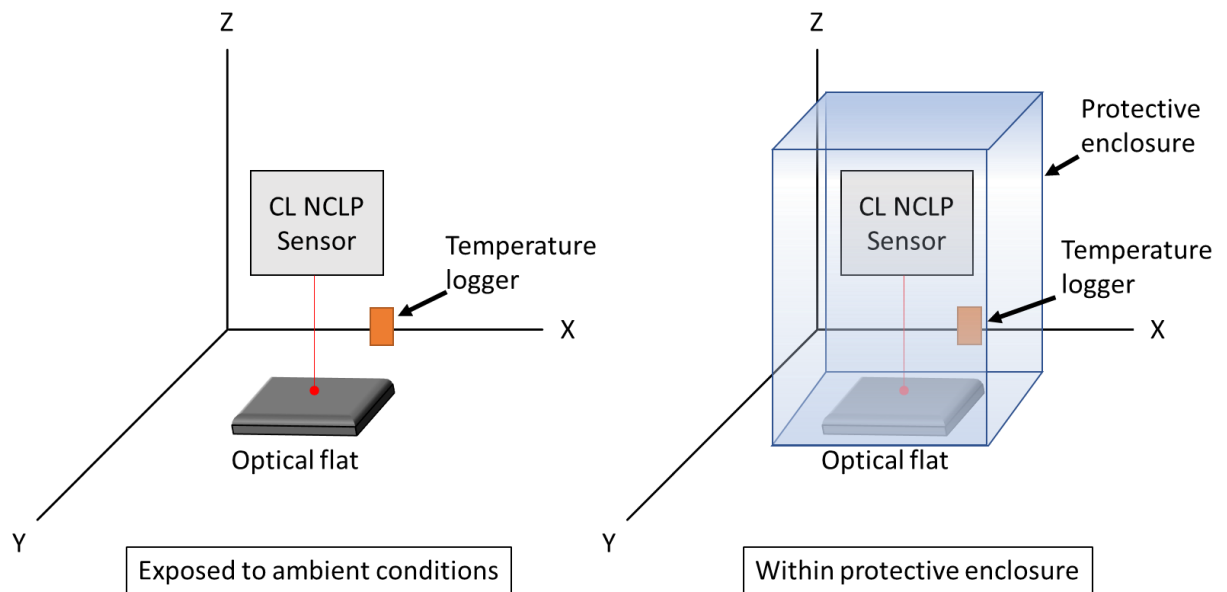
Figure 23 – Experimental set up to determine NCLP sensor displacement when exposed to ambient conditions, compared to within a protective enclosure.
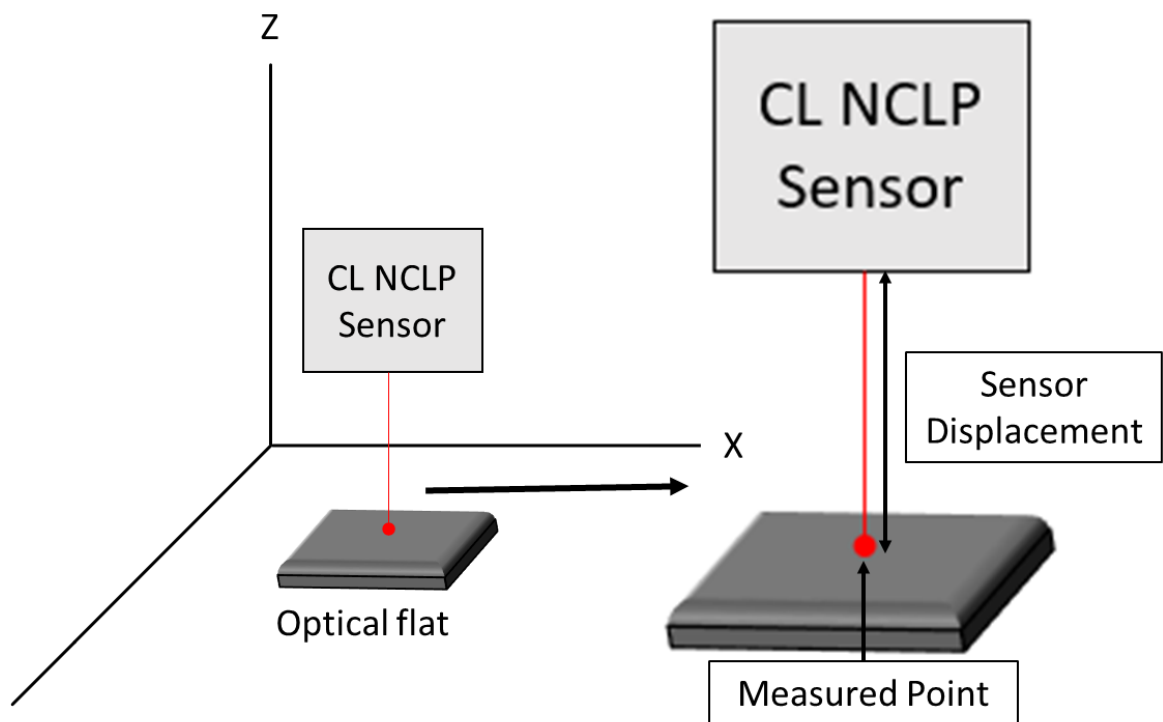
Figure 24 – The data captured is in the form of peak light intensity obtained from the laser light returned from the optical flat, indicating the displacement (µm) from the target surface. One data sample is obtained when one laser spot displacement is measured over a specific evaluation period. The data is in the form of maximum peak to trough distance of the light returned to the sensor. Over an evaluation period of 30s, 20-mins, and 2-hrs, the number of data samples measured were 690, 920, and 5500 samples respectively.

3.3.4 Investigation 3 – Determining optimum scanning parameters for surface form measurement on natural human enamel

The influence of changing the NCLP step-over distance was assessed for measuring surface form on natural enamel. A constant measurement area (1.0x1.0mm) on a natural enamel sample was utilised. The step-over distances (µm) evaluated in *x* and *y* were: 300, 150, 100, 80, 40, 20, 10, 8, 4, 2, 1, using medium and low precision mode. For each scan, the following measurements were recorded: total number of points measured, raw Sa value, and scan duration.

Once the optimum step over distance was obtained (10 µm), it was kept constant, the scan dimensions were then altered to determine which was optimum for surface form measurement on natural enamel. A natural enamel sample was scanned with scan dimensions: 4.5x4.5mm, 4.0x4.0mm, 3.5x3.5mm, 3.0x3.0mm, using 10 µm step over distance. For each scan, the following measurements were recorded: total number of points measured, raw Sa value, and scan duration.

3.3.5 Investigation 4 – Characterising effects of early citric acid-induced enamel erosion on natural human enamel

3.3.5.1 Novel barrier creation

Two methods were tested for suitability in isolating the enamel surface to produce reference areas or uneroded enamel and allow for the formation and measurement of an isolated enamel lesion: strips of PVC tape (used and described in Chapter 2 Section 2.3.1) and a hole-punched circle in clear PVC tape (Figure 25). Holes were punched using a 1.5mm surgical biopsy punch (Kai Medical, Kai Industries ltd, Japan) and placed over the highest peak of the enamel sample; known as the bulbosity of the enamel sample. Twenty samples were created, 10 isolated using strips of PVC tape, and 10 using hole-punched PVC tape, before being immersed for 5 minutes in 0.3% citric acid, pH 3.2, under constant agitation and subsequently washed with deionised water (Chapter 2 Section 2.3.1). Samples were then dried (5s oil-free air) and analysed for the presence/attachment of the tape to the enamel surface post-erosion, and water-tightness (no seepage under the tape). After this, the repeatability of creating a hole-punched circle in the clear PVC tape was investigated for the size of the hole produced (diameter) and whether taping on the natural tooth alters its dimensions (compared to a flat surface).

Ten holes were punched into clear PVC tape which was mounted flat onto a glass microscopy slide. Each hole was scanned using NCLP scan dimensions (x,y) 3.0 x 3.0mm and settings 601x601 points, 5 μm step-over in low precision mode. These settings were chosen to ensure tape edges were scanned for evaluation. Each data set was adjusted using metrology software, (Boddies v1.92, Taicaan, Southampton, UK), leaving only the area of the hole. From this the surface area of the hole was

determined, the radius of the circle was calculated using the equation $r = \sqrt{\dfrac{A}{\pi}}$ (assuming a constant radius), and the diameter was calculated using the equation $d = 2r$. This method was repeated with the hole-punched PVC tape (n=10) placed on natural enamel samples (n=10). The tape was positioned so that the 1.5mm hole was placed over the bulbosity of the enamel sample; defined as the highest peak of the natural enamel surface using TSM. Each taped sample was visually assessed for air-voids/gaps at the tooth-tape interface using OCT in live scanning view/mode. Figure 26 illustrates the 10 punched holes in PVC tape mounted on a microscope slide (A), and an example on a natural enamel surface (B), the central exposed region of enamel (C), and an example of a B-scan indicating the direct contact between tape and enamel surface (D). In the OCT B-scan, there is direct contact between tape and tooth surface with no evidence of an air gap present.
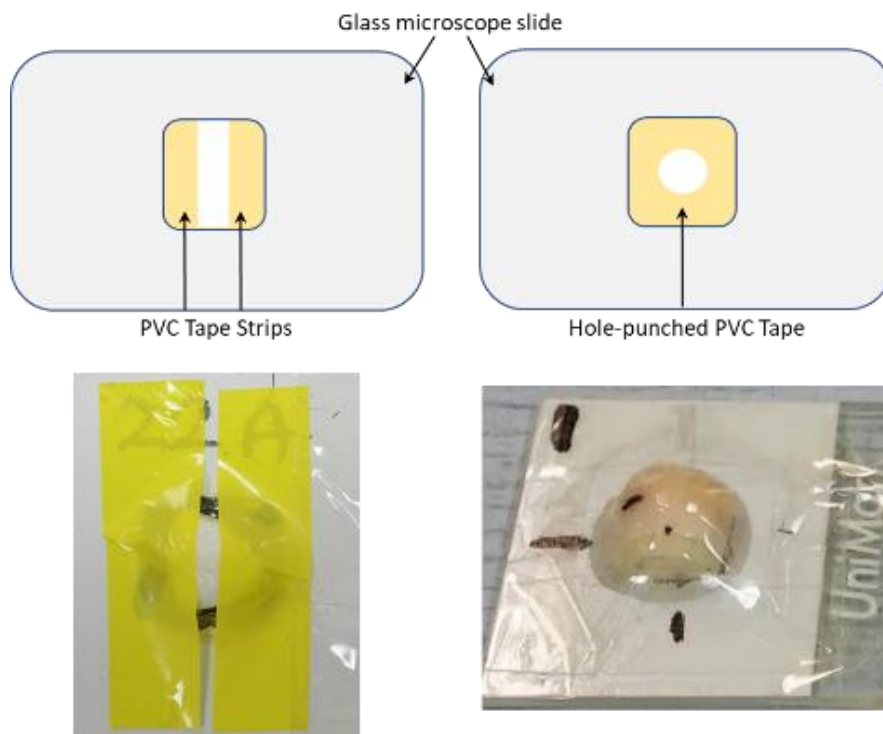
Figure 25 – Comparison between the experimental set up for taping on natural enamel. Strips of PVC tape (left) compared with hole-punched PVC tape (right)

Figure 26 – Barrier method analysis using clear PVC adhesive tape:

(A) 10 1.5mm holes in PVC tape adhered on microscope slide for analysis
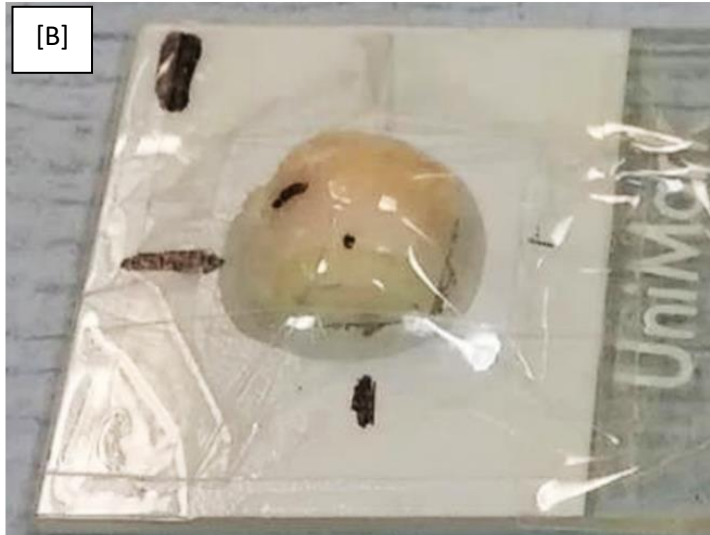
(B) natural enamel sample with PVC adhesive barrier and 1.5mm hole placed on the highest peak of the tooth.
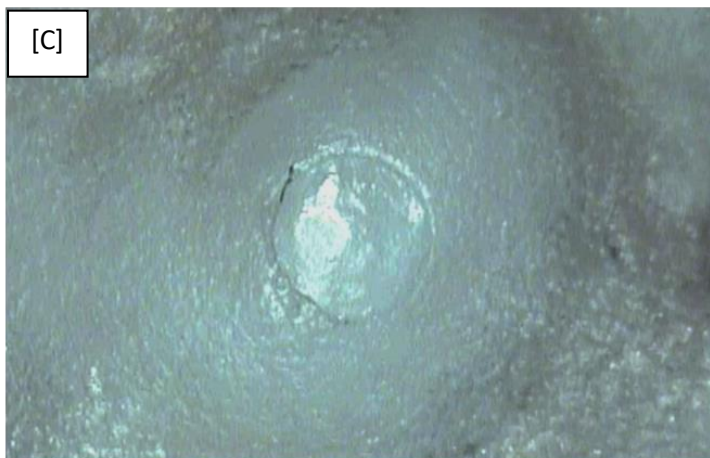
(C) close up of exposed enamel region on bulbosity of natural enamel sample
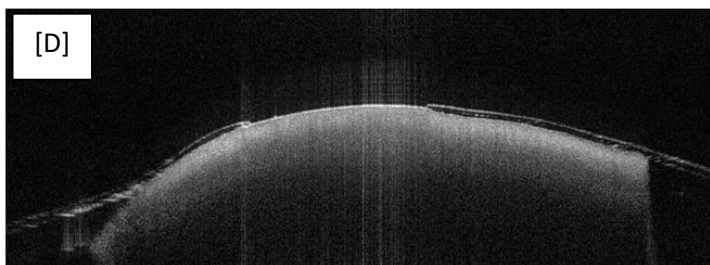
(D) A B-scan of the taped sample. For illustrative purposes, the tape is indicated in red (bottom), and the epoxy resin adhesive in green. There is no evidence of an air gap between the tape and tooth or epoxy adhesive (green).
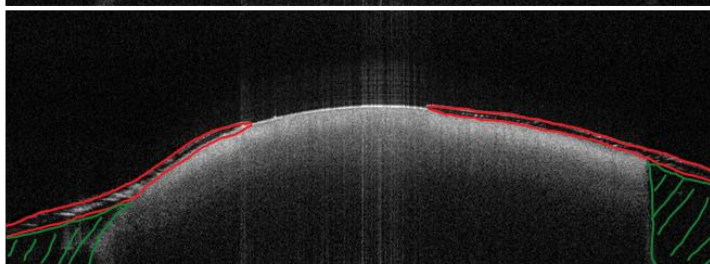
Twelve natural enamel samples were prepared as described in Section 2.2.1 and isolated using hole-punched PVC tape as described in Section 2.5.1. All samples were scanned before acid immersion to provide baseline data sets (surface form and roughness) for comparison to after erosion scan data. Citric acid (0.3%w/w) erosive solution was prepared according to the method described in Chapter 2 Section 2.3.2. and samples immersed for three cycles, of 5 mins per cycle; resulting in cumulative erosion times of 5, 10, 15 mins.

The samples were immersed in 10 ml of citric acid (per tooth) and agitated using an orbital shaker (62.5 RPM, Stuart mini-Orbital Shaker SSM1, Bibby Scientific, England), for 5 minutes before rinsing with deionised water (pH 5.8) for 2 minutes and left to air dry. Afterwards the PVC tape was carefully removed, and samples were replaced in the scanning jig, and surface form and roughness measurements recorded, and the process repeated after each erosion cycle.

3.3.5.3   Surface form change measurement and characterisation

For each NCLP data set, the first 15 lines of data was trimmed, loaded into one of three metrology software packages according to the analysis method, and transformed into a 3D surface (digital version of the enamel surface). Three methods for determining enamel loss were used: 1) scan superimposition and difference analysis using Geomagic (v 2014, Geomagic Inc, North Carolina, USA); 2) scan alignment and profile extraction analysis using MountainsMap (DigitalSurf, France) and 3) scan subtraction and residual profile extraction analysis using Boddies (v1.92, Taicaan, Southampton, UK) (Rodriguez et al., 2012a; Holme et al., 2005; Stenhagen

et al., 2010). The operator was blinded to each treatment, conducted all analyses, and samples were randomised prior to analysis.

Enamel loss was defined as step height using: mean Z-change, mean 3D total deviation, single mid-point step height (SPSH), mean single mid-point step height (mean SHC) and 3D step height. All values were calculated in µm.

3.3.5.3.1   Geomagic Method

The data were loaded into superimposition software which automatically converted the point cloud data into a polygon mesh. To superimpose the data sets, an initial best fit alignment using 300 randomly selected data points was conducted, to minimise alignment error between the baseline and eroded data sets. A more precise alignment was then performed using 1500 additional data points. After superimposition, a region of interest, 0.2 mm diameter, was selected at the central region of the eroded area; this ensured minimisation of the effects of the natural topographical variation between samples. Change between aligned scans was measured for each erosion time compared to baseline using two outputs: mean Z-change (measured change in Z) and mean 3D total deviation (measures change in X, Y, Z). The mean and SD were calculated for all time points (Figure 27).
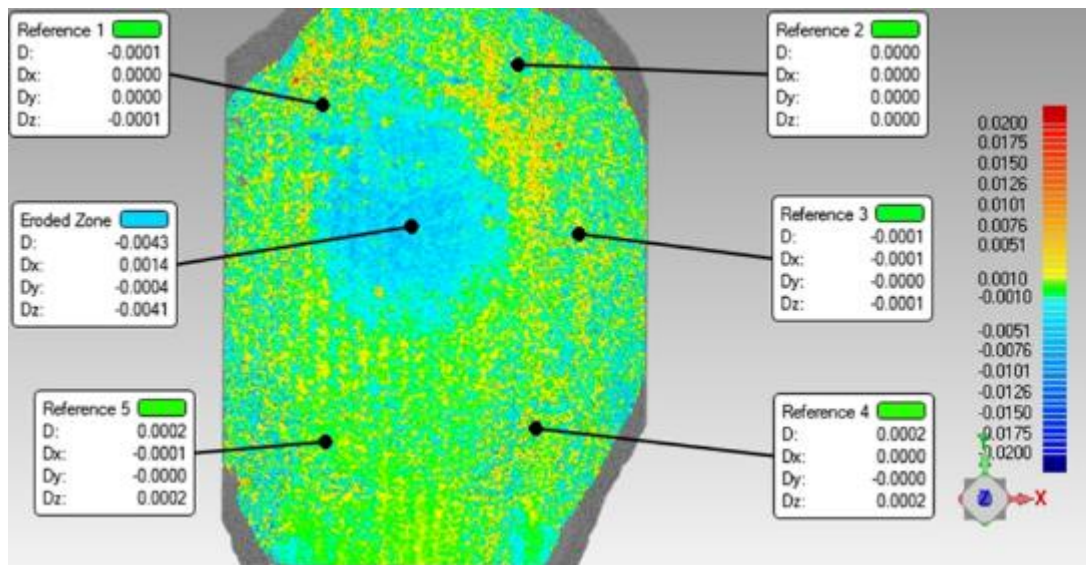
Figure 27 – Representative example of a sample with its associated dental erosion lesion using superimposition, in blue, green denotes no change, whilst yellow denotes gain post erosion. Surface form change (enamel loss) is depicted by 3D total deviation (D) and Z-deviation (Dz). The central eroded region and 5 reference regions have been analysed for allow for erosion versus non-eroded comparison.

3.3.5.3.2   MountainsMap Method

All scans were loaded into surface metrology software which automatically created a 3D point cloud. Before scan alignment, offset analysis was performed between baseline and each erosion data set. Firstly, a 0.8 µm Gaussian filter for roughness was applied to all data sets, outlier points were removed using a denoising filter; the filtered roughness data points were then processed together to form a composite series of images. The offset and rotational differences between each roughness data set were then determined automatically by the software. These offset and rotational values were used to align the original baseline and erosion data sets. The erosion data was subtracted from the baseline data to produce a difference/residual data set. Surface levelling was performed using a linear least squares plane of best fit method, excluding the 1.5mm eroded area. Using the residual data, step height at the eroded area was then calculated using mean Z-change (ZMean), and 3D step height (ISO-5436). Mean and SD for both outputs was calculated for all the data sets at each time point (Figure 28).
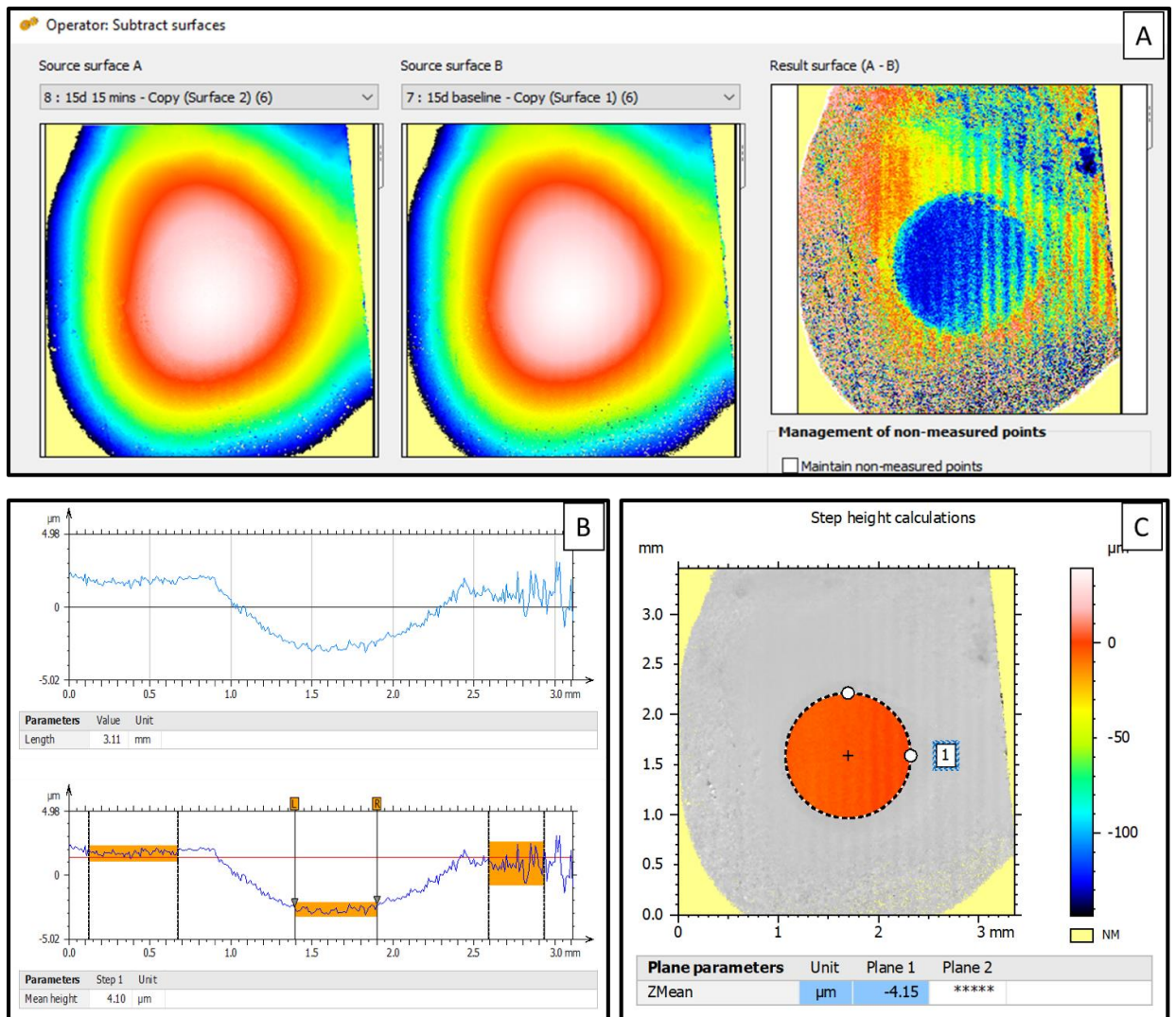
Figure 28 – Representative example of a sample with its associated erosion lesion (15 mins erosion) using scan alignment and subtracted to form a residual data set (A), which was levelled (and used for step height analysis). A mean profile was extracted to calculate 3D step height according to ISO 5346-1 (B), and a non-ISO step height was calculated on the residual data set using mean Z-change (ZMean) (C) which provides the mean difference in Z between plane 1 (the eroded surface) and plane 2 (automatically defined by the software as 0)

Data sets were loaded into surface metrology software as no prior scan alignment was required with the data. Erosion scans for each time point were subtracted from the respective baseline scans to produce a residual data set for each erosion time. The residual data was then levelled using a best fit method, with the eroded area excluded. Step height of the eroded are was calculated by comparing the height differences along: a single horizontal line of reference (single mid-point step height, SPSH) (O'Toole et al., 2015), an average across 10 horizontal lines of references across the eroded area (mean single mid-point step height, mean SHC; (Mistry et al., 2015), and the entire eroded area (3D step height, 3D SHC; (Sar Sancakli et al., 2015). An example of the method and measurement output can be seen in Figure 29.
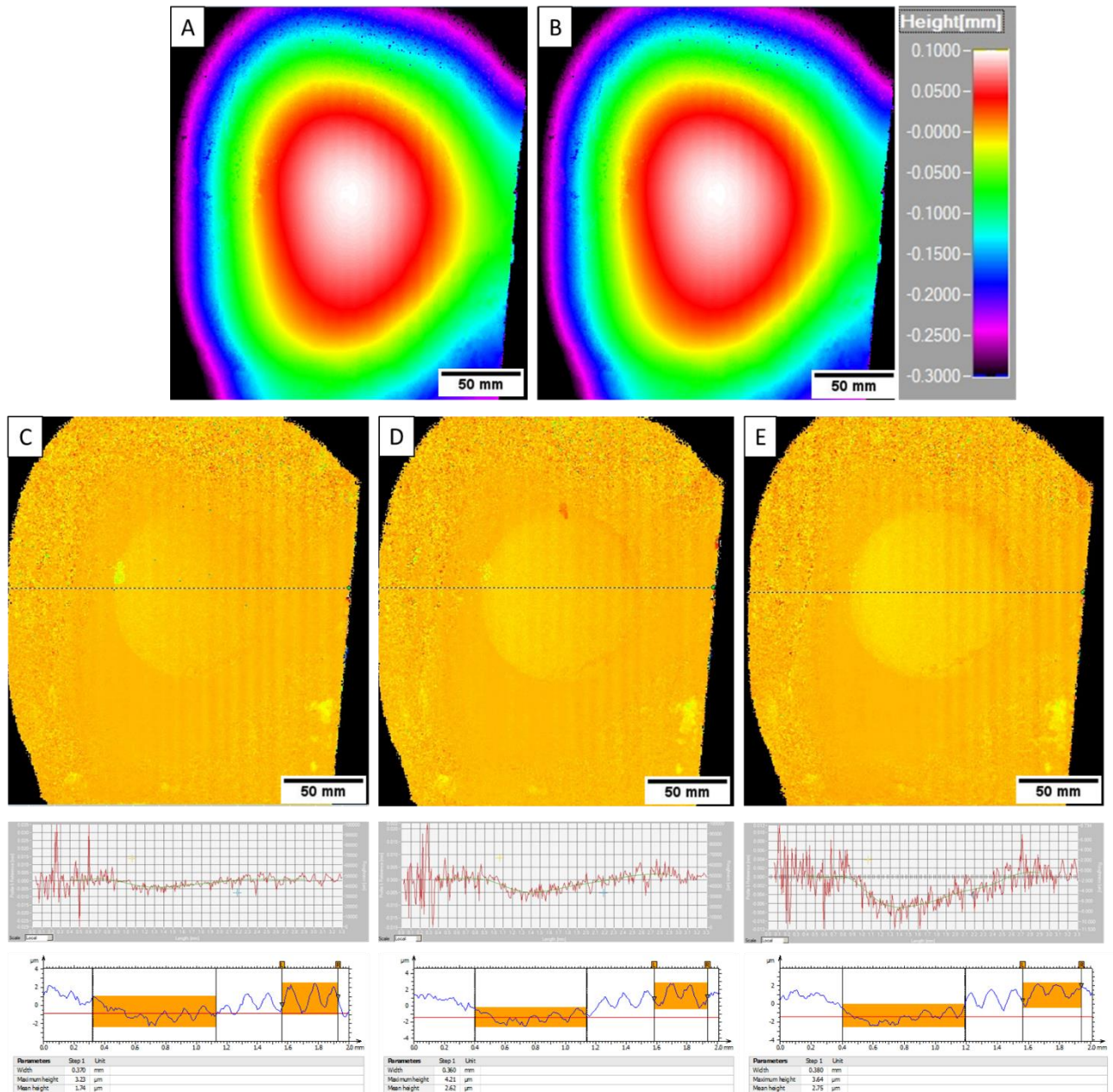
Figure 29 – Representative example of a sample undergoing longitudinal assessment of erosion.

Before erosion (A) and after 5 mins erosion (B) are subtracted to form difference image (C), this

process is continued with 10- and 15-mins erosion scans to produce difference images (D) and (E).

A single line mid-point step height is demonstrated with the line profiles (dotted line in C, D, E),

whilst 3D step height is represented as the height difference between the regions highlighted in

3.3.6 Surface roughness change measurement and characterisation

Surface roughness was measured following previously published protocols using surface metrology software (Boddies v1.92, Taicaan, Southampton, UK) (Austin et al., 2016; Mullan et al., 2017a). A cluster of five scans each measuring 0.2 x 0.2 mm (0.04 mm^2) was selected in the central peak of each natural enamel sample and scanned using a 4 µm step-over distance in low precision mode. This was performed using a custom image acquisition macro written within the motion control software (Stages^{TM}, TaiCaan Technologies, Southampton, UK) together with the assistance of a live video microscope within the NCLP system. This central cluster method was previously validated as representative of the natural enamel surface for measuring change in surface roughness (Mullan et al., 2017a).

A 25 µm Gaussian filter was applied to remove form data, leaving only roughness data. 3D roughness (S$_a$) was determined for each scan using metrology software (Boddies v1.92, Taicaan Technologies, Southampton, UK) and mean Sa calculated for each sample from the 5 scans according to ISO 25178 (Mullan et al., 2017b; Austin et al., 2016). This was done for all samples, before and after erosion cycle. The mean (SD) surface roughness was then calculated for each sample at baseline, 5, 10, and 15 mins cumulative erosion.

3.3.7 Surface reflectivity measurement and characterisation

Optical coherence tomography (OCT) was conducted, before and after each erosion cycle, using a swept-source multi-beam clinical OCT machine (VivoSight™ Michelson Diagnostics, Kent, UK) utilising a near infra-red laser (1305 nm) with optical resolution <7.5 µm. Samples (n=2, per group) were scanned in a raster pattern to produce B-

stack volumes comprising 1000 B-scans of (x,z) dimension (4x1mm) with y-step-over 4 µm; the resulting B-stack volumes consisted of dimension 4 x 4 x 1 mm(x,y,z). A custom written stack analysis programme extracted single full profile peak intensity average images from each B-stack volume; known as surface projection or reflection images. An automated macro using ImageJ (ImageJ, (Abramoff et al., 2004) was created to analyse the peak intensity of the designated region of interest (1.5mm diameter eroded region) before and after each erosion cycle. Peak intensity (reflectivity) analysis consisted of normalising all grey values against baseline and this was converted into a percentage; 100% reflectivity vs baseline indicated no erosion occurred at baseline. The percentage increase or decrease in normalised percentage peak intensity was determined for all erosion cycles(Schneider et al., 2012). An example is seen in Figure 30.

3.4   Statistical methods

Statistical analysis was conducted using GraphPad Prism 7 (GraphPad Software Inc, California, USA). Data were assessed for normality using Komogorov-Smirnov and Shapiro-Wilks tests, and visually assessed with histograms and box plots. All the data were found to be normally distributed, and therefore mean and standard deviation was reported, inter-group analysis was conducted using one-way ANOVA with post-hoc Tukey test for multiple comparisons.
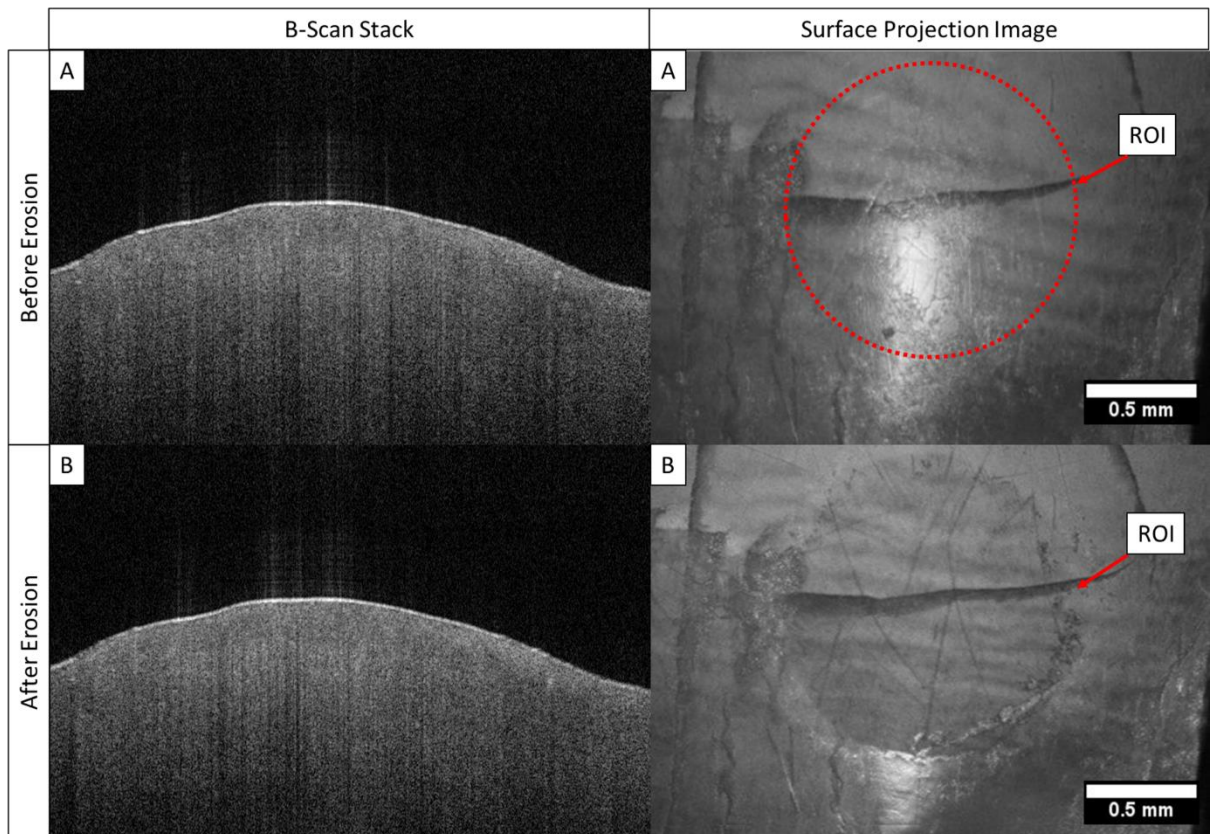
Figure 30 – Example of B-scan stack (left) and the associated surface projection images for baseline (A) and after 15 mins (B) erosion. The red circle is the region of interest (ROI) used for analysis, kept constant and saved within ImageJ. Peak intensity within the ROI was measured using ImageJ at each time point. In this sample very little difference between before/after-erosion B-stacks could be visualised, whilst

3.5 Results

3.5.1 Investigation 1 – Detection threshold determination of NCLP

For repeatability, the mean (SD) surface form difference between each scan was 0.14 (0.05) µm and the NCLP repeatability (surface form) was 0.29 µm. Similarly, the mean (SD) surface roughness difference was 0.03(0.01) µm and the NCLP repeatability (surface roughness) was 0.06 µm.

For reproducibility, the mean (SD) surface form difference between each scan was 0.23(0.07) µm and the NCLP reproducibility (surface form) was 0.44 µm. Mean (SD) surface roughness difference was 0.03(0.02) µm and the NCLP reproducibility (surface roughness) was 0.09 µm.

3.5.2 Investigation 2 – Characterising the influence of thermal variation on NCLP system stability

Figure 31 and Table 3 show thermal variance and positional variance for each evaluation period. Laboratory air conditioning produced cyclic temperature variation (20 +/- 1 ºC).

3.5.2.1 NCLP Open

During short term (30s) evaluation, thermal variance was below the resolution of the temperature logger (<0.1 ºC), with positional variation (SD) of 0.014 µm. During medium-term (20 mins) evaluation, thermal variance (SD) of 0.260 ºC was detected and corresponded with a positional variation (SD) of 0.556 µm. During long-term (2 hrs) evaluation, thermal variance (SD) of 0.473 ºC and positional variation (SD) of 1.049 µm was detected.

During short term (30s) evaluation, thermal variance was below the resolution of the

temperature logger (<0.1 °C), with positional variation (SD) of 0.013 µm. During

medium-term (20 mins) evaluation, thermal variance (SD) of 0.053 °C was detected

and corresponded with a positional variation (SD) of 0.098 µm. During long-term (2

hrs) evaluation, thermal variance (SD) of 0.069 °C and positional variation (SD) of

0.164 µm was detected.

	Scanning Evaluation Period					
	30 seconds		20 minutes		2 hours	
NCLP Condition	Thermal variance [SD] (ºC)	Positional Variation 690 samples [SD] (µm)	Thermal Variance [SD] (ºC)	Positional Variation 920 samples [SD] (µm)	Thermal Variance [SD] (ºC)	Positional Variation 5500 samples [SD] (µm)
NCLP Open	<0.1 (SD = 0)	0.014	0.260	0.556	0.473	1.049
NCLP Closed	<0.1 (SD = 0)	0.013	0.053	0.098	0.069	0.164

Table 3 – thermal variance and NCLP sensor positional variation over three scanning

evaluation periods: short-term (30s), medium-term (20 mins), and long-term (2 hrs).
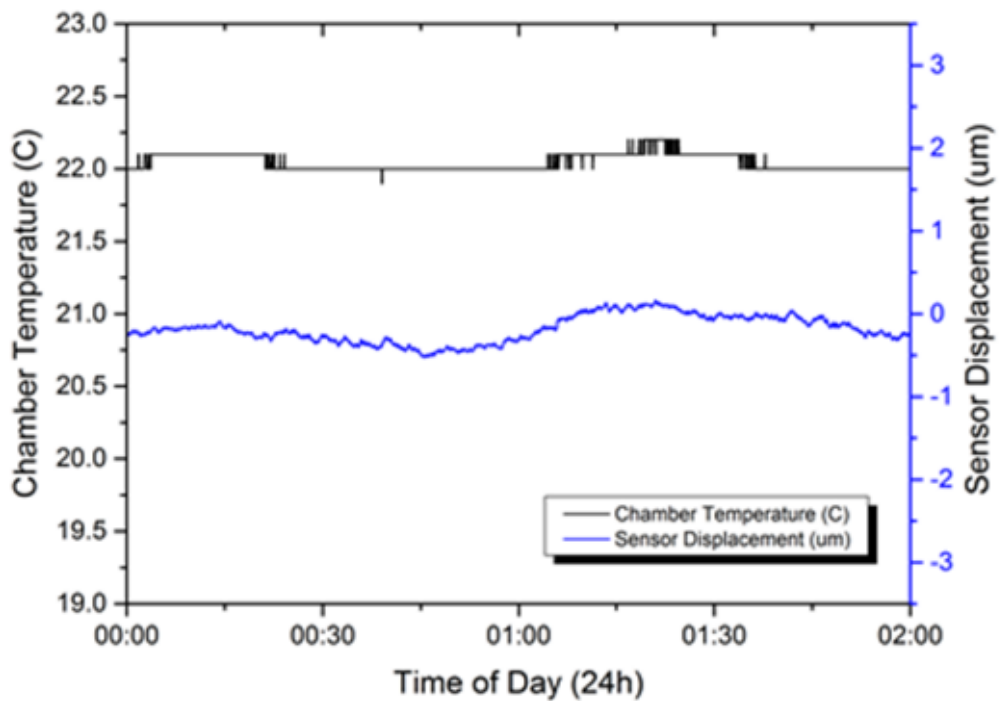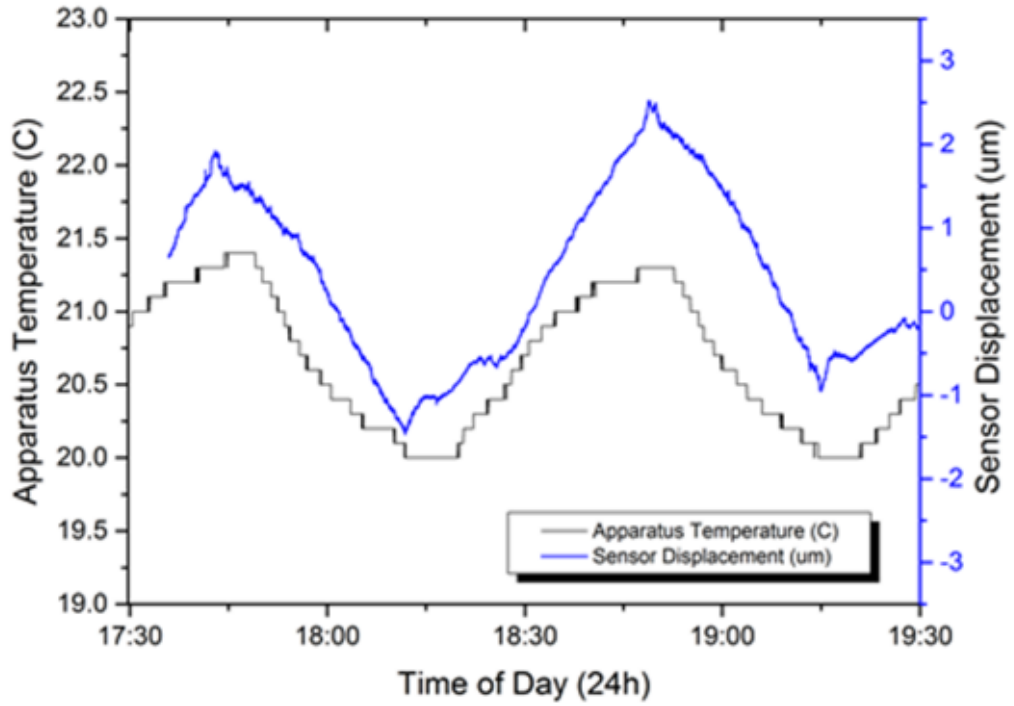
Figure 31 – Graphs of ambient temperature and the sensor displacement with NCLP open (top) and NCLP closed (bottom).

3.5.3 Investigation 3 – Determining optimum scanning parameters for surface form measurement on natural human enamel

Figure 32 and Table 4 show the total number of measured points, raw Sa value, and scan duration for each scan using 1.0 x 1.0 measurement area. Decreasing step over distance increased the total number of measured points, raw Sa value, and scan duration of each scan. Step over distance of 10 µm provided the optimum balance between scan duration (3 mins 45s, LP and 7 mins 04s, MP), total number of measured points (10,201), and raw Sa value (460.33 µm). This was determined as the optimum step over distance for surface form measurement.

Figure 33 and Table 5 show the total number of measured points, raw Sa value, and scan duration for each scan using each measurement area. As scan dimensions decreased, this resulted in a reduction in the total number of points and duration. The black regions in Figure 33 demonstrated regions of non-measured points, these areas reduced as scan dimension was decreased. The optimum scan dimension of 3.5 x 3.5 mm provided optimum balance between total number of points measured (123,201), scan duration (15 mins 23s, LP, and 50 mins 43 s, MP).
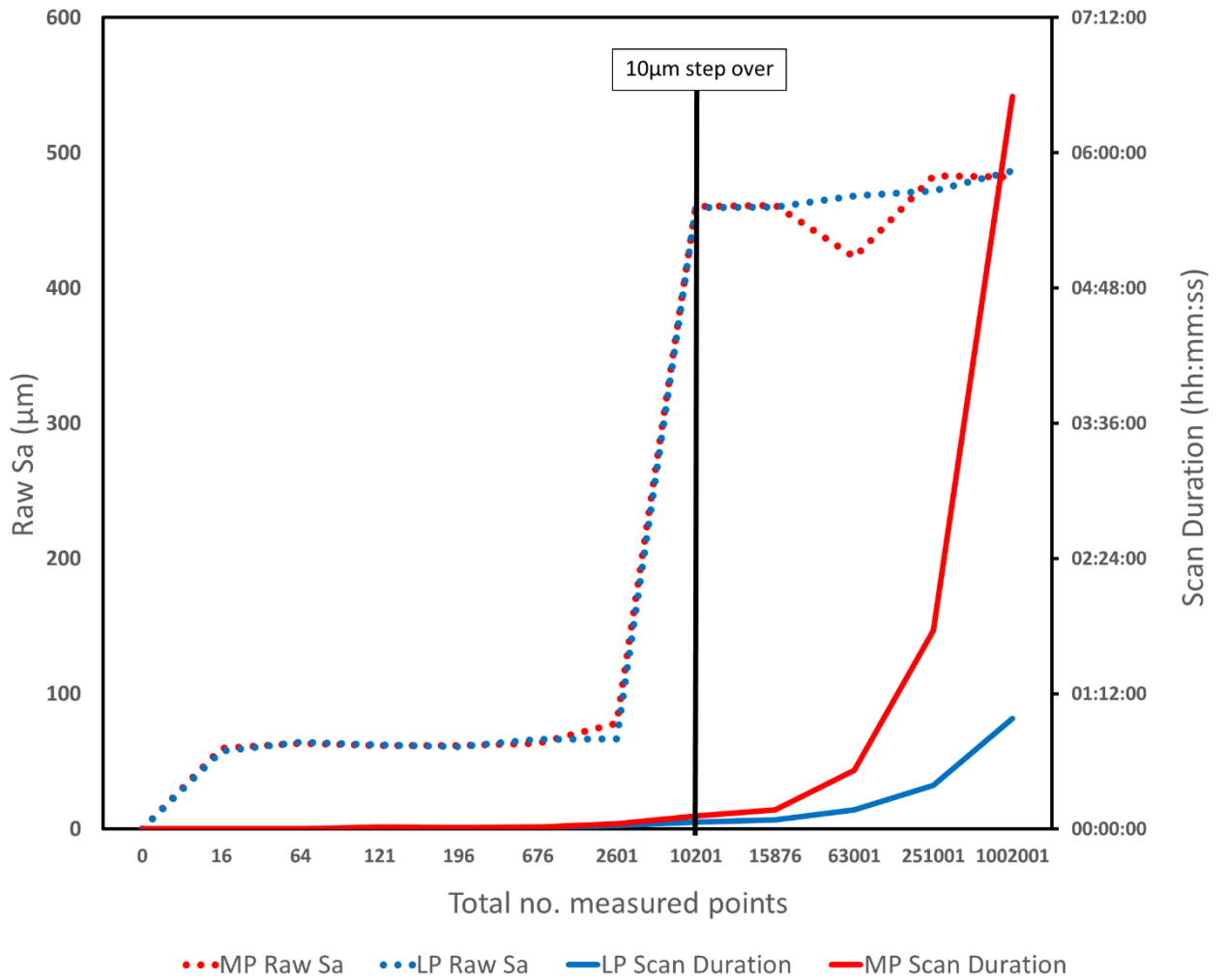
Figure 32 – Graph indicating raw Sa value and scan duration according to the total number of measured points for each scan for the 1.0x1.0mm scanning grid. The total number of measured points increased as step-over distance decreased. Similarly, scan duration increased rapidly after 10 µm step over (10,201 total no. measured points), and raw Sa value appeared to plateau.

Scan grid 1.0x1.0mm					Scan Duration (hours:mins:sec)		Raw Sa value (μm)	
x-step over distance (um)	No. points measured in x	y-step over distance (um)	No. points measured in y	Total no. points measured in scan	LP Scan Duration	MP Scan Duration	LP	MP
0	0	0	0	0	00:00:00	00:00:00	0	0
300	4	300	4	16	00:00:09	00:00:09	57.72	59.8
150	8	150	8	64	00:00:11	00:00:11	64.22	63.57
100	11	100	11	121	00:00:22	00:00:53	62.05	61.82
80	14	80	14	196	00:00:31	00:00:42	60.79	61.57
40	26	40	26	676	00:00:54	00:01:02	66.18	63.32
20	51	20	51	2601	00:01:49	00:02:47	66.87	78.33
10	101	10	101	10201	00:03:45	00:07:04	459.33	460.33
8	126	8	126	15876	00:04:45	00:10:05	460.12	461.27
4	251	4	251	63001	00:10:09	00:31:19	468.13	422.69
2	501	2	501	251001	00:23:09	01:45:32	471.79	482.83
1	1001	1	1001	1002001	00:58:53	06:29:54	486.84	482.12

Table 4 – Comparison of step-over distance in x and y, the total number of points measured in each scan, the scan duration, and raw Sa value for each scan. The total number of points was calculated by multiplying the number of points measured in x and y. As step over distance decreased, total number of points in each scan increased, scan duration increased, and raw Sa value increased. Using 10 μm step over distance provided a good balance between total number of points measured, scan duration and raw Sa value. LP – low precision mode, MP – medium precision mode.

						Time taken for scan (hours:mins:sec)	
Scan dimension (x,y) um	x-step over distance (um)	No. points measured in x	y-step over distance (um)	No.points measured in y	Total no. points measured in scan	LP Scan Duration	MP Scan Duration
5.0 x 5.0	10	501	10	501	251001	00:22:48	01:35:02
4.5 x 4.5	10	451	10	451	203401	00:20:04	01:18:16
4.0 x 4.0	10	401	10	401	160801	00:16:59	01:04:18
3.5 x 3.5	10	351	10	351	123201	00:15:23	00:50:43

Table 5 – Comparison of scan dimension (x,y), number of points measured in x and y, total number of points for each scan, and the duration of each scan. Step over distance was kept constant at 10 μm. As scan dimension was reduced, total number of points measured decreased, scan duration also decreased in both LP and MP scan modes. LP – low precision mode, MP – medium precision mode.
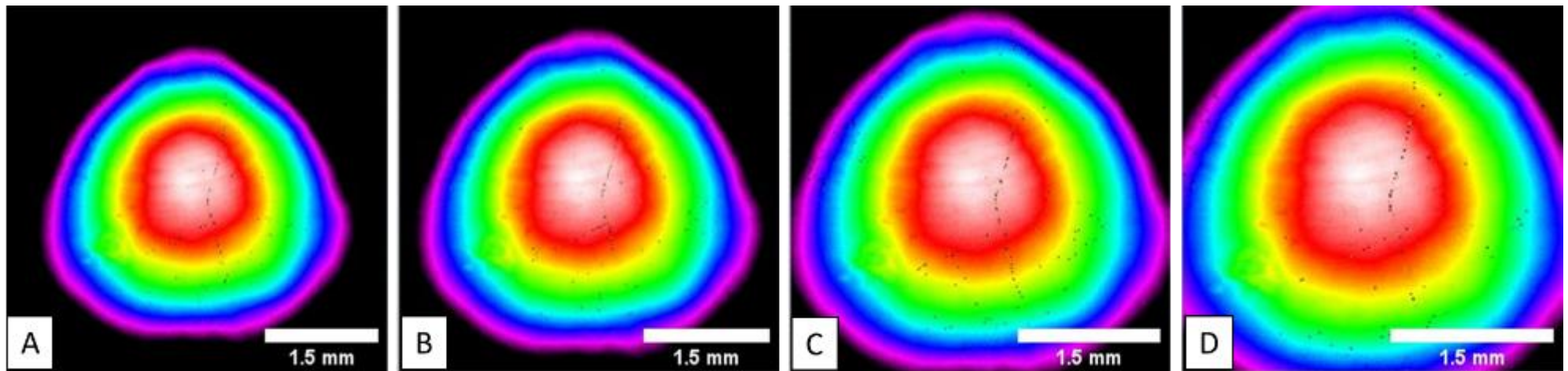
Figure 33 – Comparison of NCLP scan data obtained using the same step over distance (10 µm) but varying scan dimensions: (A) 5.0 x 5.0mm, (B) 4.5 x 4.5 mm, (C) 4.0 x 4.0 mm, and (D) 3.5 x 3.5 mm. Reducing scan dimensions results in reduction of unmeasured regions (in black) and reduces scan duration. Scan dimensions 3.5 x 3.5 mm provides balance between total number measured points (point cloud size) and scan duration. LP – low precision mode, MP – medium precision mode.

3.5.4 Investigation 4 – Characterising effects of early citric acid-induced enamel erosion on natural human enamel

3.5.4.1 Barrier creation

After 5 minutes erosion, the hole-punched tape remained on all samples whilst the PVC strips all de-bonded after the first 10s of the erosion. Hole-punch taped samples were visualised analysed under OCT live-scanning mode, there was no evidence of air gap or de-bonding from the enamel surface. Table 6 shows the repeatability hole-punched PVC barrier using the surgical biopsy punch. Figure 34 demonstrates the difference between the barrier placed flat on a glass microscope slide compared with on a natural tooth sample. The hole was created with a mean (SD) 1.48(0.03) mm when analysed flat on the microscope slide; and after application on to the natural enamel surface the size of the hole increased to mean (SD) diameter of 1.74(0.10) mm.
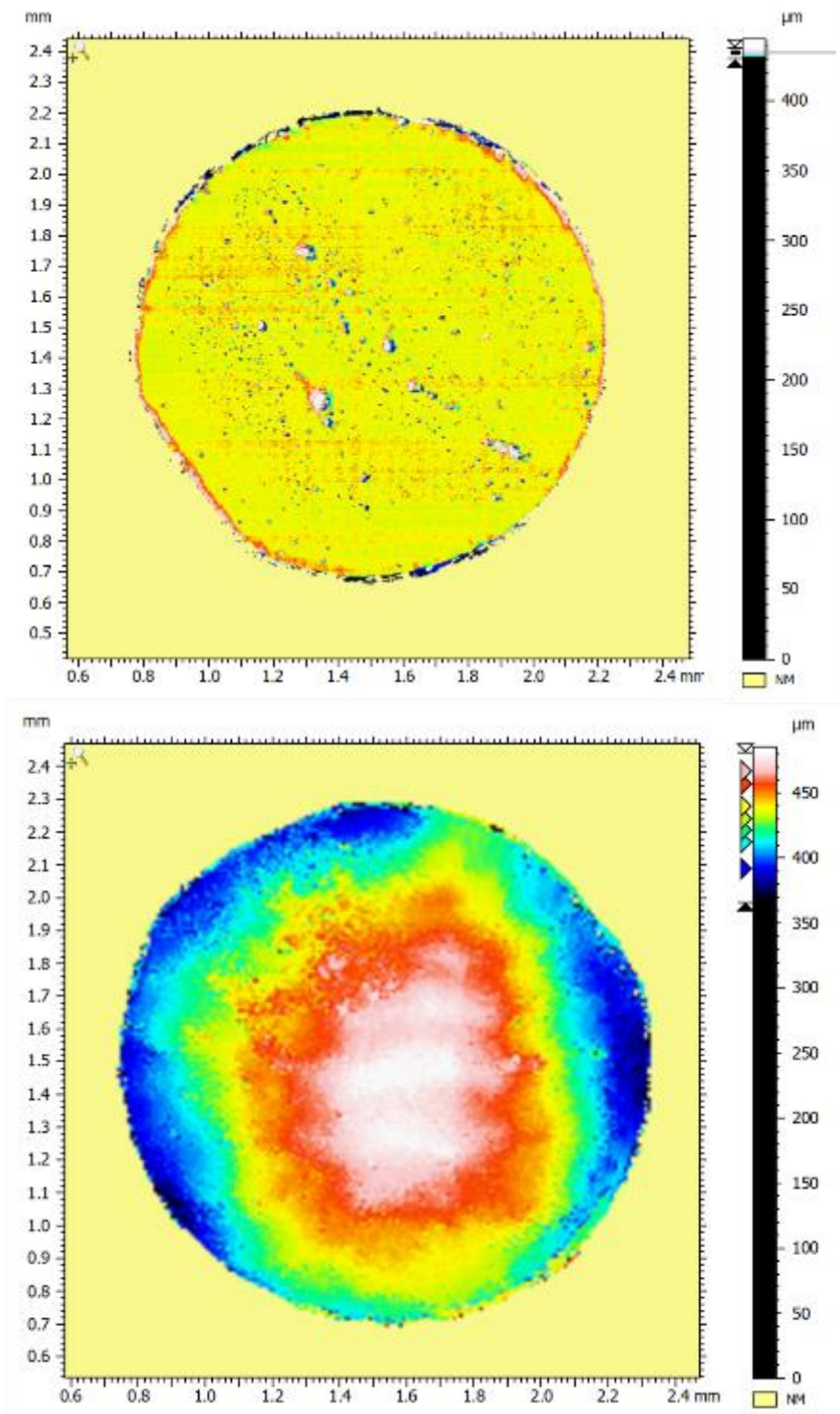
Figure 34 - Comparison between the hole created using a 1.5mm surgical punch biopsy on PVC adhesive tape: placed on microscopy slide (top) and on natural enamel sample (bottom).

PVC Tape placed on microscope slide			
Hole	Surface Area of hole (mm²)	Radius (mm)	Diameter (mm)
1	1.68	0.73	1.46
2	1.72	0.74	1.48
3	1.66	0.73	1.45
4	1.65	0.72	1.45
5	1.75	0.75	1.49
6	1.71	0.74	1.48
7	1.85	0.77	1.54
8	1.62	0.72	1.44
9	1.74	0.74	1.49
10	1.76	0.75	1.50
Mean (mm)	1.72	0.74	1.48
SD (mm)	0.06	0.01	0.03

PVC tape placed on natural enamel samples			
Hole	Surface area of hole (mm²)	Radius (mm)	Diameter (mm)
1	2.36	0.87	1.73
2	3.09	0.99	1.98
3	2.45	0.88	1.77
4	2.20	0.84	1.67
5	2.05	0.81	1.62
6	2.49	0.89	1.78
7	2.28	0.85	1.71
8	2.17	0.83	1.66
9	2.26	0.85	1.70
10	2.40	0.87	1.75
Mean (mm)	2.38	0.87	1.74
SD (mm)	0.27	0.05	0.10

Table 6 – Comparison of surface area, radius, and diameter of holes produced in PVC tape using surgical punch biopsy and placed on microscopy slide (left), and on the natural enamel samples (right).

3.5.4.2   Surface form change measurement and characterisation

Enamel loss measured using three different methods: (1) Geomagic (scan superimposition and difference), (2) MountainsMap (scan imposition and profile extraction), and (3) Boddies (scan subtraction and profile extraction) using each programme and the data are shown in Table 7.

3.5.4.2.1   Geomagic Method

There was a statistically significant increase in erosion lesion depth for both measurement outputs, compared to baseline at all time points (p<0.0001). Mean (SD) Z-change (μm) at 5, 10, and 15 minutes was 1.1(0.9), 2.2(1.1), 3.7(1.6) μm and the mean (SD) total deviation (μm) for the same erosion times were 1.1(0.8), 2.1(1.0), and 3.5(1.6) μm respectively. There was no statistically significant difference in step height values compared to the mean Z-change and mean 3D total deviation for all erosion times (p>0.05). Representative example of superimposition and difference analysis can be seen in Figure 35.

3.5.4.2.2   MountainsMap Method

Mean (SD) Z-change (μm) after 5, 10, and 15 minutes erosion was 1.05 (0.59), 2.12 (1.06), 3.40 (1.75) μm respectively, and using mean (SD) 3D step height (μm) it was 1.49 (0.26), 2.47 (0.85), 3.71 (1.58) μm respectively. There was a statistically significant difference in mean 3D step height between 5 mins and 15 mins (p<0.05). Additionally, there was no statistically significant difference in the step height calculation using either mean Z-change or mean 3D step height measurement output (p>0.05).

3.5.4.2.3   Boddies Method

Table 7 shows mean SPSH, mean SHC and 3D SHC after 5, 10, and 15 minutes. Differences between each step height calculation method were statistically

significant after 10 minutes erosion (mean SPSH vs mean 3D SHC, p< 0.05) and 15 minutes erosion (mean SPSH vs mean SHC, p<0.01, mean SPSH vs mean 3D SHC, p<0.0001). There was no statistically significant difference in the erosion lesion depth calculation after 5 minutes erosion (p>0.05); as seen in Figure 36.

3.5.4.3 Comparing Step Heights Between Analysis Method

A comparison between the step heights measured using each analysis method, and their associated measurement outputs can be seen in Figure 37. There was no statistically significant (p>0.05) differences in step height calculated using any of the three methods after 5- and 10-mins erosion. However, after 15 mins, statistically significant differences in step height were evident between Geomagic, MountainsMap, and Boddies.

Mean step height (µm) measured using Boddies as mean(SD) SPDH (7.06(1.26)) and mean(SD) SHC (6.01(1.12)) were both statistically significantly (p<0.0001) larger than step heights measured using Geomagic mean (SD) Z-change (3.70(1.60)) and mean 3D total deviation (3.50(1.60)), and MountainsMap mean Z-change (3.40(1.75) and mean 3D SHC (3.71(1.58)).

3.5.4.4 Surface roughness change measurement and characterisation

The mean (SD) surface roughness values, using Boddies, for all natural enamel samples after 0, 5, 10, and 15 minutes acid immersion were, 1.13 (0.13) µm, 1.52 (0.23) µm, 1.44 (0.19) µm, and 1.43 (0.21) µm respectively (Figure 38 and Table 7) and were statistically significant at all citric acid immersion time points compared to baseline (p<0.0001). Intergroup analysis revealed statistically significant differences in mean surface roughness between 5 minutes and all other erosion time points (versus 10 mins p<0.05, and versus 15 mins, p<0.0001), however there was no

statistically significant difference between 10 minutes and 15 minutes erosion (p>0.05); as seen in Figure 37.

3.5.4.5 Surface reflectivity measurement and characterisation

Mean surface reflectivity, using OCT, before and after all acid erosion periods is shown in Table 7. Differences in surface reflectivity occurred after all erosion timepoints compared with before erosion. Mean percentage peak intensity change after 5, 10, and 15 minutes erosion were 82%, 77.7%, and 73.2% respectively, and were statistically significant ($p<0.0001$) for all erosion groups compared with before erosion (100%). However, there were no statistically significant differences in percentage peak intensity change between erosion timepoints ($p>0.05$). An example of the surface reflectivity images can be seen in Figure 39.
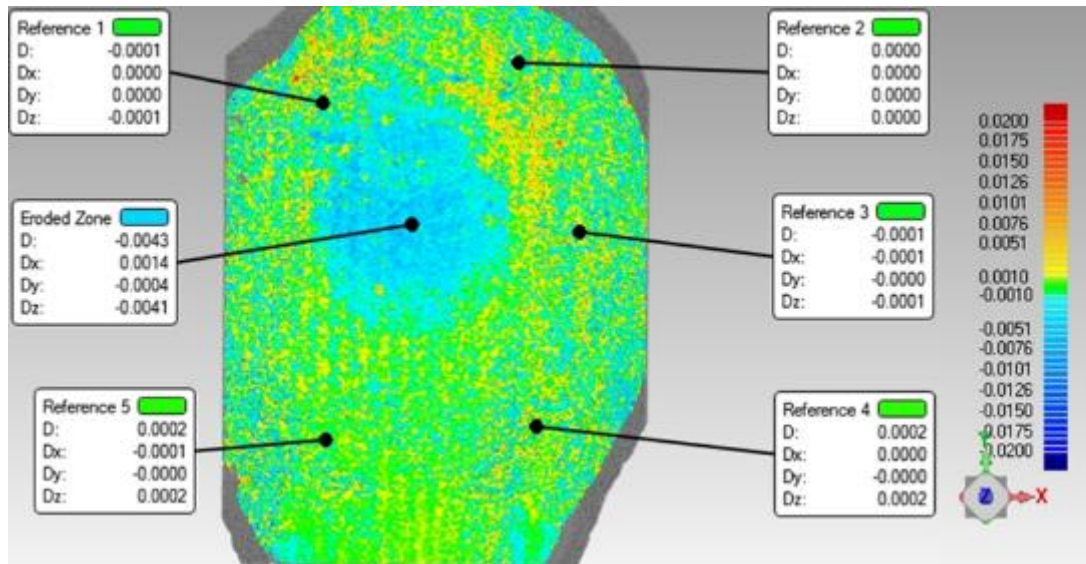
Figure 35 – Representative example of a sample with an erosion lesion (blue) using method 1, green shows no change, whilst yellow shows gain post erosion. Erosion lesion is described using by 3D total deviation (D) and Z-change (Dz). The central eroded region and 5 reference regions have been analysed for allow for erosion versus non-eroded comparison.
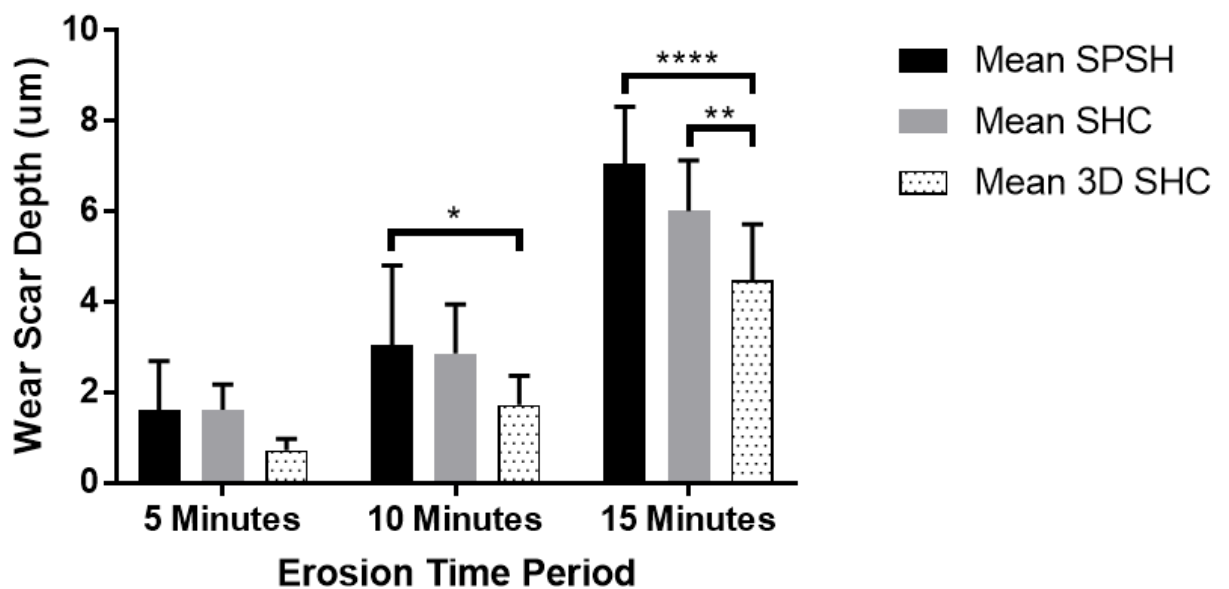
Figure 36 – For method 3, differences in the step height measured using mean single mid-point step height (SPSH), mean single point step height (SHC), and mean three-dimensional step height (3D SHC) were compared. Statistical significance is denoted by * ($p<0.05$), ** ($p<0.01$), *** ($p<0.005$), and ****($p<0.0001$).
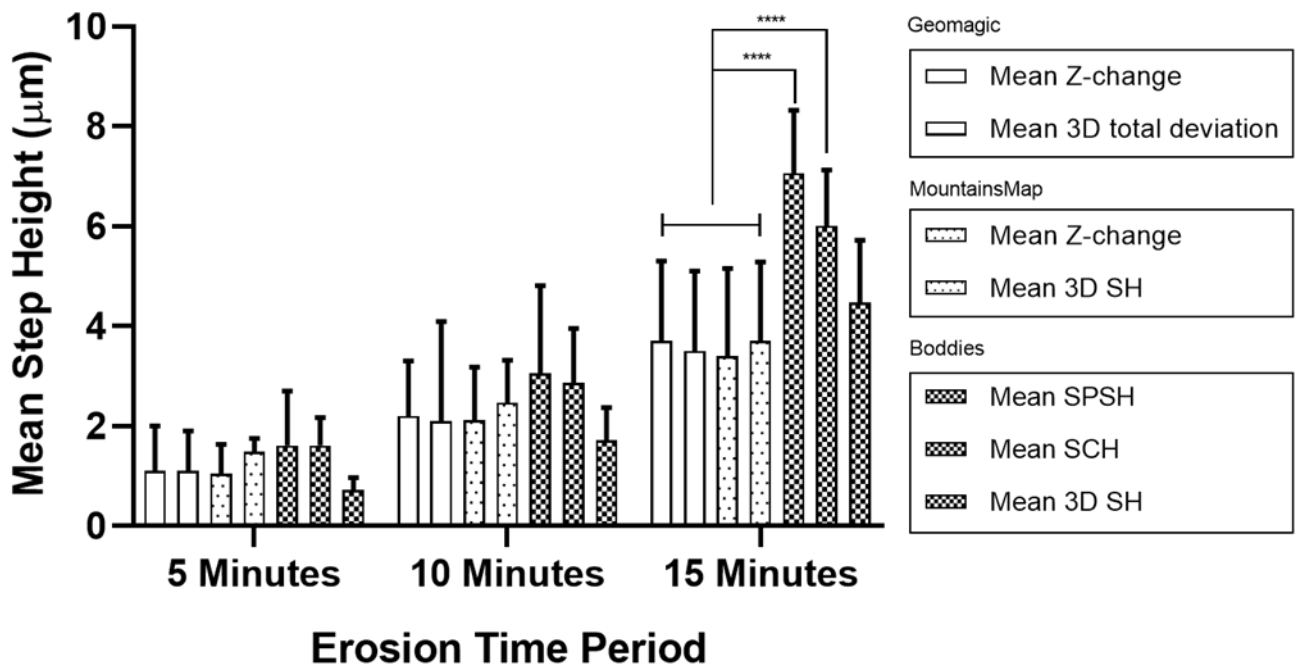
Figure 37 – Comparing the mean step heights obtained using analysis methods: Geomagic, MountainsMap and Boddies, and according to their respective measurement outputs. Statistically significant differences in mean step height data were observed after 15 mins erosion only. Statistical significance is denoted by * (p<0.05), ** (p<0.01), *** (p<0.005), and ****(p<0.0001).

	Surface Profilometry Step Height Analysis Method							Surface Roughness		Peak Intensity Analysis	
	Geomagic		MountainsMap		Boddies						
Erosion Time (mins)	Mean(SD) Z-change (μm)	Mean(SD) 3D total deviation (μm)	Mean(SD) Z-change (μm)	Mean(SD) 3D SDH (μm)	Mean(SD) SPSH (μm)	Mean(SD) SHC (μm)	Mean(SD) 3D SHC (μm)	Mean(SD) Surface Roughness (Sa, μm)	Percentage Change vs Baseline (%)	Mean(SD) Reflectivity (grey value)	Percentage Reflection vs Baseline (%)
0 (baseline)	0	0	0	0	0	0	0	1.13 (0.13)	0	48831.7	100.0
5	1.10 (0.9)	1.10 (0.8)	1.05 (0.59)	1.49 (0.26)	1.61 (1.09)	1.61 (0.56)	0.72 (0.25)	1.52 (0.23)	38.4	40026.1	82.0
10	2.20 (1.1)	2.10 (1.0)	2.12 (1.06)	2.47 (0.85)	3.06 (1.75)	2.86 (1.09)	1.72 (0.65)	1.44 (0.19)	30.3	37951.8	77.7
15	3.70 (1.6)	3.50 (1.6)	3.40 (1.75)	3.71 (1.58)	7.06 (1.26)	6.01 (1.12)	4.47 (1.25)	1.43 (0.21)	30.0	35738.8	73.2

Table 7 – Step height of the erosion lesion was measured using three methods (1) scan superimposition and difference, (2) scan superimposition and profile extraction, and scan subtraction and profile extraction. Three different software were used (1) Geomagic Control 2014, (2) MountainsMap, and (3) Boddies v1.92. Step height was measured using ISO and non-ISO methods. ISO methods included: single mid-point step height (SPSH), mean single point step height (SHC), three-dimensional step height (3D SHC). Non-ISO methods included: Z-change and 3D total deviation. Surface roughness was measured using 3D parameter Sa and expressed also has change versus baseline. Peak intensity analysis was measured as change in surface reflectivity in grey value and converted to percentage reflection versus baseline.
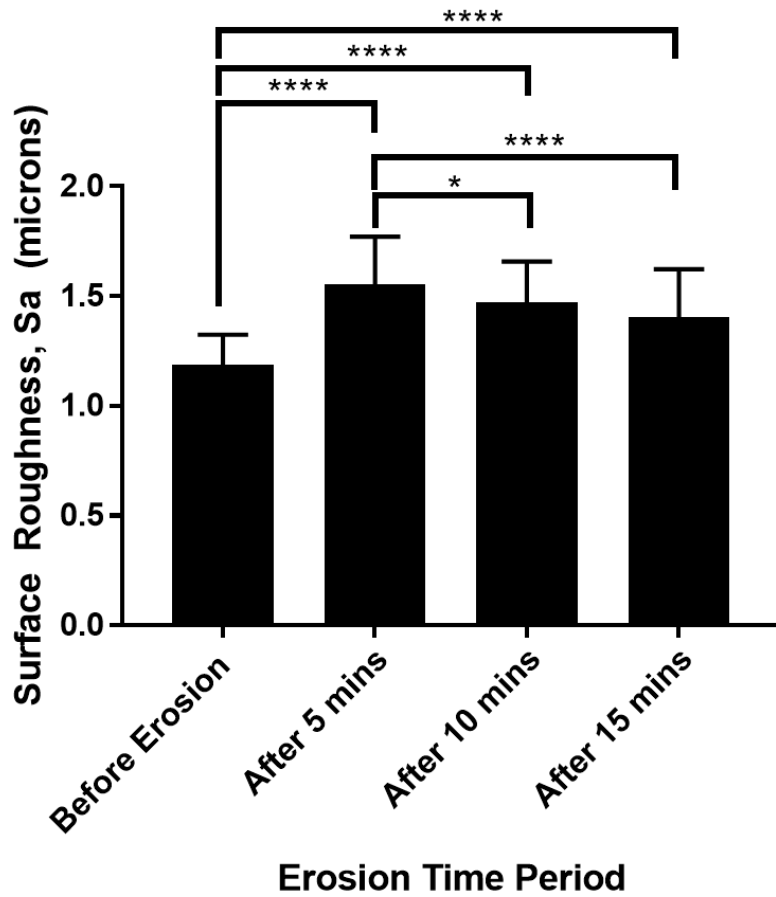
Figure 38 – Change in surface roughness of the wear scar were determined for each erosion time using 3D parameter Sa and compared to before erosion. Statistical significance is denoted by * (p<0.05), ** (p<0.01), *** (p<0.005), and ****(p<0.0001).
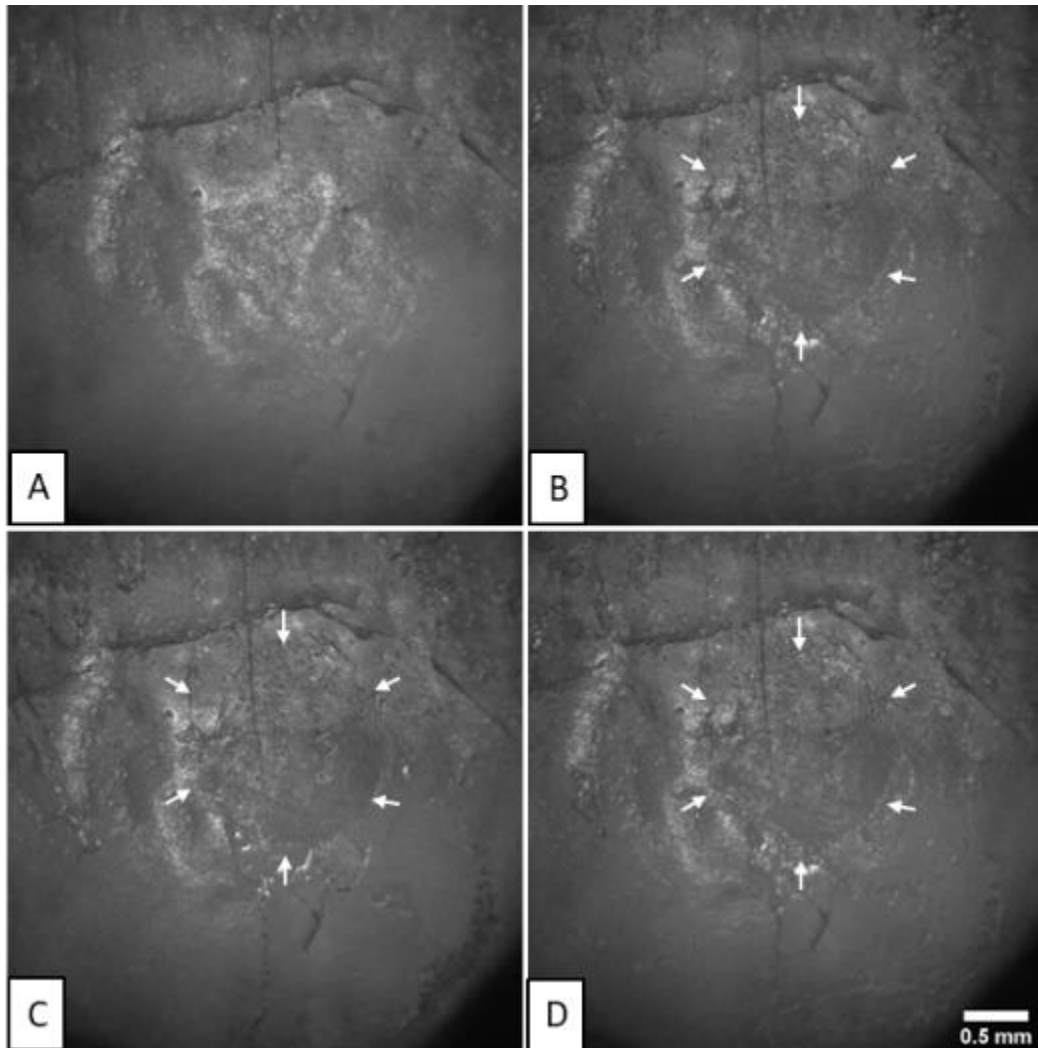
Figure 39 – Representative example of surface reflection/projection images produced with OCT. Eroded lesion is indicated by the white arrows, and erosion times are (A) baseline, (B) 5 mins, (C) 10 mins, (D) 15 mins erosion. Scale bar for all images in 0.5mm. These images were created using the B-stack volumes produced from OCT scan before and after each erosion time. The same region of interest was maintained, and peak intensity analysis performed.

3.6   Discussion

The accuracy and measurement uncertainty of chromatic confocal profilometry for surface roughness measurement of polished and natural enamel surfaces has been previously studied (Mullan et al., 2017b); however, in this Chapter we determined the detectable threshold of monochromatic NCLP for surface form and surface roughness measurements using natural human enamel. A significant challenge in using natural enamel surfaces for both early and late erosion in vitro models was the use of an effective acid-resistant barrier protocol to produce an exposed area of enamel with corresponding areas of protected/uneroded enamel to serve as reference for comparison after erosion. This was relatively easy to achieve for polished enamel samples and is one reason why in vitro research studying dental erosion has primarily used polished enamel surfaces (Huysmans et al., 2011a).

The influence of thermal variation on monochromatic CL NCLP sensor displacement has not been previously studied in the context of dental surface metrology applications. For medium (20 mins) and long-term (2-hrs) scanning periods we demonstrated a significant influence of temperature change on NCLP displacement when left uncovered/unprotected and showed that the closed situation had less deviation from the optical flat. This might have a major impact for studies attempting to evaluate the very earliest changes that occur during acid-mediated erosion of polished and natural enamel. The effect of sensor displacement varied according to the scanning time investigated. A previous study (Holme et al., 2005) demonstrated, when using white light interferometry (WSI), a 1K change in temperature resulted in a y-direction shift of 6.5 μm between the lens and the sample; this required step height calculations to be adjusted accordingly. Furthermore, no further analysis

regarding how temperature change during WSI scanning was conducted to determine its effects on subsequent scanning and step height determination. Similarly, McBride et al (2001) demonstrated the impact of ambient scanning variation on chromatic (WL) NCLP sensor displacement. After enclosing the NCLP in a Perspex enclosure, the authors noted a significant improvement in both ambient temperature fluctuations, within the enclosure, and NCLP sensor displacement values (McBride et al., 2001).

An optical flat was utilised, rather than a natural tooth sample, to determine sensor displacement, because the crystalline structure of the optical flat material will neither change size nor shape with increasing thermal changes. Therefore, a true indication of sensor displacement changes with thermal variation could be determined. Our study demonstrated a linear relationship in the region measured between sensor/apparatus temperature variation and NCLP sensor displacement. Temperature variation induced NCLP sensor displacement did not affect measurements conducted over a short scanning period (30 s). However, over medium (20 mins) and long (2 hrs) scanning periods NCLP sensor displacement was calculated at 0.556 μm and 1.049 μm respectively. The profilometric scans conducted in this study to determine wear scar depth formation were conducted over 21 minutes using an NCLP system not covered nor protected from ambient thermal changes. By characterising the influence of thermal variation on subsequent sensor displacement, it was possible to account for this error in any NCLP scans being conducted over medium and long scanning periods. All studies that seek to determine the earliest effects of acid-erosion on enamel should ideally ensure ambient/sensor temperature variations are conducted in an enclosed environment,

and controlled within 2°C (ISA, 2006) to ensure minimisation of sensor displacement over medium-long term scanning periods. It remains unknown whether the NCLP displacement with temperature variation is due to drift of the NCLP sensor or due to drift in the motion controllers that move the sample. However, the causes of the displacement are irrelevant to the requirement of an enclosure to enhance its scanning performance.

Utilising a surgical biopsy punch of 1.5mm diameter provided a reliable method to create a hole with mean (SD) diameter 1.48(0.03) µm. The exposed region of enamel represented the maximum peak of the natural enamel sample which would be the first region under erosive attack in the oral cavity (Shellis and Addy, 2012). Previously reported barrier methods for polished enamel include use of adhesive tape strips (Paepegaey et al., 2013b; Austin et al., 2016; Mullan et al., 2017a) or nail varnish (Amaechi et al., 1998a; Ganss et al., 2005) to leave a rectangular (or similar shaped) strip of exposed enamel for erosion. The use of PVC tape strips was not successful on natural enamel as they debonded almost immediately after immersion in citric acid. The use of circumferential barrier provided an easily removed barrier without damage to the erosion lesion. The use of nail varnish was not investigated in this Chapter due to the inability to remove the varnish without irreversible damage to the erosion lesion.

A 10 µm step over distance provided the optimum data providing sufficient point cloud data for analysis and duration of scan thus ensuring the longitudinal measurement of surface form measurement could be conducted in a timely manner. The use of smaller step over distances resulted in an exponential increase in NCLP

scan duration, which would be impractical for longitudinal assessment of erosion in pH-cycling in vitro models.

Measuring surface form change has presented a significant challenge in erosion research due to the complex freeform nature of natural enamel and measurement errors associated with utilising NCLP (Mullan et al., 2017b; Leach, 2009; Bell, 2001; Yang et al., 2017). Step height change calculation, ISO 5436-1, using post erosion scan data is considered the gold standard for determining erosive tooth wear *in vitro* for flat polished samples. (Huysmans et al., 2011a; Lussi and Ganss, 2014). This method cannot be utilised for natural enamel samples as conventional form removal techniques and wear scar isolation – using strips of tape or other physical barriers – is not possible on freeform organic surfaces. However, this can be determined by using either scan superimposition and comparing differences in the Z-height or by profile subtraction of before and after profile scan data and utilising the difference profile for analysis.

The utilisation of a difference profile or difference image produced by profile subtraction of before/after erosion scan data sets has been previously utilised to successfully determine bulk enamel loss in polished human enamel samples (Holme et al., 2005). In this study an *in vitro* stepwise etch investigation was conducted using hydrochloric acid, and utilised dental amalgam as the reference region for comparison to the eroded enamel region. By subtracting the profiles the difference was then utilised for analysis of bulk enamel loss (Holme et al., 2005). In our study, calculation of bulk enamel loss, from the different profiles on natural human enamel samples was successfully demonstrated. Additionally, by utilising a circumferential

barrier technique, using PVC tape to allow for the creation of a central window of exposed enamel surrounded by a region of uneroded/protected enamel, this allowed a direct comparison between eroded and non-eroded enamel without the use of any adjunctive dental materials as points of reference. Moreover, utilisation of a bespoke scanning jig ensured the facilitation of accurate sample placement and aided in accurate superimposition or alignment of before and after erosion data sets, which therefore allowed determination of wear scar depth by profile comparison or subtraction and analysis of the difference profile.

Profile superimposition allowed determination of changes in Z-height, either as mean Z-change or mean 3D deviation, similar to results obtained by Rodriguez and Bartlett 2010 and Rodriguez et al 2012) who also demonstrated dimensional change using superimposition software (Rodriguez and Bartlett, 2010; Rodriguez et al., 2012a). Our study, however, is the first to demonstrate step height calculation in natural human enamel using profile subtraction and mean single point step height (mean SPSHC), mean step height (mean SHC), or mean 3D step height (mean 3D SHC). Our study found no statistically significant difference ($p<0.05$) in either measurement for the shortest erosion exposure studied (5 minutes). However, there was a statistically significant difference after 10 minutes (mean SPSH vs mean 3D SHC, $p< 0.05$) and 15 minutes erosion (mean SPSH vs mean SHC, $p<0.01$, mean SPSH vs mean 3D SHC, $p<0.0001$). Mean 3D SHC, using Boddies, provided the lowest wear depth and may indicate a truer representation as this is calculated from all available profiles. This is in agreement with previous studies which have utilised 3D SHC to determine step height change in polished (Rodriguez and Bartlett, 2010; Sar Sancakli et al., 2015) and natural enamel samples (Rodriguez and Bartlett, 2010; Rodriguez et al., 2012a).

After 15 mins erosion, step height values obtained for mean single mid-point step height (mean SPSH) and mean mid-point step height (mean SHC) were significantly higher than the other measurement outputs, mean Z-change, mean 3D total deviation, and mean 3D step height. These differences were not due to the software used for analysis. Step height calculation will be higher when the analysis method utilises only 1 region (s.f. SPSH) or small number of regions (s.f. SHC) of the erosion lesion. It has been previously demonstrated that analysing the entire erosion lesion (s.f 3D SHC) will result in a lower and truer value for step height (Rodriguez and Bartlett, 2010).

Previous literature has reported characterisable changes to polished enamel surfaces at 30 seconds erosion using surface roughness (Austin et al., 2016), 30 minutes using OCT (Aden et al., 2017), and 15 minutes using TSM (Mullan et al., 2017a); however seldom have the characterisable changes to natural enamel surfaces been considered. Mullan et al (Mullan et al., 2017a) demonstrated the differences in the changes in surface roughness in natural enamel samples compared with polished enamel samples; polished samples became significantly rougher (increasing Sa values) with increased erosion compared with natural enamel samples which became significantly smoother (decreasing S_a values) after prolonged citric acid exposure times (Mullan et al., 2017a).

The results of this study indicate that during the early erosion period (5 minutes) surface roughness increased significantly from baseline S_a of 1.13 (0.13), up to 1.52 (0.23) μm (p<0.0001), and then decreased after 10 and 15 minutes. This may mean

the early erosive process in natural enamel is slower compared to polished enamel samples, but further work is needed to evaluate the effect of time.

OCT provided an evaluation of the effect of early citric acid erosion on surface reflectivity. The eroded zone demonstrated reduced percentage surface reflection compared with uneroded regions as erosion time increased. This indicated that the optical properties of the amorphous surface layer were adversely affected by acid erosion. This is supported by previous *in vitro* study utilising natural human incisors embedded in resin; OCT was able to detect changes to the enamel surface following 5 and 10 minutes of acid erosion and detectable changes were significant after 50 and 60 minutes erosion (Chew et al., 2014). Whilst, an in-vivo study demonstrated increase in backscattering of the OCT signal intensity as acid erosion increased, which occurred due to surface and subsurface demineralisation which was calculated up to a depth of 33 μm after 60 minutes erosion (Austin et al., 2017). However, this study required 60 minutes of orange juice mediated acid erosion to produce a detectable effect (Chew et al., 2014; Aden et al., 2017; Austin et al., 2017).

This *in vitro* study has demonstrated the formation of the early erosive lesion in natural enamel, and many different methodological challenges have been overcome relating to sample isolation, and lesion characterisation. Natural enamel samples can be considered for use in *in vitro* studies to investigate the formation and progression of early acid erosion, as well as the assessment of enamel lesion remineralisation. Future work is necessary in determining how the natural variability in physicochemical composition of natural enamel samples – due to the presence of the intact surface enamel layer – interacts with the dental erosion process.

3.7 Conclusions

The NCLP detection threshold for measuring changes in surface form and surface roughness was determined for natural human enamel; 0.29 µm and 0.06 µm respectively. Thermal variation during NCLP scanning resulted in characterisable NCLP sensor displacement over 20 mins (0.556 µm) and 2 hrs (1.049 µm), when NCLP was placed in an enclosure NCLP sensor displacement was reduced over the same time periods to 0.098 µm and 0.164 µm. A scanning enclosure can significantly enhance NCLP measurement stability and thus measurement accuracy.

Acid-induced dental erosion wear scars in natural human enamel could be characterised using surface profilometry, surface roughness, OCT, and TSM. Our study is the first to demonstrate step height calculation in natural human enamel using superimposition (Geomagic), profile alignment/extraction (MountainsMap), and profile extraction (Boddies) techniques; after 5 mins enamel loss was measured between 1.05 – 1.61 µm.

4 Chapter 4 – Effect of single application fluoride treatment, and the acquired enamel pellicle on step height formation in natural human enamel

4.1 Introduction

In Chapter 3 it was demonstrated how dental erosion lesions can be created and characterised in natural human enamel using changes in surface form (3D step height), surface roughness, surface reflectivity, and surface morphology.

This new in vitro erosion model using natural enamel has potential for many applications to simulate the clinical environment in a controlled laboratory environment. Two of the most common factors which impact on dental erosion clinically, as described in Chapter 1, are the use of sodium fluoride toothpaste and human saliva.

As a result, this Chapter focused on the impact of a common toothpaste (F as sodium fluoride) and the acquired enamel pellicle (AEP) on the dental erosion on natural enamel in vitro model developed in Chapter 3; this was conducted as two separate investigations. The impact of sodium fluoride pre-treatment was investigated for its impact on step height formation, whilst the AEP was investigated for its impact on erosion lesion formation.

4.2 Chapter Aims, Objectives and Null Hypotheses

4.2.1 Chapter Aim

The aim of this study was to:

1. Determine the effect of single application sodium fluoride (NaF) toothpaste pre-treatment on the early and late erosion on natural human enamel

2. Determine the effect of natural saliva and artificial saliva as a remineralising solution after toothpaste treatment

3. Determine the effect of the AEP formed over different time periods on the early erosion process on natural human enamel

4.2.2 Chapter Objectives

The objectives of this Chapter are linked to and expand on Thesis Objective 3 (page 114):

1. Compare the use of fluoride vs non-fluoride toothpaste slurry mixture in a pre-treatment model on natural human enamel

2. Compare the remineralisation effects of natural saliva and artificial saliva after toothpaste pre-treatment

3. Compare the short duration (3 mins) and long duration (24 hrs) AEP on dental erosion on natural human enamel

4. Ascertain whether 5-mins erosion could produce a detectable change in surface form, surface roughness and surface morphology

4.2.3 Chapter Null Hypotheses

1. There will be no difference in erosion lesions formed between fluoride and non-fluoride treated natural human enamel samples

2. There will be no difference in erosion lesions formed between artificial saliva and natural human saliva mineralisation solutions

3. There will be no difference in erosion lesions formed between natural human enamel samples with 3 min and 24 hrs AEP

4. There will be no detectable change in surface form, surface roughness and surface morphology with either 3-min or 24-hrs AEP

4.3 Materials and Methods

4.3.1 Sample creation

Extracted human permanent clinically sound and disease-free molar teeth were collected under ethical approval (REC: 12/LO/1836) with informed consent. Natural enamel samples (n=60) were sectioned, bonded to glass microscope slides, and cleaned according to the same method described in Chapter 3 section 3.3.1.

4.3.2 Test solutions

Citric acid (0.3%, pH 3.2) was prepared for use according to method described in Chapter 3 section 3.3.5.2.

Slurries of identical formulation of toothpaste with or without fluoride (1450ppm) were produced in 1:2 (toothpaste:deionised water, w:v) ratio and rapidly homogenised using a magnetic orbital shaker (Fisherbrand, Isotemp, Fisher Scientific, USA). The mean (SD) pH of the resultant fluoride and non-fluoride toothpaste slurries were 6.90(0.01) and 6.61 (0.04) respectively. Artificial saliva was prepared according to the method previously described by Eisenburger et al 2001 and titrated to pH 7 using 0.1M NaOH; the constituent ingredients are shown in Table 8 (Eisenburger et al., 2001). All solutions were stored at room temperature (22 $\pm$ 0.5°C).

Paraffin-stimulated whole mouth human natural saliva was collected from healthy volunteers under ethical approval (Northampton REC, 14/EM/0183) and with patient consent. Saliva was collected in 20ml polypropylene tubes after an absence of food and drink for 1 hour prior to donation and were ice-chilled immediately upon collection and frozen at -80°C for long term storage. Prior to use in experimentation

samples were defrosted for the same length of time (3 hours) at room temperature according to previously published protocol (Mutahar et al., 2017); and immediately pooled with a vortex mixer to resuspend any precipitated proteins.

Chemical name	Formula	Amount added to 1L deionised water (g)
Calcium chloride dihydrate	$CaCl_2.H_2O$	0.1029
Magnesium chloride	$MgCl_2$	0.01904
Potassium dihydrogen phosphate	KH_2PO_4	0.544
HEPES acid buffer	$C_8H_{18}N_2O_4S$	5.206
Potassium chloride	KCL	2.2365

Table 8 – Artificial saliva formulation according to Eisenburger et al 2001

4.3.3 Natural enamel erosion model

Eighty natural enamel specimens were created and mounted on glass microscope slides according to the method outlined in Chapter 3 Section 3.3.1. All enamel specimens (n=80) were numbered and randomly assigned (random number generator, Microsoft Excel 2016, Microsoft, USA) to either Investigation 1 or 2. Experimental outline for Investigation 1 and 2 can be seen in Figure 40 and Figure 41.

4.3.3.1 Investigation 1 – Effect of Toothpaste Pre-treatment

Sixty enamel samples were randomised to either fluoride (F, n=30) or non-fluoride (NF, n=30) slurry pre-treatment groups, and then further sub-assigned to one of three mineralisation solutions; deionised water (negative control, DI, n=20), artificial saliva (AS, n=20), or natural human saliva (NS, n=20) (Figure 40). All samples were taped using polyvinylchloride tape with a 1.5mm diameter circle central hole to leave enamel exposed; as described in Chapter 3 Section 3.3.5.1.

One pre-treatment cycle consisted of immersing each sample in 10 ml toothpaste slurry (F or NF) under agitation (62.5 RPM, Stuart mini-Orbital Shaker SSM1, Bibby Scientific, England) for 3 minutes, before immersion in deionised water (DIW), artificial saliva (AS), or natural human saliva (NS) for 30 minutes (Hornby et al., 2009; Joiner et al., 2014). All samples were washed (1-minute, deionised water) and dried (5s, oil-free air) before 3 cycles of 5-minute citric acid demineralisation. One demineralisation cycle consisted of immersing each sample in 10ml citric acid under constant agitation (62.5 RPM, Stuart mini-Orbital Shaker SSM1, Bibby Scientific, England) for 5 minutes, followed by 2-minute rinse with deionised water with cumulative erosion times, 5, 10 and 15 minutes.

4.3.3.2 Investigation 2 – Effect of 3-min and 24-hrs AEP

Two AEP models were used in this investigation: 3-mins (short) and 24 hours (long).

Twenty natural enamel specimens were numbered and randomly assigned (random number generator, Microsoft Excel 2016, Microsoft, USA) to either 3-mins or 24-hrs NS pre-treatment groups (Figure 41). All samples were taped using PVC tape with a 1.5mm diameter circle central hole to leave enamel exposed; as described in Chapter 3 Section 3.3.5.1. Samples were then immersed and stored un-agitated at 22°C$\pm$1 in NS for either 3-mins or 24-hrs to form an AEP. After immersion, samples were gently rinsed with deionised water for 1 minute and left do air dry for 24 hours according to a similar previously published protocol (Mutahar et al., 2017).

4.3.4 Natural enamel erosion method

In both investigations, erosion period of 5 minutes was used using 10ml citric acid per sample under constant agitation (62.5 RPM, Stuart mini-Orbital Shaker SSM1, Bibby Scientific, England), followed by 2-minute rinse with deionised water. The samples were air-dried with oil free air for 5 seconds before the tape was carefully removed and allowed to dry further before undergoing characterisation. Investigation 1 utilised 3 erosion cycles, whilst Investigation 2 used only 1 erosion cycle.

4.3.5 Erosion characterisation techniques

4.3.5.1 Investigation 1

All specimens (n=60) were scanned using NCLP and imaged using tandem scanning confocal microscopy (TSM) before slurry pre-treatment (baseline assessment) and after each erosion cycle (5, 10, and 15-minute post-erosion assessment). NCLP scanning protocol utilised was described in Chapter 3 Section 3.3.5.3 3D Step height formation was calculated for each sample after each erosion cycle using the scan alignment and profile subtraction (MountainsMap) technique described in Chapter 3 Section 3.3.5.3.2. Qualitative two-dimensional images were obtained for representative samples (n=2) from each pre-treatment group using TSM (Noran Instruments; Middleton, WI, USA) described in Chapter 2 Section 2.3.3.

4.3.5.2 Investigation 2

All specimens were scanned using NCLP, OCT, and TSM before and after the erosion cycle to obtain surface form, surface roughness, surface reflectivity and surface morphology. This was done according to methods described in Chapter 3 Section 3.3.5.2

4.4 Statistical methods

Data were collected, tabulated and statistically analysed using GraphPad Prism 7 (GraphPad Software Inc, USA). For Investigation 1: based on previous pilot data, a power calculation, using GPower 3.0.1, based on ANOVA comparing mean 3D step height between treatment groups was conducted, and indicated a total sample size of 54 would be required for an effect size 0.45 yielding 80% power. However, for Investigation 2 a convenience sample of 20 samples were selected. Data were

assessed for normal distributing using Shapiro-Wilks and Komogorov-Smirnov tests and visually assessed with box-plots and histograms. Since the data was normally distributed, means and standard deviations were reported. Inter-group analysis was conducted with two-way repeated measured ANOVA with post-hoc Tukey's test for multiple intra group comparisons.
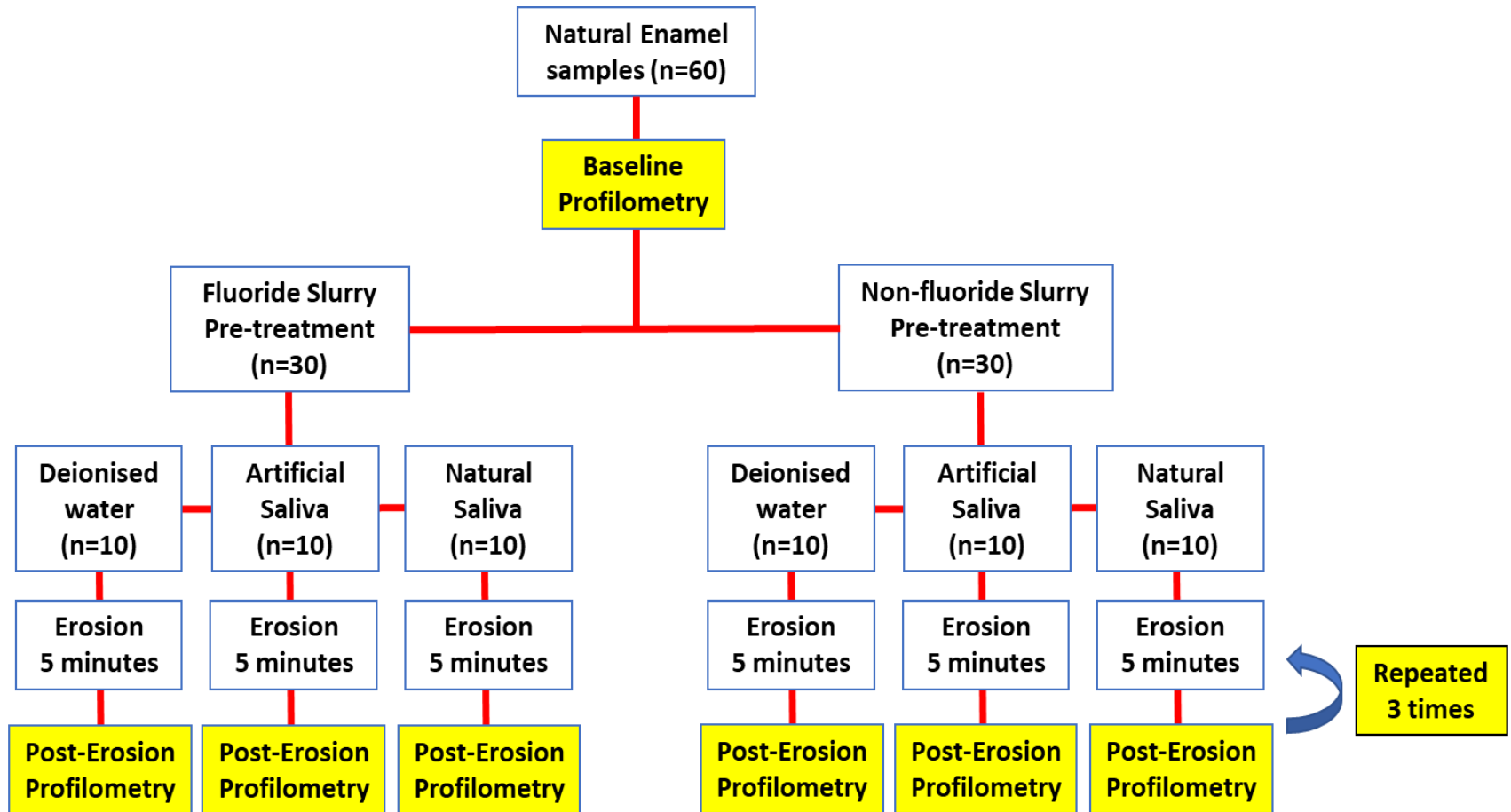
Figure 40 – Investigation 1 simplified outline of the experimental process. Only bulk enamel loss (step height) was investigated, to determine the impact of sodium fluoride toothpaste
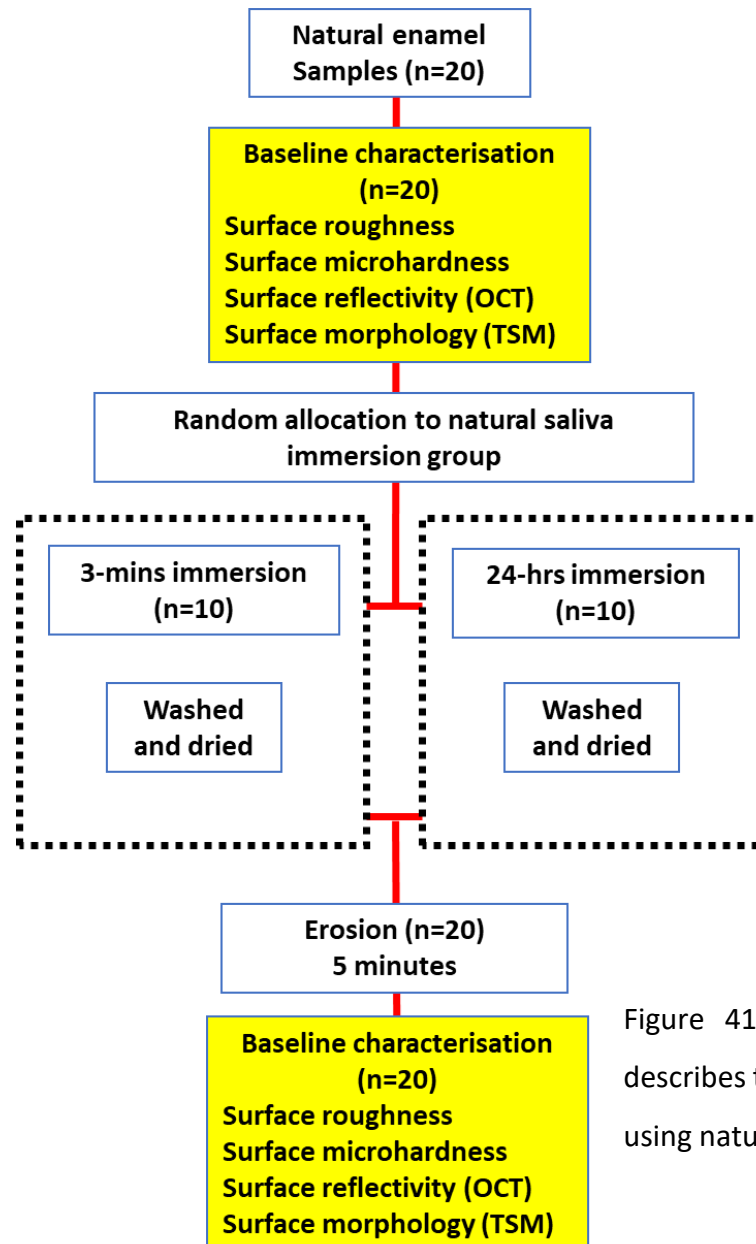
Figure 41 – Investigation 2 simplified outline. This describes the method of creating a 3-min and 24-hrs AEP using natural human enamel.

4.5   Results

4.5.1   Investigation 1

Mean (SD) 3D step height formation after 5, 10, and 15 minutes for each treatment group and their statistical associations are summarised in Figure 42. The lowest mean (SD) 3D step height (μm) after 5, 10- and 15-minutes erosion was demonstrated by F + AS group: 0.38 (0.20) μm, 1.07 (0.34) μm, and 1.73 (0.6) μm respectively. Whilst the largest mean (SD) after 5, 10, and 15 minutes was in the NF +AS group with 1.28 (0.33), 2.03 (0.91), and 3.07 (1.37) μm.

After 5 minutes erosion, mean (SD) 3D step height (μm) was significantly lower for F + AS than F + DIW (0.38(0.20) vs 1.17(0.11), p<0.05), and NF + AS (0.38(0.20) vs 1.28(0.33), p<0.0001), and then NF + NS (0.38(0.20) vs 1.23(0.28), p<0.0001) respectively. Mean (SD) 3D step height was significantly lower for F + NS than NF + AS (0.65(0.36) vs 1.28(0.33), p<0.001) and NF + NS (0.65(0.36) vs 1.23(0.28), p<0.001). There was no statistically significant (p>0.05) differences in mean (SD) 3D step height between both control groups F + DI (1.17(0.11)) and NF + DI (1.09(0.15)).

After 10 minutes erosion, mean (SD) 3D step height (μm) was significantly lower only for F + NS than NF + NS (1.36(0.48) vs 1.72(0.36), p<0.01). There were no statistically significant difference (p>0.05) in mean 3D step height between all other groups.

After 15 minutes erosion, mean (SD) 3D step height (μm) was significantly lower for F + AS than NF + AS (1.730(0.60) vs 3.07(1.37), p<0.0001) and then NF + NS (1.730(0.60) vs 2.59(0.67), p<0.001). Mean (SD) 3D step height was also significantly lower for F + NS than NF + AS (1.90(0.73) vs 3.07(1.37), p<0.05).

Qualitative analysis of TSM images for each treatment group showed progressive erosive destruction of the surface enamel with increasing erosion (Figure 43). Differences in the erosive patterns can be visualised for all treatment groups with progressive visualisation of an etch pattern with increasing erosion. At 5 minutes erosion, a clear difference in eroded enamel appearance can be seen between each treatment group; erosive effects appear least prominently in the F + AS group whilst they are more apparent in the NF + NS group. Additionally, both fluoride treatment groups indicate less erosive destruction compared with both non-fluoride treatment groups. After 10 minutes, the qualitative differences between each treatment group reduce with only the F + AS group showing more resistance to acid erosion. After 15 minutes however, the effects of erosion appear similar across all treatment groups.
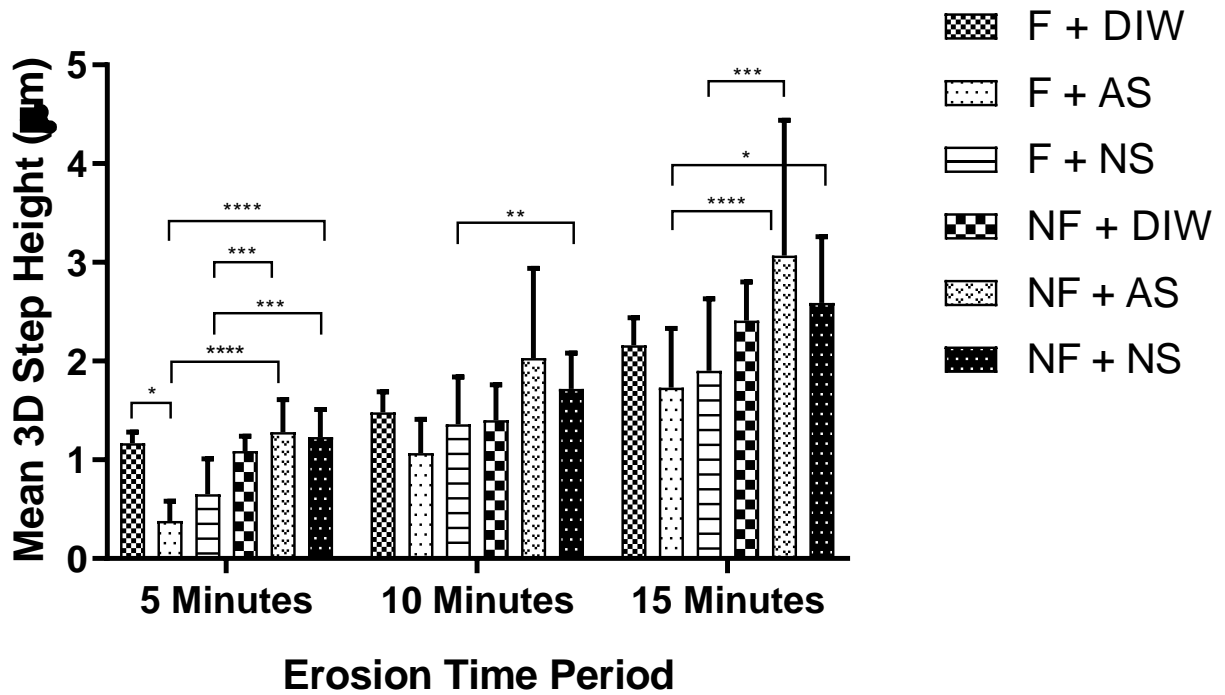
Figure 42 – Mean (SD) 3D step height formation (μm) for each erosion cycle totalling 5, 10, and 15 minutes erosion is shown for each treatment group. Two-way ANOVA and Tukey's multiple comparisons post-hoc analysis was conducted, and statistical significance is denoted by * (p<0.05), ** (p<0.01), *** (p<0.005), and ****(p<0.0001). Groups are labelled using combination of the following letters: F (fluoride slurry), NF (non-fluoride slurry), AS (artificial saliva), NS (natural saliva), DI (deionised water).
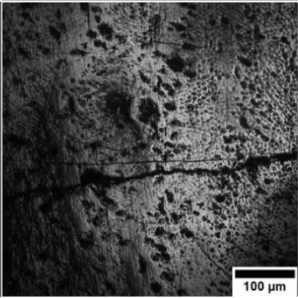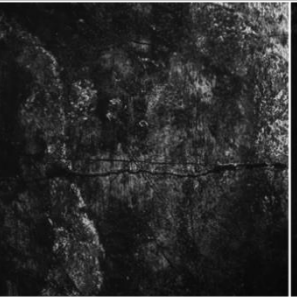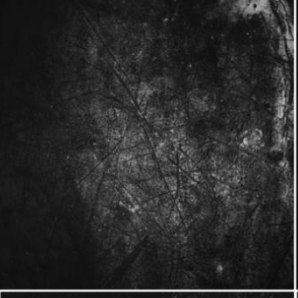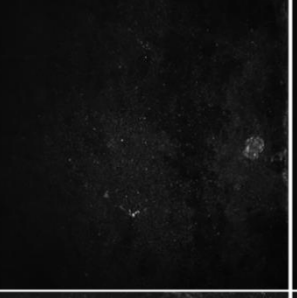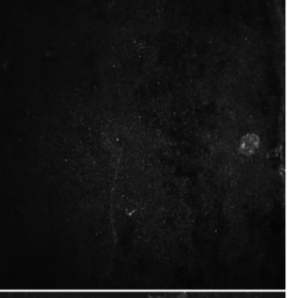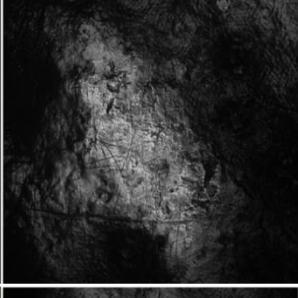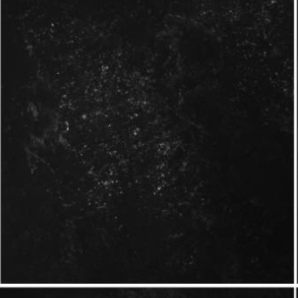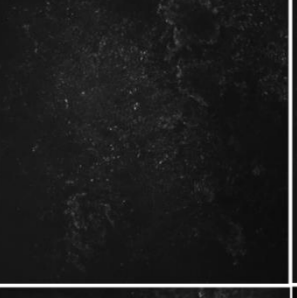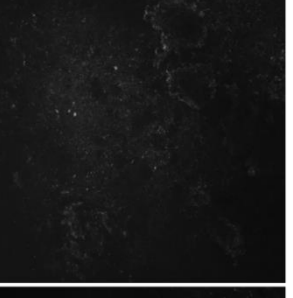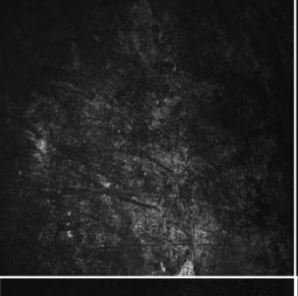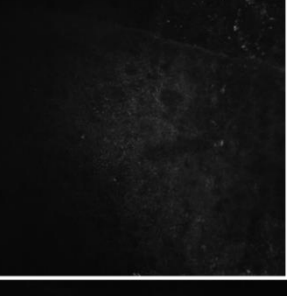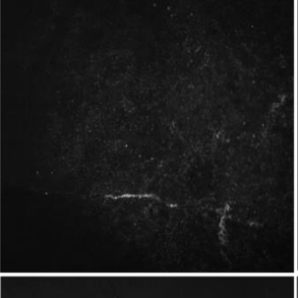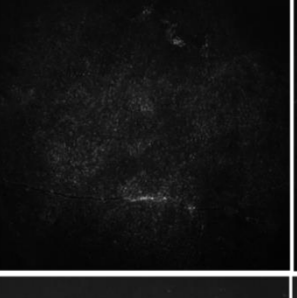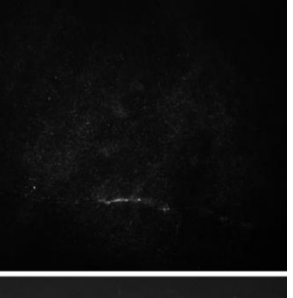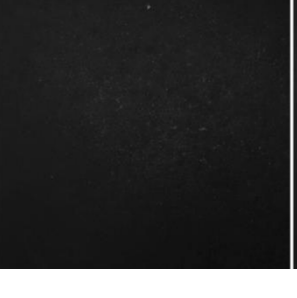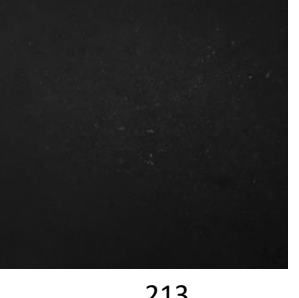
| | | Erosion Time | | |
| | | Baseline | 5 Minutes | 10 Minutes | 15 Minutes |

Treatment Group: F + AS, F + NS, F + DIW, NF + AS, NF + NS, NF + DIW

100 μm

213

Figure 43 – Representative TSM images taken for each treatment group before erosion (baseline) and after 5, 10, and 15 minutes erosion. Images are arranged per group in row order, and per erosion time in column order. All images are to the same scale represented by the single scale bar. Groups are labelled using combination of the following letters: F (fluoride slurry), NF (non-fluoride slurry), AS (artificial saliva), NS (natural saliva), DIW (deionised water).

4.5.2   <u>Investigation 2</u>

Mean (SD) 3D step height formation and surface roughness after 5 minutes erosion is seen in Figure 44 and Figure 45 respectively.

Mean 3D step height formation (μm) calculated after 5 minutes erosion showed no statistically significant difference (p>0.05) between 3 mins and 24 hrs AEP (1.22(0.31) vs 1.01(0.31)); Figure 44.

Mean (SD) surface roughness (Sa, μm) at baseline was 0.66 (0.36) μm and 0.51(0.30) μm for both 3-min and 24-hrs AEP group; Figure 45. After 5 mins erosion mean (SD) surface roughness increased significantly (p<0.001) for both groups to 1.30(0.16) μm (3-mins AEP) and 1.49(0.29) μm (24-hrs AEP). There was no statistically significant difference (p>0.05) in post-erosion surface roughness between 3-mins and 24-hrs AEP groups.

Percentage reflectivity decreased for both groups from 100% (baseline) to 92% and 95% for 3-mins and 24-hrs groups respectively after 5-mins erosion compared to baseline.

Qualitative analysis of TSM images for each treatment group showed erosive destruction of the surface enamel after 5-mins erosion versus before erosion (Figure 46). Before erosion, both groups demonstrated similar surface morphology features. After erosion, both demonstrated features consistent with erosion; darkening of enamel surface, prism core dissolution, and evidence of keyhole pattern formation. There was no visualisable difference in the erosion lesions produced in 3-mins AEP vs 24-hrs AEP groups.
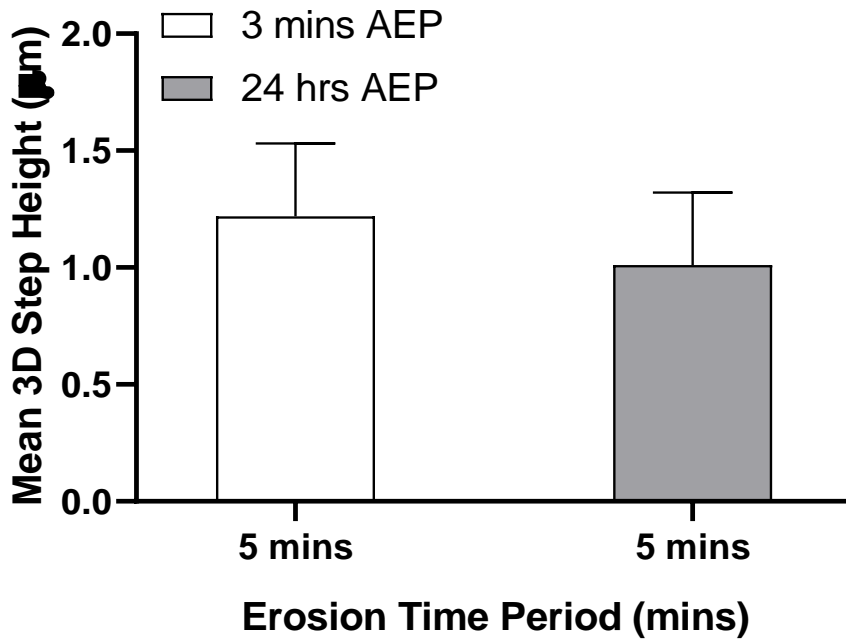
Figure 44 – Mean (SD) 3D step height formation (µm) after 5 mins

erosion for both 3 mins and 24 hrs AEP
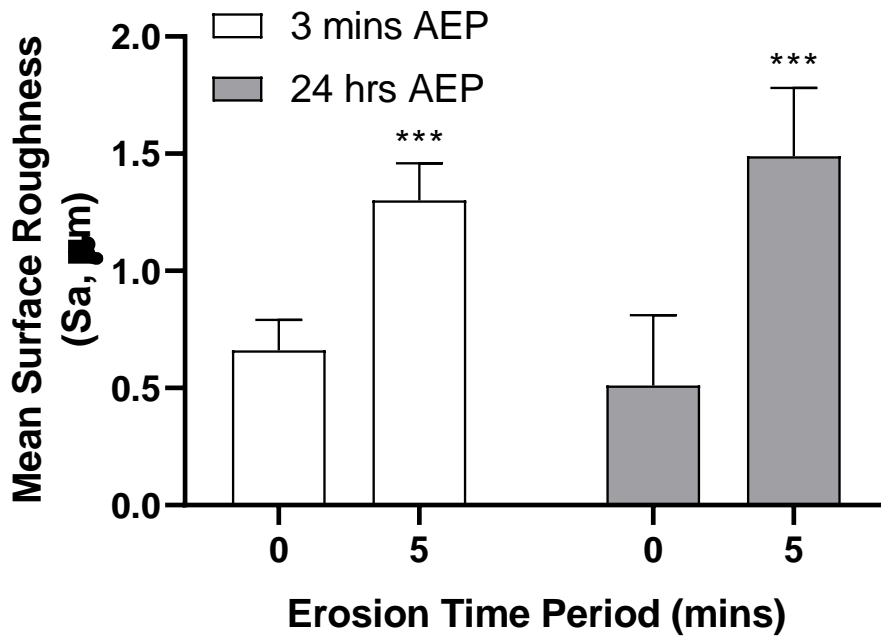
Figure 45 – Mean (SD) surface roughness for both 3-mins and 24-hrs AEP at baseline (0 mins) and after erosion (5 mins). Statistical significance is denoted by * (p<0.05), ** (p<0.01), *** (p<0.005), and ****(p<0.0001).
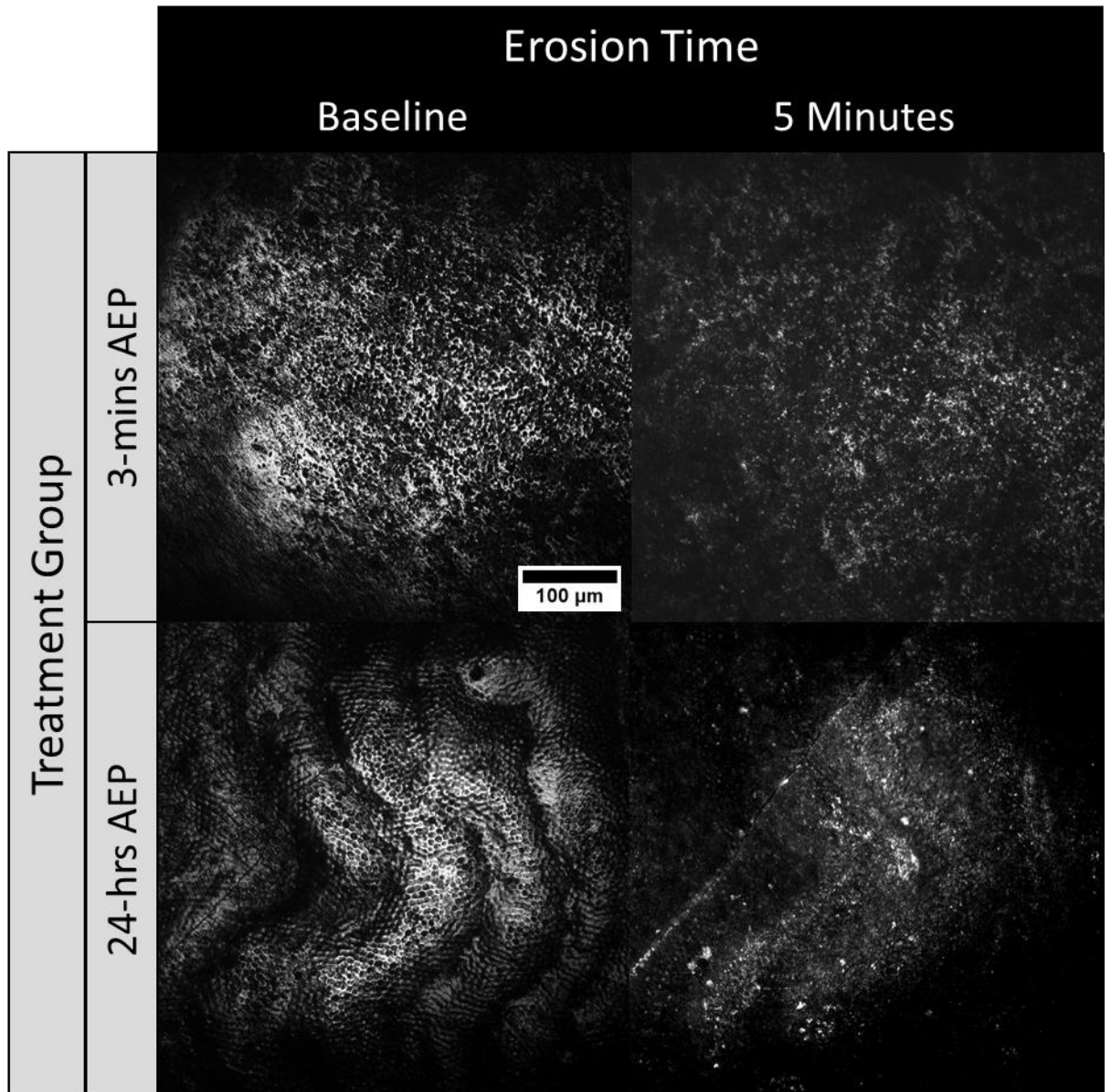
Figure 46 – Representative TSM images taken for each saliva treatment group before erosion (baseline) and after 5 mins erosion. Images are arranged per group in row order, and per erosion time in column order. All images are to the same scale represented by the single scale bar.

4.6   Discussion

In this Chapter we conducted two separate investigations to determine the impact of NaF toothpaste pre-treatment (investigation 1) and the AEP (investigation 2) on dental erosion in natural enamel.

In investigation 1, we demonstrated the effects of single application of sodium fluoride and saliva to multiple cycles of citric acid erosion on natural enamel. Sodium fluoride contained in a toothpaste slurry produced significantly less 3D step height formation on natural human enamel compared to a non-fluoride slurry; therefore, the first null hypothesis was rejected. The second null hypothesis was accepted as there was no difference in 3D step height formation between artificial or natural human saliva for both fluoride and non-fluoride pre-treatment groups, indicating either can be used as the mineralising solution after toothpaste slurry treatment.

The differences in mineralising effectiveness between natural saliva and artificial saliva might reflect their organic constituents (Chapter 1). The organic component of natural human saliva may influence the remineralisation and mineralising properties of human saliva (Lippert et al., 2004a). The artificial saliva used in this Chapter followed Eisenburger et al 2001 formulation and is considered a pure mineral solution without any organic components that could potentially affect Ca^{2+} availability for remineralisation or mineralisation (Eisenburger et al., 2001).

This Chapter evaluated the use of natural human enamel with sodium fluoride toothpaste for erosion in vitro. Previous dental erosion studies have utilised polished enamel, either of human or animal origin, because measurement using NCLP or other analytical techniques has previously not been possible (Zheng et al., 2009, 2010;

Zheng and Zhou, 2007). Utilising natural human enamel samples provides a more clinically representative substrate to test oral care products, such as fluoridated toothpastes, compared with polished samples; it has been previously discussed in Chapter 1, how the polished enamel surface is more susceptible to acid erosion and how the erosion process differs compared with natural enamel (Zheng et al., 2010; Zheng and Zhou, 2007).

Overall, sodium fluoride produced statistically lower mean 3D step height formation compared to non-fluoride slurry pre-treatment and supports findings from polished enamel studies (Lussi et al., 2008; Magalhaes et al., 2009). This suggests that the fluoride pre-treatment of natural enamel protects the surface against citric acid erosion, regardless of the effect of natural or artificial saliva. It has been previously suggested that sodium fluoride-containing toothpastes can form a layer of precipitated calcium fluoride (CaF_2) onto the enamel surface and increase the amount of fluorapatite (FA) in the enamel surface. The calcium fluoride layer is assumed to act like a physical barrier against acid attack on the underlying enamel surface and thus helps reduce demineralisation and promote remineralisation, whilst the FA is much more resistant to subsequent acid-demineralisation (Magalhães et al., 2011). However this was not investigated and was beyond the scope of this Chapter, future study would be required to investigate this further.

Additionally, our results demonstrated that a single application of sodium fluoride produced a significant protective effect against dental erosion in vitro in natural human enamel. Similar results, using a polished enamel model with highly concentrated fluoride were demonstrated in a previous study (Sar Sancakli et al.,

2015). The results of our study did not demonstrate any statistically significant differences for the influence of saliva type on mean 3D step height at all erosion times. This suggests for laboratory studies of a similar design either artificial or natural saliva can be used and supports the results of Batista et al (Batista et al., 2016).

The primary measurement outcome in our study was 3D step height formation which is an internationally recognised method of determining bulk enamel loss in dental erosion studies utilising polished enamel samples, regardless of biological origin. It is the first to utilise this measurement output for natural surfaces of human enamel. Profile subtraction has been a technique previously utilised by Holme et al 2005 to determine bulk enamel change in eroded enamel; and it has been successfully used to determine 3D step height formation in our study (Holme et al., 2005). However, Holme et al (Holme et al., 2005) used white light interferometry to determine bulk enamel change using the residual data produced from subtracting scans obtained before and after erosion using hydrochloric acid. Our study is the first to utilise this profile subtraction technique with scanned data sets obtained using non-contacting optical profilometry in a citric acid erosion model.

TSM images allowed a qualitative assessment of the eroded region of representative samples of each treatment group and supported the step height data. Baseline images indicated the presence of the amorphous surface layer of the natural human enamel samples and the associated topographical features. Qualitative differences are evident between samples pre-treated with fluoride toothpaste slurry compared to those treated with non-fluoride toothpaste. After 5 minutes erosion, both fluoride

treatment groups demonstrated less erosive destruction compared with the non-fluoride treatment groups, with a more intact topographical and morphological features present, hills and dells, and less honeycomb-appearance (compared with before erosion). After 15 minutes, the pattern of erosive destruction appears similar across all treatment groups, whilst at 10 minutes only the F + AS group indicate less erosive effects. This suggests the effects of fluoride and artificial saliva pre-treatment resulted in protection against erosion for longer erosion periods. These findings are also supported by previous studies which have utilised scanning electron microscopy to show differences in erosion pattern of enamel samples treated with non-fluoride, and different fluoride type products (Wang et al., 2011b; Alexandria et al., 2017).

In investigation 2, the short (3-min) and long (24-hrs) term AEP was tested for their erosive protective benefit on natural human enamel against a previously published dietary citric acid in vitro model. No statistically significant difference in the protective benefits between either AEP group could be demonstrated; both experimental groups resulted in characterisable erosion lesions after 5-mins erosion. As a result, both null hypotheses were accepted.

The protective benefit of the AEP against dietary erosion in vitro is still a matter of debate within the wider erosion literature; some studies have demonstrated a protective effect of the AEP (Hannig et al., 2004a; Mutahar et al., 2017) whilst others have demonstrated no or a limited protective effect (Nekrashevych and Stosser, 2003; Brevik et al., 2013). In this Chapter, step height formation was measurable in both AEP groups, indicating there was no protective effect from either the 3-mins or 24-hrs AEP. Hannig et al 2004 evaluated the protective effect of the AEP formed over

three different time periods, 3, 60, and 120 minutes, on polished bovine enamel, subjected to 1-min erosion (1% citric acid pH 3.6). Their results demonstrated the erosive protective benefit of all three types of AEP; demonstrating surface microhardness loss and calcium release were both lower in those samples treated with 3-min AEP vs no-AEP; indicating that the protective effect of short-term (3-min) pellicle against short duration citric acid erosion (Hannig et al., 2004a). This contrasts with the results obtained in our study, using surface profilometry, and showed no difference between the 3-min or 24-hrs pellicle. This could be due to the differences in the method used to generate the AEP or the evaluation of change. Hannig et al 2004 utilised human volunteers to create the AEP on the enamel samples by wearing an oral appliance housing the polished bovine samples; they therefore tested an in situ formed AEP as compared to a purely in-vitro pellicle derived from previously collected frozen whole human saliva which was pooled and vortexed. Further investigation is required to determine whether there are differences in the formation, composition, and erosive-protective properties of AEP depending on how it was formed, in vitro versus in situ.

Mutahar et al 2017 demonstrated the erosion protective benefit of a 24-hrs AEP using an in-vitro AEP using a method similar to the one used in the present study. This study immersed polished human enamel samples in pooled vortexed whole human saliva, derived from previously collected frozen samples, for 24 hours, washing and drying for another 24 hours before then subjecting samples to five 10-mins erosion cycles (0.3% citric acid pH 3.2). Their results demonstrated significantly ($p < 0.05$) lower mean step height formation in 24-hrs AEP group versus no-AEP group,

but interestingly, an increased surface microhardness loss compared to no-AEP. The findings from our study demonstrated that step height was still measurable after one 5-min erosion period, with values similar to those demonstrated in Chapter 3. Whilst it was beyond the scope of this PhD to analyse the proteomics of the collected human saliva, and the subsequent AEP formation, it may be hypothesised that the saliva used to create the AEP may have had a low protein content or those proteins may have been lost during the thawing process. Further investigations are therefore warranted to determine whether an in-vivo formed AEP would produce different results compared with the in vitro formed AEP. Additionally it is unknown whether the collected human saliva samples were contaminated with bacteria. Further investigation is required to determine whether their presence would impact on the subsequent AEP formed using those saliva samples.

The use of surface roughness in this study provided evidence that the surface microtextural features following citric acid erosion were not significantly different (p>0.05) between 3 mins AEP (1.30(0.16) μm) and 24-hrs AEP (1.49(0.29) μm). However, surface roughness was significantly increased compared to baseline values for both groups, 0.66(0.36) microns and 0.51(0.30) μm respectively. This therefore suggests the in-vitro AEP formed in this study at both time points did not result in protective benefit, which would have manifested as a non-significant increase or lack of increase in surface roughness following erosion. The erosive protective ability of the AEP has been previously discussed in Chapter 1 and has been shown to vary according to the erosive solution used and the type of AEP model utilised. In this Chapter, it may be the case that the erosive challenge was too strong for the AEP that

formed on the samples. Whilst it was beyond the scope of this Chapter, further analysis of the AEP itself is warranted as well as further work using weaker acid solutions to determine whether the AEP model in this chapter provide any erosive-protective capabilities.

The use of surface reflectivity to analyse the effects of acid erosion and subsequent impact of the AEP demonstrated a subtle difference in percentage normalised surface reflectivity between 24 hrs (95%) and 3-mins (92%) AEP. Previous studies using OCT to analyse the effect of the AEP on dental erosion have used OCT signal backscatter intensity as their measurement output, and to our best knowledge, none have used surface projection images. Breivik et al 2013, characterised changes in surface reflectivity in polished human samples using a previously validated reflectometer. Polished human enamel samples were immersed in whole human saliva for 15 hours to form 15-hrs AEP or kept in a humid environment, and then eroded with citric acid (1%, pH 3.6) for 2 4, 8, 10 and 15 minutes. This study demonstrated that specular reflection intensity was significantly different between AEP and non-AEP treated samples; with higher specular reflection intensity in AEP treated samples after 2 and 4 mins erosion (Brevik et al., 2013). The authors concluded the 15-hrs AEP produced a protective benefit helping to maintain a higher level of surface reflection after 2- and 4-mins erosion versus non-AEP treatment enamel. However, Austin et al 2017 demonstrated erosive change as the increase in overall mean decay of backscattered OCT signal intensity compared to enamel immersed in water only (Austin et al., 2017). This study used natural human enamel and 60 mins orange juice erosion.

TSM images supported the data obtained using NCLP and OCT. Baseline images indicated presence of highly variable topography comprising the surface layer of the natural enamel samples. Qualitative differences in surface morphology is evident after erosion (Figure 7) for both 3-mins and 24-hrs AEP when compared to their respective baseline images. Features indicative of erosive attack include, loss of surface topography features, presence of keyhole erosive pattern, and destruction of prism cores. These findings are also supported by previous studies utilising TSM to study erosion on natural human enamel, which indicate a similar erosion destruction features (Mullan et al., 2017a).

This study only utilised a single 5-min erosion cycle to demonstrate no protective benefit of AEP, compared to previous studies that have utilised multiple erosion cycles to measure the longitudinal effect of acid erosion and the impact of the AEP. This was sufficient to demonstrate the lack of erosion protection of the AEP, given that the erosion lesions could be measured and characterised using changes in surface form, roughness, reflectivity, and morphology.

4.7 Conclusion

Within the limitations of this in-vitro study, investigation one demonstrated that sodium fluoride pre-treatment resulted in a protective effect against citric acid mediated dental erosion, regardless of the remineralisation solution used. Either artificial saliva or natural human saliva can be used as the remineralisation solution after fluoride pre-treatment, without significantly affecting step height formation, and thus can provide a better understanding of the effects of the type of fluoride used. Whilst Investigation two demonstrated that dental erosion could still be characterised in natural enamel regardless of the AEP present before erosion.

5 Chapter 5 – Effect of calcium silicate/sodium phosphate treatment on early and late erosion in natural human enamel

5.1 Introduction

In Chapter 4, two factors were investigated for their impact on the dental erosion model created in Chapter 3. The impact of single application NaF toothpaste application on the natural enamel was investigated using a previously published oral healthcare product testing laboratory model (Parker et al., 2014; Hornby et al., 2014; Wood et al., 2018). Additionally, a short term (3-mins) and long term (24-hrs) laboratory formed AEP model was used in accordance with previous protocols (Hannig et al., 2004b; Mutahar et al., 2017).

This Chapter investigates the impact of an existing calcium silicate, sodium phosphate and sodium monofluorophosphate toothpaste formulation (NR5) on dental erosion on natural enamel. This formulation has been previously studied and its erosive-protective benefits have been demonstrated in an in vitro erosion model. NR5 formulation has been shown to produce calcium silicate, and calcium fluoride particles which deposit on the surface of polished enamel; providing an erosive-protective benefit(Parker et al., 2014; Hornby et al., 2014; Wood et al., 2018). These studies used polished human and bovine enamel, the effects of this toothpaste formulation have not been evaluated on natural human enamel.

This Chapter therefore utilises the same erosion model described in Chapter 3 and the same oral product testing model outlined in Chapter 4 with artificial saliva as the mineralisation solution.

5.2 Chapter Aims, Objectives and Null Hypotheses

5.2.1 Chapter Aim

The aim of this study was to:

1. Determine the effect of single application of calcium silicate, sodium phosphate and sodium monofluorophosphate toothpaste pre-treatment on the early and late erosion process on natural human enamel

5.2.2 Chapter Objectives

The objectives of this Chapter are linked to and expand on Thesis Objective 3 (page 114):

1. Compare the use of calcium silicate, sodium phosphate and sodium monofluorophosphate toothpaste vs sodium monofluorophosphate (positive control) vs non-fluoride (negative control) toothpaste slurry mixture in a pre-treatment model on natural human enamel and determine the effect on step height formation, surface roughness, surface reflectivity, and surface morphology of natural enamel in vitro

5.2.3 Chapter Null Hypotheses

1. There will be no difference in erosion lesions formed on natural human enamel samples pre-treated with calcium silicate, sodium phosphate and sodium monofluorophosphate toothpaste, sodium monofluorophosphate and non-fluoride toothpaste

2. There will be no difference between artificial saliva and natural human saliva mineralisation solutions

5.3 Materials and Methods

5.3.1 Sample creation

Natural human enamel specimens (n=60) were sectioned, bonded onto glass microscope slides, and thoroughly cleaned according to the method described in Chapter 3 Section 3.3.1.

5.3.2 Test solutions

Citric acid (0.3%, pH 3.2) was prepared for use according to the method described in Chapter 3 section 3.3.5.2

Three toothpaste slurries were created according to the mixing ratios and quantities outlined in Chapter 4 Section 4.3.2 (Hornby et al., 2014; Wood et al., 2018).

The toothpaste slurries used in this study were as follows:

1. Calcium silicate/sodium phosphate and sodium monofluorophosphate (NR5) toothpaste (1450 ppm F as SMFP)

2. Sodium monofluorophosphate (SMFP) toothpaste (1450 ppm F as SMFP)

3. Non-fluoridated (NF) toothpaste (0 ppm F)

All slurries were immediately used within 30s of their homogenisation to ensure equal use of active ingredients across all test groups. The mean (SD) pH of each test slurry was: (1) 9.83(0.02), (2) 6.76(0.04), (3) 6.62(0.02). All slurries were used at room temperature ($22 \pm 0.5^{o}C$).

Paraffin stimulated whole mouth natural human saliva was collected from healthy volunteers using 15ml polypropylene tubes, immediately stored in $-80^{o}c$ freezer, and prepared for use according to the method described in Chapter 4 Section 4.3.2.

Artificial saliva was created according to the method described in Chapter 4 Section 4.3.2 and formulation provided by (Eisenburger et al., 2001).

5.3.3   Natural enamel erosion model

All specimens (n=60) were numbered and randomly assigned (random number generator, Microsoft Excel 2016, Microsoft, USA) to pre-treatment groups (1), (2), or (3) with 20 samples per group (Figure 47).

Pre-treatment consisted of immersion (10ml per sample, 3 mins) of all samples followed by 1 rinse (1-minute, deionised water), dried (5s oil-free air), and placement in mineralisation solution (30 mins) artificial saliva (AS, n=30) or deionised water (DIW, n=30). This produced six experimental groups shown (Table 9).

After pre-treatment, samples were eroded in citric acid (0.3%, pH 3.2) for three cycles of 5 minutes erosion (cumulative erosion times 5, 10, 15 mins erosion), whereby one erosion cycle consisted of erosion (10ml, 5-mins) under constant agitation (62.5 RPM, Stuart mini-Orbital Shaker SSM1, Bibby Scientific, England) followed by 2-minute rinse with deionised water

The resulting lesions were measured/characterised quantitatively using changes in surface form (mean 3D step height change) and surface roughness (mean Sa) using non-contacting laser profilometry (NCLP), surface reflectivity using optical coherence tomography (OCT) and qualitatively using tandem scanning confocal microscopy (TSM).

Experimental Group	Abbreviation
Calcium silicate/sodium phosphate and sodium monofluorophosphate + Artificial Saliva	NR5 + AS
Calcium silicate/sodium phosphate and sodium monofluorophosphate + Deionised Water	NR5 + DIW
Sodium monofluorophosphate + Artificial Saliva	SMFP + AS
Sodium monofluorophosphate + Deionised Water	SMFP + DIW
Non-fluoride + Artificial Saliva	NF + AS
Non-fluoride + Deionised Water	NF + DIW

Table 9 – Experimental groups in this Chapter and their associated abbreviations
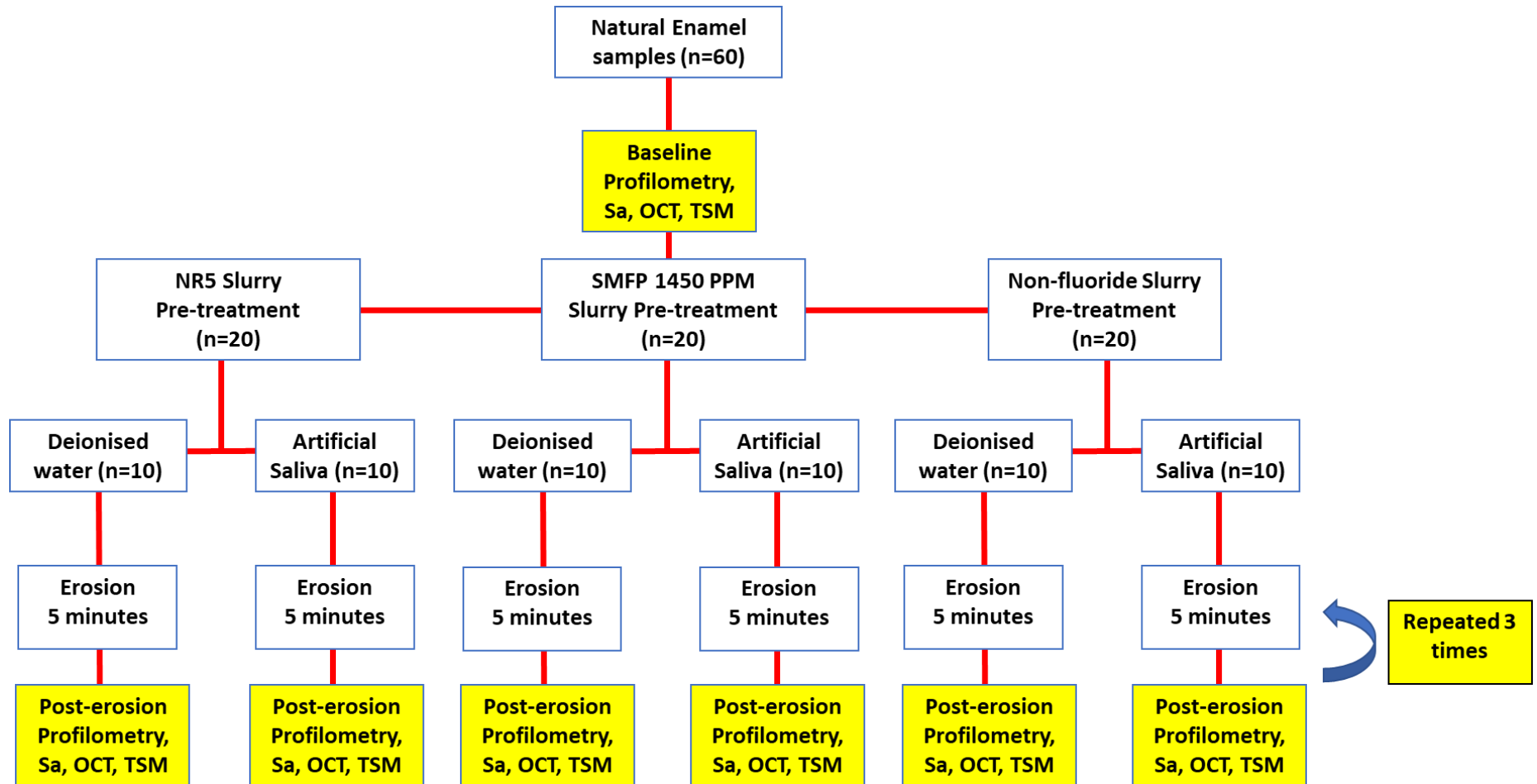
Figure 47 – Simplified outline of the experimental process

5.3.4 Erosion characterisation techniques

All specimens (n=80) were scanned using NCLP, and representative samples (n=2, per group) were scanned with OCT and TSM before slurry pre-treatment (baseline assessment) and after each erosion cycle (5, 10, and 15-minute post-erosion assessment). NCLP scanning protocol for surface form and roughness measurement, and calculation of 3D step height formation (Chapter 3 Section 3.3.5.3) and surface roughness (Chapter 3 Section 3.3.6). OCT scanning protocol and analysis of surface reflection images was conducted according to the method described in Chapter 3 Section 3.3.7. Qualitative two-dimensional images were obtained and analysed for representative samples from each pre-treatment group and after each erosion cycle using TSM using the method described in Chapter 2 Section 2.3.3.

5.4 Statistical methods

Data were collected, tabulated and statistically analysed using GraphPad Prism 7 (GraphPad Software Inc, USA). From previous pilot data, a power calculation, using GPower 3.0.1, based on ANOVA comparing the treatment groups was conducted, and indicated a sample size of 8 per treatment group (54 total sample size) would be required for an effect size 0.45 yielding 80% power. Data were assessed for normal distribution using Shapiro-Wilks and Komogorov-Smirnov tests and visually assessed with box-plots and histograms. Data were normally distributed, therefore mean and standard deviations were reported. Inter-group analysis was conducted with two-way repeated measures ANOVA with post-hoc Tukey's test for multiple intra group comparisons. Pearson correlation and linear regression analysis was performed between mean 3D step height and mean surface roughness; $p < 0.05$ was considered

statistically significant, R^2 values determined for all correlation measures and r values

for association between variables.

5.5 Results

Mean (SD) 3D step height formation after 5, 10, and 15 minutes for each treatment group and their statistical associations are summarised in Figure 48.

The lowest mean (SD) 3D step height formation in either deionised water or artificial saliva immersion after 5, 10- and 15-minutes erosion was demonstrated by NR5 + AS group: 0.51 (0.2) μm, 1.08 (0.27) μm, and 1.96 (0.4) μm respectively.

For deionised water immersion, mean (SD) 3D step height was significantly lower for NR5 than NF at 5 mins (0.86(0.38) vs 1.34(0.36), p<0.05) and 15 mins (1.83(0.44) vs 2.40(0.41), p<0.05). However, there were no statistically significant differences between NR5 and SMFP for all immersion time points (p<0.05).

For artificial saliva immersion, mean (SD) 3D step height was significantly lower for NR5 than NF at 5 mins (0.51(0.22) vs 1.15(0.40), p<0.05), 10 mins (1.08(0.27) vs 2.06(0.61), p<0.0001), and 15 mins (1.96(0.40), 2.75(0.79), p<0.01), and compared to SMFP at 10 (1.08(0.27) vs 1.77(0.49) p<0.05), and 15 mins (1.96(0.40) vs 2.75(0.49), p<0.01). There were no statistically significant differences between NF and SMFP for all immersion time points (p<0.05).

Mean (SD) surface roughness for each treatment group can be seen in Figure 49. When comparing all treatment and immersion groups to their respective baseline values after 5 mins erosion, the lowest mean (SD) surface roughness values were obtained for NR5 + AS group roughness compared to baseline (0.83(0.13) vs 1.15(0.17) μm, p<0.001). The highest mean (SD) surface roughness value was found in NF + AS group 1.10(0.40) μm (p<0.01) compared with its own baseline 0.54(0.24) μm.

For deionised water immersion, there were no statistically significant differences in surface roughness between any toothpaste treatment group.

However, for artificial saliva immersion, there was a statistically significant higher surface roughness for NF than NR5 at 10 (1.98(0.74) vs 1.27(0.18), p<0.0001) and 15 mins (1.76(0.58) vs 1.29(0.09), p<0.001) and then SMFP at 10 mins (1.98(0.74) vs 1.22(0.13), p<0.0001) and 15 mins (1.76(0.58) vs 1.29(0.13), p<0.001). There was no statistically significant difference between NR5 and SMFP at any erosion time point (p>0.05).

Linear regression and correlation analysis for mean 3D step height versus mean surface roughness is shown for treatment groups NR5 (Figure 50), SMFP (Figure 51) and NF (Figure 52) toothpastes. All treatment groups demonstrated a positive linear relationship and very weak positive correlation, which was statistically significantly only for NR5 + AS (p<0.05).

Surface reflectivity changes from OCT are indicated in Table 10 for each treatment group. Within artificial saliva immersion treatment groups, percentage peak intensity normalised against baseline values were highest in NR5 slurry group with 91.2% reflection after 5 minutes, compared to 87.2% and 86.6% for SMFP and NF respectively. This trend continued after 10 and 15 minutes when compared to both SMFP and NF slurry groups. Within deionised water immersion groups, highest percentage peak intensity values were for non-fluoride slurry group with 94.6% reflection after 5 minutes, compared with 84.7% and 92.7% for NR5 and SMFP respectively.

Qualitative analysis of TSM images for each treatment group showed progressive erosive destruction of the surface enamel with increase of erosion time (Figure 53). Differences in the erosive patterns can be visualised for all treatment groups with progressive visualisation of an etch pattern with increasing erosion. At 5 minutes erosion, a clear difference in eroded enamel appearance was seen between each treatment group; erosive effects appeared least prominently in the NR5 + AS and NR5 + DIW groups whilst they were more apparent in the NF + DIW and NF + AS groups. Additionally, both NR5 and SMFP treatment groups indicated less erosive destruction compared with both NF treatment groups. After 10 minutes, the qualitative differences between each treatment group reduced with only the NR5 + AS group showing more resistance to acid erosion. After 15 minutes however, the effects of erosion appeared similar across all treatment groups.
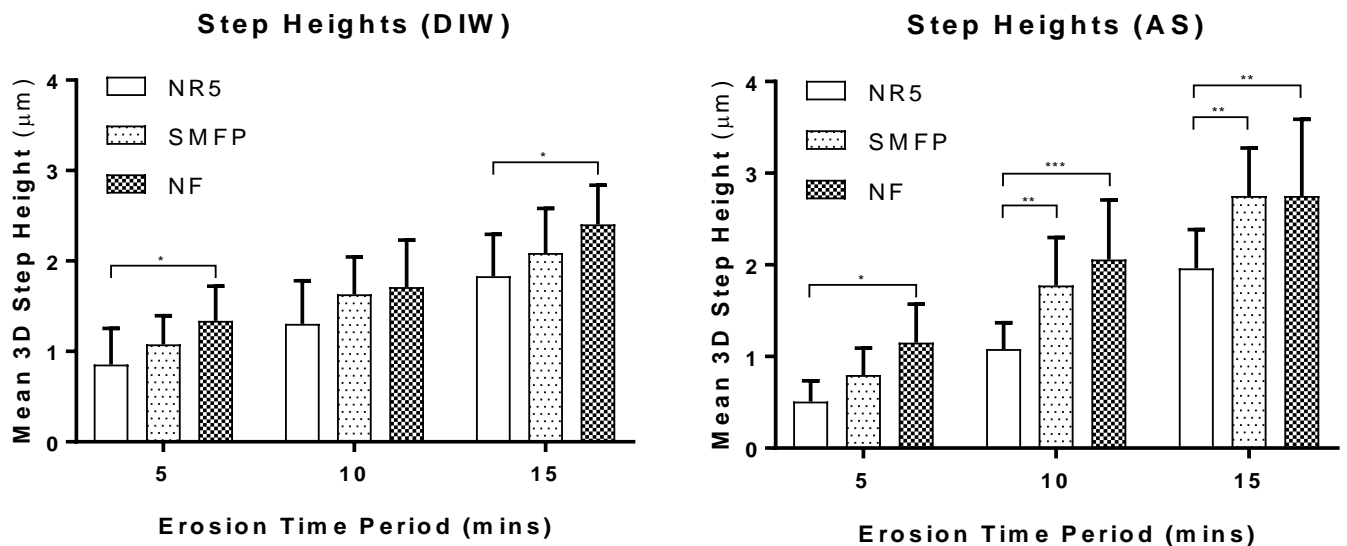
Figure 48 – Mean (SD) 3D step height for each erosion time point and treatment group. Statistical significance is denoted by- *p<0.05, **p<0.01. ***p<0.001, ****p>0.0001
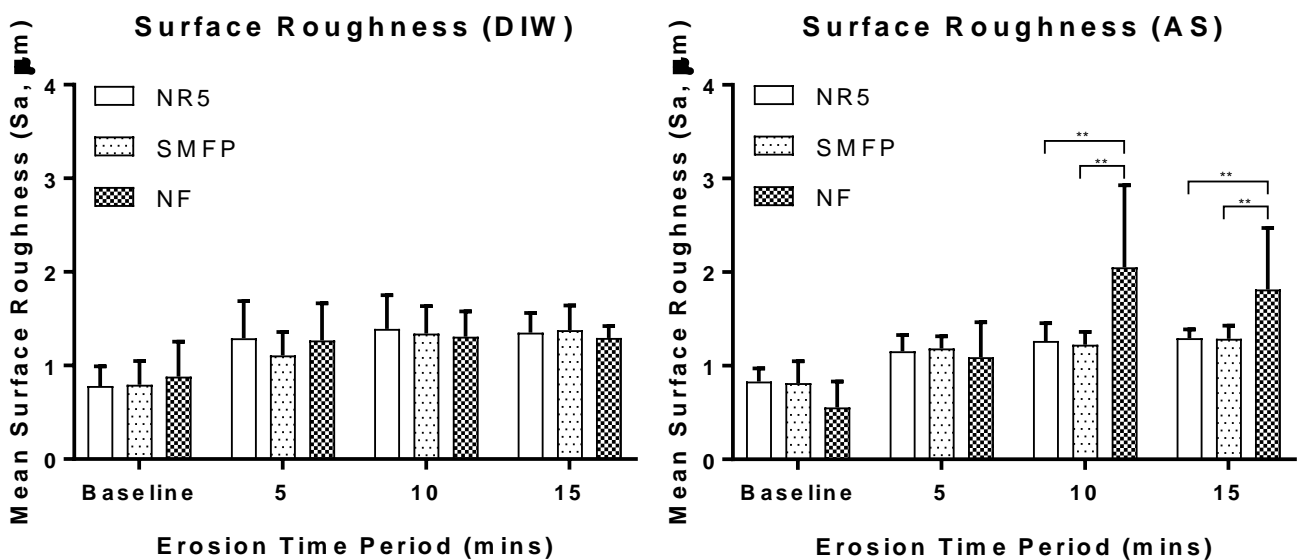
Figure 49 – Mean (SD) surface roughness for each treatment group. Statistical significance is denoted by- *p<0.05, **p<0.01. ***p<0.001, ****p>0.0001

	Percentage Peak Intensity vs Baseline (%)					
Erosion Time (mins)	NR5 + AS	SMFP + AS	NF + AS	NR5 + DIW	SMFP + DIW	NF + DIW
0 (Baseline)	100.0	100.0	100.0	100.0	100.0	100.0
5	91.2	87.2	86.6	84.7	92.7	94.6
10	85.9	85.2	84.2	80.2	84.8	91.5
15	86.7	82.1	81.1	77.9	82.1	90.9

Table 10 – Percentage peak intensity vs baseline for each treatment group

238
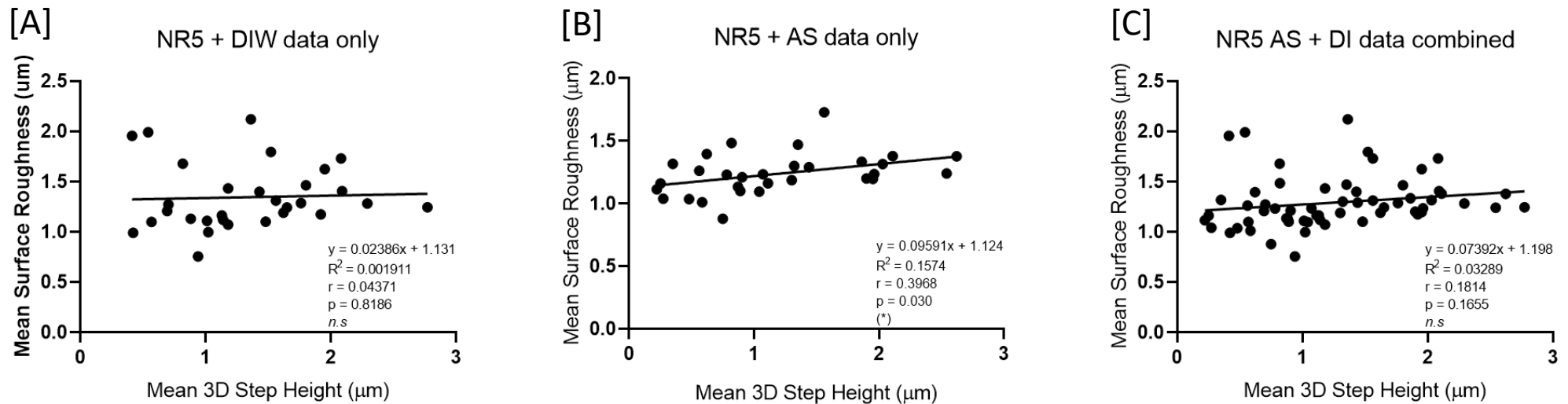
Figure 50 – Linear regression and Pearson's correlation coefficient is demonstrated for NR5 treated group. Analysis was performed for each immersion group (A) Deionised water, DIW, (B) artificial saliva, AS, and (C) with the data combined. A positive linear relationship and very weak correlation is demonstrated for all three data sets; this is statistically significant only for (A) NR5 + AS data. Statistical significance is shown by: (*) $p<0.05$, (**) $p<0.01$, (***) $p<0.001$, (****) $p<0.0001$. R^2 indicates strength of association (0 is lowest, 1 is highest), r indicates strength and direction of linear relationship (0 is no linear relationship, +0.3 is weak positive, +0.5 is moderate positive, +0.7 is strong positive, +1 is perfect positive)
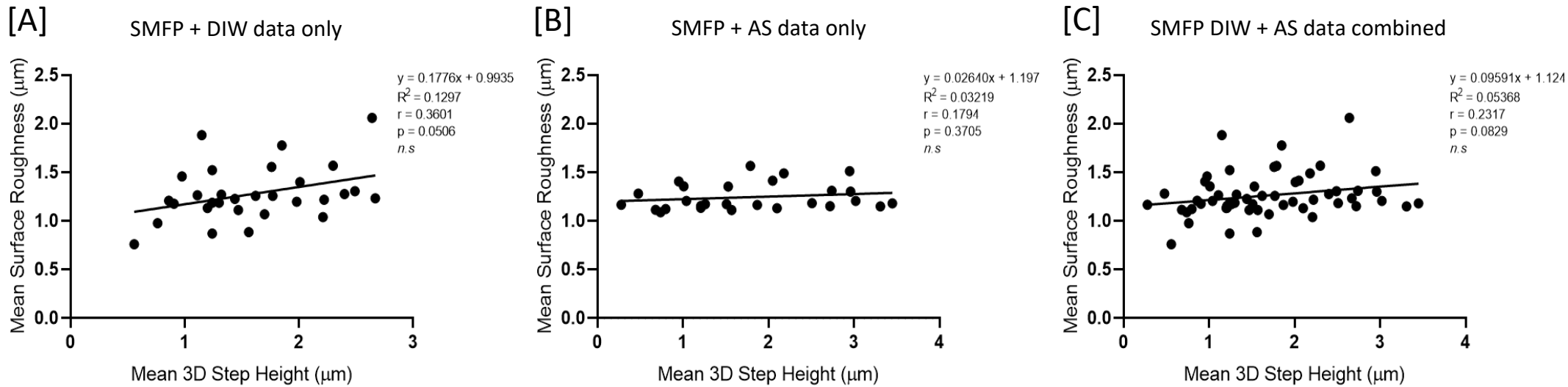
Figure 51 – Linear regression and Pearson's correlation coefficient is demonstrated for SMFP treated group. Analysis was performed for each immersion group

(A) Deionised water, DIW, (B) artificial saliva, AS, and (C) with the data combined. A positive linear relationship and very weak correlation is demonstrated for

all three data sets; none were statistically significant. Statistical significance is shown by: (*) $p < 0.05$, (**) $p < 0.01$, (***) $p < 0.001$, (****) $p < 0.0001$.

R^2 indicates strength of association (0 is lowest, 1 is highest), r indicates strength and direction of linear relationship (0 is no linear relationship, +0.3 is weak

positive, +0.5 is moderate positive, +0.7 is strong positive, +1 is perfect positive)

[A] NF + DIW data only

Mean Surface Roughness (μm) vs Mean 3D Step Height (μm)

$y = 0.08864x + 1.129$
$R^2 = 0.03988$
$r = 0.1997$
$p = 0.2900$
n.s

[B] NF + AS only

Mean Surface Roughness (μm) vs Mean 3D Step Height (μm)

$y = 0.1601x + 1.314$
$R^2 = 0.0417$
$r = 0.1848$
$p = 0.356$
n.s

[C] NF AS + DIW data combined

Mean Surface Roughness (μm) vs Mean 3D Step Height (μm)

$y = 0.15871x + 1.151$
$R^2 = 0.04165$
$r = 0.2044$
$p = 0.1278$
n.s
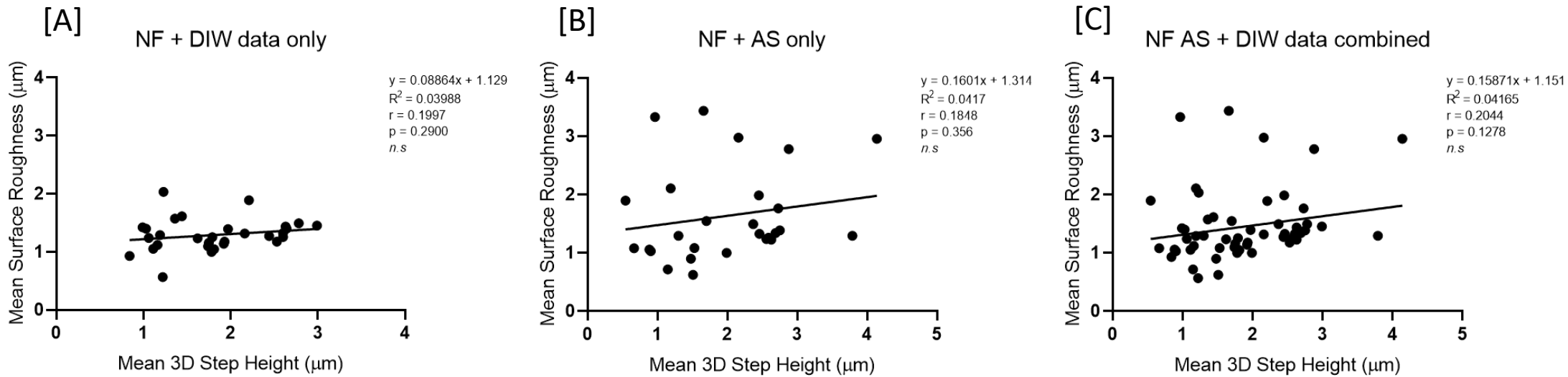
Figure 52 – Linear regression and Pearson's correlation coefficient is demonstrated for NF treated group. Analysis was performed for each immersion group (A) Deionised water, DIW, (B) artificial saliva, AS, and (C) with the data combined. A positive linear relationship and very weak correlation is demonstrated for all three data sets; none were statistically significant. Statistical significance is shown by: (*) $p<0.05$, (**) $p<0.01$, (***) $p<0.001$, (****) $p<0.0001$. R^2 indicates strength of association (0 is lowest, 1 is highest), r indicates strength and direction of linear relationship (0 is no linear relationship, +0.3 is weak positive, +0.5 is moderate positive, +0.7 is strong positive, +1 is perfect positive)

242
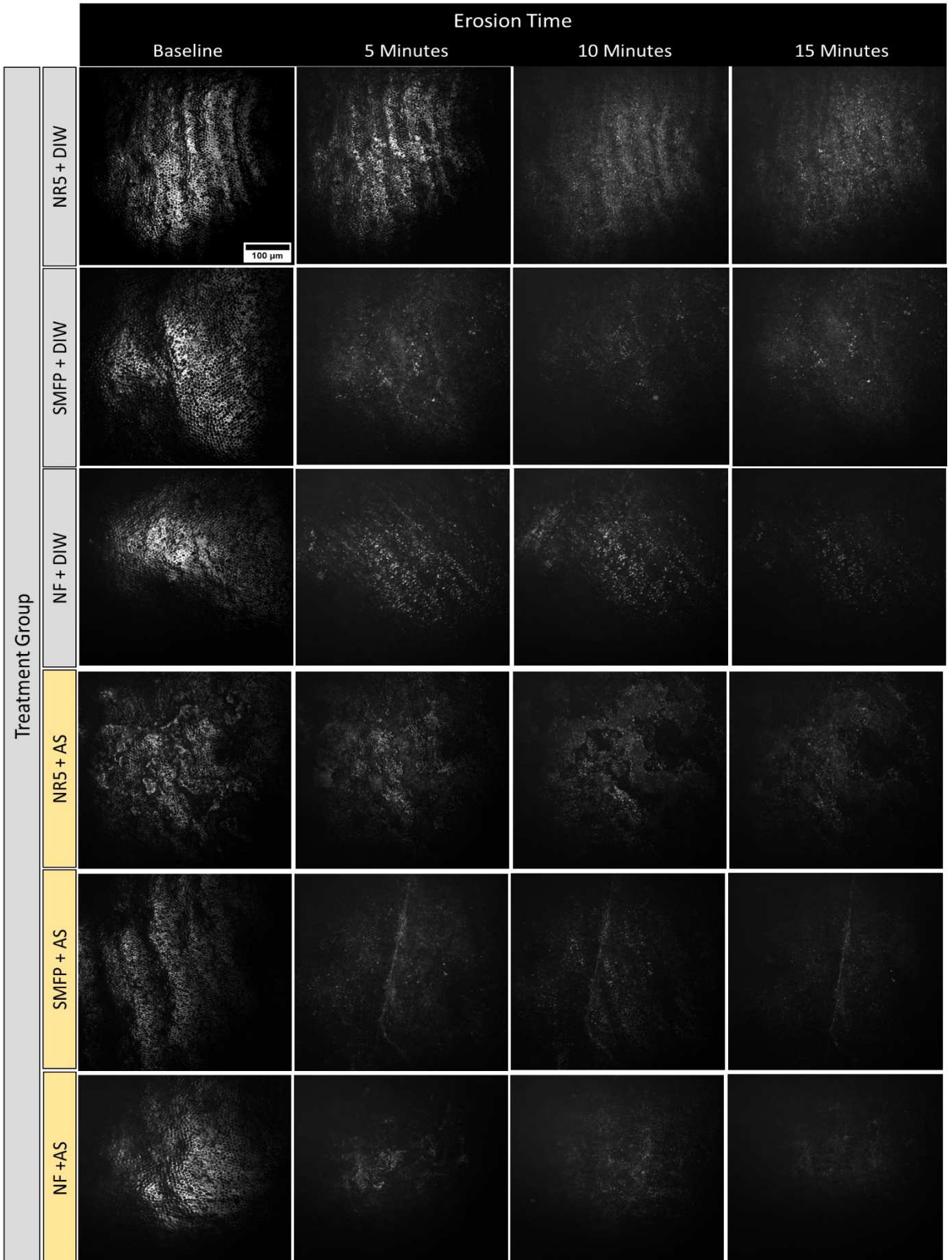
Figure 53 – Representative TSM images taken for each treatment group before erosion (baseline) and after 5, 10, and 15 minutes erosion. Images are arranged per group in row order, and per erosion time in column order. All images are to the same scale represented by the single scale bar. Groups are labelled using combination of the following letters: NR5 (calcium silicate/sodium phosphate, SMFP slurry), NF (non-fluoride slurry), AS (artificial saliva), NS (natural saliva), DIW (deionised water).

5.6   Discussion

The erosive protective benefits of a novel calcium-silicate/sodium phosphate and fluoride containing toothpaste against dietary-acid mediated dental erosion in natural human enamel in vitro has been demonstrated in this study. The NR5 toothpaste slurry provided erosive-protective benefits against citric acid erosion as evidenced by reduced 3D step height formation, reduced surface roughness, les changes in surface reflectivity (OCT) and less morphological topographical destruction versus SMFP (positive fluoride control) and NF (negative control) toothpaste slurries. As a result, under the current experimental conditions, the null hypothesis has been rejected.

Previous studies have investigated the protective and remineralising effects of different calcium-silicate/sodium phosphate formulations with or without additional fluoride. Parker et al (Parker et al., 2014) demonstrated the efficacy of 2 minute application of calcium silicate (1mg/ml) slurry in phosphate buffer (pH7) in remineralising eroded bovine enamel. Additionally, they demonstrated the efficacy of the same calcium silicate slurry after immersion in fluoride solution (2 minutes, 1000ppm sodium fluoride) in protecting bovine enamel against subsequent acid erosion (nitric acid pH3). Similarly, Hornby et al (Hornby et al., 2014) demonstrated the erosive-protective benefit of calcium silicate/sodium phosphate and fluoride toothpaste against citric-acid mediated erosion compared with a sodium fluoride control (Hornby et al., 2014).

In the current study, the NR5 toothpaste slurry after immersion in artificial saliva produced the best erosive-protective benefit. This was evidenced with continued reduction in mean 3D step height formation resulting in statistically significantly lower step height after 10- and 15-minutes cumulative erosion compared to both SMFP and NF control toothpaste slurries. In previous laboratory studies, artificial saliva has been shown to provide better mineralisation and remineralisation properties compared with natural human saliva (Amaechi and Higham, 2001; Hara et al., 2008a). This is because artificial saliva is a pure mineral solution containing no organic material (depending on the formulation). The organic material in natural human saliva impacts on calcium and phosphate availability and therefore the mineralisation and remineralisation properties when used in the laboratory.

It is hypothesised that the reduction in bulk enamel loss, through less step height formation, is due to the previously demonstrated ability of calcium silicate/sodium phosphate slurry to deposit calcium silicate particles onto the enamel surface (Parker et al., 2014). Moreover, the erosive-protective benefit of this slurry mixture was previously demonstrated as a result of its rapid calcium release profile which is at its fastest within the first minute of the slurry's formation, pH buffering/modulating effect, as well as its ability to deposit calcium silicate particles on the enamel surface (Parker et al., 2014).

The present study demonstrated the effect of NR5 toothpaste slurry was at its maximum when utilised in conjunction with artificial saliva as the remineralisation solution compared with deionised water only. This is due to the chemical mode of action of calcium silicate-based biomaterials which have been previously

demonstrated to occur in the presence of an ionic solution such as artificial saliva or simulated body fluid (Parker et al., 2014; Wood et al., 2018). The presence of H+ in these solutions causes an exchange with the calcium ions in the calcium silicate and thus resulting in an increase in local pH that results in an attraction of phosphate ions which interact with the calcium ions to precipitate hydroxyapatite (Parker et al., 2014). This interaction would not occur if calcium silicate is immersed in deionised water alone. The interaction between calcium silicate/sodium phosphate and artificial saliva (or ionic solutions) has been previously demonstrated as essential for the precipitation and deposition of hydroxyapatite onto the enamel surface (Hornby et al., 2014; Parker et al., 2014; Wood et al., 2018).

Previous studies evaluating calcium silicate/sodium phosphate formulations in vitro have been conducted on polished enamel surfaces either of bovine (Hornby et al., 2014; Parker et al., 2014) or human (Joiner et al., 2014; Sun et al., 2014; Wood et al., 2018) origin. Investigating the erosive-protective benefit of NR5 on natural human enamel samples provides a clinically realistic laboratory method, improving our understanding of what is likely occurring in the clinical environment. The use of scan alignment and profile subtraction analysis, as described in Chapter 3, provided a way of assessing the erosive protective behaviour of NR5 formulation. This method could therefore be utilised for any other oral healthcare product such as oral mouthwashes or dental varnishes.

Additionally, the current study demonstrated a reduced surface roughness following initial citric-acid attack only for NR5+AS when compared to those in the SMFP and NF control groups after 10 and 15 minutes respectively; indicating the surface roughness of the natural enamel surface was not as rough after acid-attack when it was treated

with NR5 and immersed in artificial saliva. Lower surface roughness values after initial acid attack, indicated by lower Sa (μm) values, have been previously used to denote regions of reduced surface topography destruction following acid attack (Austin et al., 2016). It is hypothesised that this may be due to calcium silicate having been previously shown to nucleate hydroxyapatite and thus alter the demineralisation/remineralisation equilibrium in favour of remineralisation reducing mineral loss from the enamel surface resulting in less surface topography destruction (Hornby et al., 2014; Parker et al., 2014). Interestingly, there was no statistically significant difference in surface roughness when comparing deionised water and artificial saliva toothpaste slurry pre-treatment groups. This may due to the lack of differentiation in erosion lesion types created using deionised water or artificial saliva remineralisation solutions, when utilising the areal parameter of arithmetic average height of the surface, *Sa*. Hara et al (Hara et al., 2016) demonstrated that the use of *Sa* as a parameter to differentiate between erosion-only lesions between eroded and non-eroded enamel surfaces and more complex parameters were required to differentiate further surface microtextural features caused by additional factors such as abrasion and attrition (Hara et al., 2016). In this present study, it is unknown whether there are any differences in the surface microtextural features in erosion lesions produced between the samples immersed in deionised water and artificial saliva due to the use of *Sa* to quantify surface roughness. Further study is therefore required to utilise more surface microtexture analytical parameters to determine whether there is a difference in the dental erosion lesions produced after immersion in either deionised water or artificial saliva remineralisation solution after toothpaste slurry pre-treatment.

OCT analysis provided information on the surface reflective behaviour of the natural enamel samples treated with NR5, SMFP or NF toothpaste slurries. Differences in surface reflectivity between the toothpaste slurries were found with NR5 providing the lowest reduction compared with SMFP or NF. Analysing the surface reflectivity of surface projection images may be a useful surrogate marker for the presence or absence of erosion. Further work is necessary to understand the clinical significance of OCT data, correlating its findings with other investigation techniques such as calcium or phosphate release analysis. Rakhmatullina et al 2011 demonstrated a correlation between the specular reflection of polished enamel and surface roughness and calcium release. Specular reflection decreased with increasing erosion, which correlated with an increase in calcium release and surface roughness (Rakhmatullina et al., 2011). TSM provided qualitative assessment of natural enamel erosion at each erosion cycle. Whilst there were visualisable differences between the different treatment groups at increasing erosion, further morphological analysis would be required using higher magnification techniques such as SEM and EDX. This would help determine differences in the depositions after each toothpaste slurry pre-treatment and ascertain differences in enamel morphology in high detail after erosion. However, a disadvantage to such a technique is in the sample preparation required; this would mean samples can only be used once and erosion could not be studied longitudinally on the same samples. Environmental SEM could also be utilised as no sample surface modification is required for imaging, however, the impact of the vacuum required on the enamel structure would need to be investigated

This current study demonstrated the erosive-protective benefit after a single application of calcium silicate/sodium phosphate and fluoride toothpaste slurry. The effect of single application/treatment using calcium silicate/sodium phosphate against enamel erosion has been also previously demonstrated (Parker et al., 2014). Previously, a single 2 minute treatment phase using calcium silicate/sodium phosphate slurry in phosphate buffer (pH7) was sufficient to reduce the rate of calcium loss from polished bovine enamel surfaces by approximately 39% when compared to non-treated reference enamel regions (Parker et al., 2014). The results of this current study also utilised a similar application time, 3-minutes and 30-minute remineralisation solution period and demonstrated erosive-protective benefits of a calcium silicate/sodium phosphate toothpaste slurry. This agrees with previous literature on the application time required for calcium silicate/sodium phosphate to produce an erosive-protective benefit on enamel samples (Hornby et al., 2014; Parker et al., 2014; Sun et al., 2014).

Further evaluation of the effect of calcium silicate/phosphate technologies on the natural human enamel surface in vitro is required to aid in the understanding of how this technology interacts with the complex morphology of the natural enamel surface.

5.7 Conclusion

Within the limitations of this in-vitro study, calcium silicate-based toothpaste provided erosion-protective benefits evidenced by reduced 3D step height formation over prolonged erosion periods in natural enamel versus fluoride only (MFP) and non-fluoride toothpaste groups. Additionally, surface roughness increase after initial erosion was lowest after calcium silicate-based toothpaste application compared with all other treatment groups. Natural human enamel is a viable test substrate for the evaluation of oral care products, with 3D step height allowing for determination of the protective effect against bulk enamel loss in vitro.

6 Chapter 6 – Overall Discussion, Limitations, and Conclusions

6.1 Overall Discussion and Limitations

The focus of this Thesis was to characterise the micro and macro scale changes occurring on polished and natural human enamel after citric acid attack. The characterisation methodologies used were non-destructive to ensure the erosion process could be studied longitudinally on the same samples. As a result, methods such as SEM and AFM were not utilised, as some degree of surface modification occurs during their use (Paepegaey et al., 2013a; Häßler-Grohne et al., 2011). However, further research is warranted to determine if the mechanisms of erosion are affected by an initial modification of the enamel surface using surface destructive techniques such as SEM and AFM (Field et al., 2010).

In Chapter 2 the measurement techniques and erosion times required to produce measurable erosion lesions differed between the two sample types. Enamel loss could not be calculated using step height using the same method for the polished enamel samples. This was due to two fundamental limitations with the laboratory technique: 1) sample isolation and enamel exposure for erosion, and 2) sample measurement with profilometry. The principles used in sample creation and measurement for polished enamel did not work on the natural enamel surface. The two surfaces were inherently different (as discussed in Chapter 1) and therefore the natural enamel surface was explored further in Chapter 3. The calculation of step height in polished enamel followed the method previously utilised by Austin et al 2014, using ISO 5436-1, which required a region of uneroded reference enamel (Austin et al., 2014). As this was not present in the natural enamel samples step height calculation was not possible.

In Chapter 3 investigation 1 the detection threshold was calculated using one slice of natural enamel mounted on the glass microscope slide. Whilst this provided sufficient data for subsequent analysis, it is unknown whether the detection threshold values would differ if other natural enamel samples were scanned using this method. Potentially, every natural enamel sample could have been scanned ten times consecutively and the minimum detection threshold calculated per experimental group to allow for comparison with subsequent erosion lesion values. The problem however of the total CL NCLP scan time may limit the number of scans required for this purpose potentially limiting the feasibility of such investigations.

In Chapter 3 investigation 2, the changes in thermal variation and their impact on CL NCLP were determined using an optical flat, rather than a natural enamel sample, consisting of lithium-aluminosilicate glass. This was done to measure sensor displacement related to temperature changes on a dimensionally stable target surface. However, this method could also have been conducted using a natural enamel sample as the target surface. Whilst this was not investigated in this Thesis, the curvature of the enamel sample could have potentially affected the CL NCLP sensor displacement when compared to the optical flat. It is unknown whether the sensor error is affected when using natural enamel and would therefore require further investigation. Additionally, whilst a relationship between sensor displacement and temperature was demonstrated, it is still unknown whether a true sensor shift was measured or a shift in the motion control which moves the sample itself. Whilst the data for this Investigation was obtained at a designated metrology laboratory using the same CL NCLP setup as the one used for this Thesis, it would

have been ideal to use the same recording equipment to determine the thermal variances and NCLP displacement in the KCL laboratory as well as a matter of comparison.

In Chapter 3 investigation 3, the scanning parameters were limited by the type of profilometer used in this Thesis. The CL NCLP had Z-axis gauge range of 600 μm and reported 17° angular tolerance (Boltryk et al., 2008; Bull and McBride, 2018). This would have limited the amount of data returned to the sensor at the extreme edges of the natural enamel sample due to its curvature exceeding the sensor gauge range. It its unknown whether a different displacement sensor such as a white light (WL) sensor would improve on the quantity of data obtained from the natural enamel samples and whether this would improve on the results already obtained using CL NCLP in this Thesis.

In Chapter 3 investigation 4 the use of clear PVC tape and a surgical punch biopsy to cut circles at approximately 1.5mm diameter was both technique sensitive and time consuming to produce. This method was limited by the experience of the user, cleanliness and sharpness of the biopsy punch, and integrity of the PVC tape used. This Thesis did not investigate the effect of different biopsy punches nor the different brands of clear PVC tapes available on the market. It is therefore unknown whether someone in a different laboratory could replicate this method exactly, and hence the generalisability and user-friendliness of this method was not explored. The taping method was very challenging and required a lot of time and practice to ensure its correct placement on the natural tooth surface. It was much more technique sensitive compared to the PVC tape method for polished enamel in Chapter 2, and

the placement of new PVC tape after each erosion cycle was impossible to keep at the same location each time. As a result, further research is required for alternative taping methods which would eliminate the requirement for removal and replacement each time profilometric scanning is required.

The geometry of the erosion lesion in natural enamel (Chapter 3) was different to compared to polished enamel in Chapter 2. In natural enamel the erosion lesions were irregular semi-circular/hemispherical shaped whilst in polished enamel (Chapter 2) they were more uniform and rectangular in their geometry. The investigation of the three different analytical methods for calculating enamel loss in Chapter 3 provided valuable insights into studying irregular enamel lesions. However, further analysis is required to determine whether other volumetric based methods could also be utilised in analysing these natural enamel lesions. In previous studies analysing erosion-attrition and erosion-abrasion lesions in polished enamel, which produced irregular wear lesions, it was concluded that the following measurement methods could all be used to assess enamel loss: average wear depth (volume of enamel loss, mm^3 / surface area of enamel lesion μm^2) (Vieira et al., 2007) normalised enamel loss (3D step height, μm / surface area, μm^2) (Rodriguez and Bartlett, 2010), and volume loss (mm^3) (Ruben et al., 2019). Whilst these measurement methods were not utilised in this study, it would be interesting to determine whether they can be used to study erosion lesions formed on natural enamel in a dental erosion only in vitro model.

In Chapter 4 Investigation 1, the erosive protective benefit of sodium fluoride toothpaste was evaluated using two parameters: enamel loss (3D step height) and

surface morphology (using TSM). It would have been preferred if the natural enamel samples were also evaluated for changes in surface texture (surface roughness), and surface reflectivity (OCT) to allow for full comparison with samples tested in Chapter 3 and 5. In Investigation 2, step height could still be measured regardless of the AEP formed on the natural enamel samples. This Investigation was an initial exploratory study to determine the viability of the in vitro method, and as such would require further evaluation with sufficient statistical power. Additionally, the proteomics of the human saliva collected was not evaluated as this was beyond the scope of this Thesis and there may have been bacterial contamination which could have affected the AEP quality. Similarly, this Investigation did not utilise other techniques such transmission electron microscopy to evaluate the AEP itself, again as this was beyond the scope of the Thesis. Future study of the mechanism of AEP formation on natural enamel in vitro, and the impact of the proteomic composition of the collected saliva would be required.

In Chapter 5 the treatment protocol followed those developed previously to ensure correct preparation and application of the NR5 formulation (Hornby et al., 2014; Wood et al., 2018). However, this method did not utilise a phosphatase enzyme which is normally present in human saliva to fully liberate the fluoride ion from SMFP (Farley et al., 1987). It is therefore possible that the benefits of SMFP may have been underestimated and further study is required using a treatment protocol that maximises the benefits of each individual toothpaste treatment. Additionally, the viscosity of each toothpaste was not analysed for their potential impact on their erosion potential. The NR5 formulation, which is anhydrous in storage, was found to

be much more viscous and more difficult to homogenise compared with SMFP and NF toothpastes. The impact of toothpaste viscosity and wettability on the tooth surface was beyond the scope of this Thesis and would merit future study.

6.2 Comparing step height at 5 mins for each chapter

A comparison was conducted of the mean (SD) 3D step heights obtained for Chapter 3s (dry field), 4 (F pre-treatment, 3-min AEP, 24-hrs AEP), and 5 (NR5 pre-treatment, SMFP pre-treatment); this can be seen in Figure 54 and Table 11. Data were assessed for normal distribution using Shapiro-Wilks and Komogorov-Smirnov tests and visually assessed with box-plots and histograms. Data were normally distributed and inter-group analysis was conducted with one-way ANOVA with post-hoc Tukey's test for multiple intra group comparisons.

When comparing between the different pre-treatment methods used in each chapter, NaF + AS (Chapter 4) resulted in the lowest mean(SD) 3D step height formation, this was statistically significant when compared to dry field (Chapter 3) (0.38(0.20) vs 1.04(0.41) μm, $p<0.0001$), 3-mins AEP (Chapter 4) (0.38(0.20) vs 1.01(0.31) μm, $p<0.05$), 24-mins (0.38(0.20) vs 1.22(0.75)μm, $p<0.001$). There was no statistically significant difference in mean 3D step height between all NaF and NR5 and SMFP (Chapter 5) pre-treatment groups ($p>0.05$).

Whilst NaF + AS produced the lowest mean 3D step height measured in this Thesis, there was no significant difference between the values obtained for NR5 and SMFP pre-treatment. This may suggest that NaF, NR5 and SMFP may have similar erosive-protective properties, however, their effects were not directly compared; future work would therefore be necessary to determine any differences.
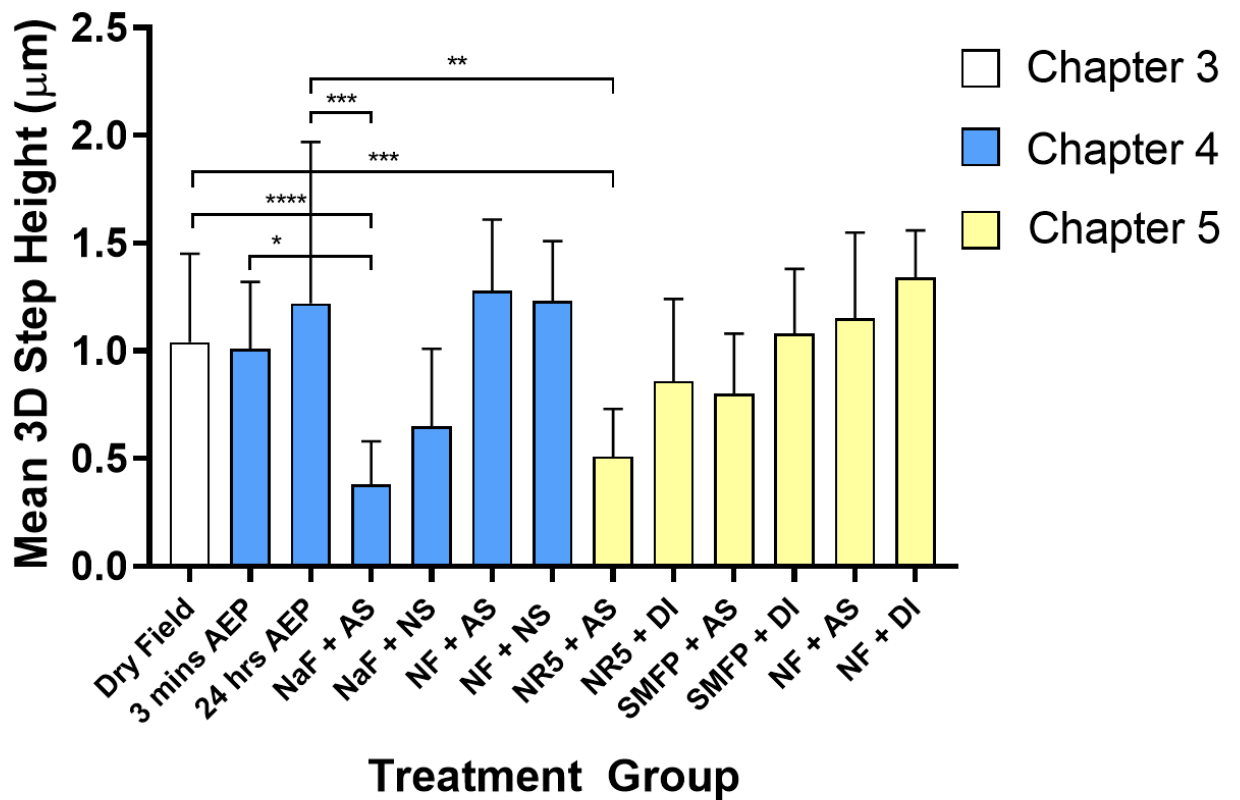
Figure 54 – A graphical comparison of the mean(SD) 3D step heights obtained after 5 mins erosion in natural human enamel for the conditions tested in this Thesis. Colour coding indicates the Chapter of origin. White (chapter 3), Blue (chapter 4), Orange (chapter 5). Statistical comparison between the main experimental treatment factors (dry field, 3-min AEP, 24-hrs AEP, NaF, NR5, and SMFP) was conducted with one-way ANOVA. Statistical significance is shown by: (*) $p<0.05$, (**) $p<0.01$, (***) $p<0.001$, (****) $p<0.0001$.

Treatment Regime	Erosion Time (mins)	
	5	
	Mean 3D SH (µm)	SD
Dry field (acid only) n=12	**1.04**	0.41
3 min AEP (only) n=10	**1.01**	0.31
24 hrs AEP (only) n=10	**1.22**	0.75
NaF + AS n=10	**0.38**	0.20
NaF + NS n=10	**0.65**	0.36
NF + AS n=10	**1.28**	0.33
NF + NS n=10	**1.23**	0.28
NR5 + AS n=10	**0.51**	0.22
NR5 + DI n=10	**0.86**	0.38
SMFP + AS n=10	**0.80**	0.28
SMFP + DI n=10	**1.08**	0.30
NF + AS n=10	**1.15**	0.40
NF + DI n=10	**1.34**	0.22

Table 11 – A comparison of the mean(SD) 3D step heights obtained after 5 mins erosion in natural human enamel for the conditions tested in this Thesis. Colour coding indicates the Chapter of origin. White (chapter 3), Blue (chapter 4), Orange (chapter 5).

6.3   Overall Conclusion

In polished human enamel, the early erosive lesion could be measured using changes in surface roughness, surface microhardness, surface reflectivity and surface morphology after 10s citric acid erosion; surface form change could be measured after 120s.

In natural human enamel surface form change could be measured using a comparison between before and after erosion scans with NCLP using either superimposition and difference analysis, scan alignment and profile subtraction analysis, or scan subtraction and residual profile analysis.

The calculation of surface form change in natural human enamel was possible due to the understanding of the measurement errors inherent within NCLP. Thermal variation was demonstrated to affect NCLP sensor stability resulting in displacement over medium and long duration scan times.

Whilst the AEP did not affect erosion in natural human enamel, sodium fluoride and NR5 toothpastes demonstrated a protective benefit against citric acid erosion in vitro.

7 Chapter 7 - Suggestions for future work

Whilst this Thesis has provided a significant step forward in dental surface metrology by providing a method to characterise and calculate step height formation due to acid erosion in natural human enamel in vitro, there are a number of further investigations that still require exploration.

Whilst a number of different ISO and non-ISO standard methods of step height were used throughout this Thesis to evaluate enamel loss, there would certainly be merit in investigating other methods of enamel loss in natural enamel including: volume of erosion lesion (μm^3), and normalised lesion depth (μm, volume of lesion/surface area of lesion); Additionally, correlations analysis would be interesting, correlating this with enamel loss methods described in Chapter 3.

Investigating the impact of different NCLP sensors on the erosion lesion measurement and step height measurement on natural human enamel. The same natural enamel samples would be scanned with triangulation laser (TL), white light (WL), and confocal laser (CL) sensors to determine whether the spot size, angular tolerance, gauge range and axial resolution of the sensor impacts on the measurement of dental erosion lesions in natural enamel and calculation of enamel loss (Boltryk et al., 2009)

The natural enamel in vitro erosion model developed in Chapter 3 should be explored further using other common acidic food stuffs, e.g. cola, orange juice, fruit teas etc, and investigating their erosive capabilities on natural human enamel in vitro. Whilst laboratory citric acid solutions provide a standardisable method to study erosion in

vitro, ultimately, the use of dietary foods is necessary to best match the clinical scenario

Additionally, the differences in erosive-protective mechanisms between NaF, NR5, and SMFP toothpaste products should be investigated using the natural enamel in vitro model from Chapter 3 to determine whether one product is superior to the other. Each product would be used to pre-treat natural enamel samples before being eroded in a cyclic erosion model and analysed as described in Chapter 4 and prepared according to the optimum working conditions for that product.

The AEP has previously been demonstrated to provide protective benefits against erosion on polished enamel (Mutahar et al., 2017), however, as our Thesis did not demonstrate this in natural enamel, a comparative study of the formation of AEP on both natural and polished human enamel samples is required. This will investigate whether there is a difference in the AEP produced on both sample types in vitro. And if so, to determine any differences, biological or otherwise, between the two AEP types.

Further exploration of the effect of attrition and abrasion on the erosion process in natural human enamel is required to determine their impact, as well as an investigation on the characterisation methods for these erosive tooth wear lesions. An analysis of the taping method is required to ensure its viability within an attrition/abrasion model; so far its integrity has only be evaluated in a dental erosion only model.

Appendices

Patient consent form (tooth collection)

King's College London — King's College Hospital NHS Foundation Trust — Guy's and St Thomas' NHS Foundation Trust

---

Consent Form (Version 2: 22/07/2015)
Title of project: Protection of erosive tooth wear (donation of extracted tooth)
REC ref: REC ref: 12/LO/1836
Investigator: Professor David Bartlett

Please complete this form after you have read the Information Sheet and/or listened to an explanation about the research

Patient Identification: Date

Thank you for considering taking part in this research. The person organising the research and/or a member of the clinical team who is trained for this purpose must explain the project before you agree to take part.

If you have any questions arising from the Information Sheet or explanation given to you, please ask the researcher before you decide whether or not to join in. You will be given a copy of this Consent Form to keep and refer to at any time.

I confirm that I have read and understand the information sheet dated (version 1) for the above study.

I have had the opportunity to consider the information, ask questions and have had these answered satisfactorily.

I understand that my participation is voluntary and that I am free to withdraw at any time without giving any reason, without my medical care or legal rights being affected.

I agree to take part in the above study.

Name of Patient..
Signature...Date..

Name of Person taking consent..
Signature...Date..

1 for patient, 1 for researcher site file, 1 (original) to be kept in medical notes, 1 to be kept with donated tooth
Page 1 of 1

Patient information leaflet (tooth collection)

Guy's, King's and St Thomas' Dental Institute Department of Fixed and Removable Prosthodontics
25th Floor, Guy's Tower Guy's Hospital London Bridge London SE1 9RT Tel 0207 188 5390 Fax 0207 188 7488

KING'S College LONDON

King's College Hospital NHS NHS Foundation Trust

Guy's and St Thomas' NHS NHS Foundation Trust

Volunteer information sheet (Version 2) 15/07/2015
Title of project: Protection of erosive tooth wear (donation of extracted tooth)
REC ref: 12/LO/1836
Investigator: Professor David Bartlett

You will be given a copy of the information sheet and a signed consent form to keep.

Part 1
Invitation paragraph

You are being invited to donate your tooth for a research study. Before you decide it is important for you to understand why the research is being done and what it will involve:

Part 1 tells you the purpose of the potential studies and what will happen if you decide to participate.
Part 2 gives you more detailed information about the conduct of the potential studies.

Please take time to read the following information carefully. Ask us if there is anything that is not clear. Talk to others about the research if you wish and the following organization could give you independent advice:
Guy's and St Thomas' Hospital NHS Foundation Trust Patient Advice and Liaison Service Telephone 020 7188 8801 or 020 7188 8803 email: pals@gstt.nhs.uk
Post: Patient information team, Knowledge and information centre, St Thomas' Hospital London, Westminster Bridge Road, SE1 7EH

What is the purpose of the study?
Tooth wear is a condition where the teeth wear away faster than normal and is caused by acid erosion (from acidic foods and drinks and stomach acid), tooth grinding and over brushing. Tooth wear is a common condition that can affect anyone and it appears to be happening more and more nowadays. Severe tooth wear can cause teeth to become very sensitive, as well as causing cosmetic and chewing problems due to shortened teeth and in severe cases can cause tooth loss. Certain toothpastes and mouth rinses have the potential to prevent and treat tooth wear. However the scientific evidence for this is lacking and the studies we plan to carry out may provide important information regarding the disease process, progression of the disease and possible prevention of the disease.
Why have I been chosen?
You are suitable for this study because you are a healthy individual who needs a tooth removed.

Do I have to take part?
It is up to you to decide whether or not to take part. If you do, you will be given this information sheet to keep and be asked to sign a consent form. You are still free to withdraw

---

at any time and without giving a reason. A decision to withdraw at any time, or a decision not to take part, will not affect the standard of care you receive.

What will happen to me if I decide to take part?
At your first visit, when you are consulted about the tooth extraction, you will be invited to join the study by a clinician. At your second visit we will confirm that you still want to donate your tooth and then you will have your tooth removed in the normal way. After your tooth is extracted it will be transferred to the Biomaterials laboratory at King's College Hospital Dental Institute (Department of Biomaterials, 17th Floor, Guy's Tower, Guy's Hospital, London Bridge SE1 9RT). Once the tooth is extracted your participation in the study is over.

What do I have to do?
You will just have to attend your set appointments as normal.

What is the drug, device or procedure being tested?
Various methods of studying the surface changes of the extracted teeth and the effects of dietary acids, fluorides and other protective agents are being investigated in this study on the extracted teeth.

What are the alternatives for diagnosis or treatment?
The research does not involve any volunteer treatment and you will receive your routine standard treatment as usual.

What are the side effects of any treatment received when taking part?
There are no risks associated with this study, other than the usual risks of a tooth extraction which will be explained to you by the clinical team who are carrying out the treatment.

What are the other possible disadvantages or risks of taking part?
There are no risks associated with this study, other than the usual risks of a tooth extraction which will be explained to you by the clinical team who are carrying out the treatment.

What are the possible benefits of taking part?
We do not expect that you will receive any benefit from taking part in this study.

What happens when the research study stops?
We aim to publish the results in medical journals.

What if there is a problem? And contact details:
No problems can be foreseen however the contact number for complaints or concerns is for: Professor David Bartlett 0207 188 5390 or email david.bartlett@kcl.ac.uk

Will my taking part in the study be kept confidential?
We will not be collecting any information about you and your confidentiality is safeguarded during and after the study. Our procedures for handling, processing, storage and destruction of your data are compliant with the Data Protection Act 1998.

Guy's, King's and St Thomas' Dental Institute Department of Fixed and Removable Prosthodontics
25th Floor, Guy's Tower Guy's Hospital London Bridge London SE1 9RT Tel 0207 188 5390 Fax 0207 188 7488

KING'S College LONDON

King's College Hospital NHS NHS Foundation Trust

Guy's and St Thomas' NHS NHS Foundation Trust

Contact for further information:
Professor David Bartlett 0207 188 5390 or email david.bartlett@kcl.ac.uk

This completes Part 1 of the Information Sheet. If the information sheet in Part 1 has interested you and you are considering participation, please continue to read the additional information in Part 2 before making any decision.

Part 2

What if relevant new information becomes available?
We are a leading establishment in this area of research and if any new information relevant to this study becomes available the researchers will discuss this with you. You are free to withdraw from the study at any time.

What will happen if I don't want to carry on with the study?
You can withdraw from study. Just advise the clinician treating you that you do not want to donate your tooth and your tooth will be disposed of once extracted, or you can keep it to take home.

What if there is a problem?
If you have any concern about any aspect of this study, you should ask to speak with the researchers who will do their best to answer their questions.
Professor David Bartlett 0207 188 5390 or email david.bartlett@kcl.ac.uk

If you remain unhappy and wish to complain formally, you can do this through the NHS complaints procedure. If you are harmed by taking part in this research project there are no special compensation arrangements. If you are harmed due to someone's negligence, then you may have grounds for a legal action but you may have to pay privately for it. Regardless of this, if you wish to complain, or have any concerns about any aspect of the way that you have been approached or treated during the course of this study, the normal NHS complaints mechanisms should be available to you.

Details of how to complain can be obtained from the Volunteer Advice and Liaison Service (PALS)
Guy's and St Thomas' Hospital NHS Foundation Trust Patient Advice and Liaison Service
Telephone 020 7188 8801 or 020 7188 8803 email: pals@gstt.nhs.uk
Post: Patient information team, Knowledge and information centre, St Thomas' Hospital London, Westminster Bridge Road, SE1 7EH

Will my taking part in this study be kept confidential?
We will not be collecting any information about you and your confidentiality is safeguarded during and after the study. Our procedures for handling, processing, storage and destruction of your data are compliant with the Data Protection Act 1998.

What will happen to any samples that I give?
After your tooth has been removed, it will be anonymised (i.e. there will be no way of linking the tooth to your personal data or medical records) and then transported to the Biomaterials laboratory at King's College Hospital Dental Institute (Department of Biomaterials, 17th Floor, Guy's Tower, Guy's Hospital, London Bridge SE1 9RT). The tooth will be used in a laboratory study or clinical study investigating erosive tooth wear. The study may be laboratory experiment which involves simulating erosive wear on the enamel blocks from the donated teeth in the laboratory, as well as exposure to topical protection or it may be a clinical study where participants may wear mouthguards containing sterilised blocks containing the enamel from the donated teeth. In both cases, measurements of the amount of wear on the tooth surface are taken.

What will happen to the results of the research study?
The results of the study will be published in medical journals. Participants will not be identified in any report or publication.

Who has reviewed the study?
This study was given a favourable ethical opinion REC ref: 12/LO/1836

Will any genetic tests be done?
No.

Thank you for considering taking part and for taking time to read this sheet – please ask any questions if you need to.

ARTICLE IN PRESS

Available online at www.sciencedirect.com

ScienceDirect

dental
materials

Detection threshold of non-contacting laser profilometry and influence of thermal variation on characterisation of early surface form and textural changes in natural human enamel

Petros Mylonas[a,*], *Thomas Bull*[b], *Rebecca Moazzez*[a], *Andrew Joiner*[c], *David Bartlett*[a]

[a] *Centre for Oral, Clinical and Translational Sciences, King's College London Faculty of Dentistry, Oral & Craniofacial Sciences, UK*
[b] *Mechatronics Research Group, Engineering and the Environment, University of Southampton, UK*
[c] *Unilever Oral Care, Bebington, Wirral, UK*

ABSTRACT

Objectives. To determine the detection threshold of non-contacting laser profilometry (NCLP) measuring surface form and surface roughness change in natural human enamel *in vitro*, characterise how ambient scanning thermal variation affects NCLP measurement, and calculate bulk enamel loss in natural human enamel.

Methods. NCLP repeatability and reproducibility accuracy was determined by consecutively scanning natural human enamel samples with/without sample repositioning. Ambient thermal variation and NCLP sensor displacement over short (30 s), medium (20 min), and long (2 h) scanning periods were evaluated for their standard deviation. Natural human enamel specimens (n = 12) were eroded using citric acid (0.3% w/w pH3.2) for 5, 10, and 15 min and characterised using surface profilometry, tandem scanning confocal microscopy (TSM), and optical coherence tomography (OCT).

Results. Repeatability and reproducibility error of NCLP for surface form was 0.28 μm and 0.43 μm, and for surface roughness 0.07 μm and 0.08 μm. Ambient thermal variation resulted in NCLP sensor displacement of 0.56 μm and 1.05 μm over medium and long scanning periods. Wear scar depth (μm) was calculated between 0.72–1.61 at 5 min, 1.72–3.06 at 10 min, and 3.40–7.06 at 15 min. Mean (SD) surface roughness (μm) was 1.13 (0.13), 1.52 (0.23), 1.44 (0.19), and 1.43 (0.21) at baseline, 5, 10, and 15 min. Qualitative image analysis indicated erosive change at the surface level, progressing after increasing erosion time.

Significance. Minimum detectable limits for NCLP measuring surface form and surface roughness changes were characterised. Ambient thermal variation, subsequent sensor displacement, and its impact on NCLP performance were characterised. Dental erosion lesions in natural human enamel could be characterised using surface profilometry, surface roughness, OCT, and TSM. Step height formation could be calculated within NCLP and temperature operating limits using profile superimposition and profile subtraction techniques.

Natural enamel samples can now be used in *in-vitro* studies to investigate the formation and development of early acid erosive tooth wear, as well as the assessment of methods for enamel lesion remineralisation and repair.

© 2019 Published by Elsevier Inc. on behalf of The Academy of Dental Materials.

1.   Introduction

Non-contacting laser profilometry (NCLP) is considered the gold standard measurement technique for the detection and quantification of surface wear in dental tribology and dental erosion studies of acid-mediated attack on dental hard tissue samples [1–3]. NCLPs utilise a laser displacement probe and precision motion system to map the surface topography of an object as a three-dimensional point cloud. The point cloud data can subsequently be analysed and compared, using metrology or superimposition software, to extract, quantify and compare the surfaces [1,4].

Quantification of the effects of acid-mediated erosion on enamel surfaces using NCLP have previously focused on extensively eroded surfaces, where the extent of the wear is clinically visible and thus well within the detection threshold of current NCLPs [5].

In dental erosion studies, the detection threshold of NCLPs is primarily determined by three factors: the size of the laser spot [6] determines lateral/spatial (XY) resolution, the optics of the displacement laser determines vertical/axial (Z) resolution, and lateral precision [4,6] of the motion system used which in-turn determines the repeatability of measurement.

Vertical resolution (Z height) is defined as the smallest measurable height difference between surface features, whilst lateral resolution (XY) is the smallest measurable distance between two surface features in the x–y plane [7]. Early erosive lesions have been previously characterised using changes in surface form [8] and surface roughness (amplitude parameter, Sa) [8,9].

Surface form and textural measurements can be affected by differences in both NCLP vertical and lateral resolution, and the step-over distance (sampling interval distance) of the motion system utilised [7,10]. Both the vertical and lateral resolution of the NCLP system are important for the detection threshold of early erosive lesions. Previously it has been shown that a lateral resolution <2.5 μm was sufficient to resolve surface textural features on the polished and natural enamel surface [11], and vertical resolution 10 nm to resolve small changes in surface form in polished enamel [8,12]; no study has yet to evaluate this in natural human enamel.

Surface form detection is dependent primarily on NCLP vertical resolution whilst surface roughness will be primarily affected by lateral resolution [6]. Surface form measurement comprises long wavelength features, compared to the short wavelength features for surface roughness.

NCLP detection threshold is therefore different depending on whether surface form or roughness is being measured; this has yet to be evaluated in natural human enamel. Evaluating both detection thresholds are important to ensure early

erosion can be evaluated for changes in surface form and roughness.

However, other sources of error can affect the overall accuracy of NCLP measurement. Thermal variation during the period of the measurement is considered one of the largest sources of measurement error in surface metrology where the NCLP is required to detect submicron scale changes in surface texture or form [4,6,13,14]. Dimensional metrology studies in the manufacturing sector have demonstrated thermal induced measurement errors in X, Y, and Z axes using optical profiling to assess measurement accuracy [14]. To date, there have been no studies which have considered, measured, or determined the effects of thermal variation in dental surface metrology measurements with NCLPs.

Additional measurement error is also introduced depending on the enamel model utilised. Natural unpolished enamel is considered an organic freeform structure comprising a series of complex curved surfaces and randomly varying topographical features [15,16]. The topography of the enamel surface is highly variable due to the presence of: perikymata grooves which add wave-like concentric surface features, and focal holes and enamel caps which add additional peak and valley features [17], This results in an additional level of topography complexity increasing the difficulty of accurately measuring natural enamel surface features using NCLP; this is due to measurement errors inherent to scanning complex curved surfaces [6,10]. The nature of the surface topography also impacts on the formation and progression of acid-induced erosion which is non-uniform and heterogenous, and this increases the difficulty in characterising and measuring surface changes with NCLP [15,16,18]. As a result, polished enamel has been the most commonly used substrate to study the effects of acid-mediated erosion as the polishing process removes the aprismatic surface layer and produces a more topographically flat and uniform surface with near standardised surface characteristics [6,10].

The polishing process, however, affects the wear characteristics of enamel and its susceptibility to acid-induced erosion increases as the dentinal–enamel junction (DEJ) is reached [16]. The preservation of the outer amorphous surface layer of natural enamel may present a more representative substrate with which to study the *in vitro* effects of acid-mediated erosion and subsequent modifying factors or therapeutic agents [19,20].

Previous studies quantifying surface form change in natural or polished enamel samples have investigated the differences between before- and after-erosion datasets using either superimposition alignment with quantified Z-axis deviations [1,21], or by subtraction analysis involving the subtraction of before- and after- erosion datasets (with or without prior scan alignment) to produce a difference or residual

dataset from which form change is calculated [22,23]. These methods have either utilised NCLP with large spot size (15 μm) displacement sensors [1], handheld intraoral scanners [21], or white light interferometry [22], which are unable to detect very early surface form or roughness change *in vitro*. Additionally, these methods have yet to be investigated for suitability in measuring surface form and texture measurement using NCLP with very small spot size (2 μm) displacement sensor.

The aim of this study is therefore to investigate the minimum detectable threshold of surface profile and roughness changes in natural enamel and develop a relevant *in vitro* model to study the effects of early acid-induced erosion.

2. Materials and methods

2.1. Sample preparation

Extracted human permanent erupted-molar teeth free from clinical disease or prior restoration, were collected under ethical approval (REC: 12/LO/1836) and with patient informed consent. Twelve enamel sections were produced with approximately equal dimensions (5 mm × 5 mm ×3 mm), the buccal, palatal and/or lingual portions, were sectioned using a 300 μm diamond wafering blade, and fixed on 76 mm × 26 mm × 1 mm glass microscope slides (Marienfield GmbH & Co. KG, Germany) using epoxy resin (EverStick, Everbuild Products Ltd, UK) to produce microscope slides with 4 enamel specimens bonded to the surface; 2 buccal and 2 palatal or lingual sections from the same unpolished or natural surface from the tooth.

A bespoke positioning jig was manufactured to ensure repeatable placement of each microscope specimen slides onto the NCLP prior to scanning.

To ensure all samples were cleaned of all organic and inorganic surface contaminants, a minimally invasive cleaning process was utilised. This consisted of chemical-only cleaning technique involving 10-min immersion in 4.7% sodium hypochlorite, followed by 30-min ultrasonication in distilled water, air drying, then 2-min alcohol wipe using cotton buds. Samples were inspected under tandem scanning confocal microscopy (TSM) before and after cleaning to ensure cleanliness.

An overview of the study design can be seen in Fig. 1.

2.2. Investigation 1—detection threshold determination

An NCLP with a 655-nm confocal laser mounted on an automatic motion system (XYRIS 2000CL, Taicaan, Southampton, UK) was used throughout this study; the NCLP has a 2 μm lateral (XY) laser spot size, 10 nm axial (Z height) resolution and 0.6 mm Z-range. The repeatability study (instrument accuracy) was conducted by scanning one natural human enamel sample 10 times consecutively, according to good metrology scanning guidelines [13], without pick up and replacement, whilst for the reproducibility study (pick and replacement accuracy), the sample was scanned 10 times consecutively with the sample picked up and replaced on the scanning jig every 21 min; the time taken to complete one measurement.

To ensure minimisation of thermal variation on scanning, the samples were allowed to thermally equilibrate for period of 10 min prior to initiating each scan.

To quantify NCLP precision (repeatability and reproducibility) in measuring surface form and surface roughness, the mean variability between the 10 measurements was calculated by firstly importing the data sets into surface metrology software (Boddies v1.92, Taicaan, Southampton, UK). Each surface scan consisted of a rectilinear grid (XY), with a height measurement (Z) taken at each intersection. Form and roughness data was extracted separately from the original raw profile data using a 0.8 μm Gaussian filter for form and roughness over a 10 μm sampling interval [4]. Differences between consecutive form and roughness data were then calculated by superimposing two measurement grids and subtracting one from the other. This difference was quantified by taking the absolute (modulus) of the difference at each measured point and calculating the arithmetic average (mean) of the absolute height differences between the measurements. In the case of perfectly matching data the measured points would all superimpose perfectly and there will be no difference. The detection threshold for both surface form and roughness was then calculated using a previously published method, using the equation mean + 3 SD; whereby mean and SD refer to the average and standard deviation in the arithmetic average (mean) of the absolute height differences between measurements [24].

2.3. Investigation 2—characterising the influence of thermal variation on NCLP system stability

To determine influence of thermal variation on measurement stability, the measured displacement to a flat surface held at a nominally static position orthogonal to the NCLP measurement beam, was logged over a period of several hours during variation in environmental temperature. Environmental control consisted of laboratory air conditioning (Toshiba RAV SM562KRT-E) with temperature control set at 20 ± 1 °C. The NCLP scanning room is separate from the main laboratory area accessible via a lockable door. Temperature logging was conducted out-of-hours by one operator only, to minimise variations in ambient temperature due to movement of people; the room was locked during scanning periods to ensure NCLP isolation.

A calibrated optically flat surface (Edmunds Industrial Optics, USA) made of lithium–aluminosilicate glass with low coefficient of thermal expansion ($\alpha = 0.1 \times 10^{-6}$ °C^{-1}), was used as a target surface. The target was cleaned using an acetone rinse followed by distilled water and blown dry using dry nitrogen. The surface was then arranged on the NCLP, orthogonal to the incident laser beam, with the laser displacement probe at a nominal static displacement of 6 mm above the target surface. A temperature and humidity logger (Lascar Electronics, UK) with 0.1 °C and 0.5 %RH resolution recorded environmental conditions at a rate of 0.2 Hz.

Temperature and sensor displacement were then recorded at the NCLP. Short, medium, and long scanning periods were investigated under two conditions: (a) with the NCLP uncovered (open condition) and (b) with a simple inverted box enclosure over the instrument (closed condition). The enclo-
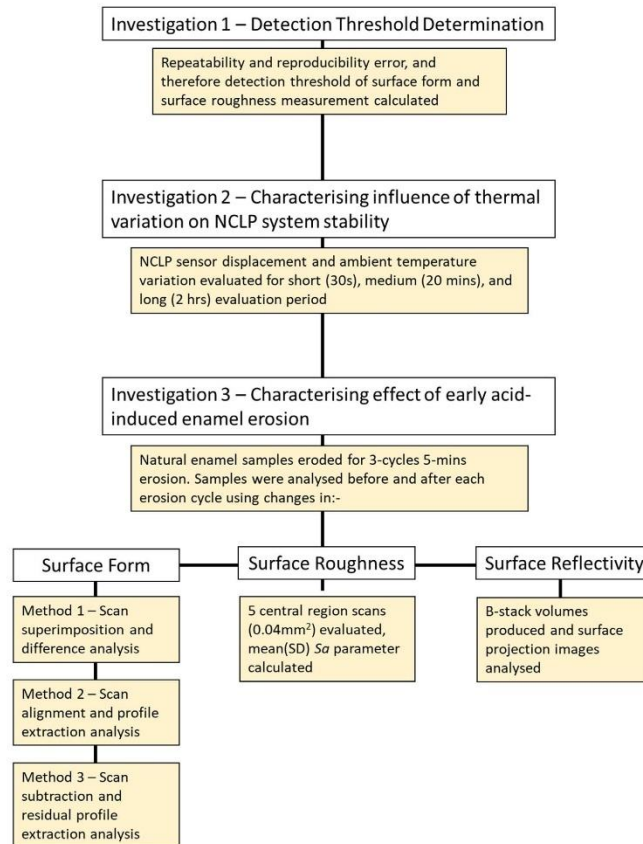
Fig. 1 – Outline of the study design.

sure provided a basic level of protection from local air currents and thus stabilises the temperature at the NCLP.

Fluctuation in scanning temperature and sensor displacement was evaluated for (1) short term stability — a 30-s evaluation period, (2) medium term stability — a 20-min period — equivalent to the time taken for a complete NCLP 3D measurement, and (3) long term stability — a 2-h evaluation. This allowed for determination of the influence of thermal effects according to the scanning time. The NCLP was programmed (Stages, Taicaan Technologies, Southampton, UK) to log the NCLP sensor displacement at 25 Hz for the short measurement and 0.8 Hz for the medium and long measurement.

The thermal variation and displacement change for each case were then evaluated for their standard deviation.

2.4. Investigation 3—characterising effects of early acid-induced enamel erosion

2.4.1. Natural enamel early acid-induced erosion model
Twelve natural enamel samples were prepared as previously described and clear polyvinyl chloride (PVC) protective barriers with a 1.5 mm diameter circular hole were placed over the maximum bulbosity of each sample. This was determined as the maximum peak detected by scanning the profile of all tooth samples prior to taping using the NCLP.

Samples were exposed to acid immersion in a repeated measures process every 5 min for three cycles, total immersion times: 5, 10, and 15 min. All samples were scanned before acid immersion to provide baseline data sets (surface form

268

and roughness) for comparison to after scan data. Citric acid (0.3% w/w) erosive solution was prepared, from anhydrous citric acid powder (Sigma Aldrich, Poole, Dorset UK) to deionised water, and pH adjusted to 3.2 using 0.1 M sodium hydroxide (Sigma Aldrich, Poole, Dorset UK) [17]. The titratable acidity was calculated as the volume of sodium hydroxide required to increase the solution pH to 7; this was 18.0 ml [10,17]. All samples were immersed in 10 ml of citric acid (per tooth) and agitated using an orbital shaker (62.5 RPM, Stuart mini-Orbital Shaker SSM1, Bibby Scientific, England), for 5 min before rinsing with deionised water (pH 5.8) for 2 min and left to air dry. After the PVC tape was removed, samples were replaced in the scanning jig, and surface form and roughness measurements recorded. This process was repeated to ensure measurements were obtained at 10 and 15 min erosion.

Previous unpublished pilot work attempted to use ISO 5436-1 to obtain a step height in natural enamel. However, there was no definable reference points to allow comparison between eroded and uneroded enamel. This was due to previous barrier methods proving unsuccessful in creating an isolated eroded lesion and reference enamel region [25]. Therefore, three methods for determining bulk enamel loss were proposed: scan superimposition and difference analysis; scan alignment and profile extraction analysis, and scan subtraction and residual profile extraction analysis [1,22,23]. An operator blinded to treatments conducted all analyses, and samples were randomised prior to analysis.

2.4.1.1. Surface form change measurement and characterisation.

2.4.1.1.1. Method 1—scan superimposition and difference analysis. The scan data, consisting of a Cartesian point cloud, were trimmed and transformed into a 3D surface using superimposition software (Geomagic Control 2014, Geomagic Inc, North Carolina, USA). To minimise effects of alignment error between baseline and eroded scan data sets, an initial best fit of alignment using 300 randomly selected data points was conducted before a more precise alignment using 1500 additional data points was performed. After completing superimposition, a region of interest, 0.2 mm diameter, was selected at the central region of the wear scar; this ensured minimisation of the effects of the natural topographical variation between samples. Tooth loss was then measured in μm for each erosion time point and a mean taken of all points in X, Y, and Z (automatically calculated by the software) using two outputs: mean Z-change and mean 3D total deviation between two consecutive scans.

2.4.1.1.2. Method 2—scan alignment and profile extraction analysis. All scans were loaded as a Cartesian point cloud into surface metrology software (MountainsMap, DigitalSurf, France), an offset analysis between each erosion cycle data set were initially conducted to facilitate accurate alignment and thus allowing wear scar analysis. Firstly, a 0.8 μm Gaussian filter for roughness was applied to all data sets, a spatial denoising (3 × 3) filter was applied to remove outlier points; the filtered data points were then processed together to form a composite series of images. Shift surface operator was applied which determined the offset and rotational values between the filtered roughness data in X, Y, Z. These offset values were used to correctly align all the original raw data sets according

to their pre-erosion scan, further wear-scar analysis was then conducted. The post-erosion scans were subtracted from the pre-erosion baseline scan using a subtraction operator, leaving the residual data set. The palette colour was manipulated to aid visualisation of the resultant wear scar. A surface levelling operator was utilised, excluding the 1.5 mm diameter eroded wear scar region, using a linear least squares plane of best fit method. This was repeated for all post-erosion time points. Determination of change at the wear scar was expressed as residual step height, which was calculated using two quantitative outputs: resultant difference in Z (Z mean, μm), and as residual 3D step height change (μm).

2.4.1.1.3. Method 3—scan subtraction and residual profile extraction analysis. Data scans after erosion were compared with their baseline pre-eroded scans using surface metrology software (Boddies v1.92, Taicaan, Southampton, UK). Post-erosion scans were mathematically subtracted from their respective baseline scan, this produced a residual data set which was subsequently used for wear scar analysis. The residual data was levelled using best fit method excluding the central wear scar region. Differences between the uneroded region and eroded region were then quantified in microns using changes in Z-axis along a single horizontal line of reference (single mid-point step height, SPSH) [26], using 10 horizontal lines of references across the wear scar (mean single mid-point step height, mean SHC) [27], and the entire wear scar (3D step height, 3D SHC) [2].

2.4.1.2. Surface roughness change measurement and characterisation. Surface roughness was measured according to previously published protocols using surface metrology software (Boddies v1.92, Taicaan, Southampton, UK) [4,24]. A cluster of five scans each measuring 0.2 × 0.2 mm (0.04 mm²) was selected in the central bulbosity of each natural enamel sample and scanned in a raster pattern with a 4 μm stepover distance. This was conducted using a bespoke image acquisition macro written within the motion control software (Stages™, TaiCaan Technologies, Southampton, UK) together with the assistance of a live video microscope attached to the NCLP system. This central cluster method was previously validated as representative of the natural enamel surface for measuring change in surface roughness [9].

A 25 μm Gaussian filter was applied to each scan in order to determine 3D roughness (Sa) data for each sample using metrology software (Boddies v1.92, Taicaan Technologies, Southampton, UK), and mean Sa calculated for each sample from the 5 scans according according to previously published protocols and ISO 25178 [4,24,25].

2.4.1.3. Surface reflectivity measurement and characterisation. Optical coherence tomography (OCT) was conducted, before and after each erosion cycle, using a swept-source multi-beam clinical OCT machine (VivoSight™ Michelson Diagnostics, Kent, UK) utilising a near infra-red laser (1305 nm) with optical resolution <7.5 μm. Samples were scanned in a raster pattern to produce B-stack volumes comprising 1000 B-scans of (x,z) dimension (4 × 1 mm) with y-step-over 4 μm; the resulting B-stack volumes consisted of dimension 4 × 4 × 1 mm (x,y,z). A stack analysis programme [8] extracted single full profile peak intensity average images from each B-stack volume; known

as surface projection/ reflection images. An automated macro created using ImageJ (ImageJ, Abramoff et al. [28]) was created to analyse the peak intensity (grey value) of the designated region of interest (1.5 mm diameter eroded region) before and after each erosion cycle. Peak intensity (reflectivity) analysis consisted of normalising all grey values against baseline and this was converted into a percentage; 100% reflectivity vs baseline indicated no erosion occurred at baseline. The percentage increase or decrease in normalised percentage peak intensity was determine for all erosion cycles [8,29].

2.5. Statistical methods

Statistical analysis was conducted using GraphPad Prism 7 (GraphPad Software Inc, California, USA). Data was assessed for normality using Komogorov–Smirnov and Shapiro–Wilks tests, and visually assessed with histograms and box plots. All the data were found to be normally distributed, and therefore mean and standard deviation was reported, between group analysis was conducted using parametric testing one-way repeated measures ANOVA with post-hoc Tukey test for multiple comparisons.

3. Results

3.1. Investigation 1—detection threshold determination

For the NCLP repeatability investigation, the mean (SD) surface form difference between each scan was calculated as 0.14 (0.05) μm and the NCLP repeatability was therefore calculated as 0.29 μm. Similarly, the mean (SD) surface roughness difference between each scan was 0.03 (0.01) μm and thus the NCLP repeatability for surface roughness was calculated as 0.06 μm.

However, for the NCLP reproducibility study, the mean (SD) surface form difference between each scan increased to 0.23 (0.07) μm and thus the NCLP reproducibility for surface form was calculated as 0.44 μm. For surface roughness measurements, the mean (SD) difference was 0.03 (0.02) μm and the NCLP reproducibility for surface roughness was calculated as 0.09 μm.

3.2. Investigation 2—characterising the influence of thermal variation on NCLP system stability

Fig. 2 and Table 1 indicate the sensor displacement variations that occur with temperature variation according to the scanning conditions of the NCLP.

During short-term evaluation, no change in scanning temperature occurred within the resolution of the temperature logger (<0.1 °C), and static stability of sensor displacement showed no significant difference between the NCLP open or closed (SD of sensor displacement 0.014 and 0.013 μm respectively). Short-term measurements were not significantly affected by thermal variation in measurement temperature, thus demonstrating the baseline repeatability of the measurement system without the influence of thermal variation in the measurement environment.

There was a cyclical temperature variation introduced by the laboratory air conditioning control (20 ± 1 °C). This produced a corresponding variation in the sensor displacement. This positive trend was evident in medium and long-term evaluations where the NCLP had no protective enclosure.

During medium-term evaluation, thermal variance (SD) of 0.260 °C was detected and corresponded with a resulting NCLP displacement SD of 0.556 μm, whilst within the enclosure NCLP thermal variance and subsequent displacement SD reduced to 0.053 °C and 0.098 μm respectively.

Similarly, during long-term evaluation, the temperature control improved (SD of 2-h temperature 0.473 °C to 0.069 °C) and the sensor displacement fluctuation dampened (1.049 μm to 0.164 μm) when the NCLP was enclosed. This relationship demonstrated a temperature sensitivity on measured displacement of the NCLP of 2218 nm/°C (2.218 μm/°C).

3.3. Investigation 3—characterising effects of early acid-induced enamel erosion

3.3.1. Surface form change measurement and characterisation

Wear scar depth as analysed using three different methods and their respective analytical outputs is shown Table 2.

3.3.1.1. Method 1—scan superimposition and difference analysis. Acid erosion caused a statistically significant increase in wear scar depth for both measurement outputs, compared to baseline, for all time points (p < 0.0001). Mean (SD) Z-change (μm) at 5, 10, and 15 min was 1.1 (0.9), 2.2 (1.1), 3.7 (1.6); whilst the mean (SD) total deviation (μm) for the same erosion times were 1.1 (0.8), 2.1 (1.0), and 3.5 (1.6) respectively. There was no statistically significant difference in mean Z-change and mean 3D total deviation measured for each erosion time point (p > 0.05). Additionally, there was no statistically significant difference in the wear scar depth calculation using either Z-mean or 3D total deviation measurement output (p > 0.05). Representative example of superimposition and difference analysis can be seen in Fig. 3.

3.3.1.2. Method 2—scan superimposition and profile extraction analysis. Mean (SD) Z-change (μm) after 5, 10, and 15 min erosion was 1.05 (0.59), 2.12 (1.06), 3.40 (1.75) respectively, and using mean (SD) 3D step height (μm) it was 1.49 (0.26), 2.47 (0.85), 3.71 (1.58) respectively. There was a statistically significant difference in mean 3D step height between 5 min and 15 min (p < 0.05). Additionally, there was no statistically significant difference in the wear scar depth calculation using either mean Z-change or mean 3D step height measurement output (p > 0.05).

3.3.1.3. Method 3—scan subtraction and residual profile extraction analysis. For all three measurement outputs, acid erosion after 5, 10, and 15 min caused a statistically significant increase in wear scar depth (p < 0.0001). Differences between each wear scar calculation method were noted and were statistically significant after 10 min erosion (mean SPSH vs mean 3D SHC, p < 0.05) and 15 min erosion (mean SPSH vs mean SHC, p < 0.01, mean SPSH vs mean 3D SHC, p < 0.0001). There was no
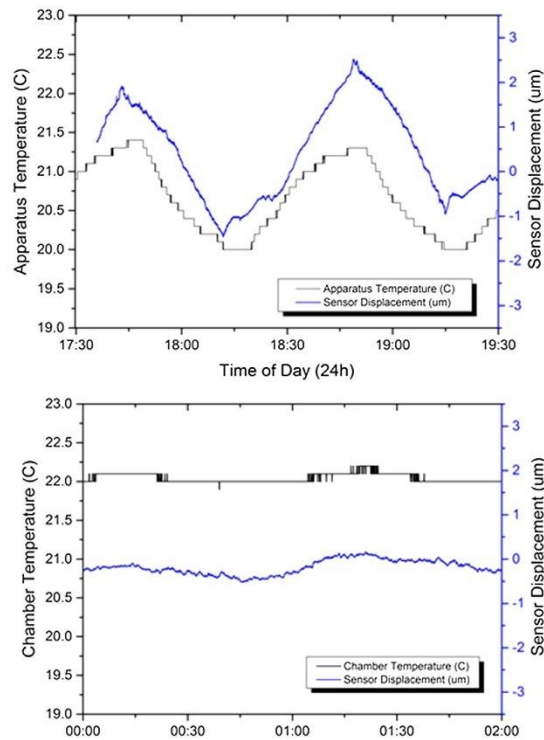
Fig. 2 – Graphs of apparatus ambient temperature and the sensor displacement without apparatus enclosure (above) and with apparatus enclosure (below). There is a clear relationship between sensor displacement and apparatus ambient temperature. The use of a thermal enclosure leads to a significant reduction in chamber and apparatus temperature which in turn minimises sensor displacement, resulting in a more stable scanning outcome.

Table 1 – Indicates the dependence of the NCLP positional accuracy on control of environmental temperature. It is apparent that a simple, low cost enclosure provides a significant improvement in thermal control and positional stability. $T = 30\,s$ indicates environmental noise floor for short term influences (non-thermal considerations). $T = 20\,min$ indicates maximum influence of thermal variance over a single NCLP 3D measurement. $T = 2\,h$ indicates maximum influence of cyclic thermal variance in the environment.

| NCLP condition | Scanning evaluation period | | | | | |
| | 30 s | | 20 min | | 2 h | |
	Thermal variance [SD] (^{0}C)	Positional variation 690 samples [SD] (μm)	Thermal variance [SD] (^{0}C)	Positional variation 920 samples [SD] (μm)	Thermal variance [SD] (^{0}C)	Positional variation 5500 samples [SD] (μm)
Exposed to ambient laboratory air	<0.1 (SD = 0)	0.014	0.260	0.556	0.473	1.049
Within protective enclosure	<0.1 (SD = 0)	0.013	0.053	0.098	0.069	0.164

Table 2 – Results for surface profile, surface profilometry, and peak intensity analysis are shown. For surface profile measurements, 3 methods were analysed, scan superimposition with/without profile extraction, and scan subtraction with profile extraction. Mean (SD) for each data output is determined.

Erosion time (min)	Surface profilometry							Surface roughness		Peak intensity analysis	
	Scan superimposition and difference method		Scan superimposition and profile extraction method		Scan subtraction and profile extraction method						
	Mean (SD) Z-change (μm)	Mean (SD) 3D total deviation (μm)	Mean (SD) Z-change (μm)	Mean (SD) 3D step height (μm)	Mean (SD) SPSH (μm)	Mean (SD) SHC (μm)	Mean (SD) 3D SHC (μm)	Mean (SD) surface roughness (Sa, μm)	Percentage change vs baseline (%)	Mean (SD) reflectivity (grey value)	Percentage reflection vs baseline (%)
0 (baseline)	0	0	0	0	0	0	0	1.13 (0.13)	0	48831.7	100.0
5	1.10 (0.9)	1.10 (0.8)	1.05 (0.59)	1.49 (0.26)	1.61 (1.09)	1.61 (0.56)	0.72 (0.25)	1.52 (0.23)	38.4	40026.1	82.0
10	2.20 (1.1)	2.10 (1.0)	2.12 (1.06)	2.47 (0.85)	3.06 (1.75)	2.86 (1.09)	1.72 (0.65)	1.44 (0.19)	30.3	37951.8	77.7
15	3.70 (1.6)	3.50 (1.6)	3.40 (1.75)	3.71 (1.58)	7.06 (1.26)	6.01 (1.12)	4.47 (1.25)	1.43 (0.21)	30.0	35738.8	73.2

Fig. 3 – Representative example of a sample with its associated wear scar using superimposition, in blue, green denotes no change, whilst yellow denotes gain post erosion. Wear scar depth is depicted by 3D total deviation (D) and Z-deviation (Dz). The central eroded region and 5 reference regions have been analysed for allow for erosion vs non-eroded comparison (For interpretation of the references to colour in this figure legend, the reader is referred to the web version of this article).
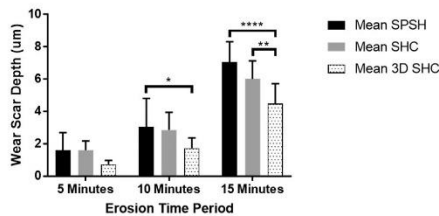
Fig. 4 – Differences between the three wear scar depth measurements were compared for the scan subtraction and profile extraction methodology. Statistical significance is denoted by * (p < 0.05), ** (p < 0.01), * (p < 0.005), and ****(p < 0.0001).**

statistically significant difference in the wear scar calculation after 5 min erosion (p > 0.05); as seen in Fig. 4.

3.3.2. Surface roughness change measurement and characterisation

The mean (SD) surface roughness values for all natural enamel samples after 0, 5, 10, and 15 min acid immersion were, 1.13 (0.13) μm, 1.52 (0.23) μm, 1.44 (0.19) μm, and 1.43 (0.21) μm respectively (Table 2 and Fig. 5) and were statistically significant at all citric acid immersion time points compared to before erosion (baseline) (p < 0.0001). Intergroup analysis revealed statistically significant differences in mean surface roughness between 5 min and all other erosion time points (vs 10 min p < 0.05, and vs 15 min, p < 0.0001), however there was no statistically significant difference between 10 min and 15 min erosion (p > 0.05).

3.3.3. Surface reflectivity measurement and characterisation

Analysis of sample surface reflectivity, using OCT, before and after all acid erosion periods can be seen in Table 2.
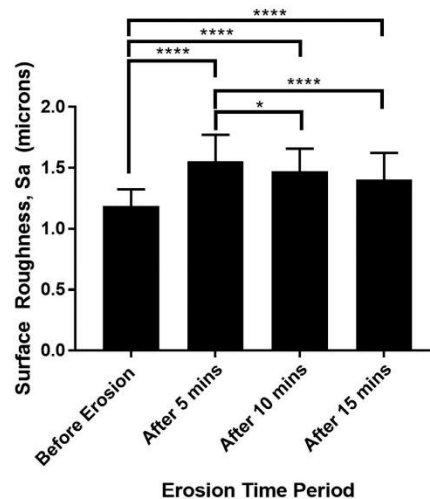
Fig. 5 – Change in surface roughness of the wear scar were determined for each erosion time point and compared to before erosion. Statistical significance is denoted by * (p < 0.05), ** (p < 0.01), * (p < 0.005), and ****(p < 0.0001).**

273
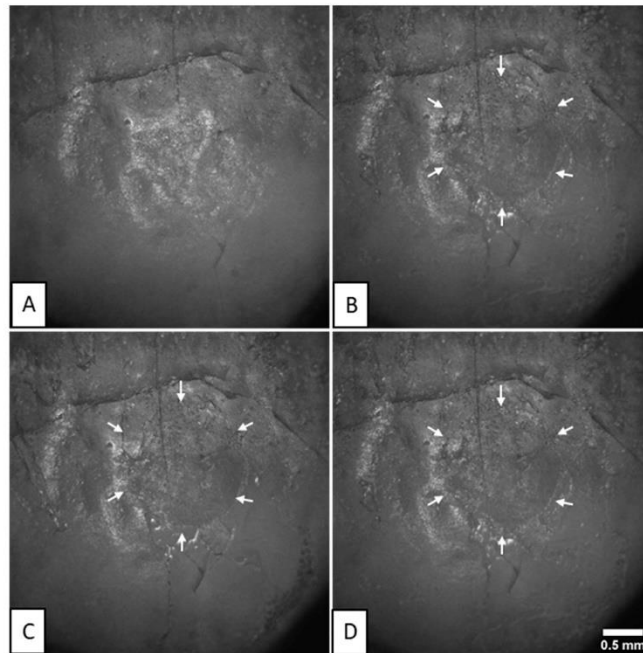
Fig. 6 – Representative example of surface reflection/projection images produced with OCT. Eroded lesion is indicated by the white arrows, and erosion times are (A) baseline, (B) 5 min, (C) 10 min, (D) 15 min erosion. Scale bar for all images in 0.5 mm.

Differences in surface reflectivity occurred after all erosion timepoints compared with before erosion. Percentage peak intensity change after 5, 10, and 15 min erosion were 82%, 77.7%, and 73.2% respectively, and were statistically significant (p < 0.0001) for all erosion groups compared with before erosion. However, there were no statistically significant differences in percentage peak intensity change between erosion timepoints (p > 0.05). An example of the surface reflectivity images can be seen in Fig. 6.

4.   Discussion

The accuracy and measurement uncertainty of chromatic confocal profilometry for surface roughness measurement of polished and natural enamel surfaces has been previously studied [4], however, to the authors' knowledge, this study is the first to determine detectable threshold of monochromatic NCLP for surface form and surface roughness measurements using natural human enamel. A significant challenge in using natural enamel surfaces for both early and late erosion *in vitro* models is defining an effective barrier protocol to produce an exposed area of enamel with corresponding areas of pro-

tected/uneroded enamel to serve as reference for comparison after erosion. This is relatively easy to achieve for polished enamel samples and is one reason why *in vitro* research studying dental erosion has primarily used polished enamel surfaces [30]. However, this study is the first to utilise a novel barrier technique to provide isolation and thus creation of an eroded enamel region for comparison to region of uneroded natural enamel. This is this first study utilising a circumferential barrier creation method using adhesive tape to create dental erosion lesions on natural enamel. Surgical biopsy punch of 1.5 mm diameter provided a reliable method to reproducibly create a hole with mean (SD) 1.49 (0.03) mm. The exposed region of enamel represented the bulbosity of the natural enamel sample, this region was utilised as this would be the first region under erosive attack in the oral cavity [31]. Previously reported barrier methods utilised on polished enamel include use of adhesive tape strips [4,8,11], or nail varnish [32,33] to leave a rectangular (or similar shaped) strip of exposed enamel for erosion. In unpublished pilot work by the same authors, these barrier methods could not be successfully utilised on natural enamel to produce dental erosion lesions; adhesive tapes detached almost immediately when immersed in citric acid, and nail

274

varnish removal damaged the delicate eroded enamel surface.

The influence of scanning environment thermal variation on NCLP sensor displacement has not been previously studied, and for medium and long-term scanning periods it appears to have a significant influence on NCLP displacement. This will have a major impact for studies attempting to evaluate the very earliest changes that occur during acid-mediated erosion of polished and natural enamel. The effect of sensor displacement varied according to the scanning time investigated. A previous study by Holme et al. [22] indicated, but did not further evaluate, that for their scanning set up using white light interferometry (WSI), a 1 K change in temperature would result in a y-direction shift of 6.5 μm between the lens and the sample. Furthermore, no further analysis regarding how thermal variation during WSI scanning was conducted to determine its effects on subsequent scanning and step height determination. Within our study, however, we have demonstrated the effect of changing ambient temperature on NCLP sensor displacement for three different scanning time periods (short, medium, long) to reflect the different scanning durations that may occur according to the scanning parameters required to scan an object using NCLP. By doing this, our study has shown that using a scanning enclosure to stabilise ambient scanning conditions led to an improvement in NCLP sensor stability and in turn improved its measurement accuracy. Future studies utilising NCLP should therefore consider the use of a scanning enclosure to improve accuracy of subsequent measurements.

An optical flat was utilised, rather than a natural tooth sample, to determine sensor displacement, because the crystalline structure of the optical flat material will neither change size nor shape with increasing thermal changes. Therefore, a true indication of sensor displacement changes with thermal variation could be determined. Our study demonstrated a linear relationship in the region measured between sensor/apparatus temperature variation and NCLP sensor displacement. Temperature variation induced NCLP sensor displacement did not affect measurements conducted over a short scanning period (30 s). However, over medium (20 min) and long (2 h) scanning periods NCLP sensor displacement was calculated at 0.556 μm and 1.049 μm respectively. The profilometric scans conducted in this study to determine wear scar depth formation were conducted over 21 min using an NCLP system not covered nor protected from ambient thermal changes. By characterising the influence of thermal variation on subsequent sensor displacement, it was possible to account for this error in any NCLP scans being conducted over medium and long scanning periods. All studies that seek to determine the earliest effects of acid-erosion on enamel should ideally ensure ambient/sensor temperature variations are conducted in an enclosed environment, and controlled within 2 °C [34] to ensure minimisation of sensor displacement over medium-long term scanning periods.

Measuring surface form change has presented a significant challenge in erosion research due to the complex freeform nature of natural enamel and measurement errors associated with utilising NCLP [4,6,13,14]. Step height change calculation, ISO 5436-1, using post erosion scan data is considered the gold standard for determining erosive tooth wear in vitro for flat polished samples [30,35]. This method cannot be utilised for natural enamel samples as conventional form removal techniques and wear scar isolation — using strips of tape or other physical barriers — is not possible on freeform organic surfaces.

However, this can be determined by using either scan superimposition and comparing differences in the Z-height or by profile subtraction of before and after profile scan data and utilising the difference profile for analysis.

The utilisation of a difference profile or difference image produced by profile subtraction of before/after erosion scan data sets has been previously utilised to successfully determine bulk enamel loss in polished human enamel samples [22]. In this study by Holme et al. [22], they conducted an in vitro stepwise etch study using hydrochloric acid, and utilised dental amalgam as the reference region for comparison to the eroded enamel region. By subtracting the after erosion profile from the before erosion profile, the resulting difference profile was then utilised for subsequent analysis of bulk enamel loss [22]. In our study, calculation of bulk enamel loss, from the difference profile producing using profile subtraction, on natural human enamel samples as successfully demonstrated. Additionally by utilising a novel barrier technique, using PVC tape to allow for the creation of a central window of exposed enamel surrounded by region of uneroded/protected enamel, this tallowed for a direct comparison between eroded and non-eroded enamel without the use of any adjunctive dental materials as points of reference. Moreover, by utilising a bespoke scanning jig sample alignment before and after erosion was ensured to facilitate accurate superimposition or alignment of before and after erosion data sets, which therefore allowed determination of wear scar depth by profile comparison or subtraction and analysis of the difference profile.

Profile superimposition allowed for determination of changes in Z-height, either as mean Z-change or mean 3D deviation, similar to results obtained by Rodriguez et al. [1,2] who also demonstrated dimensional change using superimposition software [1,2]. Our study, however, is the first to demonstrate step height calculation using profile subtraction and either mean single point step height (mean SPSHC), mean step height (mean SHC), or mean 3D step height (mean 3D SHC). This study found no statistically significant difference (p < 0.05) in either measurement for the shortest erosion exposure studied (5 min). However, there was a statistically significant difference after 10 min (mean SPSH vs mean 3D SHC, p < 0.05) and 15 min erosion (mean SPSH vs mean SHC, p < 0.01, mean SPSH vs mean 3D SHC, p < 0.0001). Mean 3D SHC provided the lowest number for wear depth and may indicate a truer representation of wear scar depth as this is calculated from all available profiles in the wear scar. This is in agreement with previous studies which have utilised 3D SHC to determine step height change in polished [2,36] and natural enamel samples [1,2].

Previous literature has reported characterisable changes to polished enamel surfaces at 30 s erosion using surface roughness [11], 30 min using OCT [37], and 15 min using TSM [9]; however seldom have the characterisable changes to natural enamel surfaces been considered. Mullan et al. [9] demonstrated the differences in the changes in surface roughness in natural enamel samples compared with

polished enamel samples; polished samples became significantly rougher (increasing Sa values) with increased erosion compared with natural enamel samples which became significantly smoother (decreasing Sa values) after prolonged citric acid exposure times [9].

However, the results of this study indicate that during the early erosion period (5 min) surface roughness increased significantly from baseline Sa of 1.13 (0.13), up to 1.52 (0.23) μm (p < 0.0001), and then decreased after 10 and 15 min. Suggesting the early erosive process in natural enamel is much slower than in polished enamel samples, and the use of surface roughness can allow for determination of early changes to the surface layer of natural enamel during early erosion.

TSM demonstrated qualitative changes occurring at the amorphous surface layer and provided clear evidence at the eroded/uneroded enamel boundary which was protected by the taping isolation method. This work is supported by Mullan et al. [4] who also demonstrated surface changes to natural enamel samples after acid erosion using TSM, however, they utilised longer erosion time periods and orange juice as their erosive medium [4].

OCT provided an evaluation of the effect of early citric acid erosion on surface reflectivity. The eroded zone demonstrated reduced percentage surface reflection compared with uneroded regions as erosion time increased. This indicated that the optical properties of the amorphous surface layer were adversely affected by acid erosion. This is supported by previous *in vitro* study utilising natural human incisors embedded in resin, OCT was able to detect changes to the enamel surface following 5 and 10 min of acid erosion and detectable changes were significant after 50 and 60 min erosion [38]. Whilst, an *in-vivo* study demonstrated increase in backscattering of the OCT signal intensity as acid erosion increased, which occurred due to surface and subsurface demineralisation which was calculated up to a depth of 33 μm after 60 min erosion [39]. However, this study required 60 min of orange juice mediated acid erosion to produce a detectable effect [37–39].

This *in vitro* study has demonstrated the formation of the early erosive lesion in natural enamel, and many different methodological challenges have been overcome relating to sample isolation, and lesion characterisation. Natural enamel samples can be considered for use in *in vitro* studies to investigate the formation and progression of early acid erosion, as well as the assessment of enamel lesion remineralisation.

Whilst this was beyond the scope of this study, future work is necessary to determine the variability in physicochemical composition of natural enamel samples (due to the difference in tooth source, exposure to saliva, fluoride etc) and ascertain its impact on the dental erosion process.

5. Conclusions

NCLP detection threshold for measuring changes in surface form and surface roughness was determined for natural human enamel. Thermal variation during scanning resulted in NCLP sensor displacement over medium (20 min) and long (2 h) scanning periods, therefore this should be characterised, and its effects minimised when scanning natural enamel samples. A scanning enclosure can significantly enhance NCLP measurement stability and thus measurement accuracy. Acid-induced dental erosion wear scars in natural human enamel could be characterised using surface profilometry, surface roughness, OCT, and TSM; step height could be calculated using profile superimposition and profile subtraction techniques.

REFERENCES

[1] Rodriguez JM, Austin RS, Bartlett DW. A method to evaluate profilometric tooth wear measurements. Dent Mater 2012;28:245–51, http://dx.doi.org/10.1016/j.dental.2011.10.002.

[2] Rodriguez JM, Bartlett DW. A comparison of two-dimensional and three-dimensional measurements of wear in a laboratory investigation. Dent Mater 2010;26:e221–5, http://dx.doi.org/10.1016/j.dental.2010.07.001.

[3] Paepegaey A, Barker ML, Bartlett DW, Mistry M, West NX, Hellin N, et al. Measuring enamel erosion: a comparative study of contact profilometry, non-contact profilometry and confocal laser scanning microscopy. Dent Mater 2013;29:1265–72, http://dx.doi.org/10.1016/j.dental.2013.09.015.

[4] Mullan F, Bartlett D, Austin R. Measurement uncertainty associated with chromatic confocal profilometry for 3D surface texture characterisation of natural human enamel. Dent Mater 2017;33(6):e273–81, http://dx.doi.org/10.1016/j.dental.2017.04.004.

[5] Attin T, Wegehaupt FJ. Methods for assessment of dental erosion. Monogr Oral Sci 2014;25:123–42, http://dx.doi.org/10.1159/000360355.

[6] Leach R. Fundamental principles of engineering nanometrology. Oxford, UK: Elsevier Inc.; 2009.

[7] de Groot P. The meaning and measure of vertical resolution in optical surface topography measurement. Appl Sci 2017;7:54, http://dx.doi.org/10.3390/app7010054.

[8] Mylonas P, Austin R, Moazzez R, Joiner A, Bartlett D. In vitro evaluation of the early erosive lesion in polished and natural human enamel. Dent Mater 2018;34:1391–400.

[9] Mullan F, Austin RS, Parkinson CR, Hasan A, Bartlett DW. Measurement of surface roughness changes of unpolished and polished enamel following erosion. PLoS One 2017;12:0–11, http://dx.doi.org/10.1371/journal.pone.01824.

[10] Austin RS, Mullen F, Bartlett DW. Surface texture measurement for dental wear applications. Surf Topogr Metrol Prop 2015;3:23002, http://dx.doi.org/10.1088/2051-672X/3/2/023002.

[11] Austin RS, Giusca CL, Macaulay G, Moazzez R, Bartlett DW. Confocal laser scanning microscopy and area-scale analysis used to quantify enamel surface textural changes from citric acid demineralization and salivary remineralization in vitro. Dent Mater 2016;32:278–84, http://dx.doi.org/10.1016/j.dental.2015.11.016.

[12] Mullan F, Mylonas P, Parkinson C, Bartlett D, Austin R. Precision of 655nm confocal laser profilometry for 3D surface texture characterisation of natural human enamel

undergoing dietary acid mediated erosive wear. Dent Mater 2018;34:531–7.

[13] Bell S. Measurement Good Practice Guide No. 11 (Issue 2), A Beginner's Guide to Uncertainty of Measurement. Middlesex, United Kingdom: National Physical Laboratory Teddington; 2001.

[14] Yang B, Ross-Pinnock D, Muelaner J, Mullineux G. Thermal compensation for large volume metrology and structures. Int J Metrol Qual Eng 2017;8, http://dx.doi.org/10.1051/ijmqe/2017004.

[15] Zheng J, Xiao F, Qian LM, Zhou ZR. Erosion behavior of human tooth enamel in citric acid solution. Tribol Int 2009;42:1558–64, http://dx.doi.org/10.1016/j.triboint.2008.12.008.

[16] Zheng J, Xiao F, Zheng L, Qian LM, Zhou ZR. Erosion behaviors of human tooth enamel at different depth. Tribol Int 2010;43:1262–7, http://dx.doi.org/10.1016/j.triboint.2009.12.008.

[17] Berkovitz BK, Holland G, Moxham B. Oral anatomy, histology, and embryology. 6th ed. Edinburgh: Mosby/Elsevier; 2009.

[18] Zheng J, Zhou ZR. Friction and wear behavior of human teeth under various wear conditions. Tribol Int 2007;40:278–84, http://dx.doi.org/10.1016/j.triboint.2005.09.025.

[19] Young A, Tenuta LMA. Initial erosion models. Caries Res 2011;45:33–42, http://dx.doi.org/10.1159/000325943.

[20] Shellis R, Featherstone JDB, Lussi A. Understanding the chemistry of dental erosion. Erosive tooth wear from diagnosis to therapy. Monogr Oral Sci 2014;25:163–79, http://dx.doi.org/10.1159/000359943.

[21] Kumar S, Keeling A, Bartlett D, Osnes C, O'Toole S. The sensitivity of digital intraoral scanners at measuring early erosive wear. J Dent 2018;81:39–42.

[22] Holme B, Hove LH, Tveit AB. Using white light interferometry to measure etching of dental enamel. Meas J Int Meas Confed 2005;38:137–47, http://dx.doi.org/10.1016/j.measurement.2005.04.003.

[23] Stenhagen KR, Hove LH, Holme B, Taxt-Lamolle S, Tveit AB. Comparing different methods to assess erosive lesion depths and progression in vitro. Caries Res 2010;44:555–61, http://dx.doi.org/10.1159/000321536.

[24] Attin T, Becker K, Roos M, Attin R, Paqu F. Impact of storage conditions on profilometry of eroded dental hard tissue. Clin Oral Investig 2009;13:473–8, http://dx.doi.org/10.1007/s00784-009-0253-9.

[25] Mylonas P, Austin RS, Moazzez R, Joiner A, Bartlett DW. In vitro evaluation of the early erosive lesion in polished and natural human enamel. Dent Mater 2018;34:1391–400.

[26] O'Toole S, Mistry M, Mutahar M, Moazzez R, Bartlett D. Sequence of stannous and sodium fluoride solutions to prevent enamel erosion. J Dent 2015;43:1498–503, http://dx.doi.org/10.1016/j.jdent.2015.10.003.

[27] Mistry M, Zhu S, Moazzez R, Donaldson N, Bartlett DW. Effect of model variables on in vitro erosion. Caries Res 2015;49:508–14, http://dx.doi.org/10.1159/000438725.

[28] Abramoff M, Magalhaes P, Ram S. Image processing with ImageJ. Biophotonics Int 2004;11:36–42.

[29] Schneider C, Rasband W, Eliceiri K. NIH Image to ImageJ: 25 years of image analysis. Nat Methods 2012;9:671–5.

[30] Huysmans MC, Chew HP, Ellwood RP. Clinical studies of dental erosion and erosive wear. Caries Res 2011;45:60–8, http://dx.doi.org/10.1159/000325947.

[31] Shellis RP, Addy M. The interactions between attrition, abrasion and erosion in tooth wear. erosive tooth wear from diagnosis to therapy. Monogr Oral Sci 2012;25:32–45.

[32] Amaechi BT, Higham SM, Edgar WM. Use of transverse microradiography to quantify mineral loss by erosion in bovine enamel. Caries Res 1998;32:351–6, http://dx.doi.org/10.1159/000016471.

[33] Ganss C, Lussi A, Klimek J. Comparison of calcium/phosphorus analysis, longitudinal microradiography and profilometry for the quantitative assessment of erosive demineralisation. Caries Res 2005;39:178–84, http://dx.doi.org/10.1159/000084795.

[34] ISA-TR52.00.01. Recommended Environments for Standards Laboratories. North Carolina, United States of America: The Instrumentation, Systems, and Automation Society; 2006.

[35] Lussi A, Ganss C. Erosive tooth wear: from diagnosis to therapy. 2nd ed. Switzerland: S. Karger AG; 2014.

[36] Sar Sancakli H, Austin R, Al-Saqabi F, Moazzez R, Bartlett D. The influence of varnish and high fluoride on erosion and abrasion in a laboratory investigation. Aust Dent J 2015;60:38–42, http://dx.doi.org/10.1111/adj.12271.

[37] Aden A, Anderson P, Burnett G, Lynch R, Tomlins P. Longitudinal correlation of 3D OCT to detect early stage erosion in bovine enamel. Biomed Opt Express 2017;8:1092–3.

[38] Chew HP, Zakian CM, Pretty IA, Ellwood RP. Measuring initial enamel erosion with quantitative light-induced fluorescence and optical coherence tomography: An in vitro validation study. Caries Res 2014;48:254–62, http://dx.doi.org/10.1159/000354411.

[39] Austin R, Taha M, Festy F, Cook R, Andiappan M, Gomez J, et al. Quantitative swept-course optical coherence tomography of early enamel erosion in vivo. Caries Res 2017;51(4):410–8, http://dx.doi.org/10.1159/000477098. Epub 2017 Jun 22.

In vitro evaluation of the early erosive lesion in polished and natural human enamel

P. Mylonas[a,*], R.S. Austin[a], R. Moazzez[b], A. Joiner[c], D.W. Bartlett[a]

[a] Prosthodontic Department, King's College London, London, UK
[b] Mucosal and Salivary Biology Division/Restorative Department, King's College London, London, UK
[c] Unilever Oral Care, Bebington, Wirral, UK

ARTICLE INFO

ABSTRACT

Objective. This study evaluated the capability of profilometry, microhardness, Optical Coherence Tomography (OCT) and Tandem Scanning Confocal Microscopy (TSM) in characterising the early erosive lesion in polished and natural human enamel *in vitro*.

Methods. Polished (n = 60) and natural (n = 60) human enamel surfaces, were immersed and agitated in 0.3% citric acid erosion at 0 s, 10 s, 30 s, 60 s, 120 s, and 300 s (n = 10). Changes in the surface were measured with 3D-step height change (μm), surface roughness (μm), surface microhardness (KHN), and images were assessed qualitatively with OCT and TSM.

Results. Mean (SD) 3D-step height change (μm) was measurable for polished enamel at: 60 s (0.24 ± 0.1), 120 s (1.16 ± 0.71), 300 s (2.01 ± 0.47; $p < 0.05$); a step height change was not detectable on acid challenged natural enamel surfaces. Mean (SD) surface roughness (μm) of polished enamel was detected at 10 s (0.270 ± 0.013; $p < 0.05$) and all erosion periods; and in natural enamel detected after 120 s (0.830 ± 0.125) and 30 s (0.800 ± 0.140; $p < 0.005$). Polished enamel Mean (SD) microhardness (KHN) statistically significantly decreased at all time points ($p < 0.001$); this was unmeasurable for natural enamel. Qualitative image analysis of both surface types indicated erosive change at the surface level, with progression after increasing erosion time.

Significance. The early erosive lesion in polished enamel could be characterised quantitatively surface roughness and microhardness and qualitatively using OCT and TSM; whilst in natural enamel only surface roughness could be utilised. Further investigation of early erosion in natural enamel is required to develop new more clinically relevant models.

© 2018 The Academy of Dental Materials. Published by Elsevier Inc. All rights reserved.

1.   Introduction

Erosive tooth wear is a common oral condition which if not treated can compromise the longevity of teeth and a person's quality of life [1]. Understanding what happens in the early stages of this condition, particularly to the integrity of the enamel surface, should enable a better understanding of prevention [2]. The time acidic foods or drinks are exposed

278

in the mouth during eating and or drinking is not precisely known, due to individual variation, but it's likely to be only for a few seconds. But how long it takes for acidic challenge to change the enamel surface is unknown. It is apparent that frequency of consumption of acidic foods and drinks creates a greater risk of developing erosion but they are cleared quickly from the mouth [3]. Current understanding of erosive tooth wear suggests that following a short duration (less than 5 min) acid exposure the enamel surface may soften to a depth of between 0.2 μm and 5 μm [4,5]. This softening is believed to reflect partial loss of surface minerals leading to increasing surface roughness and decreased surface microhardness [5–8]. But these times are derived from laboratory investigations which are partly influenced by the model, presence of artificial or natural saliva, the biofilm, but also by the sensitivity of the measuring technique. Clinically, we appreciate that irreversible loss of tooth structure occurs if acid exposure is prolonged, and increases if further attritive or abrasive factors are introduced [4,9–12]. The definition of what is 'short duration' acid-erosion, in the literature, has not been specified to one particular time period or to the number of acid erosion cycles used, but rather by the duration of acid exposure utilised; typically lasting for several seconds or minutes, and which do not exceed 5 min duration [4,11,13–15].

The physical properties of the early erosive lesion are ill-defined due to the difficulty in detecting quantifiable changes to the enamel structure within short acid erosion time periods [16]. This is primarily a consequence of the sensitivity of most methods to measure any change. Studies have evaluated the formation of early erosive lesions with a range of acid immersion periods and/or number of immersion cycles and varies from 5 s [17] up to 2 h [7] for 1 acid cycle [6,7,11,18–24] to greater than 5 cycles of acid erosion with varying immersion times [17,23,25–27]. Most early enamel erosion studies have been conducted on polished enamel surfaces to ensure consistency of sample preparation, and allow reproducible and accurate measurement of effects occurring from acid exposure [16,18,28,29]. Laboratory simulation of the early erosive lesion on natural, unpolished enamel has been challenging due to its topography and morphology [30].

Previous erosion studies have utilised surface profilometry, to measure step height loss [17,22,27,31] and surface microhardness to determine surface and sub surface softening [6,18,27,29]. Moreover, the equipment and acquisition parameters utilised, varied between studies, and thus it is difficult to generalise the overall detection capabilities of specific measurement techniques. However, these techniques have produced varying degrees of success when detecting the earliest changes following acid erosion. To complicate matters further different measuring systems produce different data, although it appears that the comparative changes are consistent between them [31,32]. A recent study concluded that chromatic non-contacting optical profilometry had measurement uncertainty of 0.49 μm [33] suggesting enamel loss from early enamel erosion may not be reliably detected below 0.4 microns. Whilst another study reported areal textural changes after 30 s exposure to citric acid, utilising non-contacting optical microscopy [27]. Surface microhardness has been shown to be sensitive in detecting early changes due to acid erosion after 30 s exposure to citric acid [27], and this technique may be

useful for times less than this on polished or natural enamel surfaces. Scanning electron microscopy (SEM), has been used to evaluate morphological changes following exposure to acid, however this technique alters the sample surface to allow imaging [21,24]. Tandem scanning microscopy (TSM), involves no sample preparation and high image acquisition, has previously been evaluated for dentine occlusion studies [34,35] but its use in evaluating enamel erosion has yet to be considered. Optical coherence tomography (OCT) has been used to determine surface [16,36] and subsurface [16,37,38] changes that occur to enamel after erosion but to different degrees of success. A recent study determined that alterations in enamel surface reflectivity could be utilised to study the early erosive lesion with change detectable after 1 min acid exposure in polished bovine enamel surfaces [36]. However, longer erosive time periods of 60 min [38] up to 6 h [37] were required in order for subsurface changes in natural enamel to be detectable.

The aim of the study was to determine the minimum time that acid exposure causes change on the enamel surface can be measured by profilometry, surface roughness, surface microhardness, OCT, and TSM. Our null hypothesis was that the formation of an early erosive lesion is independent of time

2. Methods

Enamel slabs (n = 120) were sectioned from the mid-buccal surfaces of previously extracted caries-free human molar teeth (REC ref 12/LO/1836), using a water-cooled 300 μm diamond wafering blade (XL 12205, Benetec Ltd., London, UK). Each slab was mounted, unpolished enamel surface down, in self-cured bisacryl material (Protemp™4, 3M ESPE, Seefeld, Germany) using a custom-made silicone mould. Sixty slabs were polished using successively finer silicon-carbide discs (Versocit, Struers A/S, Copenhagen, Denmark) of grit 500, 1200, 2000, and 4000 for 25 s, 30 s, and 60 s respectively, using a water-cooled rotating polishing machine at 150 rpm and 10 N constant pressure (LaboPol-30, Struers ApS, Ballerup, Denmark) removing approximately 300 μm of enamel and achieving flatness tolerance ±0.2 μm. The newly polished surfaces were then ultrasonicated (GP-70, Nusonics, Lakewood, USA) in 100 ml deionised water (pH 5.8) for 15 min to remove smear layer and air-dried for 24 h at room temperature. PVC adhesive tape was placed on the polished enamel slab/bis-acryl embedding material surface such that each the polished enamel surface had a 1 mm × 3 mm window of exposed enamel, protected by two zones of reference tape either side; allowing for comparison of eroded and protected enamel regions after erosion and after tape removal [27].

Natural surfaces were not cleaned using the same method as for the polished surfaces because this did not result in a sufficiently cleaned enamel surface upon which to conduct the acid erosion challenge. As a result, to ensure they were free from surface debris and organic contamination, all natural enamel surfaces (n = 60) underwent a standardised cleaning regime consisting of: a 10-min immersion in 4.7% sodium hypochlorite solution (Coventry Chemicals Ltd, Coventry, UK), followed by 30-min ultrasonic cleaning in deionised water and air dried for 1 h followed by a 2-min clean with ethanol and cotton wipes, and final air dry for 1 h. They were examined under

TSM before and after cleaning to ensure surface cleanliness which was determined as the visible lack of surface material after cleaning and clear visualisation of enamel surface topography.

All samples were then randomly assigned to one of six treatment groups according to period of acid immersion: 0, 10, 30, 60, 120, or 300 s; 10 natural and 10 polished surfaces per group. Citric acid (0.3%w/w) was prepared, using previously published protocols, by adding anhydrous citric acid powder (Sigma Aldrich, Poole, Dorset UK) to deionised water, and the pH adjusted to 3.2 using 0.1 M sodium hydroxide (Sigma Aldrich, Poole, Dorset UK) [27]. The titratable acidity was calculated according to the volume of sodium hydroxide required to increase the solution pH to 7, which was 18.0 ml [23,27]. Each group of teeth were immersed in 100 ml 0.3% citric acid solution (10 ml per sample) and agitated (62.5 rpm) using an orbital shaker (Stuart mini-Orbital Shaker SSM1, Bibby Scientific, England), at differing times for only 1 erosion cycle. All surfaces were washed with deionised water (pH 5.8) and left to dry overnight before data collection to ensure consistent profilometry scanning of all surfaces under the same scanning conditions [27,33].

Baseline surface microhardness was tested for all polished surfaces utilising a Knoop microhardness tester (Duramin-5, Struers Ltd, Rotherham, UK) and those surfaces outside the range 270–400 KHN were rejected [22]. After acid immersion and drying, adhesive tape for polished enamel surfaces was carefully removed and surfaces assessed. Post erosion microhardness was conducted from 6 indentations produced 100 μm apart, selected conveniently in the eroded and uneroded enamel regions, at 981.2 mN load and 10 s press time and the mean change calculated from the difference between the them according to previously published protocols and ASTM E384 17 [22,27,39].

Profilometric measurement was conducted using a 2 μm laser spot sized red light (655 nm) confocal laser scanning profilometer (Taicaan, XYRIS 2000, UK) with 0.01 μm z height resolution, vertical gauge range 0.6 mm, sensor spatial resolution (x,y) < 1 μm, and (x,y) scanning interval of 10 μm, using previously published protocols [23,32]. Two reference marks made using indelible pen on the bis-acryl material of each sample was used to allow scan co-localisation. Analysis for mean 3D step height was conducted using surface metrology software (MountainsMap®, Digitalsurf, France) using the ISO 5436-1 standard [40]. Surface roughness was measured according to previously published protocol [33] using five representative areas, each 0.04 mm², over the sample were imaged, scanning occurred in a raster pattern, at scanning interval of 4 μm. A 25 μm Gaussian filter was applied to each scan in order to determine 3D roughness (Sa) data for each sample, according to previously published protocols and ISO 25178-2 [27,33].

OCT was conducted by a swept-source multi-beam clinical OCT machine (VivoSight™ Michelson Diagnostics, Kent, UK) utilising a near infra-red laser (1305 nm), with <7.5 μm optical resolution [38], on representative samples of polished enamel surfaces for each erosion group. The refractive index of sound enamel has been previously approximated as 1.65 [36], the resolution of this system for measuring sound enamel is 4.06 μm (x direction) and 3.32 μm (z direction) in air respec-

tively. Each sample was scanned in a raster pattern to produce B-stack volumes consisting of 500 B-stacks of x,z dimension (6 × 1 mm) with y-dimension of 4 μm between each scan. OCT data were semi-quantitatively analysed by using a stack analysis algorithm that was custom designed for this study to extract single full profile peak intensity average images from each B-stack volume. These images were semi-quantitatively analysed using image processing software (ImageJ, Abramoff et al. [41]) by assessing the peak intensity of the eroded enamel compared with non-eroded reference enamel in polished enamel surfaces. This method could not be used for the natural surfaces and thus they were only evaluated qualitatively with TSM.

TSM (Noran Instruments; Middleton, WI, USA) used a ×20 objective lens (×20/0.35 NA objective) filtered light projection (green, 550 nm), to acquire representative 2D images of surfaces before and after acid erosion. A camera (iXon 885 EM-CCD Andor Technology; Northern Ireland, UK) and image acquisition software Micromanager v1.4.22 (Open Imaging; Inc. San Francisco, CA, USA), was used together with image processing software (ImageJ, Abramoff et al. [41]) to qualitatively analyse the 2D images [42]. The images produced using TSM were evaluated qualitatively to determine any visual changes between eroded and uneroded/protected enamel in polished surfaces, and between co-localised images of before/after eroded natural enamel surfaces. Co-localisation was conducted by means of utilising distinct surface features on each natural sample as fiducial markers for comparison of each sample against itself before/after erosion; in accordance with previous protocol [42].

2.1. Statistical analysis

Statistical analysis was conducted using OriginPro 8.5 Statistical Software (OriginPro version 8.5, OriginLab Corp, MA, United States). Kolmogorov–Smirnov test confirmed data conformed to normal distribution, therefore means and standard deviations of each acid immersion group were calculated. Intra-group analysis compared with baseline values for uneroded enamel utilising dependent T-tests, whilst inter-group analysis was conducted with one-way ANOVA; $p < 0.05$ was considered statistically significant. Correlation statistics was performed for all quantitative measurement outputs for the polished surfaces.

Non-linear regression analysis and Spearman rank correlation coefficient comparing 3D step height and surface microhardness (mean KHN) was conducted, whilst linear regression analysis and Pearson correlation coefficient was conducted to compare surface roughness (mean SA) with both 3D step height and surface microhardness; $p < 0.05$ was considered statistically significant and R^2 values expressed for all correlation measures and r values for the association between the variables.

3. Results

Surface microhardness results for the polished surfaces are shown in Table 1. Surface microhardness changes after 10 s, 30 s, 60 s, 120 s, and 300 s citric acid immersion were 40.9

Table 1 – Descriptive statistics for 3D step height change (μm), mean(SD) surface roughness (μm), and the number of analysable samples for each characterisation method for both polished and natural enamel groups. Data is represented as mean (SD) after citric acid erosion. Statistical significance is compared to baseline according to asterisk assignment *p<0.05, **p<0.01.

Immersion period (s)	Polished enamel group						Natural enamel group					
	3D step height change (μm)	Analysable samples	Mean (SD) surface roughness (μm)	Analysable samples	Mean (SD) microhardness change (KHN)	Analysable samples	3D step height (μm)	Analysable samples	Mean (SD) surface roughness (μm)	Analysable samples	Mean (SD) microhardness change (KHN)	Analysable samples
0	0	0	0.18 (0.001)	10	4.4 (1.44)	10	–	0	0.99 (0.265)	10	–	0
10	0.16 (0.04)	5	0.27 (0.002)*	10	40.9 (2.03)*	10	–	0	0.95 (0.098)	10	–	0
30	0.20 (0.10)	3	0.30 (0.028)*	10	60.7 (1.79)*	10	–	0	0.88 (0.241)	10	–	0
60	0.24 (0.10)**	7	0.51 (0.068)*	10	91.7 (3.08)*	10	–	0	0.86 (0.481)	10	–	0
120	1.16 (0.71)**	8	0.95 (0.201)*	10	100.1 (2.07)*	10	–	0	0.83 (0.125)**	10	–	0
300	2.01 (0.47)**	9	1.28 (0.146)*	10	119.9 (4.34)*	10	–	0	0.80 (0.140)**	10	–	0

(2.03) KHN, 60.7 (1.79) KHN, 91.7 (3.08) KHN, 100.1 (2.07) KHN, and 119.9 (4.34) KHN and were statistically significant for all groups compared to baseline (p<0.01). Polished enamel surfaces became statistically softer with increasing citric acid immersion (p<0.01). Microhardness data could not be derived from natural surfaces. The mean (SD) step height change for 10, 30, 60, 120, and 300s acid immersion groups for the polished surfaces were, 0.16(0.04) μm, 0.20(0.1) μm, 0.24(0.1) μm, 1.16(0.71) μm, and 2.01(0.47) μm respectively and these were statistically different compared to baseline (Table 1). Mean (SD) step height change was detected at all times but the number of surfaces that could be analysed was not consistent, the number of analysable surfaces for 10, 30, 60, 120, and 300s were 5, 3, 7, 8, and 9 respectively. Results below 60s were considered unreliable and discounted. Step height data was not obtainable from the natural surfaces.

The mean surface roughness for polished enamel for 10, 30, 60, 120, and 300s acid immersion groups the mean (SD) surface roughness were, 0.27(0.024) μm, 0.30(0.028) μm, 0.51(0.068) μm, 0.95(0.201) μm, and 1.28(0.146) μm respectively and were statistically significant at all citric acid immersion time points compared to before erosion (p<0.05). The mean (SD) surface roughness for the natural enamel decreased for all citric acid immersion time points compared to baseline (Table 1), but were only statistically significant at 120s and 300s; 0.83(0.125) μm and 0.80(0.140) μm respectively (p<0.01). Intergroup analysis revealed no statistically significant differences in mean surface roughness between immersion groups (p>0.05).

Correlation analysis between surface microhardness, surface profilometry, and surface roughness in the polished surfaces group, can be seen in Fig. 1. There was a negative curvilinear relationship (r=−0.7676) and positive correlation (R^2=0.6593) between surface microhardness mean KHN and 3D step height (Fig. 1A), positive linear relationship (r=0.854) and positive correlation (R^2=0.7293) between surface roughness and 3D step height (Fig. 1B), and negative linear relationship (r=−0.8811) and positive correlation (0.7764) between surface roughness and surface microhardness (Fig. 1C); the correlation between each measurement output/method was highly significant (p<0.0001).

Percentage peak intensity analysis of representative polished enamel surfaces using OCT revealed significant differences in surface reflectivity between eroded and non-eroded regions for different citric acid immersion groups (see Fig. 2). Percentage peak intensity change after 10s, 30s, 60s, 120s, and 300s were 88.8%, 86.8%, 77.9%, 69.2%, and 49.1% respectively and were statistically significant for all groups compared with baseline (p<0.01). Surface reflectivity analysis could not be determined for the natural surfaces.

Micrographic analyses of polished and natural enamel surfaces revealed differences between eroded and non-eroded surfaces for each acid erosion group (Figs. 3 and 4). The honeycomb structure of polished enamel could be seen after 10s erosion (Fig. 3 B) and progressed with increased erosion immersion time. The eroded regions became subsequently darker, and scratch marks present after the polishing process progressively were lost. This indicated that the erosive process resulted in further loss of enamel with increasing erosion time. Changes to the surface of natural enamel surfaces were
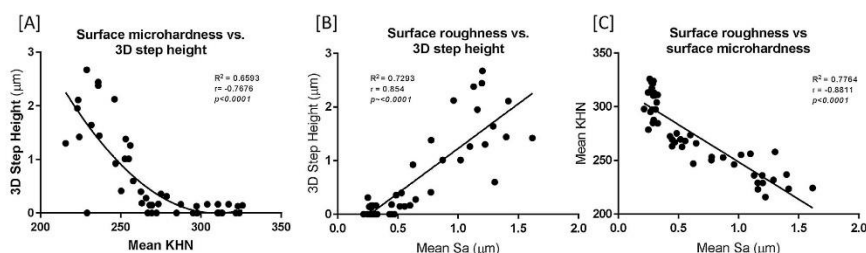
Fig. 1 – [A] Negative curvilinear relationship and large correlation is demonstrated between surface microhardness (mean KHN) and 3D step height (μm) for all samples evaluated. [B] Positive linear relationship and large correlation is demonstrated between surface roughness (mean Sa, μm) and 3D step height (μm) for all samples evaluated. [C] Negative linear relationship and large correlation is demonstrated between surface roughness (mean Sa, μm) and surface microhardness (mean KHN) for all samples evaluated.
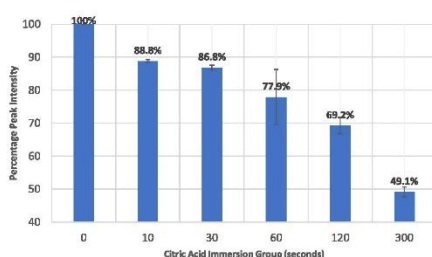
Fig. 2 – Optical coherence tomography, surface reflectivity percentage peak intensity change for representative samples from each acid erosion group compared with baseline/before acid erosion. A decrease in enamel surface reflectivity is evident after acid erosion and continues to decrease with increasing acid erosion.

more subtle, with changes appearing to occur in the prism-inter prism interface after 10 s (Fig. 4) and progressed to further generalised destruction of enamel prism structure and surface topography after 300 s (Fig. 4).

4.   Discussion

The surface microhardness results indicate surface softening of polished enamel surfaces occurred after 10 s, which is much earlier than previously reported in the literature [27]. This suggests that the effects of citric acid on polished enamel, involving the processes of phosphate leaching and calcium chelation from the enamel surface, occur rapidly during acid exposure resulting in surface softening [16]. It was not possible to obtain any accurate, reproducible, or measurable Knoop indentations on natural enamel surfaces to ascertain the minimum time that changes in surface microhardness occurred. This is partly due to the curvature of the enamel surface but also the variations in surface topography and profile that exist

in all natural enamel surfaces, making the measurement of a standardised Knoop diamond indent impossible to conduct; which is why this technique is used only on polished uniformly flat enamel surfaces [16,43].

The findings from this study demonstrated that the current NCLP scanning settings and method was sufficient to measure the formation of the early erosive lesion in polished enamel (after 10 s), and in natural enamel (after 120 s) but only using surface roughness parameters. The surface roughness (Sa) data indicated that in polished enamel statistically significant ($p < 0.05$) changes in Sa from baseline could be detected after just 10 s citric acid erosion; whilst these changes could only be detected after 120 s in natural enamel (Table 1). The disparity in in the erosive characteristics between polished and natural enamel is likely due to the presence of the aprismatic enamel surface layer present in the natural enamel surfaces which is removed and thus missing in all the polished surfaces. The surface layer contains a higher concentration of fluoride and phosphate, and fewer impurities such as magnesium and carbonate, and has been previously shown to be more highly resistant to acid dissolution [18,29]. In a study by Zheng et al. [18] the mechanical properties of enamel differed according to its distance from the dentino-enamel junction (DEJ); erosion resistance decreased as the DEJ was reached and subsequent wear loss of eroded enamel was significantly lower for surface layer enamel *versus* enamel close to the DEJ. Further study of the natural enamel surface and the implications of changes in surface roughness following acid attack are required.

Within the scanning protocol and specifications of the non-contacting optical profilometer used in this study, we were able to detect significant changes in surface roughness after 10 s of acid exposure, which is much earlier when compared with studies utilising longer erosion time periods [13,22,24,27,29]. Current findings are consistent with a previous report which demonstrated that changes in surface roughness, as a measurement output, could be detected after 10 s [21], however this was conducted on polished bovine enamel using pH 2 hydrochloric acid and atomic force microscopy as the measurement technique and Ra as
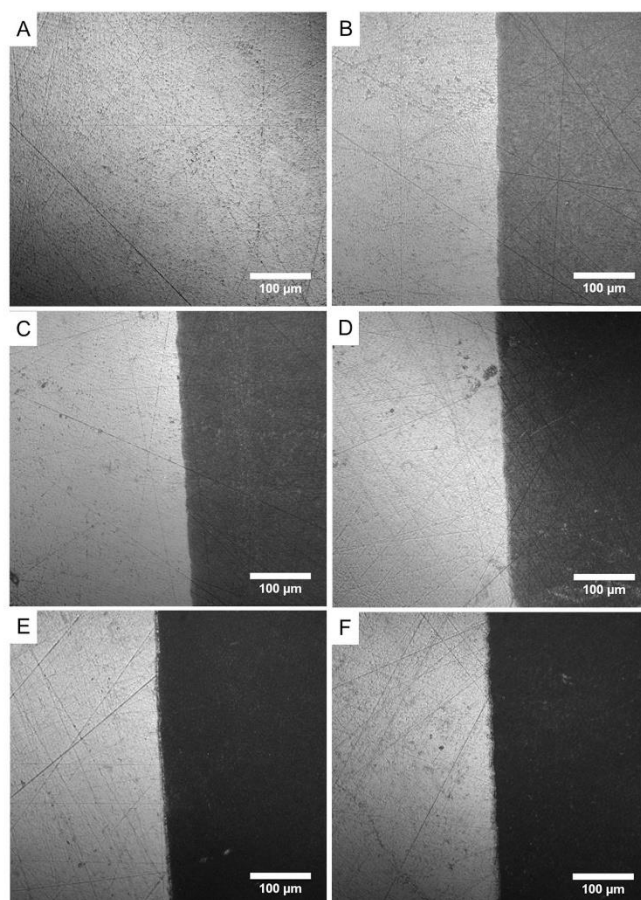
Fig. 3 – Tandem scanning confocal microscopic assessment of changes in appearance of the enamel surface of polished enamel samples: 0 s (A), 10 s (B), 30 s (C), 60 s (D), 120 s (E), 300 s (F). Early erosive changes include appearance of honeycomb structure, progressive darkening of eroded region, and progressive loss of post-polishing scratch marks.

the amplitude parameter for surface roughness. The earliest reported change in surface roughness for polished human enamel occurred after 30 s citric acid exposure [27]. Enamel surfaces in the current study were polished to higher flatness tolerance of $\pm 0.2\,\mu m$ compared with some previous studies which utilised $0.4\,\mu m$ [27] and $0.25\,\mu m$ [24]. This may have helped in the detection of the earliest deviations in the polished enamel surface due to acid erosion in the current study. This is consistent with suggestions from previous reports indicating the importance of sample preparation and its potential

influence on surface texture feature detection [27]. The detection with non-contacting profilometry of changes in surface roughness after 10 s citric acid exposure suggest that the physiological processes occurring during early erosive attack, such as calcium and phosphate release from the enamel surface, occur relatively quickly [17,24,27].

The surface roughness of natural enamel surfaces decreased as acid immersion time increased, indicating smoothening of the aprismatic enamel surface, and contrasts to the results from polished surfaces which became

283
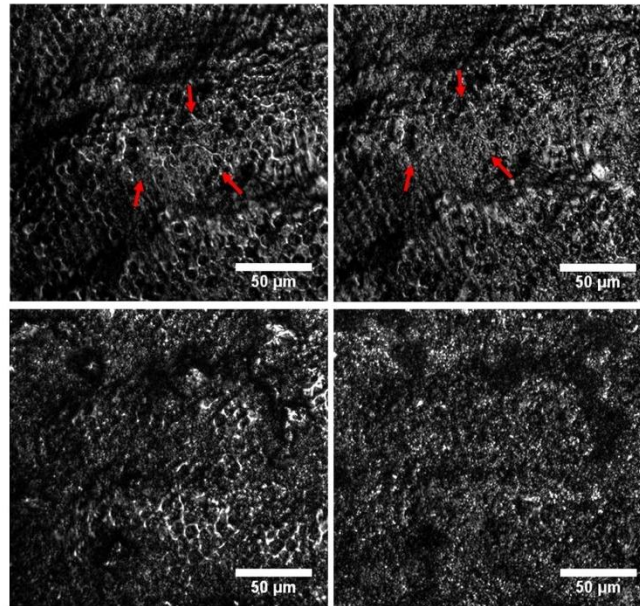
Fig. 4 – Tandem scanning confocal microscopic assessment of changes in appearance of the enamel surface of natural enamel samples: before citric acid immersion (top left and bottom left); after citric acid immersion 10 s (top right) and 300 s (bottom right). Early changes include initial breakdown of prism-interprism interfaces (indicated with red arrows), further increasing size of the prisms relative to their 'Before' acid erosion image, loss of superficial and deeper topographical features. (For interpretation of the references to colour in this figure legend, the reader is referred to the web version of this article.)

rougher with increasing erosion. This difference in the wear behaviour and surface characteristics between polished and natural human enamel after erosion was also observed in a study by Mullan et al. [44] who found the median (IQR) surface roughness (Sa) of natural enamel reduced significantly (p < 0.0001) (baseline Sa of 1.45(2.58) μm to 0.38(0.35) μm) after three 15-min cycles of orange juice mediated erosion, whilst the median (IQR) surface roughness (Sa) for polished enamel increased (baseline 0.04 (0.17) μm to 0.27 (0.08) μm) after the same erosion period [44]. This supports what is observed clinically in patients who suffer from erosive tooth wear, where natural enamel surfaces become progressively smoother and shinier due to loss of surface structure and texture [1].

In the polished enamel group, there was a lack of consistent outputs for 3D step height formation in surfaces with citric acid exposure below 60 s. This could indicate that below this time the integrity of the enamel remains unchanged or was not detected using our non-contacting optical profilometry methods. The barrier method of choice, PVC taping in 1:3 ratio to leave an exposed region of enamel, has been widely published previously has been shown to not influence the effect of acid-mediated erosion on enamel [22,23,27,42,44]. Additionally the calculation of 3D step height using ISO 5435-1 utilises three relatively flat regions, two in the reference regions and one in the central portion of the eroded region; and thus any influence from the use of taping to protect the reference regions such as left over adhesive at the eroded-uneroded region or slight diffusion of acid under the tape is unlikely to affect 3D step height calculation [32,40]. The progression from early erosive lesion to erosive tooth wear with measurable loss of enamel would appear to occur in the presence of prolonged citric acid attack greater than 60 s duration. In natural enamel however, 3D step height change was undetectable. This was due to a number of technical challenges faced in trying to measure the natural enamel surface: the PVC tape barriers would not adhere to the natural enamel, which meant a referenced region of exposed enamel could not be produced. In addition, utilising a non-contacting optical profilometers to measure 3D step height in natural enamel is very difficult due to the curvature and non-uniform surface topography of the natural enamel surface [33]. These compar-

isons were conducted without either natural or artificial saliva and their impact is unknown. This study's aim was to assess the sensitivity of the measuring systems, the next will be to determine the influence of salvia.

To the authors knowledge this is the first study to correlate the use of changes in surface profilometry (3D step height), surface roughness (Sa) and surface microhardness (KHN) when measuring the same co-localised eroded regions to characterise the early erosive lesion within an *in-vitro* early-erosion model. Results indicated there was a strong positive correlation between all three measurement methods, whilst the association between each variable differed. The negative curvilinear relationship between surface microhardness and 3D step height indicates as bulk loss of enamel occurs, the microhardness of the underlying enamel reduces. Additionally, there was a positive linear relationship between surface roughness – of the enamel surface at the base of the erosion trough – and 3D step height formation. Both these findings may be explained by the fact that surface microhardness and surface roughness was conducted on the acid- softened enamel left behind after bulk enamel loss occurred. This acid-softened enamel is formed as a result of the softening process that occurs during citric-acid mediated dental erosion where penetration of the acid into the enamel subsurface occurs before bulk superficial enamel is lost due to prolonged acidic attack [45,46]. The negative linear relationship between surface roughness and surface microhardness indicates that in polished enamel surfaces, surface roughness may be a surrogate marker for the enamel softening that occurs following citric acid erosion. Future studies will need to be conducted to correlate surface roughness (Sa) changes with associated calcium release analysis to determine whether surface roughness can be used as a surrogate measurement for the chemical changes occurring on the eroded enamel surface.

OCT did not produce quantifiable data for enamel subsurface/depth changes for any of the acid exposure times. However, OCT allowed surface intensity changes of the profile of eroded surfaces to be quantified and analysed. Differences in surface reflectivity between the eroded and non-eroded (reference) region of each sample, denoted by gradual decrease in percentage peak intensity, indicated that early acid erosion did result in changes in surface optical properties of enamel. This is likely due to the loss of calcium and phosphate from the enamel surface resulting in an increase in surface roughness and hence change in the optical properties of enamel producing a less reflective and more optically diffuse surface [38,47]. Aden et al. [36] used OCT to conduct quantitative analysis of mean local pixel intensities on polished bovine enamel specimens *in-vitro* with increasing acid exposure time. Their results indicated pixel intensity decreased with increased acid erosion, suggesting that surface change due to acid exposure could be detected after 1, 2, and 5 min [36]. However, longer acid exposure times were required to measure sub-surface changes using OCT in natural enamel *in-vivo*, for example, Austin et al. [38] demonstrated sub-surface changes in the superficial 33 μm of enamel after 60 min rinsing with orange juice *in-vivo*. Although saliva and salivary pellicle may affect the erosive process *in-vivo* [38], this suggests that short acid immersion periods produce alterations in the enamel surface characteristics with minimal subsurface changes whilst more

extended acid exposure times are required before subsurface changes in enamel occur. Significant additional changes to subsurface enamel may also be required before quantitative changes in 3D step height can be detected with the OCT as supported by the work of Chan et al. [37] who reported that polarisation-sensitive OCT detected subsurface enamel changes after 6 h immersion in a pH 4.5 demineralisation solution cycled over 2 days [37].

TSM images allowed qualitative assessment of the eroded zone for each erosion period, and as time increased the presence of the honeycomb-like structure of eroded enamel became more prominent and was best visualised after 300 s of citric acid exposure. This supports the work by Zheng et al. [29] who reported that after 5 min acid erosion, the formation of a honeycomb-like structure could be distinguished, which was due to the preferential dissolution of the prism inter-prism interface [29]. SEM could have also been used in our study to further corroborate surface structural changes; however, TSM allows for sample scanning without further surface modification.

The *in vitro* methods used in the current study demonstrate the formation of erosive lesions in polished enamel. Using polished enamel specimens, it was possible to detect relatively small changes in enamel surface characteristics following short acid exposures and sensitive enough to discriminate between different acid exposure times. Thus, polished enamel specimens are appropriate for studies that aim to investigate the formation of erosive lesions and studies that aim to investigate the prevention or repair of erosive lesions. Indeed, such specimens are commonly used in the evaluation of enamel remineralisation agents and formulations [16,22,23,26]. This study did not consider the impact of the acquired salivary pellicle on the formation of the early erosive lesion, as it was necessary to overcome the significant challenges in developing a working dry-field model first before additional influencing factors were introduced. The presence of saliva and/or the use of artificial saliva has been previously shown to influence the erosive patterns observed following acid mediated erosion of enamel for more extensive erosion periods, greater than 5 and 10 min, however there is a paucity of literature on the effect of the AEP on the formation and progression of the early erosive lesion; this will be the focus of future work in this area [27,48–50].

One potential limitation of this study is that the resolution of the optical profilometer used to determine 3D step height change may not have been sufficient enough to detect changes consistently/reliably below 60 s in polished enamel surfaces. Any enamel loss which may be occurring during the initial 60 s citric acid exposure may not have been detected by the current non-contacting optical profilometer, and therefore whether or not enamel bulk material loss is occurring at such early erosion times may not be entirely excluded without further analysis, such as with atomic force microscopy. Additionally, this study sought to determine the level of dental erosion which could be detected using current and previously utilised scanning parameters/techniques and did not consider how different data acquisition variables may affect the NCLP detection performance. Fleming et al. [51] explored the minimum data acquisition variables for contact profilometry on the measurement of artificial wear scars created on resin-

based composite samples, and determined the minimum x-and y- axis spacing required to ensure accurate quantification of mean total volumetric wear. Whilst their results may be extrapolated to non-contacting white profilometry, it is unknown whether this would be case for the NCLP used in this study which used a red-laser mono-chromatic based displacement sensor. Future study is therefore required to consider the effect of altering the scanning parameters on the accuracy of the measurements obtained using NCLP's that utilise this type of displacement sensor.

Using the current methods utilised, neither 3D step height nor surface microhardness data could be obtained in natural enamel surfaces. Future studies may consider using different measurement techniques to obtained quantifiable data for determining changes that occur in natural enamel surfaces after citric acid demineralisation.

5. Conclusion

Changes in surface roughness, surface microhardness and qualitative image analysis were evident for polished enamel surfaces and demonstrated that 0.3% citric acid (pH 3.2) alters the surface after only 10 s of citric acid exposure. Changes in surface roughness (Sa) and surface microhardness (KHN) were sensitive enough to allow the determination of the early erosive lesion; and their use in early enamel erosion studies is recommended. Natural enamel surfaces, however, required much longer erosion periods before any measurable change could be quantified; neither profilometric changes nor microhardness measurements were possible using the specific measurement equipment and data acquisition methods selected for this study.

Acknowledgement

REFERENCES

[1] Bartlett D. A personal perspective and update on erosive tooth wear–10 years on: part 2—restorative management. Br Dent J 2016;221:167–71, http://dx.doi.org/10.1038/sj.bdj.2016.555.

[2] Lussi A, Ganss C. Erosive tooth wear: from diagnosis to therapy. 2nd ed. Switzerland: S. Karger AG; 2014.

[3] O'Toole S, Bernabe E, Moazzez R, Bartlett D. Timing of dietary acid intake and erosive tooth wear: a case-control study. J Dent 2017;56:99–104, http://dx.doi.org/10.1016/j.jdent.2016.11.005.

[4] Voronets J, Lussi A. Thickness of softened human enamel removed by toothbrush abrasion: an in vitro study. Clin Oral Investig 2010;14:251–6, http://dx.doi.org/10.1007/s00784-009-0288-y.

[5] Lussi A, Schlueter N, Rakhmatullina E, Ganss C. Dental erosion—an overview with emphasis on chemical and histopathological aspects. Caries Res 2011;45:2–12, http://dx.doi.org/10.1159/000325915.

[6] Cheng Z-J, Wang X-M, Cui F-Z, Ge J, Yan J-X. The enamel softening and loss during early erosion studied by AFM, SEM and nanoindentation. Biomed Mater 2009;4:15020, http://dx.doi.org/10.1088/1748-6041/4/1/015020.

[7] Mathews MS, Amaechi BT, Ramalingam K, Ccahuana-Vasquez RA, Chedjieu IP, MacKey AC, et al. In situ remineralisation of eroded enamel lesions by NaF rinses. Arch Oral Biol 2012;57:525–30, http://dx.doi.org/10.1016/j.archoralbio.2011.10.010.

[8] Amaechi BT, Higham SM, Edgar WM, Milosevic A. Thickness of acquired salivary pellicle as a determinant of the sites of dental erosion. J Dent Res 1999;78:1821–8, http://dx.doi.org/10.1177/00220345990780120901.

[9] Eisenburger M, Shellis RP, Addy M. Scanning electron microscopy of softened enamel. Caries Res 2004;38:67–74, http://dx.doi.org/10.1159/000073923.

[10] Eisenburger M, Addy M, Hughes JA, Shellis RP. Effect of time on the remineralisation of enamel by synthetic saliva after citric acid erosion. Caries Res 2001;35:211–5, http://dx.doi.org/10.1159/000047458.

[11] Wiegand A, Kowing L, Attin T. Impact of brushing force on abrasion of acid-softened and sound enamel. Arch Oral Biol 2007;52:1043–7, http://dx.doi.org/10.1016/j.archoralbio.2007.06.004.

[12] Arsecularatne JA, Hoffman M. An in vitro study of the microstructure, composition and nanoindentation mechanical properties of remineralizing human dental enamel. J Phys D Appl Phys 2014;47:315–403, http://dx.doi.org/10.1088/0022-3727/47/31/315403.

[13] Lippert F, Parker DM, Jandt KD. In situ remineralisation of surface softened human enamel studied with AFM nanoindentation. Surf Sci 2004;553:105–14, http://dx.doi.org/10.1016/j.susc.2004.01.040.

[14] Voronets J, Jaeggi T, Buergin W, Lussi A. Controlled toothbrush abrasion of softened human enamel. Caries Res 2008;42:286–90, http://dx.doi.org/10.1159/000148160.

[15] Jaeggi T, Lussi A. Toothbrush abrasion of erosively altered enamel after intraoral exposure to saliva: an in situ study. Caries Res 1999;33:455–61.

[16] Attin T, Wegehaupt FJ. Methods for assessment of dental erosion. Monogr Oral Sci 2014;25:123–42, http://dx.doi.org/10.1159/000360355.

[17] Hannig C, Becker C, Yankeu-Ngalene V, Attin T. Applicability of common methods for short time erosion analysis in vitro. Oral Health Prev Dent 2008;6:239–48.

[18] Zheng J, Xiao F, Zheng L, Qian LM, Zhou ZR. Erosion behaviors of human tooth enamel at different depth. Tribol Int 2010;43:1262–7, http://dx.doi.org/10.1016/j.triboint.2009.12.008.

[19] Lippert F, Parker DM, Jandt KD. In vitro demineralization/remineralization cycles at human tooth enamel surfaces investigated by AFM and nanoindentation. J Colloid Interface Sci 2004;280:442–8, http://dx.doi.org/10.1016/j.jcis.2004.08.016.

[20] Lussi A, Jaeggi T, Gerber C, Megert B. Effect of amine/sodium fluoride rinsing on toothbrush abrasion of softened enamel in situ. Caries Res 2004;38:567–71, http://dx.doi.org/10.1159/000080588.

[21] Derceli J dos R, Faraoni JJ, Pereira-da-silva MA, Palma-Dibb RG. Analysis of the early stages and evolution of dental enamel erosion. Braz Dent J 2016;27:313–7, http://dx.doi.org/10.1590/0103-6440201600667.

[22] O'Toole S, Mistry M, Mutahar M, Moazzez R, Bartlett D. Sequence of stannous and sodium fluoride solutions to prevent enamel erosion. J Dent 2015;43:1498–503, http://dx.doi.org/10.1016/j.jdent.2015.10.003.

[23] O'Toole S, Bartlett DW, Moazzez R. Efficacy of sodium and stannous fluoride mouthrinses when used before single and multiple erosive challenges. Aust Dent J 2016;61:497–501, http://dx.doi.org/10.1111/adj.12418.

[24] Mann C, Ranjitkar S, Lekkas D, Hall C, Kaidonis JA, Townsend GC, et al. Three-dimensional profilometric assessment of early enamel erosion simulating gastric regurgitation. J Dent 2014;42:1411–21, http://dx.doi.org/10.1016/j.jdent.2014.06.011.

[25] Hjortsj C, Jonski G, Thrane PS, Saxegaard E, Young A. The effects of acidic fluoride solutions on early enamel erosion in vivo. Caries Res 2009;43:126–31, http://dx.doi.org/10.1159/000209345.

[26] Hjortsj C, Jonski G, Young A, Saxegaard E. Effect of acidic fluoride treatments on early enamel erosion lesions—a comparison of calcium and profilometric analyses. Arch Oral Biol 2010;55:229–34, http://dx.doi.org/10.1016/j.archoralbio.2010.01.003.

[27] Austin RS, Giusca CL, Macaulay G, Moazzez R, Bartlett DW. Confocal laser scanning microscopy and area-scale analysis used to quantify enamel surface textural changes from citric acid demineralization and salivary remineralization in vitro. Dent Mater 2016;32:278–84, http://dx.doi.org/10.1016/j.dental.2015.11.016.

[28] Young A, Tenuta LMA. Initial erosion models. Caries Res 2011;45:33–42, http://dx.doi.org/10.1159/000325943.

[29] Zheng J, Xiao F, Qian LM, Zhou ZR. Erosion behavior of human tooth enamel in citric acid solution. Tribol Int 2009;42:1558–64, http://dx.doi.org/10.1016/j.triboint.2008.12.008.

[30] Lin WT, Kitasako Y, Nakashima S, Tagami J. A comparative study of the susceptibility of cut and uncut enamel to erosive demineralization. Dent Mater J 2016;36:48–53, http://dx.doi.org/10.4012/dmj.2016-239.

[31] Paepegaey A, Barker ML, Bartlett DW, Mistry M, West NX, Hellin N, et al. Measuring enamel erosion: a comparative study of contact profilometry, non-contact profilometry and confocal laser scanning microscopy. Dent Mater 2013;29:1265–72, http://dx.doi.org/10.1016/j.dental.2013.09.015.

[32] Mistry M, Zhu S, Moazzez R, Donaldson N, Bartlett DW. Effect of model variables on in vitro erosion. Caries Res 2015;49:508–14, http://dx.doi.org/10.1159/000438725.

[33] Mullan F, Bartlett D, Austin R. Measurement uncertainty associated with chromatic confocal profilometry for 3D surface texture characterisation of natural human enamel. Dent Mater 2017;33(6):e273–81, http://dx.doi.org/10.1016/j.dental.2017.04.004.

[34] Olley R, Parkingson C, Wilson R, Moazzez R, Bartlett D. A novel method to quantify dentine tubule occlusion applied to in situ. Caries Res 2014;48:69–72, http://dx.doi.org/10.1159/000354654.

[35] Mullan F, Paraskar S, Bartlett DWW, Olley RCC. Effects of tooth-brushing force with a desensitising dentifrice on dentine tubule patency and surface roughness. J Dent 2017;60:50–5, http://dx.doi.org/10.1016/j.jdent.2017.02.015.

[36] Aden A, Anderson P, Burnett G, Lynch R, Tomlins P. Longitudinal correlation of 3D OCT to detect early stage erosion in bovine enamel. Biomed Opt Express 2017;8:1092–3.

[37] Chan KH, Chan AC, Darling CL, Fried D. Methods for monitoring erosion using optical coherence tomography. Proc SPIE – Int Soc Opt Eng 2013:8566, http://dx.doi.org/10.1117/12.2011013.

[38] Austin R, Taha M, Festy F, Cook R, Andiappan M, Gomez J, et al. Quantitative swept-course optical coherence tomography of early enamel erosion in vivo. Caries Res 2017;51(4):410–8, http://dx.doi.org/10.1159/000477098.

[39] ASTM E384-17, Standard Test Method for Microindentation Hardness of Materials, ASTM International, West Conshohocken, PA, 2017.

[40] ISO 5436-1:2000, Geometrical Product Specifications (GPS) – Surface Texture: Profile method; Measurement Standards - Part 1: Material Measures, International Organization for Standardization, Geneva, 2000.

[41] Abramoff M, Magalhaes P, Ram S. Image processing with imageJ. Biophotonics Int 2004;11:36–42.

[42] Mullan F, Mylonas P, Parkinson C, Bartlett D, Austin R. Precision of 655 nm Confocal Laser Profilometry for 3D surface texture characterisation of natural human enamel undergoing dietary acid mediated erosive wear. Dent Mater 2018;34:531–7.

[43] Wiegand A, Attin T. Design of erosion/abrasion studies—insights and rational concepts. Caries Res 2011;45:53–9, http://dx.doi.org/10.1159/000325946.

[44] Mullan F, Austin RS, Parkinson CR, Hasan A, Bartlett DW. Measurement of surface roughness changes of unpolished and polished enamel following erosion. PLoS One 2017;12:0–11, http://dx.doi.org/10.1371/journal.pone.01824.

[45] Attin T, Meyer K, Hellwig E, Buchalla W, Lennon AM. Effect of mineral supplements to citric acid on enamel erosion. Arch Oral Biol 2003;48:753–9, http://dx.doi.org/10.1016/S0003-9969(03)00156-0.

[46] Shellis RP, Featherstone JDB, Lussi A. Understanding the chemistry of dental erosion. Erosive tooth wear from diagnosis to ther. Monogr Oral Sci 2014;25:163–79, http://dx.doi.org/10.1159/000359943.

[47] Rakhmatullina E, Bossen A, H schele C, Wang X, Beyeler B, Meier C, et al. Application of the specular and diffuse reflection analysis for in vitro diagnostics of dental erosion: correlation with enamel softening, roughness, and calcium release. J Biomed Opt 2011;16:107–19, http://dx.doi.org/10.1117/1.3631791.

[48] Hara AT, Gonzalez-Cabezas C, Creeth J, Zero DT. The effect of human saliva substitutes in an erosion abrasion cycling model. Eur J Oral Sci 2008;116:552–6.

[49] Hannig M, Fiebiger M, G ntzer M, D bert A, Zimehl R, Nekrashevych Y. Protective effect of the in situ formed short-term salivary pellicle. Arch Oral Biol 2004;49:903–10, http://dx.doi.org/10.1016/j.archoralbio.2004.05.008.

[50] Mutahar M, Carpenter G, Bartlett D, German M, Moazzez R. The presence of acquired enamel pellicle changes acid-induced erosion from dissolution to a softening process. Sci Rep 2017;7:10920, http://dx.doi.org/10.1038/s41598-017-11498-1.

[51] Fleming GJP, Reilly E, Dowling AH, Addison O. Data acquisition variability using profilometry to produce accurate mean total volumetric wear and mean maximum wear depth measurements for the OHSU oral wear simulator. Dent Mater 2016;32:e176–84, http://dx.doi.org/10.1016/j.dental.2016.05.004.

Precision of 655 nm Confocal Laser Profilometry for 3D surface texture characterisation of natural human enamel undergoing dietary acid mediated erosive wear

F. Mullan[a], P. Mylonas[b], C. Parkinson[c], D. Bartlett[b], R.S. Austin[b,*]

[a] Restorative Dentistry, School of Dental Sciences, Newcastle University, Framlington Place, Newcastle upon Tyne NE2 4BW, United Kingdom
[b] Tissue Engineering and Biophotonics, King's College London Dental Institute, Room 36, Floor 17, Tower Wing, Guy's Hospital, London SE1 9RT, United Kingdom
[c] GSK, St Georges Avenue, Weybridge, Surrey KT13 0DE, United Kingdom

ARTICLE INFO

ABSTRACT

Objectives. To assess the precision of optical profilometry for characterising the 3D surface roughness of natural and polished human enamel in order to reliably quantify acid mediated surface roughness changes in human enamel.

Methods. Forty-two enamel samples were prepared from extracted human molars and either polished flat or left unmodified. To investigate precision, the variability of thirty repeated measurements of five areas of one polished and one natural enamel sample was assessed using 655 nm Confocal Laser Profilometry. Remaining samples were subjected to forty-five minutes orange juice erosion and microstructural changes were analysed using Sa roughness change (μm) and qualitatively using surface/subsurface confocal microscopy.

Results. Enamel surface profilometry from the selected areas revealed maximal precision of 5 nm for polished enamel and 23 nm for natural enamel. After erosion, the polished enamel revealed a 48% increase in mean (SD) Sa roughness of 0.10 (0.07) μm ($P < 0.05$), whereas in contrast the natural enamel revealed a 45% decrease in mean (SD) roughness of -0.32 (0.42) μm ($P < 0.05$). These data were supported by qualitative confocal images of the surface/subsurface enamel.

Significance. This study demonstrates a method for precise surface texture measurement of natural human enamel. Measurement precision was superior for polished flat enamel in contrast to natural enamel however, natural enamel responds very differently to polished enamel when exposed to erosion challenges. Therefore, thus future studies characterising enamel surface changes following erosion on natural enamel may provide more clinically relevant responses in comparison to polished enamel.

© 2017 The Academy of Dental Materials. Published by Elsevier Ltd. All rights reserved.

288

1.   Introduction

Human enamel has a complex hierarchal microstructure, constituting 96% mineral, 3% water and 1% organic protein [1]. The mineral content is a hydroxyapatite, sometimes referred to as a calcium deficient hydroxyapatite (HA) due to the constant dynamic flux of metal ions occurring with the oral environment [2,3]. Prior to tooth eruption, secretory ameloblasts form the fundamental microstructural unit of enamel. The enamel rod or prism, runs from the edge of the inner dentine to the outer enamel surface, having only 3–7 μm diameter whilst up to 4 mm length, with each prism interlocked by an organic protein complex [1,4]. The orientation and alignment of the prisms as they course within the enamel are so variable that it is very difficult to trace any individual prism's path through the tooth [5–7]. However, some important microstructural patterns are known, such that each prism interlocks in a honey-comb or fish-scale like pattern and travels in a sinusoidal pattern towards the surface to decussate perpendicular to the occlusal surface whereas on the axial surfaces of the tooth the prisms are angulated around 60° to the surface [8]. Ultra-structurally within the prism, the orientation of crystallites are not uniform [9,10] and further structural considerations include Retzius lines and prism cross striations which are linked to the formation of the enamel [7].

All these variations affect the biomechanical performance of the enamel as it undergoes wear whether from chemical (acid erosion) or mechanical (attrition and abrasion) challenges. In vitro erosive tooth wear models normally employ polishing of enamel to remove the outer layer to reduce structural variations, and thus facilitate measurement [11]. However, this means the outer layer, which contains areas of aprismatic and prismatic enamel which is less susceptible to erosion [12–16], has been removed and therefore the erosion model maybe less clinically relevant.

However, the measurement of enamel in its naturally curved state has perceived difficulties. Contact and optical systems map the surface either using a stylus or a light source combined with software containing specific algorithms [17]. However, for both types of system the overall shape and type of surface can affect the measurement capability. Specifically, accuracy which is the closeness in agreement to a measured value or its 'true' value, whereas, resolution is smallest detectable measurement that a device can record and finally precision is the closeness in agreement to a series of measurements, and expressed as SD. All these factors differ for flat and curved surfaces [18,19]. Hewlett et al. [20] demonstrated by measuring a sphere gauge, using a contact profilometer, that accuracy and precision decreased over sloped areas. The light source of an optical system distorts and elongates over slopes reducing accuracy and precision [21]. It has previously been identified that profilometric step height measurements of natural enamel resulted in a precision (SD) of 3.9 μm compared with 2.2 μm for polished enamel [22]. Surface roughness measurements have been advocated and increasingly used for the quantification of early erosive tooth wear, but with limited success in natural enamel samples [15,23,24]. In a study investigating the microstructure of dental hard tissues, Ranjitkar et al. noted that measuring sloped regions resulted in increased drop out from the laser [25]. These developments have significance when trying to establish appropriate lab-
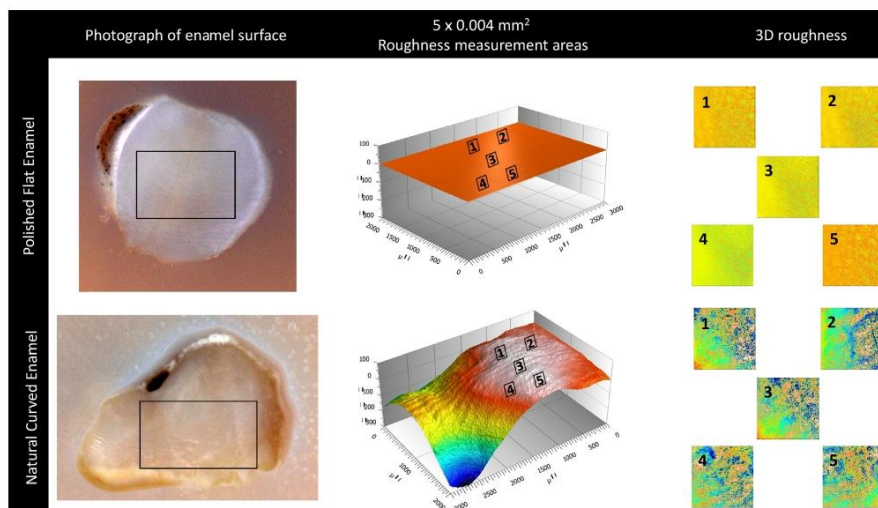

Fig. 1 – Showing photographs of representative polished and natural enamel surfaces, the five Sa roughness measurement areas and the pseudo-topography images used for 3D surface roughness measurements for both polished and natural enamel samples.

289

oratory protocols to effectively assess the effects of enamel erosion. Whilst studies suggest that natural enamel is more resistant to roughness change, to fully interpret this type of data the measurement error for both enamel substrates (natural and polished) must also be investigated, which so far has not been done.

The aims of this study were to determine the precision of surface roughness measurements of naturally curved (natural) enamel and polished flat enamel and to compare the surface effects of a dietary erosive challenge on the 3D roughness of these two types on enamel substrates.

2.   Methods

Forty-two enamel sections (5 mm × 5 mm × 3 mm) were prepared from the mid-buccal aspect of sound human molars donated under ethical agreement (REC: 12/LO/1836) and embedded in bisacryl composite material (Protemp4™ 3 M ESPE, Germany) prior to random allocation to either natural or polishing. Twenty-one enamel samples were partially embedded with their maximum buccal convexity positioned centrally leaving their outer surface accessible to ultrasonication and alcohol cleaning, thus resulting in 3 mm × 2 mm of natural exposed enamel, as shown in Fig. 1. The remaining twenty-one enamel samples were fully submerged and polished to a flatness tolerance of 0.4 μm using a series of silica carbide grits and a water cooled rotating polishing machine (Struers LaboPol-30, Struers, Copenhagen, Denmark) and ultrasonicated on completion of polishing regime following previously published protocols [11].

A 655 nm Confocal Laser Displacement sensor (LT–9010M, Keyence Corporation, Japan) and motion controlled profilometry stage (Xyris 2000, Taicaan, UK) were used throughout the study, in combination with surface metrology software (MountainsMap® v7.3, DigitalSurf, France) to measure 3D Sa surface roughness following ISO texture measurement standards [26]. The profilometer had a spot size of 2 μm and vertical resolution of 100 nm, with a 4 μm lateral scanning interval. An image analysis workflow was designed to apply a 25 μm robust Gaussian filter and extract 3D (Sa) roughness values (μm) centred around the centre of the polished enamel surface and the zenith (maximum bulbosity) of the natural enamel sample surface as shown in Fig. 1, following previously published protocols [27].

The precision of 3D surface texture measurement was determined by performing repeated scans following good practice measurement guidelines [28]. Five measurement areas (each 0.04 mm²) were selected from the centre of each sample using an image acquisition macro written within the motion control software (Stages™, TaiCaan Technologies, Southampton, UK) to ensure consecutive repeated scanning of each area 30 times, thus ensuring there were no changes to conditions. Following image acquisition, the mean (SD) Sa surface roughness (MountainsMap® v7.3, DigitalSurf, France) of the 30 scans of each area measured and the precision was expressed by calculating the variability of measurement (i.e. SD in nm) [29].

To simulate dietary wear an erosion model was designed to investigate surface roughness changes following in vitro exposure to dietary acid, based upon previously published protocols [14,27]. A 3-cycle erosion regime was investigated using a total of 40 enamel samples (20 polished and 20 natural). Enamel samples were fully immersed in 100 mL of a commercial orange juice with pH 3.2 and titratable acidity 41.3 mmol OH/L (Sainsbury's basic orange juice drink, Sainsbury's, London, UK) for 15 minutes per cycle under constant agitation at 62 rpm using an orbital shaker (Stuart Scientific, Mini Orbital Shaker S05, Bibby), thus giving a total erosion time of 45 min. A single operator located and analysed five scan areas per sample, at baseline and after erosion, in order to calculate the mean (SD) Sa surface roughness change (μm), as shown in Fig. 1.

To qualitatively characterise the enamel surface changes, representative confocal images were acquired from polished and natural samples using tandem scanning microscopy in white light reflection mode (Noran Instruments, Middleton, WI, USA) in conjunction with a ×20 objective lens (M-Plan SLWD Brightfield × 20/0.35 NA) and an automatic z-stage piezo electric controller (E-662.SR LVPZT Piezo Amplifier/Position Servo Controller, Physik Instrumente, Germany). For each sample an 85 μm Z stack at 0.5 μm intervals was acquired using proprietary image acquisition software (Micromanager v1.4.22, Open Imaging; Inc. San Francisco, CA, USA) in order to capture information from the surface and immediate subsurface (<85 μm) enamel. The resulting stack of 2D images was processed by a stack analyser programme (ImageJ,

Table 1 – Precision of 3D surface roughness measurements of 30 measurements of five scan areas from the centre of polished and natural enamel samples (SD in nm) with superscript letters indicating statistically significant differences between rows (P values below table).

		Area of enamel section				
		1 (top left)	2 (top right)	3 (central)	4 (bottom left)	5 (bottom right)
SD Sa roughness (nm)	Polished enamel	4[a]	5[b]	1[c]	1b[c]	1[a]
	Natural enamel	23[d]	23[e]	7[d,e]	13[d,e]	11[d,e]

[a] (P < 0.001).
[b] (P < 0.05).
[c] (P < 0.001).
[d] (P < 0.001).
[e] (P < 0.001).

Table 2 – Mean (SD) Sa roughness changes (μm) of polished and natural enamel before erosion (baseline) values and after 45 min immersion in an orange juice drink with * indicating statistically significant differences between rows (P < 0.05).		Before erosion	After erosion
Mean (SD) Sa roughness (μm)	Polished enamel	0.11 (0.07)	0.21 (0.08)*
	Natural enamel	0.74 (0.37)	0.41 (0.10)*

US National Institutes of Health, Bethesda, MD) to produce an optimised 533 μm × 533 μm pseudo-topography image for qualitative texture analysis.

2.1.　Statistical analysis

Precision was expressed by calculating the variability (SD) of the 30 repeated measurements (nm) for each of the 5 analysis areas. 3D roughness data were exported from the surface analysis software to spreadsheet software (Microsoft Excel 2010) and the mean Sa roughness of the five measurement areas was calculated (μm) per sample for statistical analyses. Histogram plots were used to data were normally distributed, data sets which were not normally distributed were log transformed if positively skewed. F tests were used to compare the variability (standard deviation) and P < 0.05 considered statistically significant.

For the analysis of 3D surface roughness during erosion, the mean Sa from the five measurement areas were calculated per sample prior to calculation of the group change in Sa roughness before vs. after erosion. The group roughness change data were normally distributed therefore Independent T Tests were used to compare Sa roughness changes before vs. after erosion times and P < 0.05 considered statistically significant.

3.　Results

Table 1 shows the precision of 3D enamel surface (Sa) roughness measurements. The data shows optimal precision at the central measurement area (Area 3) for both the polished enamel (1 nm) and natural enamel (7 nm) and worst precision of 5 nm for the natural enamel and 23 nm for the polished enamel. Therefore, for polished enamel there were statistical differences between the precision of measurement for the top left and bottom right measurement areas (i.e. 1 vs 5) (P < 0.001), top right and bottom left measurement areas (i.e. 2 vs 4) (P < 0.05) and the central and bottom left measurement areas (i.e. 3 vs 4) (P < 0.001). Equally for the natural enamel, there were statistical differences between the precision of measurement for the central; top right; bottom left and bottom right measurement areas (i.e. 1 vs 3, 4 and 5) (P < 0.001) and the central; top right and bottom right measurement areas (i.e. 2 vs 3, 5) (P < 0.001).

The results of the surface texture changes after the erosion are shown in Table 2. The polished enamel samples displayed a statistically significant increase of 48% in roughness after erosion resulting in a mean (SD) roughness change of 0.10 (0.07) μm after 45 min immersion in orange juice (P < 0.05). In contrast, natural enamel displayed almost the opposite trend with a statistically significant 45% decrease in roughness and thus became significantly smoother, resulting in a mean (SD) roughness change of −0.32 (0.42) μm after 45 min immersion in orange juice (P < 0.05).

Fig. 2 shows the confocal images acquired from the 85 μm of surface/subsurface enamel surfaces which revealed substantially different baseline surface features prior to erosion. The polished enamel surface before erosion was essentially featureless with no discernible micro-structural histological features evident, whereas the natural enamel surface was highly textured. The natural enamel surface displayed smaller scale surface features which took the form of a round honeycomb like lattice, superimposed on longer range features which had the appearance of undulating hills and dales, which were in turn superimposed on an irregularly curved profile of the natural enamel surface. However, the appearance of the two surfaces after erosion revealed greater similarities, with both revealing a predominance of very smaller features across the entirety of the enamel surface which was appearing to obliterate the longer range features seen in the natural enamel surface prior to erosion.

4.　Discussion

This study identified that the optical measurement system could reliably identify Sa roughness changes as small as 5 nm for polished enamel and 23 nm for natural enamel. Whilst there were differences in the precision of measurement across the five measurement areas, these differences were minimal of 4 nm for polished and 16 nm for natural enamel therefore suggesting that the level of precision is within the limits of detection required for reliable measurement of 3D surface texture changes of enamel undergoing erosion [18,20,27].

There has recently been increased interest in investigating surface changes of natural enamel surfaces which are a more clinically relevant substrate [14,15,31,32]. However, difficulties have been identified specific to optical devices, whereby measurement drop out occurs over curvatures with push the angular tolerance of the device [25]. Previously, we conducted a study comparing the Sa roughness over different locations of natural and polished enamel samples, identifying that measurements from the centre of a natural enamel sample could be considered representative of the overall sample [27]. This area could also be described as 'zenith' or apex of the curvature which is attributed to area 3 of measurement in this study. This region had the highest level of precision for natural enamel. Therefore, this would reaffirm that to increase precision of measurement and allow genuine interpretation of surfaces changes of natural enamel, measurements should be taken from this 'zenith'. Interestingly there were statistically significant differences between the five areas for both natural and polished enamel, suggestive of the involvement of some element of biological variation in the surface enamel.

The level of roughness change detected for both polished enamel and natural enamel were within the capabilities of the device. By determining the equipment was capable of
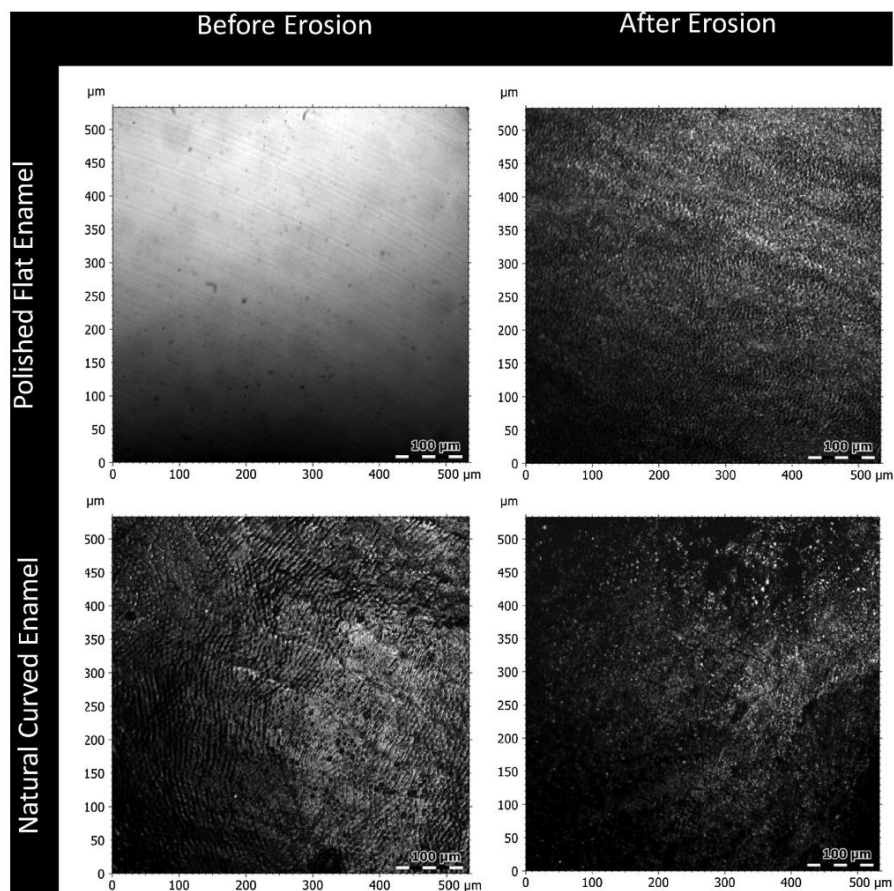
Fig. 2 – Representative images of polished and natural enamel surfaces before and after erosion dietary acid for 45 min.

truly identifying changes at this level one can be confident that this statistical inference is indeed a true negative. Baseline values for natural enamel indicate a complex textured surface, which is supported by visual evidence from the confocal images, thereby the effect of roughness change value is partly determined by the baseline values and the variation within the sample micro-structure. Natural enamel became significantly smoother after erosion whilst polished enamel became rougher, following recent trends [15,24,27,33]. These differences in behaviour between the two surfaces cannot be attributed to the differences in measurement capabilities and remain true representations. Therefore, they suggest natural enamel becoming smoother following acid exposure is a true quantification of the surface textural changes. Following erosion, the micro-histological textural features of natural enamel such as perikymata were reduced, the overall surface flattened and an increased number of enamel prisms exposed. This suggests that acid erosion of human enamel has the effect of eliminating longer wavelength features which dominate the natural enamel surface [34], however it is not yet known to what extent this may be used to prevent progression of erosion. Natural enamel has been described as being more resistant to erosion compared to polished enamel and certainly the effects of erosion are less pronounced [12,13,15,16,33]. This study supports this previous work and has identified that natural or polished enamel surfaces exhibit contrasting responses to a similar erosive challenges, thus suggesting that preserving the acid-resistant outer layer of

enamel may be essential for clinical management for erosive wear [35].

5. Conclusion

This study demonstrates a method for precise surface texture measurement of both polished and natural enamel. This opens up further possibilities for characterising the initial effects of acid erosion in natural enamel in order to develop optimal effective prevention methods prior to irreversible structural enamel loss occurs. Future studies should investigate the response of natural enamel to erosive and protective factors in order to provide a clinically representative model for greater understanding of the erosive process.

Funding

REFERENCES

[1] Cuy JL, Mann AB, Livi KJ, Teaford MF, Weihs TP. Nanoindentation mapping of the mechanical properties of human molar tooth enamel. Arch Oral Biol 2002;47:281–91, http://dx.doi.org/10.1016/S0003-9969(02)00006-7.

[2] Featherstone JDB, Lussi A. Understanding the chemistry of dental erosion. Monogr Oral Sci 2006;20:66–76, http://dx.doi.org/10.1159/000093351.

[3] West NX, Joiner A. Enamel mineral loss. J Dent 2014;42(Suppl. 1):S2–11, http://dx.doi.org/10.1016/S0300-5712(14)50002-4.

[4] Ten Cate JM, Larsen MJ, Pearce EIF, Fejerskov O. Chemical interactions between the tooth and oral fluids. In: Fejerskov O, Kidd EAM, editors. Dental caries. The disease and its clinical management. 2nd ed. Blackwell Publishing Ltd.; 2008. p. 209–31.

[5] Hirota F. Prism arrangement in human cusp enamel deduced by X-ray diffraction. Arch Oral Biol 1982;27:931–7, http://dx.doi.org/10.1016/0003-9969(82)90099-1.

[6] Raue L, Gersdorff N, Rödiger M, Klein H. New insights in prism orientation within human enamel. Arch Oral Biol 2012;57:271–6, http://dx.doi.org/10.1016/j.archoralbio.2011.08.015.

[7] Li C, Risnes S. SEM observations of Retzius lines and prism cross-striations in human dental enamel after different acid etching regimes. Arch Oral Biol 2004;49:45–52, http://dx.doi.org/10.1016/S0003-9969(03)00195-X.

[8] Whittaker DK. Structural variations in the surface zone of human tooth enamel observed by scanning electron microscopy. Arch Oral Biol 1982;27:383–92, http://dx.doi.org/10.1016/0003-9969(82)90147-9.

[9] Al-Jawad M, Steuwer A, Kilcoyne SH, Shore RC, Cywinski R, Wood DJ. 2D mapping of texture and lattice parameters of dental enamel. Biomaterials 2007;28:2908–14, http://dx.doi.org/10.1016/j.biomaterials.2007.02.019.

[10] Simmons LM, Al-Jawad M, Kilcoyne SH, Wood DJ. Distribution of enamel crystallite orientation through an entire tooth crown studied using synchrotron X-ray diffraction. Eur J Oral Sci 2011;119:19–24, http://dx.doi.org/10.1111/j.1600-0722.2011.00909.x.

[11] Mistry M, Zhu S, Moazzez R, Donaldson N, Bartlett DW. Effect of model variables on in vitro erosion. Caries Res 2015;49:508–14, http://dx.doi.org/10.1159/000438725.

[12] Meurman JH, Frank RM. Progression and surface ultrastructure of in vitro caused erosive lesions in human and bovine enamel. Caries Res 1991;25:81–7.

[13] Ganss C, Klimek J, Schwarz N. A comparative profilometric in vitro study of the susceptibility of polished and natural human enamel and dentine surfaces to erosive demineralization. Arch Oral Biol 2000;45:897–902, http://dx.doi.org/10.1016/S0003-9969(00)00041-8.

[14] Mullan F, Bartlett D, Austin RS. Measurement uncertainty associated with chromatic confocal profilometry for 3D surface texture characterization of natural human enamel. Dent Mater 2017;33:e273–81, http://dx.doi.org/10.1016/j.dental.2017.04.004.

[15] Hara AT, Livengood SV, Lippert F, Eckert GJ, Ungar PS. Dental surface texture characterization based on erosive tooth wear processes. J Dent Res 2016;95:537–42, http://dx.doi.org/10.1177/0022034516629941.

[16] Lin WT, Kitasako Y, Nakashima S, Tagami J. A comparative study of the susceptibility of cut and uncut enamel to erosive demineralization. Dent Mater J 2017;36:48–53, http://dx.doi.org/10.4012/dmj.2016-239.

[17] Field J, Waterhouse P, German M. Quantifying and qualifying surface changes on dental hard tissues in vitro. J Dent 2010;38:182–90, http://dx.doi.org/10.1016/j.jdent.2010.01.002.

[18] Durakbasa MN, Osanna PH, Demircioglu P. The factors affecting surface roughness measurements of the machined flat and spherical surface structures — the geometry and the precision of the surface. Measurement 2011;44:1986–99, http://dx.doi.org/10.1016/j.measurement.2011.08.020.

[19] Giusca CL, Leach RK. Calibration of the metrological characteristics of imaging confocal microscopes (ICMs). Measurement Good Practice Guide No. 128. 2013; National Physical Laboratory.

[20] Hewlett ER, Orro ME, Clark GT. Accuracy testing of three-dimensional digitizing systems. Dent Mater 1992;8:49–53, http://dx.doi.org/10.1016/0109-5641(92)90053-F.

[21] Jovanovski V, Lynch E. Analysis of the morphology of oral structures from 3-D co-ordinate data. Monogr Oral Sci 2000;17, http://dx.doi.org/10.1159/000061641.

[22] Schlueter N, Ganss C, De Sanctis S, Klimek J. Evaluation of a profilometrical method for monitoring erosive tooth wear. Eur J Oral Sci 2005;113:505–11, http://dx.doi.org/10.1111/j.1600-0722.2005.00253.x.

[23] Joshi M, Joshi N, Kathariya R, Angadi P, Raikar S. Techniques to evaluate dental erosion: a systematic review of literature. J Clin Diagn Res 2016;10:ZE01–7, http://dx.doi.org/10.7860/JCDR/2016/17996.8634.

[24] Arnold WH, Haddad B, Schaper K, Hagemann K, Lippold C, Danesh G. Enamel surface alterations after repeated conditioning with HCl. Head Face Med 2015;11:32, http://dx.doi.org/10.1186/s13005-015-0089-2.

[25] Ranjitkar S, Turan A, Mann A, Gully G, Marsman M, Edwards S, et al. Surface-sensitive microwear texture analysis of attrition and erosion. J Dent Res 2016:1–8.

[26] Blunt L (Liam), Jiang X. ISO 25178-2:2012(en). Geometrical product specifications (GPS) — surface texture: areal — part 2: terms, definitions and surface texture parameters. Kogan Page Science; 2012. p. 355.

[27] Mullan F, Austin RS, Parkinson CR, Hasan A, Bartlett DW. Measurement of surface roughness changes of unpolished and polished enamel following erosion. PLoS One 2017;12:e0182406, http://dx.doi.org/10.1371/journal.pone.0182406.

[28] Bell S. The Beginner's Guide to Uncertainty of Measurement. Measurement Good Practice Guide No. 11. 2001. National

Physical Laboratory – Measurement Good Practice Guide, 2012.

[29] Leach R. Fundamental principles of engineering nanometrology. Elsevier Science; 2014.

[31] Borrero-Lopez O, Pajares A, Constantino PJ, Lawn BR. Mechanics of microwear traces in tooth enamel. Acta Biomater 2015;14:146–53, http://dx.doi.org/10.1016/j.actbio.2014.11.047.

[32] Somasundaram G, Ribnick E, Sivalingam R, Eid A, Meyer T, Golnari G, et al. Detecting tooth wear using intra-oral 3d scans. WO2016003787 A1, 2015.

[33] Mullan F, Bartlett D, Austin RS. Measurement uncertainty associated with chromatic confocal profilometry for 3D surface texture characterization of natural human enamel. Dent Mater 2017;33:e273–81, http://dx.doi.org/10.1016/j.dental.2017.04.004.

[34] Nanci A, Ten Cate AR, Arnold R. Ten Cate's oral histology: development, structure, and function. Mosby; 2008.

[35] Loomans B, Opdam N, Attin T, Bartlett D, Edelhoff D, Frankenberger R, et al. Severe tooth wear: European consensus statement on management guidelines. J Adhes Dent 2017;19:111–9, http://dx.doi.org/10.3290/j.jad.a38102.

❝ DETECTING TOOTH ENAMEL EROSION WITH MOUNTAINS®

Surface metrology is a discipline embraced by more and more sectors of science than ever before. Researchers in tissue engineering & biophotonics at King's College London (UK) seeking to attain better understanding of tooth enamel erosion recently applied its methods to bring to light micro-scale surface changes over time.

Dental erosion (erosive tooth wear) is a widely recognized dental health problem. Most commonly caused by acidic foods and drinks, it involves the etching away of enamel from the tooth surface, giving the tooth a dull yellow appearance and resulting in tooth sensitivity and pain.

Petros Mylonas is part of a team of researchers at King's College London working on ways to improve understanding of dental erosion in order to find new, innovative solutions for clinicians dealing with the problem.

"The research we've been conducting utilizes two types of enamel samples: flat and unpolished." explains Petros. "Each sample was measured using a 3D profilometer then subjected to acid erosion. New measurements were performed after 5, 10 and 15 minutes."

"For the flat samples it was very simple to evaluate erosion by examining differences in step height over time as we have a flat datum either side of the eroded lesion. However, the results could not be considered clinically relevant because humans do not have artificially flat teeth! The use of unpolished natural enamel is therefore much more relevant.

That said, the problem we found was that the surface of unpolished enamel varies randomly and the topography of the erosion lesion itself also varies randomly. It seemed very difficult to define a zero height-value (or baseline) and so at first we thought we would be unable to use step height to determine erosion. Another problem was, for the measurement taken after 5 minutes, the evolution of erosion height was very small (sub-micrometer scale).

Despite these difficulties, with the help of the Mountains® support team, we were able to find a method based on surface metrology and ISO standards, to achieve accurate step height comparison

1. CORRECTING AND ALIGNING DATA USING THE SHIFT TOOL

The biggest challenge was to position the different surfaces exactly at the same level before subtracting their heights from that of the original sample.

When we first observed our data using the "4D view" feature, it became clear that there was a slight shift between the measured surfaces. Using Mountains® we were able to align the surfaces at the same XY location.

Gaussian filtration (cut-off 0.8mm) according to ISO 16610 was applied in order to obtain surface roughness and better see the differences and position of the measured samples.

Then the Shift surface operator was used to correctly align surfaces on the XY plane. At this stage, there was no visible erosion when watching the 4D view series.
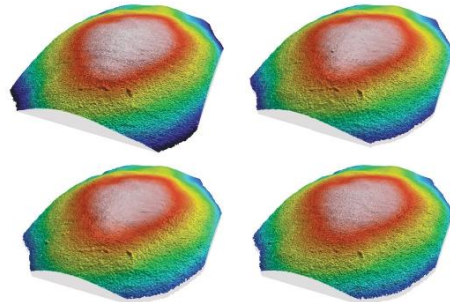
Above. *The measured surfaces were correctly aligned with the Shift surface operator and ready for further analysis.*
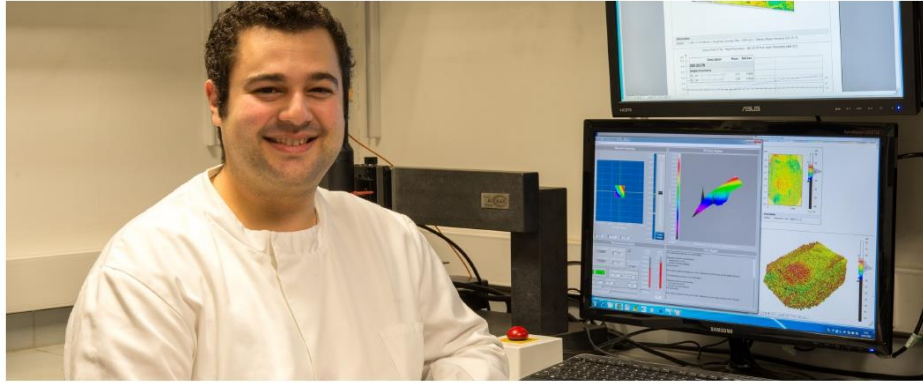
2. FROM 4D VIEW TO STEP HEIGHT HIGHLIGHTING CHANGE OVER TIME

From the shifted series, we extracted the surfaces in order to perform height subtraction from the original and thus detect erosion zones.

We applied leveling - at the same time excluding the eroded circular zone - and we were able to define the plane obtained as our Z-axis origin (or baseline).

After 5 mins

After 10 mins

After 15 mins

Above & left. Erosion zones (in blue) at 5, 10 and 15 minute intervals.
Right. Extracted height of the erosion zone at 15 minutes (with control chart).
Top. Petros Mylonas, KCL researcher.

Information		
Profile	Subtraction 15 min - before (Profile 3 / 3)	
Parameters	Step 1	Unit
Mean height	-3.9	µm

The final step was to measure the difference of height between steps. Using the Step height study in Mountains® we were able to accurately visualize and quantify sub-micrometer height differences between measurements.
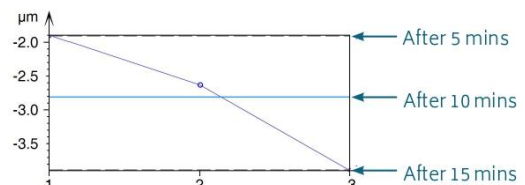
Please note: all series showing surface evolution with respect to time can be visualized in animated view in Mountains®. See examples: www.digitalsurf.com/detecting-tooth-enamel-erosion

READ MORE

▸ *In vitro evaluation of the early erosive lesion in polished and natural human enamel*. P. Mylonas, RS. Austin, R. Moazzez, A. Joiner, DW. Bartlett. In: Dental Materials, Vol. 34, No. 9, 09.2018, p. 1391-1400. https://doi.org/10.1016/j.dental.2018.06.018

References

Abramoff, M., Magalhaes, P. and Ram, S. (2004) Image processing with ImageJ. *Biophotonics International*, 11 (7): 36–42.

Aden, A., Anderson, P., Burnett, G., et al. (2017) Longitudinal correlation of 3D OCT to detect early stage erosion in bovine enamel. *Biomedical Optics Express*, 8 (2): 1092–1093.

Al-Sanabani, J., Madfa, A. and Al-Sanabani, F. (2014) Application of Calcium Phosphate Materials in Dentistry. *International Journal of Biomaterials*, 2013: 876132.

Albrektsson, T. and Johansson, C. (2001) Osteoinduction, osteoconduction and osseointegration. *European Spine Journal*, 10 (S2): S96–S101.

Alexandria, A.K., Valenca, A.M.G., Cabral, L.M., et al. (2017) Fluoride varnishes against dental erosion caused by soft drink combined with pediatric liquid medicine. *Brazilian Dental Journal*, 28 (4): 482–488.

Amaechi, B., Higham, S. and Edgar, W. (1998a) Efficacy of sterilisation methods and their effect on enamel demineralisation. *Caries research*, 32 (6): 441–446.

Amaechi, B., Higham, S. and Edgar, W. (1999) Factors influencing the development of dental erosion in vitro: enamel type, temperature and exposure time. *Journal of Oral Rehabilitation*, 26 (8): 624–630.

Amaechi, B.T. and Higham, S.M. (2001) In vitro remineralisation of eroded enamel lesions by saliva. *Journal of Dentistry*, 29 (5): 371–376.

Amaechi, B.T., Higham, S.M. and Edgar, W.M. (1998b) Use of Transverse Microradiography to Quantify Mineral Loss by Erosion in Bovine Enamel. *Caries Research*, 32 (5): 351–356.

Arsecularatne, J.A. and Hoffman, M. (2014) An in vitro study of the microstructure, composition and nanoindentation mechanical properties of remineralizing human dental enamel. *Journal of Physics D: Applied Physics*, 47 (31): 315–403.

ASTM E384 - 17 (2017) *Standard Test Method for Microindentation Hardness of Materials*. West Conshohocken, PA.

Attin, T., Becker, K., Roos, M., et al. (2009) Impact of storage conditions on profilometry of eroded dental hard tissue. *Clinical Oral Investigations*, 13 (4): 473–478.

Attin, T., Meyer, K., Hellwig, E., et al. (2003) Effect of mineral supplements to citric acid on enamel erosion. *Archives of Oral Biology*, 48 (11): 753–759.

Attin, T. and Wegehaupt, F.J. (2014) Methods for assessment of dental erosion. *Monographs in Oral Science*, 25: 123–142.

Austin, R., Stenhagen, K., Hove, L., et al. (2014) The effect of single-application fluoride treatment on simulated gastric erosion and erosion-abrasion of enamel in vitro. *International Journal of Prosthodontics*, 27 (5): 425–426.

Austin, R.S., Giusca, C.L., Macaulay, G., et al. (2016) Confocal laser scanning microscopy and area-scale analysis used to quantify enamel surface textural changes from citric acid demineralization and salivary remineralization in vitro. *Dental Materials*, 32 (2): 278–284.

Austin, R.S., Haji Taha, M., Festy, F., et al. (2017) Quantitative swept-source optical coherence tomography of early enamel erosion in vivo. *Caries Research*, 51 (4): 410–418.

Austin, R.S., Mullen, F. and Bartlett, D.W. (2015) Surface texture measurement for dental wear applications. *Surface Topography: Metrology and Properties*, 3 (2): 23002.

Austin, R.S., Stenhagen, K.S., Hove, L.H., et al. (2011) A qualitative and quantitative investigation into the effect of fluoride formulations on enamel erosion and erosion-abrasion in vitro. *Journal of Dentistry*, 39 (10): 648–655.

Azadi-Schossig, P., Becker, K. and Attin, T. (2016) Chelating effect of citric acid is negligible for development of enamel erosions. *Clinical Oral Investigations*, 20 (7): 1577–1587. doi:10.1007/s00784-015-1634-x.

Barbour, M.E., Finke, M., Parker, D.M., et al. (2006) The relationship between enamel softening and erosion caused by soft drinks at a range of temperatures. *Journal of Dentistry*, 34 (3): 207–213.

Barbour, M.E. and Rees, J.S. (2004) The laboratory assessment of enamel erosion: A review. *Journal of Dentistry*, 32 (8): 591–602. doi:10.1016/j.jdent.2004.05.001.

Bartlett, D. (2016) A personal perspective and update on erosive tooth wear – 10 years on: Part 2 – Restorative management. *British dental journal*, 221 (4): 167–171.

Bartlett, D., Evans, D., Anggiansah, A., et al. (1996) A study of the association between gastro-oesophageal reflux and palatal dental erosion. *British Dental Journal*, 181 (4): 125–131.

Bartlett, D.W., Lussi, A., West, N.X., et al. (2013) Prevalence of tooth wear on buccal and lingual surfaces and possible risk factors in young European adults. *Journal of Dentistry*, 41 (11): 1007–1013.

Batista, G.R., Torres, C.R.G., Sener, B., et al. (2016) Artificial saliva formulations versus human saliva pretreatment in dental erosion experiments. *Caries Research*, 50 (1): 78–86.

Baumann, T., Kozik, J., Lussi, A., et al. (2016) Erosion protection conferred by whole human saliva, dialysed saliva, and artificial saliva. *Scientific Reports*, 6 (September): 6–13.

Bell, S. (2001) *Good Practice Guide No. 11 Issue 2 - A Beginners Guide to Uncertainty of Measurement*., (11): 41.

Berkovitz, B.K.., Holland, G.. and Moxham, B.. (2009) *Oral anatomy, histology, and embryology*. 6th ed. Edinburgh: Mosby/Elsevier.

Boltryk, P.J., Hill, M., McBride, J.W., et al. (2008) A comparison of precision optical displacement sensors for the 3D measurement of complex surface profiles. *Sensors and Actuators, A: Physical*, 142 (1): 2–11.

Boltryk, P.J., Hill, M. and McBride, J.W. (2009) Comparing laser and polychromatic confocal optical displacement sensors for the 3D measurement of cylindrical artefacts containing microscopic grooved structures. *Wear*, 266 (5–6): 498–501.

Brevik, S.C., Lussi, A. and Rakhmatullina, E. (2013) A new optical detection method to assess the erosion inhibition by in vitro salivary pellicle layer. *Journal of Dentistry*, 41 (5): 428–435.

Bull, T.G. and McBride, J.W. (2018) In-Situ Contact Surface Characterization in a MEMS Ohmic Switch under Low Current Switching. *Technologies*, 6 (2).

Buzalaf, R.M.A., Hannas, R.A. and Kato, T.M. (2012) Saliva and dental erosion. *Journal of Applied Oral Science*, 20 (5): 493–502.

Carpenter, G., Cotroneo, E., Moazzez, R., et al. (2014) Composition of enamel pellicle from dental erosion patients. *Caries Research*, 48 (5): 361–367.

Carpenter, G.H. (2013) The Secretion, Components, and Properties of Saliva. *Annual Review of Food Science and Technology*, 4 (1): 267–276.

Carvalho, F.G. de, Carlo, H.L., Castro, R.D. de, et al. (2014) Effect of Remineralizing Agents on the Prevention of Enamel Erosion: A Systematic Review. *Pesquisa Brasileira em Odontopediatria e Clinica Integrada*, 14 (1): 55–64.

Chan, K.H., Chan, A.C., Darling, C.L., et al. (2013) Methods for monitoring erosion using optical coherence tomography. *Proceedings of SPIE - International Society of Optical Engineering*, 8566 (856606).

Cheng, Z.-J., Wang, X.-M., Cui, F.-Z., et al. (2009) The enamel softening and loss during early erosion studied by AFM, SEM and nanoindentation. *Biomedical Materials*, 4 (1): 015020.

Chew, H.P., Zakian, C.M., Pretty, I.A., et al. (2014) Measuring initial enamel erosion with quantitative light-induced fluorescence and optical coherence tomography: An in vitro validation study. *Caries Research*, 48 (3): 254–262.

Colgate-Palmolive (2010) *Product information: Colgate Duraphat varnish (50mg/ml) dental suspension*.

Cui, F. and Ge, J. (2007) New observations of the hierarchical structure of human enamel , from nanoscale to microscale. *Journal of Tissue Engineering and Regenerative Medicine*, 1 (3): 185–191. doi:10.1002/term.

Cuisinier, F. and Robinson, C. (2007) "The Structure of Teeth : Human Enamel Crystal Structure." In Epple, M. and Bauerlein, E. (eds.) *Handbook of Biomineralization*. Weinheim, Germany: Wiley-VCH Verlag GmbH. pp. 177–182.

Davis, W. and Winter, P. (1977) Dietary erosion of adult dentine and enamel: protection with fluoride toothpaste. *British Dental Journal*, 143 (4): 116–119.

Derceli, J. dos R., Faraoni, J.J., Pereira–da–silva, M.A., et al. (2016) Analysis of the early stages and evolution of dental enamel erosion. *Brazilian Dental Journal*, 27 (3): 313–317.

Dutta, A. and Saunders, W. (2014) Calcium Silicate Materials in Endodontics. *Dental Update*, 41 (October): 708–722.

Eisenburger, M. and Addy, M. (2002a) Erosion and attrition of human enamel in vitro Part I: Interaction effects. *Journal of Dentistry*, 30 (7–8): 341–347.

Eisenburger, M. and Addy, M. (2002b) Erosion and attrition of human enamel in vitro Part II: Influence of time and loading. *Journal of Dentistry*, 30 (7–8): 349–352.

Eisenburger, M. and Addy, M. (2003) Influence of liquid temperature and flow rate on enamel erosion and surface softening. *Journal of Oral Rehabilitation*, 30 (11): 1076–1080.

Eisenburger, M., Addy, M., Hughes, J.A., et al. (2001) Effect of Time on the Remineralisation of Enamel by Synthetic Saliva after Citric Acid Erosion. *Caries Research*, 35 (3): 211–215.

Eisenburger, M., Shellis, R.P. and Addy, M. (2004) Scanning electron microscopy of softened enamel. *Caries Research*, 38 (1): 67–74.

Ellingsen, J. (1986) Scanning electron microscope and electron microprobe study of reactions of stannous fluoride and stannous chloride with dental enamel. *Scandanavian Journal of Dental Research*, 94 (4): 299–305.

Esfahani, H., Salahi, E., Tayebifard, A., et al. (2016) Structural and morphological analysis of zinc incorporated non-stoichiometric hydroxyapatite nano powders. *Revista Materia*, 21 (3): 569–576.

Eversole, S.L., Saunders-Burkhardt, K. and Faller, R. V. (2014) Erosion protection comparison of stabilised SnF2 , mixed fluoride active and SMFP/arginine-containing dentifrices. *International Dental Journal*, 64 (S1): 22–28.

Exterkate, R., Damen, J. and ten Cate, J. (1993) A single-section model for enamel de- and remineralization studies. 1. The effects of different Ca/P ratios in remineralisation solutions. *Journal of Dental Research*, 72: 1599–1603.

Faller, R. V, Eversole, S.L. and Tzeghai, G. (2011) Enamel protection: a comparison of marketed dentifrice performance against dental erosion. *American Journal of Dentistry*, 24 (4): 205–210.

Fan, X., Li, X., Wan, H., et al. (2008) Clinical investigation of the anticaries efficacy of a 1.14% sodium monofluorophosphate (SMFP) calcium carbonate-based dentifrice: a two-year caries clinical trial on children in China. *Journal of Clinical Dentistry*, 19 (4): 134–137.

Farley, J., Tarbaux, N., Lau, K., et al. (1987) Monofluorophosphate is hydrolysed by alkaline phosphatase and mimics the actions of NaF on skeletal tissues in vitro. *Calcified Tissue International*, 40 (1): 35–42.

Featherstone, J.D.B. (1992) Consensus conference on intra-oral models: evaluation techniques. *Journal of Dental Research*, 71: 955–956.

Featherstone, J.D.B. (2008) Dental Caries: a dynamic disease process. *Australian Dental Journal*, 53 (3): 286–291.

Featherstone, J.D.B. and Lussi, A. (2006) Understanding the Chemistry of Dental Erosion. *Monographs in Oral Science*, 20: 66–76.

Field, J., German, M. and Waterhouse, P. (2013) Using bearing area parameters to quantify early erosive tooth surface changes in enamel: A pilot study. *Journal of Dentistry*, 41 (11): 1060–1067.

Field, J., Waterhouse, P. and German, M. (2010) Quantifying and qualifying surface changes on dental hard tissues In-vitro. *Journal of Dentistry2*, 38 (3): 182–190.

Field, J.C., German, M.J. and Waterhouse, P.J. (2014) Qualifying the lapped enamel surface: A profilometric, electron microscopic and microhardness study using human, bovine and ovine enamel. *Archives of Oral Biology*, 59 (5): 455–460.

Field, J.C., Waterhouse, P.J. and German, M.J. (2017) The Early Erosive and Abrasive Challenge: A Profilometric, Electron Microscopic and Microhardness Study Using Human, Bovine and Ovine Enamel. *The European Journal of Prosthodontics and Restorative Dentistry*, 25 (2): 93–100.

Finke, M., Hugues, J.A., Parker, D.M., et al. (2001) Mechanical properties of in situ determineralised human enamel measured by AFM nanoindentation. *Surface Science*, 491: 456–467.

Finke, M., Jandt, K. and Parker, D. (2000) The Early Stages of Native Enamel Dissolution Studied with Atomic Force Microscopy. *Journal of colloid and interface science*, 232: 156–164.

Fujii, M., Kitasako, Y., Sadr, A., et al. (2011) Roughness and pH changes of enamel surface induced by soft drinks in vitro - applications of stylus profilometry , focus variation 3D scanning microscopy and micro pH sensor. *Dental Materials Journal*, 30 (3): 404–410.

Ganss, C., Klimek, J., Brune, V., et al. (2004) Effects of Two Fluoridation Measures on Erosion Progression in Human Enamel and Dentine in situ. *Caries Research*, 49 (6): 561–566.

Ganss, C., Klimek, J. and Schwarz, N. (2000) A comparative profilometric in vitro study of the susceptibility of polished and natural human enamel and dentine surfaces to erosive demineralization. *Archives of Oral Biology*, 45 (10): 897–902.

Ganss, C., Lussi, A., Grunau, O., et al. (2011) Conventional and anti-erosion fluoride toothpastes: Effect on enamel erosion and erosion-abrasion. *Caries Research*, 45 (6): 581–589.

Ganss, C., Lussi, A. and Klimek, J. (2005) Comparison of calcium/phosphorus analysis, longitudinal microradiography and profilometry for the quantitative assessment of erosive demineralisation. *Caries Research*, 39 (3): 178–184.

Ganss, C., Lussi, A. and Schlueter, N. (2012) The histological features and physical properties of eroded dental hard tissues. *Erosive Tooth Wear: From Diagnosis to Therapy*, 25: 99–107.

Gelhard, T.B.F.M., Fidler, V., 's-Gravenmade, E.J., et al. (1983) Remineralization of softened human enamel in mucin- or CMC-containing artificial salivas. *Journal of Oral Pathology & Medicine*, 12 (5): 336–341.

Gracia, L.H., Rees, G.D., Brown, A., et al. (2010) An in vitro evaluation of a novel high fluoride daily mouthrinse using a combination of microindentation, 3D profilometry and DSIMS. *Journal of Dentistry*, 38 (SUPPL. 3): S12–S20.

Gregory-Head, B., Curtis, D., Kim, L., et al. (2000) Evaluation of dental erosion in patients with gastroesophageal reflux disease. *Journal of Prosthetic Dentistry*, 83 (6): 675–680.

Gyurkovics, M., Baumann, T., Carvalho, T.S., et al. (2017) In vitro evaluation of modified surface microhardness measurement, focus variation 3D microscopy and contact stylus profilometry to assess enamel surface loss after erosive–abrasive challenges. *PLoS ONE*, 12 (4): 1–13.

Hannig, C., Becker, C., Yankeu-Ngalene, V., et al. (2008) Applicability of Common Methods for Short Time Erosion Analysis in Vitro. *Oral Health & Preventive Dentistry*, 6 (3): 239–248.

Hannig, C., Hamkens, A., Becker, K., et al. (2005) Erosive effects of different acids on bovine enamel: Release of calcium and phosphate in vitro. *Archives of Oral Biology*, 50 (6): 541–552.

Hannig, M., Fiebiger, M., Güntzer, M., et al. (2004a) Protective effect of the in situ formed short-term salivary pellicle. *Archives of Oral Biology*, 49 (11): 903–910.

Hannig, M., Fiebiger, M., Güntzer, M., et al. (2004b) Protective effect of the in situ formed short-term salivary pellicle. *Archives of Oral Biology*, 49 (11): 903–910.

Hannig, M. and Joiner, A. (2006) The structure, function and properties of the acquired pellicle. *Monographs in Oral Science*, 19: 29–64.

Hannig, M. s. and Hannig, C. (2012) The Pellicle and Erosion. *Erosive Tooth Wear: From Diagnosis to Therapy*, 25: 206–214.

Hara, A.T., González-Cabezas, C., Creeth, J., et al. (2008a) The effect of human saliva substitutes in an erosion-abrasion cycling model. *European Journal of Oral Sciences*, 116 (6): 552–556.

Hara, A.T., Good, J. a, Gonzalez-Cabezas, C., et al. (2008b) The effect of human saliva substitutes in an erosion abrasion cycling model. *European Journal of Oral Sciences*, 116 (6): 552–556.

Hara, A.T., Livengood, S.V., Lippert, F., et al. (2016) Dental Surface Texture Characterization Based on Erosive Tooth Wear Processes. *Journal of Dental Research*, 95 (5): 537–542.

Häßler-Grohne, W., Hüser, D., Johnsen, K.P., et al. (2011) Current limitations of SEM and AFM metrology for the characterization of 3D nanostructures. *Measurement Science and Technology*, 22 (9). doi:10.1088/0957-0233/22/9/094003.

He, L.H. and Swain, M. V. (2007) Influence of environment on the mechanical behaviour of mature human enamel. *Biomaterials*, 28 (30): 4512–4520. doi:10.1016/j.biomaterials.2007.06.020.

Heurich, E., Beyer, M., Jandt, K., et al. (2010) Quantification of dental erosion - A comparison of stylus profilometry and confocal laser scanning microscopy (CSLM). *Dental Materials*, 26 (4): 326–336.

Hjortsjö, C., Jonski, G., Thrane, P.S., et al. (2009) The effects of acidic fluoride solutions on early enamel erosion in vivo. *Caries Research*, 43 (2): 126–131. doi:10.1159/000209345.

Hjortsjö, C., Jonski, G., Young, A., et al. (2010) Effect of acidic fluoride treatments on early enamel erosion lesions-A comparison of calcium and profilometric analyses. *Archives of Oral Biology*, 55 (3): 229–234. doi:10.1016/j.archoralbio.2010.01.003.

Holme, B., Hove, L.H. and Tveit, A.B. (2005) Using white light interferometry to measure etching of dental enamel. *Measurement: Journal of the International Measurement Confederation*, 38 (2): 137–147. doi:10.1016/j.measurement.2005.04.003.

Hornby, K., Evans, M., Long, M., et al. (2009) Enamel benefits of a new hydroxyapatite containing fluoride toothpaste. *International Dental Journal*, 59 (6): 325–331. doi:10.1922/IDJ_2492Joiner07.

Hornby, K., Ricketts, S.R., Philpotts, C.J., et al. (2014) Enhanced enamel benefits from a novel toothpaste and dual phase gel containing calcium silicate and sodium phosphate salts. *Journal of Dentistry*, 42: s39–s45. doi:10.1016/S0300-5712(14)50006-1.

Hove, L., Holme, B., Øgaard, B., et al. (2006) "The protective effect of TiF4, SnF2 and NaF on erosion of enamel by hydrochloric acid in vitro measured by white light interferometry." In *Caries Research*. 2006. pp. 440–443. doi:10.1159/000094291.

Hughes, J., West, N., Parker, D., et al. (2000) Effects of pH and concentration of citric, malic and lactic acids on enamel, in vitro. *Journal of dentistry*, 28 (2): 147–152. doi:10.1016/S0300-5712(99)00060-3.

Humphrey, S.P. and Williamson, R.T. (2001) Normal composition, flow, and function of saliva. *Journal of Prosthetic Dentistry*, 85 (2): 162–169. doi:10.1067/mpr.2001.113778.

Huysmans, M.C., Chew, H.P. and Ellwood, R.P. (2011a) Clinical studies of dental erosion and erosive wear. *Caries Res*, 45 (S1): 60–68. doi:10.1159/000325947.

Huysmans, M.C.D.N.J.M., Chew, H.P. and Ellwood, R.P. (2011b) Clinical Studies of Dental Erosion and Erosive Wear. *Caries Research*, 45 (s1): 60–68. doi:10.1159/000325947.

Ionta, F.Q., Mendonça, F.L., De Oliveira, G.C., et al. (2014) In vitro assessment of artificial saliva formulations on initial enamel erosion remineralization. *Journal of Dentistry*, 42 (2): 175–179. doi:10.1016/j.jdent.2013.11.009.

ISA (2006) *Recommended Environments for Standards Laboratories. ISA-TR52.00.01-2006*. North Carolina, USA.

ISO (2000a) *4287: 2000 - Geometrical product specification–surface texture: profile method–terms, definitions and surface texture parameters*.

ISO (2000b) *ISO 25178-2:2012. Geometrical Product Specifications - Surface texture: Areal - Part 2: Terms, definitions, and surface texture parameters*.

ISO (2000c) *ISO 5436-1. Geometrical Product Specifications (GPS) – Surface texture: Profile method; Measurement standards – Part 1: Material Measures*.

Ivoclar (2010) *Product information: Fluor Protector*. Available at: http://downloads.ivoclarvivadent.com/zoolu-website/media/document/11648/Professional+Care.

Ivoclar (2011) *Product information: Fluor Protector S*. Available at: http://www.ivoclarvivadent.co.uk/zoolu-website/media/document/16351/Fluor+Protector+S.

Joiner, A., Schäfer, F., Naeeni, M.M., et al. (2014) Remineralisation effect of a dual-phase calcium silicate/phosphate gel combined with calcium silicate/phosphate toothpaste on acid-challenged enamel in situ. *Journal of Dentistry*, 42: S53–S59. doi:10.1016/S0300-5712(14)50008-5.

Jordão, M.C., Ionta, F.Q., Bergantin, B.T.., et al. (2017) The Effect of Mucin in Artificial Saliva on Erosive Rehardening and Demineralization. *Caries Research*, 51 (2): 136–140. doi:10.1159/000454817.

Joshi, M., Joshi, N., Kathariya, R., et al. (2016) Techniques to Evaluate Dental Erosion: A Systematic Review of Literature. *Journal of Clinical and Diagnostic Research*, 10 (10): 1–7. doi:10.7860/JCDR/2016/17996.8634.

Kaidonis, J.A., Anastassiadis, P.M., Lekkas, D., et al. (2018) Prevention and control of dental erosion by professionally applied treatment. *Clinical Dentistry Reviewed*, 2 (1): 5. doi:10.1007/s41894-017-0018-9.

Kensche, A., Pötschke, S., Hannig, C., et al. (2016) Influence of calcium phosphate and apatite containing products on enamel erosion. *Scientific World Journal*, 2016. doi:10.1155/2016/7959273.

Khambe, D., Eversole, S.L., Mills, T., et al. (2014) Protective effects of SnF 2 – Part II . Deposition and retention on pellicle-coated enamel. *International Dental Journal*, 64 (S1): 11–15. doi:10.1111/idj.12097.

Klimek, J., Hellwig, E. and Ahrens, G. (1982) Fluoride taken up by plaque, by the underlying enamel and by clean enamel from three fluoride compounds in vitro. *Caries Research*, 16 (2): 156–161. doi:10.1159/000260592.

Kumar, S., Keeling, A., Bartlett, D., et al. (2018) The Sensitivity of Digital Intraoral Scanners at Measuring Early Erosive Wear. *Journal of Dentistry*, xx (xx): xx.

Kunin, A.A., Evdokimova, A.Y. and Moiseeva, N.S. (2015) Age-related differences of tooth enamel morphochemistry in health and dental caries. *EPMA Journal*, 6 (1): 1–11. doi:10.1186/s13167-014-0025-8.

Laurence-Young, A., Bozec, L., Garcia, L., et al. (2011) A review of the structure of human and bovine dental hard tissues and their physicochemical behaviour in relation to erosive challenge and remineralisation. *Journal of Dentistry*, 39 (4): 266–272. doi:10.1016/j.jdent.2011.01.008.

Leach, R. (2009) *Fundamental Principles of Engineering Nanometrology*. Oxford, UK: Elsevier Inc.

Leach, R. (2013) *Characterisation of Areal Surface Texture*. Berlin: Springer. (NULL).

LeGeros, R. (1991) "Biologically Relevant Calcium Phosphates: Preparation and Characterization." In *Monographs in Oral Science*. New York, United States: Karger. pp. 4–45. doi:10.1159/000419233.

Li, X., Wang, J., Joiner, A., et al. (2014) The remineralisation of enamel: A review of the literature. *Journal of Dentistry*, 42: S12–S20. doi:10.1016/S0300-5712(14)50003-6.

Lin, W.T., Kitasako, Y., Nakashima, S., et al. (2016) A comparative study of the susceptibility of cut and uncut enamel to erosive demineralization. *Dental Materials Journal*, 36 (1): 48–53. doi:10.4012/dmj.2016-239.

Lindh, L., Aroonsang, W., Sotres, J., et al. (2014) Salivary pellicles. *Saliva: Secretion and Functions*, 24: 30–39. doi:10.1159/000358782.

Lippert, F., Parker, D.M. and Jandt, K.D. (2004a) In situ remineralisation of surface softened human enamel studied with AFM nanoindentation. *Surface Science*, 553 (1–3): 105–114. doi:10.1016/j.susc.2004.01.040.

Lippert, F., Parker, D.M. and Jandt, K.D. (2004b) In vitro demineralization/remineralization cycles at human tooth enamel surfaces investigated by AFM and nanoindentation. *Journal of Colloid and Interface Science*, 280 (2): 442–448. doi:10.1016/j.jcis.2004.08.016.

Lussi, A. and Carvalho, T.S. (2015) "The future of fluorides and other protective agents in erosion prevention." In *Caries Research*. 2015. pp. 18–29. doi:10.1159/000380886.

Lussi, A. and Ganss, C. (2014) *Erosive Tooth Wear: From Diagnosis to Therapy*. 2nd ed. Switzerland: S. Karger AG.

Lussi, A., Megert, B., Eggenberger, D., et al. (2008) Impact of different toothpastes on the prevention of erosion. *Caries Research*, 42 (1): 62–67. doi:10.1159/000112517.

Lussi, A., Schlueter, N., Rakhmatullina, E., et al. (2011) Dental erosion - An overview

with emphasis on chemical and histopathological aspects. *Caries Research*, 45 (SUPPL. 1): 2–12. doi:10.1159/000325915.

Magalhães, A.C., Rios, D., Delbem, A.C.B., et al. (2006) Influence of fluoride dentifrice on brushing abrasion of eroded human enamel: An in situ/ex vivo study. *Caries Research*, 41 (1): 77–79. doi:10.1159/000096110.

Magalhaes, A.C., Wiegand, A., Rios, D., et al. (2009) Insights into preventive measures for dental erosion. *Journal of Applied Oral Science*, 17 (2): 75–86. doi:10.1590/S1678-77572009000200002.

Magalhães, A.C., Wiegand, A., Rios, D., et al. (2011) Fluoride in dental erosion. *Fluoride and the Oral Environment*, 22: 158–170. doi:10.1159/000325167.

Maggio, B., Guibert, R.G., Mason, S.C., et al. (2010) Evaluation of mouthrinse and dentifrice regimens in an in situ erosion remineralisation model. *Journal of Dentistry*, 38 (SUPPL. 3): S37–S44. doi:10.1016/S0300-5712(11)70007-0.

Maia, A.M.A., de Freitas, A.Z., de L. Campello, S., et al. (2016) Evaluation of dental enamel caries assessment using Quantitative Light Induced Fluorescence and Optical Coherence Tomography. *Journal of Biophotonics*, 9 (6): 596–602. doi:10.1002/jbio.201500111.

Mann, C., Ranjitkar, S., Lekkas, D., et al. (2014) Three-dimensional profilometric assessment of early enamel erosion simulating gastric regurgitation. *Journal of Dentistry*, 42 (11): 1411–1421. doi:10.1016/j.jdent.2014.06.011.

Marsh, P. and Martin, M. (2009) *Oral Microbiology*. 5th ed. London, England: Churchill Livingstone, Elsevier.

Mathews, M.S., Amaechi, B.T., Ramalingam, K., et al. (2012) In situ remineralisation of eroded enamel lesions by NaF rinses. *Archives of Oral Biology*, 57 (5): 525–530. doi:10.1016/j.archoralbio.2011.10.010.

McBride, J., Zhao, Z. and Boltryk, P. (2009) A comparison of optical sensing methods for the high precision 3D surface profile measurement of grooved surfaces. *Proceedings ASPE 2008*, (February). Available at: http://eprints.soton.ac.uk/65580/1/SiG_Free_Form_2009.pdf.

McBride, J.W. (2009) *The 3D Measurement and Analysis of Aspheric Surfaces*., (January).

McBride, J.W., Hill, M., Loh, J., et al. (2001) "Sensitivity of a 3D surface mapping system to environmental perturbations." In Preggs, G.N. (ed.) *Laser Metrology & Machine Performance V: proceedings from the 5th International Conference on Laser Metrology and Machine Performance*. 5th ed. Southampton, UK: WIT Press. pp. 187–195.

McBride, J.W., Hill, M. and Zhang, D. (2004) A feature extraction method for the assessment of the form parameters of surfaces with localised erosion. *Wear*, 256 (3–4): 243–251. doi:10.1016/S0043-1648(03)00411-3.

McBride, J.W. and Maul, C. (2004) The 3D measurement and analysis of high

precision surfaces using confocal optical methods.pdf. *IEICE Transactions on Electronics*, E87 (C(8)): 1261–1267.

van der Mei, H., Engels, E., de Vries, J., et al. (2007) Chitosan absorption on salivary pellicles. *European Journal of Oral Sciences*, 115: 303–307.

De Mello Vieira, A.E., Botazzo Delbem, A.C., Sassaki, K.T., et al. (2005) Fluoride dose response in pH-cycling models using bovine enamel. *Caries Research*, 39 (6): 514–520. doi:10.1159/000088189.

Meurman, J.H. and Frank, R.M. (1991) Progression and Surface Ultrastructure of in vitro Caused Erosive Lesions in Human and Bovine Enamel. *Caries research*, 25 (2): 81–87.

Mistry, M., Zhu, S., Moazzez, R., et al. (2015) Effect of model variables on in vitro erosion. *Caries Research*, 49 (5): 508–514. doi:10.1159/000438725.

Mita, H., Kitasako, Y., Takagaki, T., et al. (2013) Development and evaluation of a low-erosive apple juice drink with Phosphoryl- Oligosaccharides of Calcium. *Dental Materials Journal*, 32 (2): 212–218. doi:10.4012/dmj.2012-256.

Moazzez, R., Bartlett, D.W. and Anggiansah, A. (2004) Dental erosion, gastro-oesophageal reflux disease and saliva: how are they related? *Journal of Dentistry*, 32 (6): 489–494. doi:10.1016/j.jdent.2004.03.004.

Mullan, F., Austin, R.S., Parkinson, C.R., et al. (2017a) Measurement of surface roughness changes of unpolished and polished enamel following erosion. *PLoS ONE*, 12 (8): 0–11. doi:10.1371/journal.pone.01824.

Mullan, F., Austin, R.S., Parkinson, C.R., et al. (2018a) An in-situ pilot study to investigate the native clinical resistance of enamel to erosion. *Journal of Dentistry*, 70 (October 2017): 124–128. doi:10.1016/j.jdent.2018.01.005.

Mullan, F., Bartlett, D. and Austin, R. (2017b) Measurement uncertainty associated with chromatic confocal profilometry for 3D surface texture characterisation of natural human enamel. *Dental Materials*.

Mullan, F., Mylonas, P., Parkinson, C., et al. (2018b) Precision of 655nm Confocal Laser Profilometry for 3D surface texture characterisation of natural human enamel undergoing dietary acid mediated erosive wear. *Dental Materials*, 34: 531–537.

Mutahar, M., Carpenter, G., Bartlett, D., et al. (2017) The presence of acquired enamel pellicle changes acid-induced erosion from dissolution to a softening process. *Scientific Reports*, 7 (1): 10920. doi:10.1038/s41598-017-11498-1.

Nekrashevych, Y., Hannig, M. and Stosser, L. (2004) Assessment of Enamel and Protective Effect of Salivary Pellicle by Surface Roughness Analysis and Scanning Electron Microscopy. *Oral Health and Preventative Dentistry*, 2 (1): 5–11.

Nekrashevych, Y. and Stosser, L. (2003) Protective Influence of Experimentally Formed Salivary Pellicle on Enamel An in vitro Study. *Caries Research*, 37: 225–231. doi:10.1159/000070449.

Nekrashevych, Y. and Stösser, L. (2003) Protective influence of experimentally formed salivary pellicle on enamel erosion: An in vitro study. *Caries Research*, 37 (3): 225–231. doi:10.1159/000070449.

Nery, E., Lynch, K., Hirthe, W., et al. (1975) Bioceramic implants in surgically produced infrabony defects. *Journal of Periodontology*, 46 (6): 328–347.

Nieuw Amerongen, A. V., Oderkerk, C.H. and Driessen, A.A. (1987) Role of mucins from human whole saliva in the protection of tooth enamel against demineralization in vitro. *Caries Research*, 21 (4): 297–309. doi:10.1159/000261033.

O'Toole, S., Bartlett, D.W. and Moazzez, R. (2016) Efficacy of sodium and stannous fluoride mouthrinses when used before single and multiple erosive challenges. *Australian Dental Journal*, 61 (4): 497–501. doi:10.1111/adj.12418.

O'Toole, S., Mistry, M., Mutahar, M., et al. (2015) Sequence of stannous and sodium fluoride solutions to prevent enamel erosion. *Journal of Dentistry*, 43 (12): 1498–1503. doi:10.1016/j.jdent.2015.10.003.

O'Toole, S., Osnes, C., Bartlett, D., et al. (2019) Investigation into the accuracy and measurement methods of sequential 3D dental scan alignment. *Dental Materials*, xx (xx): xx.

Paepegaey, A., Barker, M.L., Bartlett, D.W., et al. (2013a) Measuring enamel erosion : A comparative study of contact profilometry , non-contact profilometry and confocal laser scanning microscopy. *Dental Materials*, 29 (12): 1265–1272. doi:10.1016/j.dental.2013.09.015.

Paepegaey, A.M., Harris, R., Barker, M.L., et al. (2013b) In vitro comparison of stannous fluoride, sodium fluoride, and sodium monofluorophosphate dentifrices in the prevention of enamel erosion. *Journal of Clinical Dentistry*, 24 (3): 73–78.

Parker, A.S., Patel, A.N., Al Botros, R., et al. (2014) Measurement of the efficacy of calcium silicate for the protection and repair of dental enamel. *Journal of Dentistry*, 42: S21–S29. doi:10.1016/S0300-5712(14)50004-8.

Petzold, M. (2001) The Influence of Different Fluoride Compounds and Treatment Conditions on Dental Enamel: A Descriptive in vitro Study of the CaF2Precipitation and Microstructure. *Caries Research*, 35 (1 SUPPL. 1): 45–51. doi:10.1159/000049110.

Poggio, C., Ceci, M., Beltrami, R., et al. (2014) Atomic force microscopy study of enamel remineralization. *Annali di stomatologia*, 5 (3): 98–102. Available at: http://www.pubmedcentral.nih.gov/articlerender.fcgi?artid=4252861&tool=pmcentrez&rendertype=abstract.

Poggio, C., Lombardini, M., Colombo, M., et al. (2010) Impact of two toothpastes on repairing enamel erosion produced by a soft drink: An AFM in vitro study. *Journal of Dentistry*, 38 (11): 868–874. doi:10.1016/j.jdent.2010.07.010.

Poon, C.Y. and Bhushan, B. (1995) Comparison of surface roughness measurements by stylus profiler. *Wear*, 190 (1): 76–88.

Pretty, I.A., Edgar, W.M. and Higham, S.M. (2004) The validation of quantitative light-induced fluorescence to quantify acid erosion of human enamel. *Archives of Oral Biology*, 49 (4): 285–294. doi:10.1016/j.archoralbio.2003.11.008.

Public Health England (2014) *Delivering Better Oral Health: an evidence-based toolkit for prevention*. Available at: https://www.gov.uk/government/publications/delivering-better-oral-health-an-evidence-based-toolkit-for-prevention.

Qasthari, A.I., Irawan, B. and Herda, E. (2018) The influence of brushing with theobromine and sodium monofluorophosphate toothpaste on enamel surface resistance to roughness after demineralization The influence of brushing with theobromine and sodium monofluorophosphate toothpaste on enamel surface re. *IOP Conf. Series: Journal of Physics*, 4567. doi:doi :10.1088/1742-6596/1073/3/032005.

Rakhmatullina, E., Bossen, A., Höschele, C., et al. (2011) Application of the specular and diffuse reflection analysis for in vitro diagnostics of dental erosion: correlation with enamel softening, roughness, and calcium release. *Journal of Biomedical Optics*, 16 (10): 107–119. doi:10.1117/1.3631791.

Ranjitkar, S., Turan, A., Mann, C., et al. (2017) Surface-Sensitive Microwear Texture Analysis of Attrition and Erosion. *Journal of Dental Research*, 96 (3): 300–307. doi:10.1177/0022034516680585.

Ren, Y., Zhao, Q., Malmstrom, H., et al. (2009) Assessing fluoride treatment and resistance of dental enamel to soft drink erosion in vitro: applications of focus variation 3D scanning microscopy and stylus profilometry. *Journal of Dentistry*, 37 (3): 167–176.

Ren, Y.F., Liu, X., Fadel, N., et al. (2011) Preventive effects of dentifrice containing 5000 ppm fluoride against dental erosion in situ. *Journal of Dentistry*, 39 (10): 672–678. doi:10.1016/j.jdent.2011.07.009.

Reynolds, E.C. (2009) Casein Phosphopeptide-Amorphous Calcium Phosphate: The Scientific Evidence. *Advances in Dental Research*, 21 (1): 25–29. doi:10.1177/0895937409335619.

Rodriguez, J.M., Austin, R.S. and Bartlett, D.W. (2012a) A method to evaluate profilometric tooth wear measurements. *Dental Materials*, 28 (3): 245–251. doi:10.1016/j.dental.2011.10.002.

Rodriguez, J.M., Austin, R.S. and Bartlett, D.W. (2012b) In vivo measurements of tooth wear over 12 months. *Caries Research*, 46 (1): 9–15. doi:10.1159/000334786.

Rodriguez, J.M. and Bartlett, D.W. (2010) A comparison of two-dimensional and three-dimensional measurements of wear in a laboratory investigation. *Dental Materials*, 26 (10): e221–e225. doi:10.1016/j.dental.2010.07.001.

Ruben, J.L., Roeters, F.J.M., Truin, G.J., et al. (2019) Cup-Shaped Tooth Wear Defects: More than Erosive Challenges? *Caries Research*. doi:10.1159/000496983.

Sanches, R., Otani, C., Damiao, A., et al. (2009) AFM characterization of bovine

enamel and dentine after acid-etching. *Micron*, 40 (4): 502–506.

Sanmartin de Almeida, M., Fernandes, G.V. de O., de Oliveira, A.M., et al. (2018) Calcium silicate as a graft material for bone fractures: a systematic review. *Journal of International Medical Research*, 46 (7): 2537–2548. doi:10.1177/0300060518770940.

Sar Sancakli, H., Austin, R., Al-Saqabi, F., et al. (2015) The influence of varnish and high fluoride on erosion and abrasion in a laboratory investigation. *Australian Dental Journal*, 60 (1): 38–42. doi:10.1111/adj.12271.

Schlueter, N., Hara, A., Shellis, R.P., et al. (2011) Methods for the measurement and characterization of erosion in enamel and dentine. *Caries Research*, 45 (SUPPL. 1): 13–23. doi:10.1159/000326819.

Schlueter, N., Klimek, J. and Ganss, C. (2009) Effect of stannous and fluoride concentration in a mouth rinse on erosive tissue loss in enamel in vitro. *Archives of Oral Biology*, 54 (5): 432–436. doi:10.1016/j.archoralbio.2009.01.019.

Schneider, C., Rasband, W. and Eliceiri, K. (2012) NIH Image to ImageJ: 25 years of image analysis. *Nature Methods*, 9 (7): 671–675.

Scott, R.M. and Halcrow, S.E. (2017) Investigating weaning using dental microwear analysis: A review. *Journal of Archaeological Science: Reports*, 11: 1–11. doi:10.1016/j.jasrep.2016.11.026.

Sewon, L. and Makela, M. (1990) A study of the possible correlation of high salivary calcium levels with periodontal and dental conditions in young adults. *Archives of Oral Biology*, 35: 211–212.

Shah, V.P., Midha, K.K., Findlay, J.W.A., et al. (2000) Bioanalytical method validation- a revisit with a decade of progress. *Pharmaceutical research*, 17 (12): 1551–1557. doi:10.1023/A:1007669411738.

Shellis, R.., Featherstone, J.D.B. and Lussi, A. (2014) Understanding the Chemistry of Dental Erosion. *Erosive Tooth Wear: From Diagnosis to Therapy*, 25: 163–179. doi:10.1159/000359943.

Shellis, R.P. and Addy, M. (2012) The Interactions between Attrition, Abrasion and Erosion in Tooth Wear. *Erosive Tooth Wear: From Diagnosis to Therapy*, 25: 32–45. doi:10.1159/000359936.

Shellis, R.P., Barbour, M.E., Jesani, A., et al. (2013) Effects of buffering properties and undissociated acid concentration on dissolution of dental enamel in relation to ph and acid type. *Caries Research*, 47 (6): 601–611. doi:10.1159/000351641.

Shellis, R.P., Finke, M., Eisenburger, M., et al. (2005) Relationship between enamel erosion and liquid flow rate. *European Journal of Oral Sciences*, 113 (3): 232–238. doi:10.1111/j.1600-0722.2005.00210.x.

Shellis, R.P., Ganss, C., Ren, Y., et al. (2011a) Methodology and models in erosion research: Discussion and conclusions. *Caries Research*, 45 (S1): 69–77. doi:10.1159/000325971.

Shellis, R.P., Ganss, C., Ren, Y., et al. (2011b) Methodology and models in erosion research: Discussion and conclusions. *Caries Research*, 45 (SUPPL. 1): 69–77. doi:10.1159/000325971.

Shellis, R.P. r., Featherstone, J.D.B. and Lussi, A. (2012) Understanding the Chemistry of Dental Erosion. *Erosive Tooth Wear: From Diagnosis to Therapy*, 25: 163–179. doi:10.1159/000359943.

Stenhagen, K.R., Hove, L.H., Holme, B., et al. (2010) Comparing different methods to assess erosive lesion depths and progression in vitro. *Caries Research*, 44 (6): 555–561. doi:10.1159/000321536.

Suk, M., Gillis, D.R. and Singh, G.P. (1999) In-situ technique for measuring wear of materials. *IEEE Transactions on Magnetics*, 35 (5 PART 1): 2352–2354. doi:10.1109/20.800822.

Sun, Y., Li, X., Deng, Y., et al. (2014) Mode of action studies on the formation of enamel minerals from a novel toothpaste containing calcium silicate and sodium phosphate salts. *Journal of Dentistry*, 42: S30–S38. doi:10.1016/S0300-5712(14)50005-X.

Svensson, O., Lingh, L., Cardenas, M., et al. (2006) Layer-by-layer assembly of mucin and chitosan – influence of surface properties, concentration and type of mucin. *Journal of Colloid and Interface Science*, 299: 608–616.

Tanaka, M. and Kadoma, Y. (2000) Comparative reduction of enamel demineralization by calcium and phosphate in vitro. *Caries Research*, 34: 241–245.

Tantbirojn, D., Pintado, M., Versluis, A., et al. (2012) Quantitative analysis of tooth surface loss associated withgastroesophageal reflux disease. *Journal of the American Dental Association*, 143 (3): 278–285.

Teixeira, L., Manarte-Monteiro, P. and Manso, M.C. (2016) Enamel lesions: Meta-analysis on effect of prophylactic/therapeutic agents in erosive tissue loss. *Journal of Dental Sciences*, 11 (3): 215–224. doi:10.1016/j.jds.2016.03.008.

Tenuta, L.M.A. and Cury, J.A. (2013) Laboratory and human studies to estimate anticaries efficacy of fluoride toothpastes. *Toothpastes*, 23: 108–124. doi:10.1159/000350479.

Tuke, M., Taylor, A., Roques, A., et al. (2010) 3D linear and volumetric wear measurement on artificial hip joints - Validation of a new methodology. *Precision Engineering*, 34 (4): 777–783. doi:10.1016/j.precisioneng.2010.06.001.

Venasakulchai, A., Williams, N.A., Gracia, L.H., et al. (2010) A comparative evaluation of fluoridated and non-fluoridated mouthrinses using a 5-day cycling enamel erosion model. *Journal of Dentistry*, 38 (SUPPL. 3): S21–S29. doi:10.1016/S0300-5712(11)70005-7.

Vieira, A., Jager, D.H.J., Ruben, J.L., et al. (2007) Inhibition of erosive wear by fluoride varnish. *Caries Research*, 41 (1): 61–67. doi:10.1159/000096107.

Vissink, A., Franken, M.H., S-Gravenmade, E.J., et al. (1985) Rehardening Properties

of Mucin- or CMC-Containing Saliva Substitutes on Softened Human Enamel. *Caries Research*, 19 (3): 212–218. doi:10.1159/000260846.

VOCO-GmbH (2010) *Product information: Bifluorid 10*.

Volpe, A., Tetrone, M. and Davies, R. (1993) A critical review of the 10 pivotal caries clinical studies used in a recent meta-analysis comparing the anticaries efficacy of sodium fluoride and sodium monofluorophosphate dentifrices. *American Journal of Dentistry*, 6: s13–s42.

Voronets, J. and Lussi, A. (2010) Thickness of softened human enamel removed by toothbrush abrasion: An in vitro study. *Clinical Oral Investigations*, 14 (3): 251–256. doi:10.1007/s00784-009-0288-y.

Vukosavljevic, D., Custodio, W., Buzalaf, M.A.R., et al. (2014) Acquired pellicle as a modulator for dental erosion. *Archives of Oral Biology*, 59 (6): 631–638. doi:10.1016/j.archoralbio.2014.02.002.

Wang, X., Megert, B., Hellwig, E., et al. (2011a) Preventing erosion with novel agents. *Journal of Dentistry*, 39 (2): 163–170. doi:10.1016/j.jdent.2010.11.007.

Wang, X., Mihailova, B., Klocke, A., et al. (2011b) Effect of artificial saliva on the apatite structure of eroded enamel. *Int J Spectroscopy*, 2011: doi:10.1155/2011/236496. doi:10.1155/2011/236496.

Watari, F. (2005) In situ quantitative analysis of etching process of human teeth by atomic force microscopy. *Journal of Electron Microscopy (Tokyo)*, 54 (3): 299–308.

Watson, T.F. (1990) The application of real time confocal microscopy to the study of high speed dental bur tooth cutting interactions. *Journal of Microscopy*, 157 (1): 51–60. doi:10.1111/j.1365-2818.1990.tb02946.x.

Watson, T.F. (1997) Facts and artefact in confocal microscopy. *Advances in Dental Research*, 11 (4): 433–441.

Watson, T.F., Atmeh, A.R., Sajini, S., et al. (2014) Present and future of glass-ionomers and calcium-silicate cements as bioactive materials in dentistry: biophotonics-based interfacial analyses in health and disease. *Dental materials : official publication of the Academy of Dental Materials*, 30 (1): 50–61. doi:10.1016/j.dental.2013.08.202.

Watson, T.F. and Boyde, A. (1985) The tandem scanning reflected light microscope (TSRLM) in conservative dentistry. *Journal of Dental Research*, 62: 512.

West, N.X., He, T., Macdonald, E.L., et al. (2017) Erosion protection benefits of stabilized SnF 2 dentifrice versus an arginine – sodium monofluorophosphate dentifrice : results from in vitro and in situ clinical studies. *Clinical Oral Investigations*, 21 (2): 533–540. doi:10.1007/s00784-016-1905-1.

West, N.X., Hughes, J.A. and Addy, M. (2000) Erosion of dentine and enamel in vitro by dietary acids: the effect of temperature, acid character, concentration and exposure time. *Journal of Oral Rehabilitation*, 27 (10): 875–880. doi:10.1111/j.1365-2842.2001.00778.x.

West, N.X., Hughes, J.A. and Addy, M. (2001) The effect of pH on the erosion of dentine and enamel by dietary acids in vitro. *Journal of Oral Rehabilitation*, 28 (9): 860–864. doi:10.1111/j.1365-2842.2001.00778.x.

West, N.X. and Joiner, A. (2014) Enamel mineral loss. *Journal of Dentistry*, 42: S2–S11. doi:10.1016/S0300-5712(14)50002-4.

Wetton, S., Hughes, J., West, N., et al. (2006) Exposure time of enamel and dentine to saliva for protection against erosion: A study in vitro. *Caries Research*, 40 (3): 213–217. doi:10.1159/000092228.

White, A.J., Yorath, C., ten Hengel, V., et al. (2010) Human and bovine enamel erosion under "single-drink" conditions. *European Journal of Oral Sciences*, 118 (6): 604–609. doi:10.1111/j.1600-0722.2010.00779.x.

Wiegand, A. and Attin, T. (2011) Design of erosion/abrasion studies - Insights and rational concepts. *Caries Research*, 45 (SUPPL. 1): 53–59. doi:10.1159/000325946.

Wiegand, A., Bichsel, D., Magalha, A.C., et al. (2009) Effect of sodium , amine and stannous fluoride at the same concentration and different pH on in vitro erosion. *Journal of Dentistry*, 37 (8): 591–595. doi:10.1016/j.jdent.2009.03.020.

Wiegand, A., Kowing, L. and Attin, T. (2007) Impact of brushing force on abrasion of acid-softened and sound enamel. *Archives of Oral Biology*, 52 (11): 1043–1047. doi:10.1016/j.archoralbio.2007.06.004.

Wood, N.J., Jones, S.B., Chapman, N., et al. (2018) An interproximal model to determine the erosion-protective effect of calcium silicate, sodium phosphate, fluoride formulations. *Dental Materials*, 34 (2): 355–362. doi:10.1016/j.dental.2017.11.017.

Yang, B., Ross-Pinnock, D., Muelaner, J., et al. (2017) Thermal compensation for large volume metrology and structures. *International Journal of Metrology and Quality Engineering*, 8 (21). doi:10.1051/ijmqe/2017004.

Young, A. and Tenuta, L.M.A. (2011) Initial erosion models. *Caries Research*, 45 (S1): 33–42. doi:10.1159/000325943.

Zavala-alonso, V., Loyola-rodríguez, J.P., Terrones, H., et al. (2012) Analysis of the molecular structure of human enamel with fluorosis using micro-Raman spectroscopy. *Journal of Oral Science*, 54 (1): 93–98.

Zhang, J., Boyes, V., Festy, F., et al. (2018a) In-vitro subsurface remineralisation of artificial enamel white spot lesions pre-treated with chitosan. *Dental Materials*, 34 (8): 1154–1167. doi:10.1016/j.dental.2018.04.010.

Zhang, J., Lynch, R.J.M., Watson, T.F., et al. (2018b) Remineralisation of enamel white spot lesions pre-treated with chitosan in the presence of salivary pellicle. *Journal of Dentistry*, 72 (December 2017): 21–28. doi:10.1016/j.jdent.2018.02.004.

Zheng, J., Xiao, F., Qian, L.M., et al. (2009) Erosion behavior of human tooth enamel in citric acid solution. *Tribology International*, 42 (11–12): 1558–1564.

Zheng, J., Xiao, F., Zheng, L., et al. (2010) Erosion behaviors of human tooth enamel at different depth. *Tribology International*, 43 (7): 1262–1267.

Zheng, J. and Zhou, Z.R. (2007) Friction and wear behavior of human teeth under various wear conditions. *Tribology International*, 40 (2): 278–284. doi:10.1016/j.triboint.2005.09.025.